



Ministry of Employment and Investment
Hon. Dan Miller, Minister

ENERGY AND MINERALS DIVISION
Geological Survey Branch

**THE STIKINE PROJECT:
GEOLOGY OF WESTERN TELEGRAPH
CREEK MAP AREA,
NORTHWESTERN BRITISH COLUMBIA
(NTS 104G/5, 6, 11W, 12 AND 13)**

By Derek A. Brown¹, Michael H. Gunning² and Charles J. Greig³

Appendix 3 — Conodont identifications by M.J. Orchard, Geological Survey of Canada

- 1. Geological Survey Branch, British Columbia Ministry of Employment and Investment**
- 2. Department of Geology, University of Western Ontario, London, Ontario**
- 3. C.G. Greig and Associates Ltd., Penticton, B.C.**

Canadian Cataloguing in Publication Data

Brown, Derek Anthony, 1959-

The Stikine project : geology of western Telegraph Creek map area, northwestern British Columbia (NTS, 104G/5, 6, 11W, 12 and 13)

Issued by Geological Survey Branch.

Includes bibliographical references: p.

ISBN 0-7726-2502-6

1. Geology - British Columbia - Telegraph Creek Region. 2. Geochemistry - British Columbia - Telegraph Creek Region. 3. Geology, Economic - British Columbia - Telegraph Creek Region. 4. Mines and mineral resources - British Columbia - Telegraph Creek Region. I. Gunning, Michael H. II. Greig, Charles James, 1956-. III. British Columbia. Ministry of Employment and Investment. IV. British Columbia. Geological Survey Branch. V. Title. VI. Title: Geology of western Telegraph Creek map area, northwestern British Columbia (NTS 104G/5, 6, 11W, 12 and 13). VII. Series: Bulletin (British Columbia. Ministry of Employment and Investment) ; 95.

QE187.B76 1996

557.11'185

C95-960208-9



VICTORIA
BRITISH COLUMBIA
CANADA

MAY 1996

Ambition Mtn.

Endeavour Mtn.



Frontispiece. View north along the Scud Glacier. Ambition Mountain is underlain by Permian limestone and metavolcanic rocks.

TABLE OF CONTENTS

CHAPTER 1		
INTRODUCTION	1	
Location, Access and Physiography	1	
Aboriginal Features	2	
Previous Work	2	
Exploration History	4	
Acknowledgments	4	
CHAPTER 2		
REGIONAL TECTONIC SETTING AND STRATIGRAPHY	7	
Regional Tectonic Setting	7	
Stratigraphy of the Project Area	7	
Paleozoic Stikine Assemblage	7	
Upper Carboniferous Strata	9	
Devils Elbow Unit	9	
Butterfly Unit	11	
Chutine River Area	13	
Barrington River and Little Tahltan Lake Areas	13	
Upper Carboniferous to Lower Permian Strata	14	
Navo Formation	14	
Lower to Upper Permian Strata	15	
Ambition Formation	15	
Scud Glacier Formation	17	
Regional Correlations	17	
Paleoenvironmental Interpretation	17	
Early Permian to Middle Triassic Wimpson Unit	18	
Permo-Triassic Contact Relationships	19	
Northeast of Devils Elbow Mountain	20	
Toe of Scud Glacier	20	
South of Scud Glacier	20	
North of the Chutine Culmination	20	
Upper Triassic or Older Mafic Metavolcanic Rocks	20	
Upper Triassic Stuhini Group	20	
Carnian to Lower Norian: Kitchener Unit	21	
Limestone Horizons	26	
Volcanic Facies	27	
Mafic Volcanic Rocks	27	
Intermediate Volcanic Rocks	27	
Tuffaceous Wacke	27	
Bladed-plagioclase Porphyry	27	
Upper Norian: Quattrin Unit	28	
Chemistry and Tectonic Setting of the Stuhini Group	30	
Depositional Environments	33	
Lower to Middle Jurassic Hazelton Group	33	
Dacite Unit	34	
Limy Wacke	35	
Andesite Flows and Tuff	35	
Rhyolite	37	
Basalt	37	
Chemistry	38	
Contact Relationships between Jurassic and Triassic Units	39	
Age and Correlation	39	
Depositional Environment	41	
Upper Cretaceous(?) to Paleocene Sustut Group	41	
Chemistry	45	
Contact Relationships	45	
Age and Correlation	47	
Depositional Environment	47	
Eocene Sloko Group	47	
Chemistry	48	
Age and Correlation	51	
Depositional Environment	51	
Miocene Or Younger (?) Flows	51	
Chemistry	51	
Age and Correlation	51	
Quaternary	51	
CHAPTER 3		
INTRUSIVE ROCKS	53	
Regional Overview	53	
Middle(?) to Late Triassic Plutons (228-220 Ma)	55	
Alaskan-type Ultramafites	55	
Mount Hickman Complex	57	
Middle Scud Ultramafite	57	
Yehiniko Ultramafite	57	
Hickman Batholith	57	
Hickman Pluton	57	
Nightout Pluton	58	
Other Stikine Suite Plutons	58	
Late Triassic to Early Jurassic - Copper Mountain Plutonic Suite (210-195 Ma)	59	
Butterfly Pluton	59	
Rugged Mountain Pluton	59	
Clinopyroxenite Phase	61	
Syenite Phase	61	
Hybrid Phase	61	
Alkaline Dike Swarm	61	
Latimer Lake and Damnation Plutons	61	
Early Jurassic Texas Creek Plutonic Suite (189-195 Ma)	62	
Limpoke Pluton	62	
Pogue and Brewery Plutons	62	
Pereleshin and Oksa Creek Plutons	62	
Early Jurassic(?) Diorite Intrusions	63	
Late Early Jurassic Cone Mountain Intrusions (187-180 Ma)	63	
Middle Jurassic Three Sisters Plutonic Suite (177-170 Ma)	64	
Yehiniko Pluton	64	
Niko Pluton	64	
Saffron Pluton	64	
Conover Pluton	64	
Middle Jurassic Dike Swarms and Dok Stocks	65	
Eocene Hyder Plutonic Suite (55-51 Ma)	65	
Christina Pluton	65	
Sawback Pluton	65	
Hamper Pluton	66	
Oksa Creek Dike Swarm	66	
Tertiary(?) Granodiorite	67	
Late Miocene (?) or Younger Dikes Geochemistry and Tectonic Discrimination of Intrusive Rocks	68	

Middle to Late Triassic	68	Galore Creek	106
Alaskan-type Ultramafic Plutons	68	Rugged Mountain Pluton	106
Stikine Suite	70	Limpoke Pluton	106
Late Triassic to Early Jurassic Alkaline and Ultramafic Plutons	70	Porphyry Molybdenum Deposits	106
Texas Creek Suite	70	Ben - Decker Creek Area	106
Cone Mountain Suite	70	Mesothermal and Transitional Vein Deposits	106
Three Sisters Suite	70	Early To Middle Jurassic	107
Hyder Suite	70	Yehiniko Fault Zone	107
Tectonic Discrimination	76	North of the Strata Glacier Pluton	107
Late Triassic	76	Helveker Creek	107
Early Jurassic	76	Conover Creek	107
Middle Jurassic	76	Scud Glacier Area	110
Eocene	76	Limpoke Glacier Area	110
Temporal Evolution of Plutons: the Orogenic Cycle	76	Eocene	110
Pendants in the Strata Glacier Pluton	110	North of the Strata Mountain Pluton	110
CHAPTER 4 STRUCTURE AND METAMORPHISM	77	Epithermal Vein Deposits	111
Pre-late Triassic Deformation	78	Volcanogenic Massive Sulphide Deposits	111
Phyllosilicate Foliation	81	Skarn Deposits	111
Development of Structural Culminations	81	Tahltan Lake	111
Little Tahltan Lake Culmination	81	Devil's Elbow	111
Barrington River Culmination	81	Scud River	111
Chutine River Culmination	81	Other Deposit Types	113
Age Constraints and Tahltanian Orogeny	82	Placer Gold	113
Post-Norian and Pre-Toarcian Contraction of Stuhini Group	84	Stratabound Uranium	113
Age Constraints	86	Cumulate Magnetite	113
Structures near Scud Glacier	86	Timing of Regional Metallogenic Events	113
Middle Jurassic or Cretaceous Contraction	86	Paleozoic: Volcanogenic Massive Sulphide Deposits	113
Folds	86	Late Triassic to Jurassic Porphyry Deposits and Transitional to Epithermal Veins	113
Contractional Faults	88	Early To Middle Jurassic: Volcanogenic Massive Sulphide Deposits	114
Cone Mountain Fault	88	Middle Jurassic: Calcalkaline Porphyry Deposits and Transitional Veins	114
Butterfly Lake and Related Faults	89	Eocene: Epithermal to Transitional Veins, Porphyry Molybdenum-copper Deposits	114
Navo Shear Zone	89	Galena-Lead Isotope Results	114
Age Constraints	89	Exploration Activity	115
Regional Correlation	92	Mineral Potential	115
Faults	92	CHAPTER 6 SUMMARY AND CONCLUSIONS	117
North-trending Faults	92	Plutonism	118
Scud Glacier Fault	92	Structure	118
Middle Scud Creek Faults	93	Metamorphism	119
Oksa Creek Dike Swarm	93	Economic Geology	119
East-Trending Faults	93	Tectonic Model	120
Kitchener Fault Zone	93	REFERENCES	121
Boomerang and Related Faults	93	APPENDICES	131
Ductile Fabrics	93	1. Macrofossil Identifications	132
Jimjack Fault System	93	2. Fusulinid Age Determinations	135
Northwest-trending Faults	95	3. Conodont Identifications	137
Metamorphism	95	4. Barren Conodont Collections	139
Conodont Colour Alteration Indices	95	5. Radiolarian Age Determinations	141
Late Permian to Early Triassic(?) Metamorphism	95	6. Samples Barren of Radiolaria	143
Jurassic to Pre-late Cretaceous Metamorphism	97	7. Palynomorph Collections	145
Eocene Burial Metamorphism	97	8. Whole-rock and Trace Element Chemistry of Stratified Rocks	147
Contact Metamorphism	97	9. Filtering of Geochemical Data	155
Summary of Metamorphism	98	10. Petrographic Notes	157
CHAPTER 5 ECONOMIC GEOLOGY	99	11. Whole-rock Lithochemical Analyses of Plutonic Rocks	161
Porphyry Deposits	99		
Calcalkaline Porphyry Copper Deposits	99		
Schaft Creek (Liard Copper)	99		
Showings near Schaft Creek	105		
Dokdaon - Strata Creek Area	105		
Alkalic Porphyry Copper Deposits	105		

12. Potassium-argon Analytical Data and Dates for Stratified and Plutonic Rocks	169	3-13. Chemical characteristics of the Middle Jurassic Three Sisters suite	73
13. Uranium-Lead Analytical Data	171	3-14. Chemical characteristics of the Eocene Hyder suite	74
14. Lithochemical Data	173	3-15. Tectonic discrimination diagrams for plutonic rocks	75
FIGURES			
1- 1. Location map for the Stikine project	1	4- 1. Distribution of major faults in northwestern British Columbia	77
1- 2. Physiographic regions of the Telegraph Creek map area	2	4- 2. Major structural elements in the Stikine project area	79
1- 3. Geographic features referred to in the text	3	4- 3. Cross-section illustrating deformed Norian clastic rocks unconformably overlain by Toarcian flows and tuffs	85
2- 1. Location of project area on a simplified terrane map	8	4- 4. Cross-section illustrating the contrast in deformation between Navo formation and overlying Ambition Formation and the series of northwest-trending reverse faults	87
2- 2. Schematic stratigraphic succession	9	4- 5. Relationship of the Cone Mountain fault to the pluton and hangingwall Stikine assemblage	88
2- 3. Distribution of Paleozoic Stikine assemblage	10	4- 6. Microfabrics associated with the Scud Glacier fault	92
2- 4. Stratigraphic column and paleoenvironmental interpretations for the Stikine assemblage	11	4- 7. Cross-sections of the Sustut Group	94
2- 5. Stratigraphic column near the Scud Glacier	18	4- 8. Distribution of Sustut Group in the Yehiniko valley	94
2- 6. Distribution of enigmatic mafic metavolcanic rocks	21	4- 9. Metamorphic facies structural features and plutons	96
2- 7. Distribution of the Upper Triassic Stuhini Group	22	4-10. Thermal maturation based on conodont colour alteration indices and metamorphic grade	97
2- 8. Schematic Stuhini Group stratigraphic columns	23	4-11. Histograms illustrating the distribution of CAI values relative to their age determinations	95
2- 9. Schematic Stuhini Group column near Strata Creek	29	5- 1. Major mineral deposits, mines and past producers between Stewart and Tulsequah	99
2-10. Major element geochemical plots for Stuhini Group	31	5- 2. Mineral occurrences in the project area	100
2-11. Trace element diagrams for Stuhini Group	32	5- 3. Galena-lead isotope signatures for mineral showings	114
2-12. Distribution of Hazelton Group	33	6-1. Schematic tectonic evolution	117
2-13. Schematic stratigraphic column of the Hazelton Group	34	6-2. Schematic Mesozoic tectonic evolution	119
2-14. Major and trace element geochemical plots for Hazelton Group volcanic rocks	36	6-3. Schematic Cretaceous and Eocene tectonic framework for northern Cordillera	120
2-15. Unconformable relationships between the Upper Triassic Stuhini Group, Jurassic Hazelton Group and Upper Cretaceous to Paleocene Sustut Group, and their relation to the Late Triassic and Middle Jurassic plutons	40	PHOTOS	
2-16. Distribution of Sustut Group, paleocurrent directions and age constraints	43	Frontispiece. View north along the Scud Glacier	
2-17. Sketch of key exposure of the Sustut Group	44	1- 1. Stone cairn above the Stikine River	4
2-18. Major and trace element geochemical plots for Sustut Group, Sloko Group and Miocene(?) volcanic rocks	46	1- 2. Obsidian flakes collected above Barrington River valley	5
2-19. Distribution of Sloko volcanic rocks	48	2- 1. Volcanic breccia of the Stikine assemblage	12
2-20. Sloko Group stratigraphic column	48	2- 2. Pillow with intrapillow micrite	14
3- 1. Distribution of plutonic rocks, and major ore deposits between Stewart and Dease Lake	53	2- 3. Reworked felsic tuff (Navo formation)	15
3- 2. Distribution of plutons in the project area	55	2- 4. Argillaceous limestone and limestone	16
3- 3. Distribution of the Middle to Late Triassic Stikine and Mount Hickman Plutonic Suites	55	2- 5. Limestone with chert layers and lenses	16
3- 4. Distribution of the Late Triassic to Early Jurassic Copper Mountain Plutonic Suite	59	2- 6. Ribbon chert	19
3- 5. Biotite ³⁷ Ar/ ³⁹ Ar plateau date for the Rugged Mountain pluton	61	2- 7. Microfabrics of the Stuhini Group	24
3- 6. Distribution of Early Jurassic Texas Creek Plutonic Suite and Early Jurassic diorites	62	2- 8. Sedimentary structures in Upper Triassic tuffs	25
3- 7. Distribution of late Early Jurassic Cone Mountain Plutonic Suite	63	2- 9. Carnian limestone cliffs southwest of Tahltan Lake	26
3- 8. Distribution of Middle Jurassic Three Sisters Plutonic Suite	64	2-10. Heterolithic breccia with volcanic and plutonic clasts	26
3- 9. Distribution of Eocene Hyder Plutonic Suite	65	2-11. Angular limestone boulder in volcanic conglomerate	28
3-10. Chemical characteristics of the Stikine suite compared with the Alaskan-type ultramafites	69	2-12. Dacitic lapilli tuff and ash-tuff beds	28
3-11. Chemical characteristics of the Rugged Mountain Complex	71	2-13. Heterolithic breccia composed of volcanic and plutonic fragments	29
3-12. Chemical characteristics of the Early Jurassic Texas Creek and late Early Jurassic Cone Mountain suites	72	2-14. Unconformable contact of Stuhini Group sedimentary rocks with Jurassic volcanic rocks	30
		2-15. Angular unconformity separating Stuhini Group from Hazelton Group	35
		2-16. Stuhini Group overlain unconformably by Jurassic flows	37
		2-17. Jurassic lithic lapilli tuff	38
		2-18. Flat-lying lava flows of the Jurassic succession	38
		2-19. Basalt fragment displaying bread-crust texture	39
		2-20. Lower Jurassic tuff-breccia north of Helveker Creek	40

2-21. Sustut Group conglomerate unconformably deposited on altered Jurassic volcanic rocks	41	4-12. Photomicrographs comparing undeformed and mylonitic Cone Mountain pluton	90
2-22. Typical conglomerates of the Sustut Group	43	4-13. Mylonitic contact of the Butterfly syenite and Carboniferous volcanic rocks (Butterfly formation)	91
2-23. View southeast to Sustut Group conglomerate	44	4-14. Brecciated dikes and diorite within mylonitic diorite	91
2-24. Sloko volcanic rocks	46	5- 1. Aerial view of propylitic alteration zone at Ben Mo-Cu-W prospect	107
2-25. Trachyandesite flows of the Sloko Group	49	5- 2. Vein textures from Deeker Creek	108
2-26. Andesitic crystal lithic lapilli tuff-breccia	50	5- 3. Vein textures from Chuckter showing	108
2-27. Flat-lying, columnar jointed basalt flow	50	5- 4. Multiphase veins	109
3- 1. Rugged Mountain syenite complex	60	5- 5. Quartz - iron carbonate breccia zone	110
3- 2. Megacrystic dike of Rugged Mountain complex	60	5- 6. Iron-carbonate quartz vein	112
3- 3. Breccia zone with Jurassic diorite and granodiorite inclusions hosted by Eocene granite	66	TABLES	
3- 4. Eocene Sawback granite pluton	67	2- 1. U-Pb and K-Ar Isotopic Dates for Stratified Rocks	12
3- 5. Phyllite xenolith within the Geology Ridge diorite	68	3- 1. Characteristics of the Intrusive Rocks	54
4- 1. Deformation in Tahltan Lake structural culmination	80	3- 2. Summary of U-Pb, K-Ar and Ar-Ar Dates for Plutonic Rocks	56
4- 2. Microfabrics in the Barrington River culmination	82	4- 1. Summary of Structural Features	78
4- 3. View northwest to the Ugly anticline	83	5- 1. Summary of Mineral Occurrence Characteristics	101
4- 4. Chevron-folded Middle Triassic chert	83	5- 2. Summary of Deposit Types and Potential Settings	115
4- 5. Tight folds of mafic schist in a pendant within the Early Jurassic Geology Ridge diorite	84	MAP	
4- 6. Structural discordance between Norian sedimentary rocks and Hazelton volcanic rocks	85	Geology Map of western Telegraph Creek map area (104G/5, 6, 11W, 12 and 13) 1:100 000 scale, including schematic cross-sections of western Telegraph Creek map area (104G/5, 6, 11W, 12 and 13) 1:100 000 scale <i>in pocket</i>	
4- 7. Chevron-folded metavolcanic rocks (Stuhini Group?)	86		
4- 8. Steeply dipping foliation in the Scud River valley	87		
4- 9. Bedding-cleavage intersections in felsic tuff	87		
4-10. Asymmetric, southwest-verging fold in limestone	88		
4-11. Minor folds in foliated tuffaceous rocks (Butterfly member)	89		

CHAPTER 1 INTRODUCTION

The Stikine project area, approximately 50 kilometres southwest of Telegraph Creek, lies astride the Stikine River, a major transportation route much used by prospectors. The project area covers part of a northwest-trending mineral-rich belt that includes important precious and base metal deposits such as Premier, Sulphurets, Eskay Creek, Johnny Mountain, Snip, Galore Creek and Golden Bear (Figure 1-1), and was selected for study due to its high mineral potential but outdated geological database. This report synthesizes and reviews previous geological work, provides new data on Paleozoic and Mesozoic stratigraphy, and describes Mesozoic plutonic suites and mineral occurrences.

LOCATION, ACCESS AND PHYSIOGRAPHY

The Stikine project area is located in northwestern British Columbia, approximately 400 kilometres northwest of Smithers and 125 kilometres southwest of Dease Lake. The closest supply and service centre is Telegraph Creek, a village of a few hundred people 50 kilometres to the northeast. Regular air and truck services to Telegraph Creek and Dease Lake operate throughout the summer months. A rough gravel road provides four-wheel-drive access from Telegraph Creek to part of the northwest corner of the project

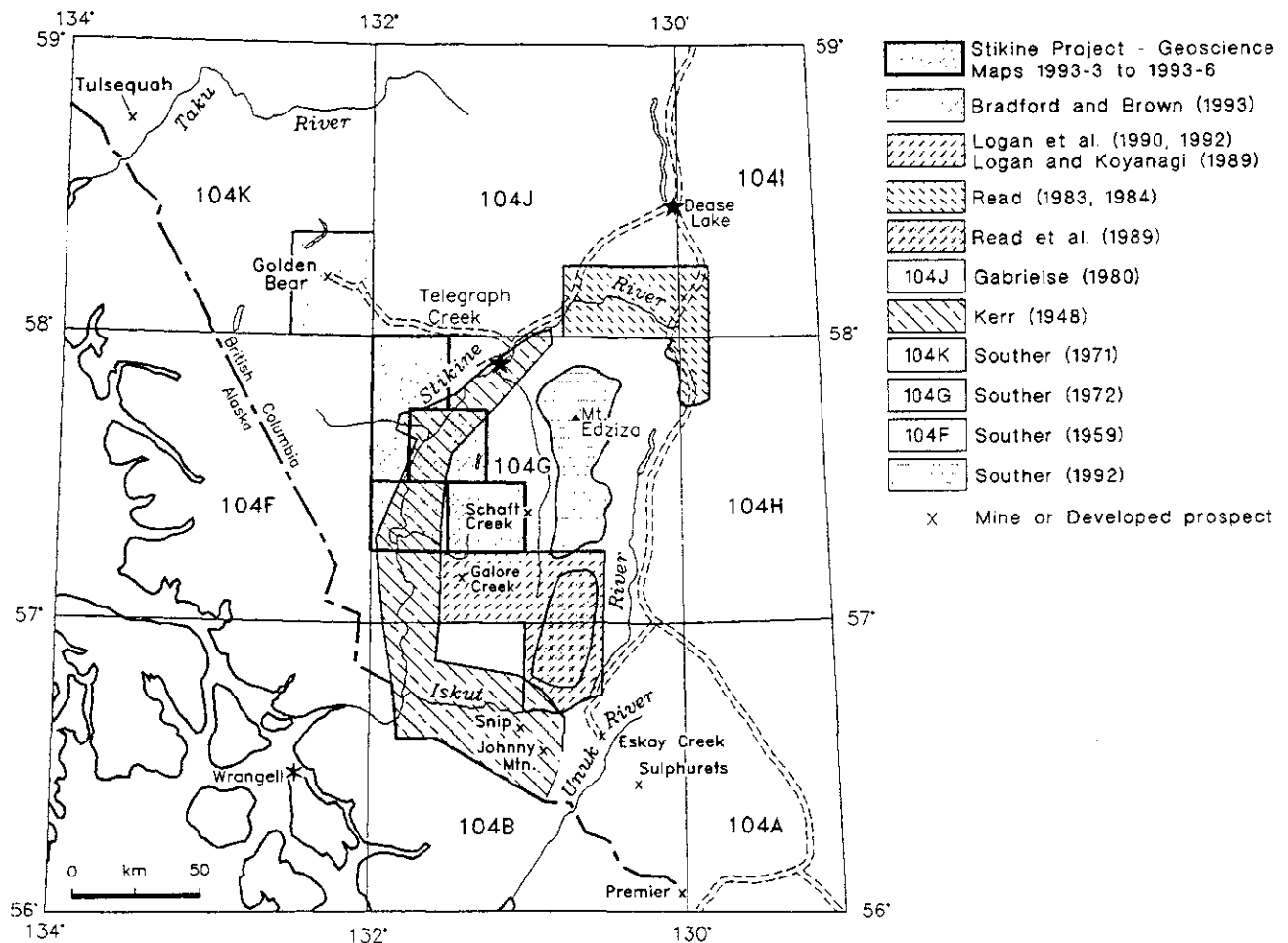


Figure 1-1. Location map showing previous geological mapping in Telegraph Creek map area and environs.

area, but practical access to most of the area is by helicopter. Gravel airstrips are located at the confluence of the Scud and Stikine rivers, at Schaft Creek and near the mouth of the Barrington River (Figure 1-2b).

The map area covers parts of two broad physiographic regions, the Coast Mountains (Boundary Ranges) on the southwest and the Tahltan Highlands on the northeast (Holland, 1976; Figure 1-2a), which were further subdivided by Ryder (1984; Figure 1-2b) into Telegraph Creek lowlands and Zagoddetchino and Tahltan Lake plateaus. The Coast Mountains comprise 75% of the area, and are characterized by steep, rugged topography, high relief, extensive alpine glaciers and snowfields, and dense rainforest at lower elevations (<1000 m elevation). In the south, the Scud icefield and glacier cover more than 50 square kilometres and jagged peaks, such as Ambition Mountain (frontispiece), reach elevations of more than 2900 metres. "Vanishing Lake", a glacially dammed lake 8 kilometres east of the Scud Glacier, is subject to outburst flooding (jokulhlaups; Figure 1-3; Perchanok, 1980). In contrast to the icy and rugged Coast Mountains in the south, the Telegraph Creek lowlands and Stikine River valley upstream of Chutine River have subdued relief, with forested, glacially rounded and elongate outcrops, and thick intervening Pleistocene and Recent glacial, glaciofluvial and fluvial deposits. Prominent northeast-trending linear features are characteristic, and local crag and tail ridges indicate that glaciers moved toward the southwest (Ryder, 1984). The northeastern part of Telegraph Creek lowland is semi-arid and open grasslands are common on south-facing terraces. In the northeast corner of the study area, Zagoddetchino plateau averages more than 1525 metres elevation and is a remnant of a larger, late Tertiary erosional surface (Souther, 1971) which includes the Tahltan Highlands and Klastine Plateau.

HISTORICAL FEATURES

More than fifty stone cairns are distributed along the Stikine valley, near the mouth of the Scud River (Figure 1-3; Photo 1-1). The cairns are completely covered by lichen and moss and vary in shape; some are domal and others rectangular. Their average height is approximately 1 metre and circular ones are about 2 metres in diameter. All are built on prominent knolls, between 1100 and 1350 metres elevation, overlooking the Stikine River. They were first described by Kerr (1948a); however, little is known of them except that they were built in the territory occupied by both ancient interior Tahltan and coastal Tlingit people.

Five obsidian flakes, presumably derived from either an arrowhead or cutting tool, were found at about 725 metres elevation immediately south of the Barrington River (150 metres above the valley floor; Photo 1-2; Figure 1-3). An obvious source is obsidian at Mount Edziza (Fladmark, 1985). Trace element signatures based on x-ray refraction analysis of the flakes confirmed their geochemical similarity to obsidian found on Mount Edziza, specifically flow 3 (M. James, Simon Fraser University, personal communication, 1994). The flakes provide evidence that native peoples travelled through the Barrington valley and possibly sharpened an obsidian tool or arrowhead at this site, probably about 4000 to 5000 years ago, in the height of the Mount Edziza microblade industry (Fladmark, 1985).

PREVIOUS WORK

Initial geological studies along the Stikine River were made in 1863 when a group of Russian geologists came to assess the area's mineral potential (Alaska Geographic Society, 1979). Dawson and McConnell were the first Canadian geologists to explore the valley (Dawson, 1889), but

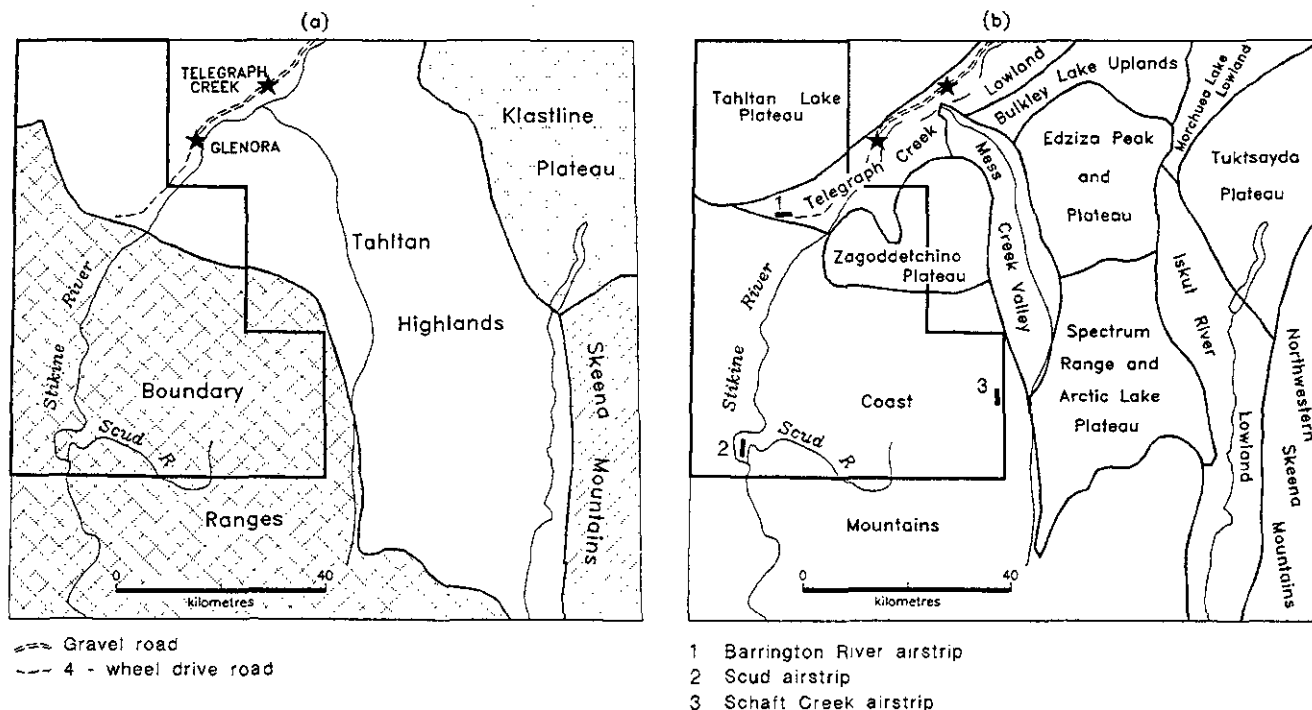


Figure 1-2. Physiographic regions of the Telegraph Creek map area (104G) after Holland (1976; a), and Ryder (1984; b).

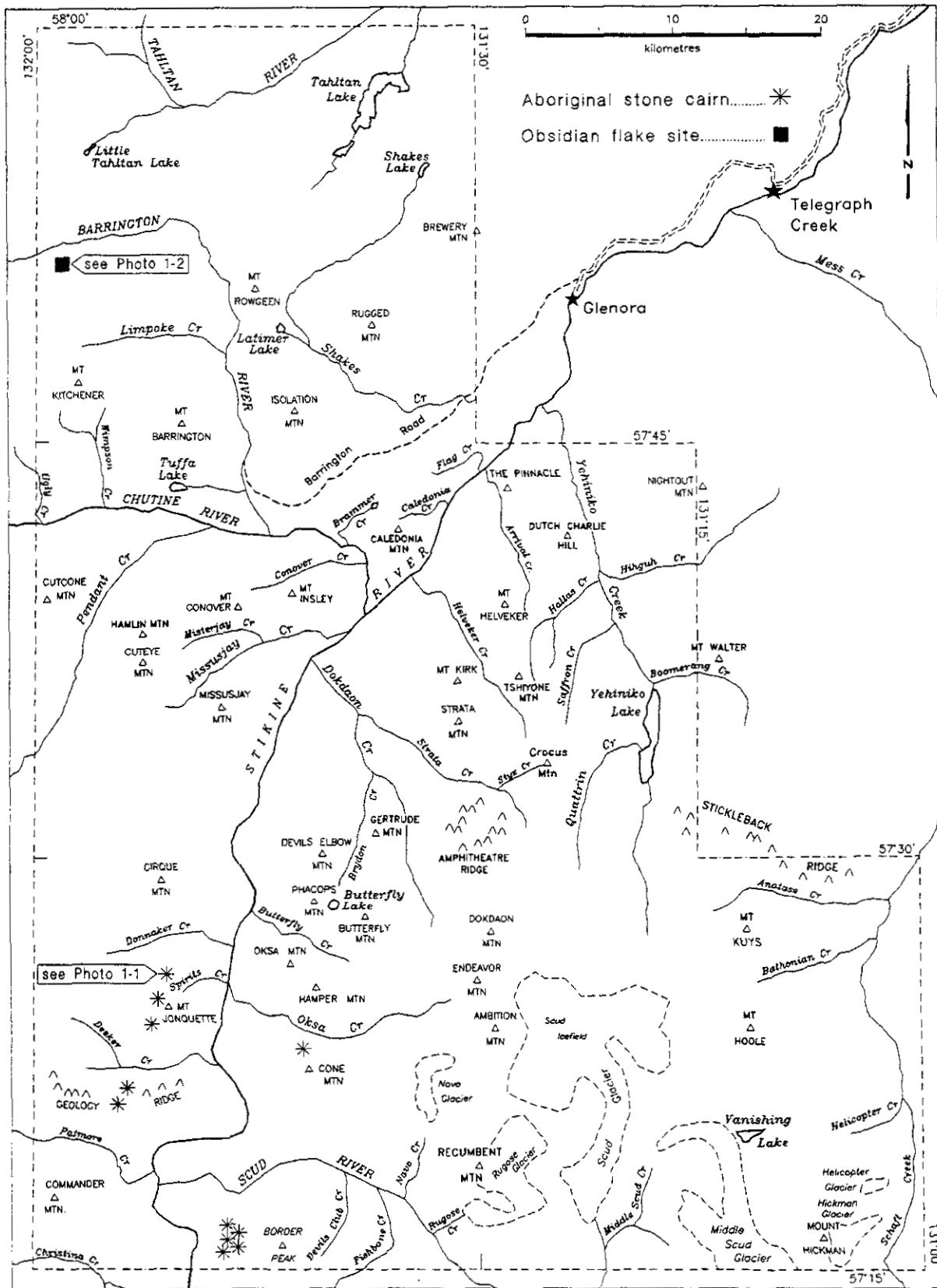


Figure 1-3. Geographic features in the project area.

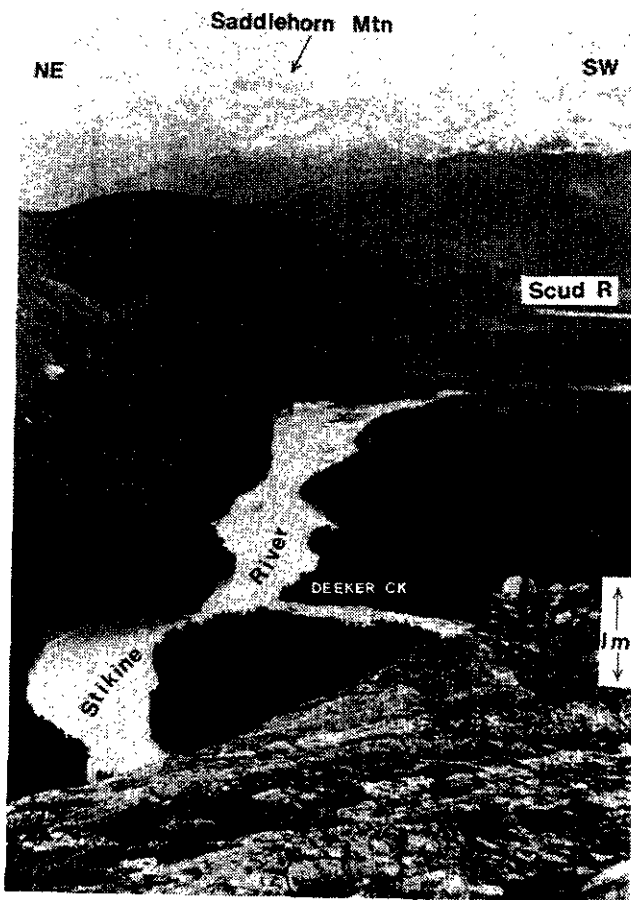


Photo 1-1. Stone cairn on a prominent knoll north of Mount Jonquette (see Figure 1-3), 1200 metres above the Stikine River.

the first geological maps (1:126 720 scale) and descriptions of the region were produced by Forrest Kerr of the Geological Survey of Canada, who worked in the Stikine River watershed between the International border and Telegraph Creek in the years 1924 to 1929 (Kerr, 1927, 1929, 1930, 1931, 1935, 1948a; Figure 1-1). Kerr proposed the original Permian and pre-Permian division of Paleozoic strata and outlined the distribution of many of the plutonic rocks.

The Geological Survey of Canada's Operation Stikine in 1956 covered much of the area in reconnaissance fashion (Geological Survey of Canada, 1957). Led by Jack Souther, it continued work in the late 1950s and 1960s and produced 1:250 000 geological maps of Chutine River (NTS 104F; Souther, 1959), Tulsequah River (NTS 104K; Souther, 1971) and Telegraph Creek (NTS 104G; Souther, 1972) areas. In Telegraph Creek map area, Souther divided the Paleozoic strata into pre-Permian, Mississippian, and Permian units, and described Triassic rocks and the Hickman batholith in detail. His work incorporated a study by Monger (1970) of Paleozoic rocks in parts of the Telegraph Creek area. The Mount Edziza Volcanic Complex, 20 kilometres northeast of the study area, was mapped at 1:25 000 scale between 1965 and 1976 (Souther, 1992).

A regional geologic framework for the Stikine River area has been developed from numerous studies, including: biostratigraphic studies of the Devonian to Permian Stikine

assemblage (Pitcher, 1960); regional synthesis by Monger (1977a); mapping to the south in the Iskut River map area by the Geological Survey of Canada (Anderson, 1989; Anderson and Thorkelson, 1990); mineral deposit studies to the southeast by Fox *et al.* (1976) and Holbek (1988), and geological mapping by Gabrielse (1980), Anderson (1983a) and Read (1983, 1984) to the northeast.

Stikine project geological mapping was completed at 1:50 000 scale in the Scud River and Scud Glacier map areas in 1988 (104G/5,6; Brown and Gunning, 1989a, b), Yehiniko Lake (west half) and Chutine River (east half) map areas in 1989 (104G/11W, 12E; Brown and Greig, 1990; Brown *et al.*, 1990), and Chutine River - Tahltan Lake map areas in 1991 (104G/12W, 13; Brown *et al.*, 1992a, b). Concurrent British Columbia Geological Survey studies have extended 1:50 000 map coverage south of the Stikine project area in the Galore Creek and Forrest Kerr Creek areas (104G/3,4 and 104B/15; Logan and Koyanagi, 1989; 1994; Logan *et al.*, 1989, 1990a, b, 1992a, b), and northwest around the Golden Bear mine (Bradford and Brown, 1993a, b; Oliver and Gabites, 1993). A stratigraphic study by Gunning (1993b) of the Forrest Kerr area is in progress.

EXPLORATION HISTORY

Prospectors first came to the Stikine River valley during the early 1860s, discovering and mining placer gold (at least 64 kilograms) at Buck's Bar, 6 kilometres southwest of Telegraph Creek (Holland, 1950). By the late 1800s, the search for placer gold had moved farther north to the Cassiar and Klondike, but the Stikine River remained a main transportation and supply route to the northern goldfields. In the late 1920s, the Barrington River placer deposit was discovered. It produced 45 kilograms of gold between 1906 and 1945 (Holland, 1950) and recent test mining yielded 12.4 kilograms of gold from about 36 000 cubic metres of gravel (Integrated Resources Ltd., News Release, October 21, 1991).

During the early part of the 20th century, attention turned to lode deposits (Kerr, 1948a). Exploration efforts prior to the 1950s were limited because access was restricted to navigable rivers. Introduction of the helicopter resulted in discovery of significant porphyry copper deposits near Galore Creek (1955) and Schaft Creek (1957; Figure 1-1). Porphyry copper exploration continued until about 1976 (Panteleyev and Dudas, 1973; Linder, 1975; Allen *et al.*, 1976; Fox *et al.*, 1976). The early 1980s brought renewed interest in the region as major companies targeted precious metal deposits. The Eskay Creek, Premier, Snip, Sulphurets, Johnny Mountain and Golden Bear projects are prime examples of nearby developments or redevelopments of precious and base metal deposits in the mineral-rich region (Figure 1-1). There remains good potential to discover new porphyry copper-gold, vein, epithermal, skarn, and volcanogenic massive sulphide deposits.

ACKNOWLEDGMENTS

Michael McDonough was a valuable member of our 1988 field crew and his data and ideas are gratefully acknowledged. David Carmichael (1988), Eric Maeckelburg

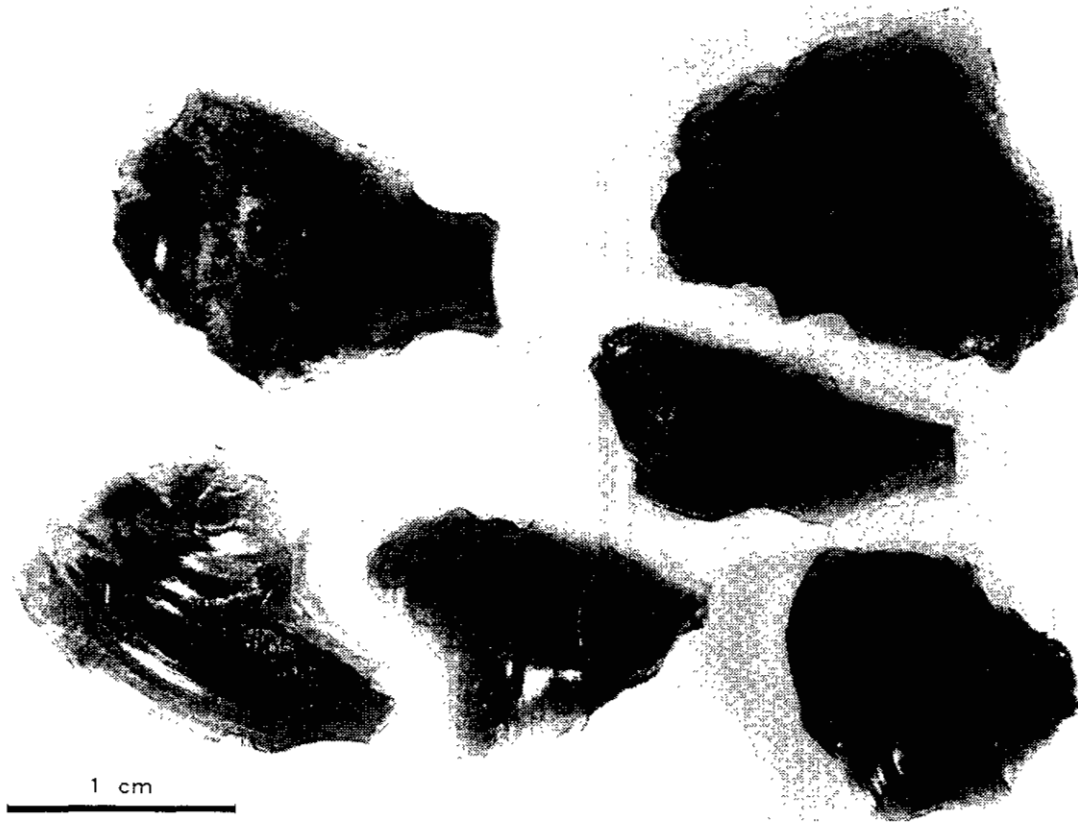


Photo 1-2. Obsidian flakes collected above the Barrington River valley (see Figure 1-3), possible evidence of ancient aboriginal hunting in the area.

(1989) and Ian Neill, David Munro and Jay Timmerman (1991) provided excellent assistance and contributed greatly to the success of the field seasons. Discussions with and field visits by Bill McMillan, Bill McClelland and Darcy Marud provided thoughtful insights. The cooperation and logistical support of Continental Gold Corporation in 1988 and of Ian Paterson, Steve Noakes and Mike Westcott of Cominco Ltd. in 1989, was greatly appreciated. Quest Canada Resource Corporation provided hospitality at its Scud camp during the 1990 field season. Central Mountain Air, Northern Mountain Helicopters Inc., Tel Air Ltd., Trans North Air Ltd., Vancouver Island Helicopters Ltd., Dease Lake Expeditors and Tundra Expeditors are acknowledged for their professional services.

John A. Bradford contributed significantly to Chapter 5, and Victor Koyanagi and Fleur Harvey-Kelly provided essential support during preparation of this manuscript. Dick Player is thanked for his photographic expertise and thin section preparation. Fossils were identified by W.E. Bamber, Lin Rui, T.P. Poulton and A.R. Sweet (GSC, ISPG, Calgary), F. Cordey, M.J. Orchard, H.W. Tipper and E.T. Tozer (GSC, Vancouver), and B.L. Mamet (University of Montreal). Isotopic work was by Joe Harakal, Dita Runkle, Janet Gabites and Anne Pickering (UBC), Mary Lou Bevier (GSC, Ottawa), Bill McClelland (University of California, Santa Barbara) and Peter Reynolds (Dalhousie University, Halifax). Joanne Schwemler performed vitrinite reflectance analyses. Thoughtful reviews and improvements to the manuscript were provided by John Newell, Bill McMillan and Brian Grant.

CHAPTER 2

REGIONAL TECTONIC SETTING AND STRATIGRAPHY

REGIONAL TECTONIC SETTING

The study area lies wholly within the Stikine Terrane (Stikinia) of the northern Intermontane Belt of the Canadian Cordillera, between the Coast Belt and Bowser Basin (Figure 2-1). In this region, Stikinia comprises Paleozoic and Mesozoic arc volcano-sedimentary successions and coeval plutonic complexes, overlain by marine clastic rocks of the Bowser Lake Group, which are overlain in turn by less extensive continental strata of the Sustut and Sloko groups.

The oldest strata are included in the Paleozoic Stikine assemblage, which is discontinuously exposed along the western flank of Stikinia for over 500 kilometres (Monger, 1977a). The assemblage consists of at least three well dated limestone units, interbedded with volcanic rocks and intruded by rare coeval plutonic rocks. This dominantly marine succession represents remnants of the paleo-Pacific oceanic arc system that spanned more than 150 Ma. The oldest rocks of the Stikine assemblage are Devonian limestones and bimodal volcanic and plutonic rocks with primitive arc signatures (Read *et al.*, 1989; Anderson, 1989; Greig and Gehrels, 1992; Logan and Drobe, 1993a, b; Logan, Drobe and McClelland in preparation; Gunning, 1993b). Carboniferous limestones and mafic volcanic rocks comprise the middle sequence. The youngest sequence comprises locally thick but laterally discontinuous Lower to Upper Permian limestones, which were deposited in an open-marine, subtropical environment, characterized by local tectonic stability. Upper Triassic and Lower to Middle Jurassic calcalkaline volcanic successions constitute island arc complexes of the Stuhini and Hazelton groups which were built on these Paleozoic strata prior to amalgamation of Stikinia with adjacent terranes; ultimate accretion to the western margin of North America occurred in the Middle Jurassic (Gabrielse and Yorath, 1991). The Bowser Lake Group formed an overlap assemblage on Stikinia in the Middle to Late Jurassic (Evenchick, 1991a). It comprises marine and nonmarine clastic rocks. The Sustut Group comprises fluvial sandstone, conglomerate and lesser tuff, the detrital material being derived from uplifted rocks of the Omineca Belt to the east and Stikinia to the west. The Sloko Group represents Eocene continental arc volcanism extruded east of the Coast Belt in a back-arc setting. The Neogene to Recent stratavolcano and surrounding plateau lavas of the Mount Edziza Complex were generated after a change in the relative movement of the North American and Pacific plates at about 40 Ma, from almost pure convergence to more oblique and hence a transtensional regime (Souther, 1992; Engerbretson *et al.*, 1985).

The time scale of Harland *et al.* (1990) is used throughout this report for isotopic ages, except for the uppermost Triassic, where the Norian is considered the youngest unit (*i.e.* Rhaetian is not included).

STRATIGRAPHY OF THE PROJECT AREA

The stratigraphic succession within the project area consists of: poorly dated Carboniferous volcanic and sedimentary rocks, and well dated Permian limestone, tuff and chert of the Stikine assemblage; Permian to(?) Middle Triassic chert; Upper Triassic, dominantly submarine mafic and felsic volcanic rocks and related sedimentary rocks of the Stuhini Group; Lower to Middle Jurassic subaerial and subordinate marine volcanic and sedimentary rocks of the Hazelton Group; Upper Cretaceous to Paleocene nonmarine molasse-type coarse-grained clastic rocks of the Sustut Group; Eocene felsic to mafic calcalkaline volcanic rocks of the Sloko Group; and Miocene to Recent (?) basalt flows (Figure 2-2). A diverse suite of granitic to ultramafic intrusive rocks ranges in age from Triassic to Eocene (Chapter 3).

PALEOZOIC STIKINE ASSEMBLAGE

Stikine assemblage rocks in the project area are Carboniferous and Permian in age. Devonian strata identified farther to the south (Logan and Drobe 1993a, b) were not recognized. The following descriptions of the assemblage are divided into age divisions — Upper Carboniferous, Upper Carboniferous to Lower Permian, and Lower to Upper Permian; and are further subdivided into six main geographical areas. These areas are: Scud River, north and south of Devils Elbow pluton, and in the Missusjay Creek, Chutine River, Barrington River and Little Tahltan Lake structural culminations (Figure 2-3; Brown *et al.*, 1992a). Descriptions of the two southernmost areas are based on detailed studies by M.H. Gunning (1993a).

A composite lithostratigraphic section comprises one formally named and four informally named divisions: the Butterfly and Devils Elbow units, and the Navo formation, Ambition Formation (Gunning *et al.*, 1994) and Scud Glacier formation (Figure 2-4; Table 2-1). Upper Carboniferous foliated sedimentary and volcanic facies are called the Devils Elbow and Butterfly units respectively. Near the Scud River, Upper Carboniferous to Lower Permian ash tuff conformably overlies the Butterfly unit and is named the Navo formation. A thick succession of well bedded, Lower to Upper Permian limestone conformably overlies the Navo for-

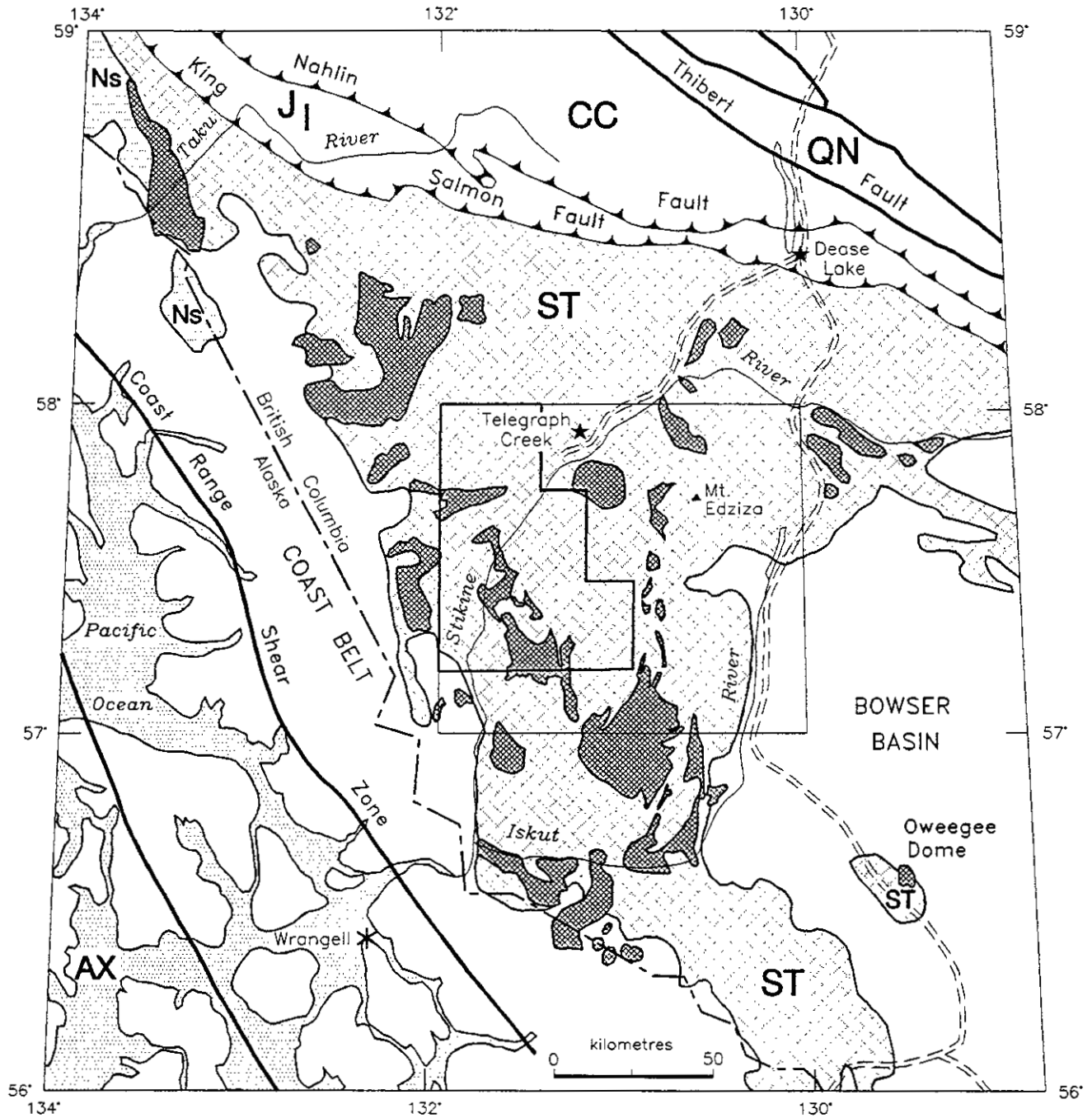


Figure 2-1. Location of project area on a simplified terrane map of northwestern British Columbia and its relationship to the regional distribution of the Stikine assemblage (modified from Wheeler and McFeely, 1991). Fine cross-hatched areas = Paleozoic strata correlated with Stikine assemblage, AX = Alexander Terrane, CC = Cache Creek Terrane, JI = Inklin assemblage (post-terrane accretion overlap assemblage), NS = Nisling terrane, ST = Stikinia (coarse cross-hatch), QN = Quesnellia. Outer box is the outline of the Telegraph Creek map area (104G), and the inner polygon represents the Stikine project area.

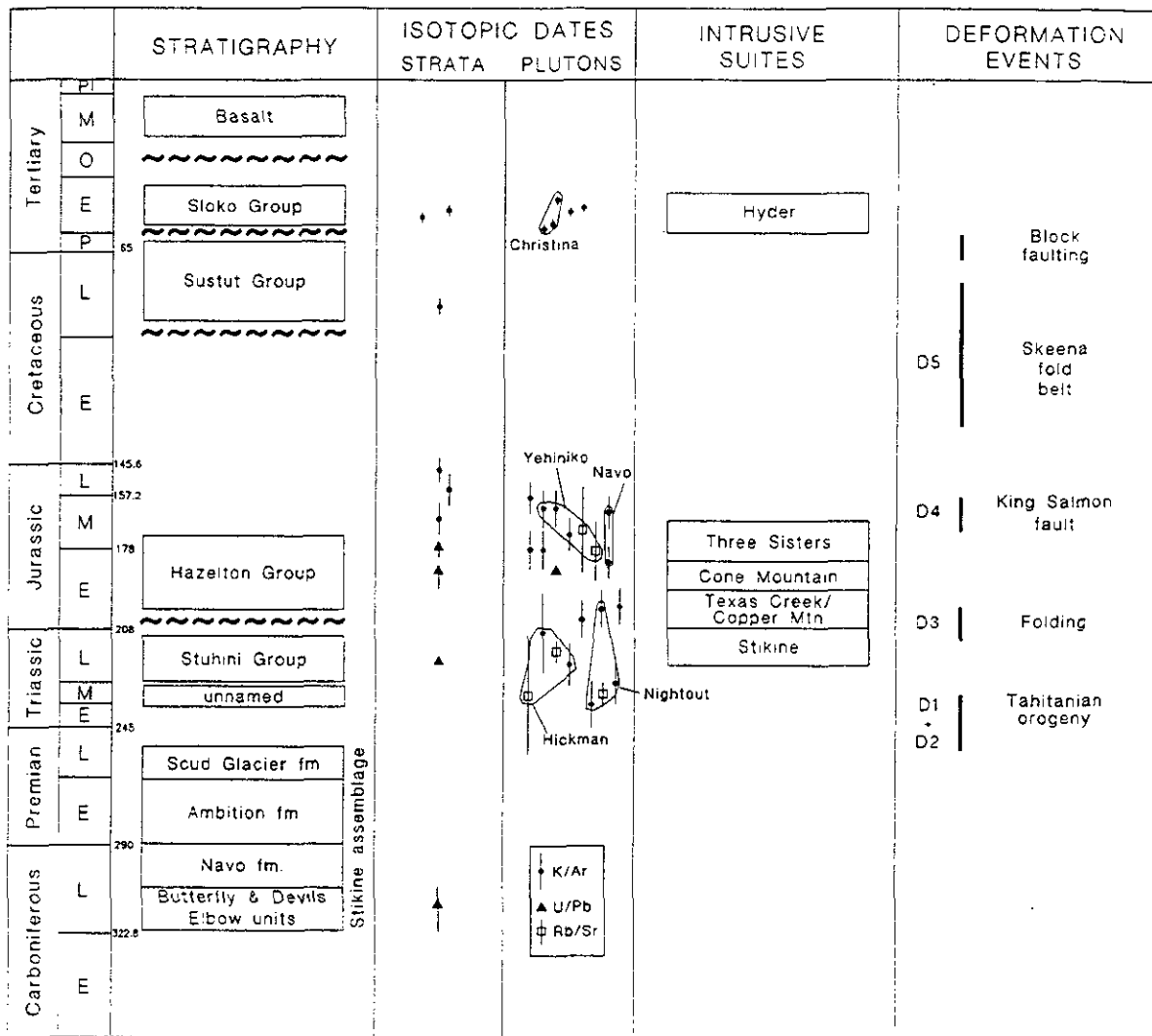


Figure 2-2. Schematic stratigraphic succession, showing intrusive events in the study area. Isotopic data from Holbek (1988), White *et al.* (1968) and M.H. Gunning (unpublished data, 1994) are included. Intrusive suites are discussed in Chapter 3. Regional deformational events shown in the last column are discussed in Chapter 4.

mation and is named the Ambition Formation. The Scud Glacier formation consists of Upper Permian tuff and chert which conformably overlie the limestone and includes the youngest strata in the assemblage.

UPPER CARBONIFEROUS STRATA (Unit uCS)

DEVILS ELBOW UNIT (Unit uCSs)

The Devils Elbow unit comprises mainly sedimentary rocks with minor intercalated volcanic rocks; it grades laterally to the south into the coeval volcanic-rich Butterfly unit. It is exposed north of Devils Elbow Mountain, from which its name was adopted, and also in the Missusjay Creek area. Correlative rocks also underlie the Chutine culmination. The total thickness of the unit is unknown because the base is not exposed and strata are folded and faulted.

The unit comprises variably foliated graphitic and siliceous argillite, graphitic phyllite and pale green ash tuff in thin laminated intervals. Recrystallized, coarse-grained,

sparry skeletal wackestone forms discontinuous intervals up to 30 metres thick. Silicified and folded colonial and solitary rugose corals (Appendix 1) occur in scattered, metre-thick concentrations. Fusulinids (Appendix 2) are rare. Echinoderm columnal fragments are evident in thin section but not in outcrop. The dark grey, massive to crudely layered limestone is recrystallized to sparry calcite and interbedded with rare, thin lenses of argillite. Volcanic components include pale green sericite schist, rare aphanitic basalt flows and chlorite schist.

The stratigraphic base of the Devils Elbow unit is not exposed. The upper contact of phyllitic rocks with massive Stuhini Group rocks, immediately east of the ridge north of Devils Elbow Mountain, is poorly exposed and interpreted to be paraconformable. An erosional contact crops out north of Missusjay Creek. Limited biostratigraphy precludes evaluating the degree of non-deposition or erosion represented by the contact (Gunning, 1993a).

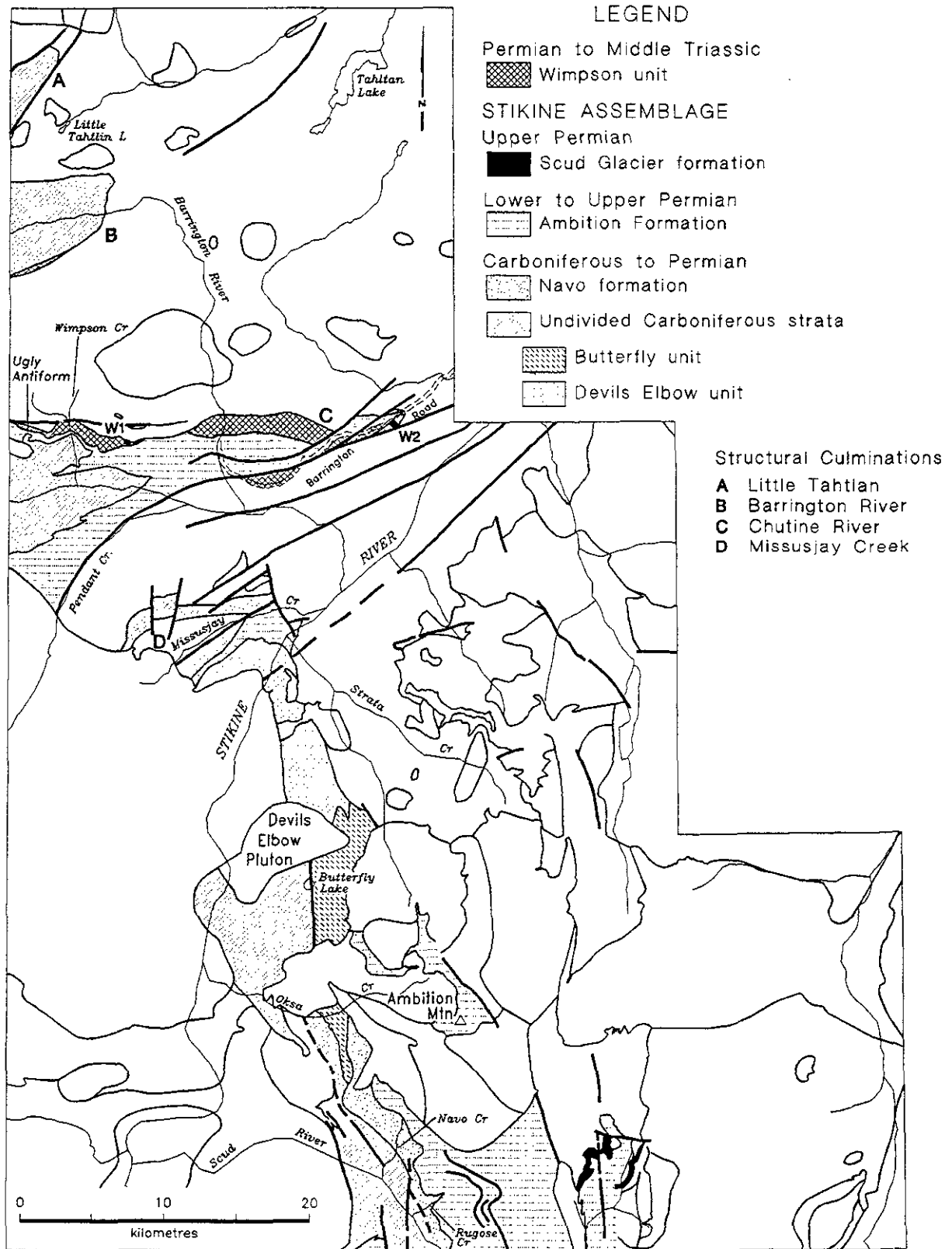


Figure 2-3. Distribution of Paleozoic Stikine assemblage in the project area, the six main areas are: (1) Scud River, (2) Devils Elbow, (3) Missussjay Creek, (4) Chutine River, (5) Barrington River and (6) northwest of Little Tahtlan Lake.

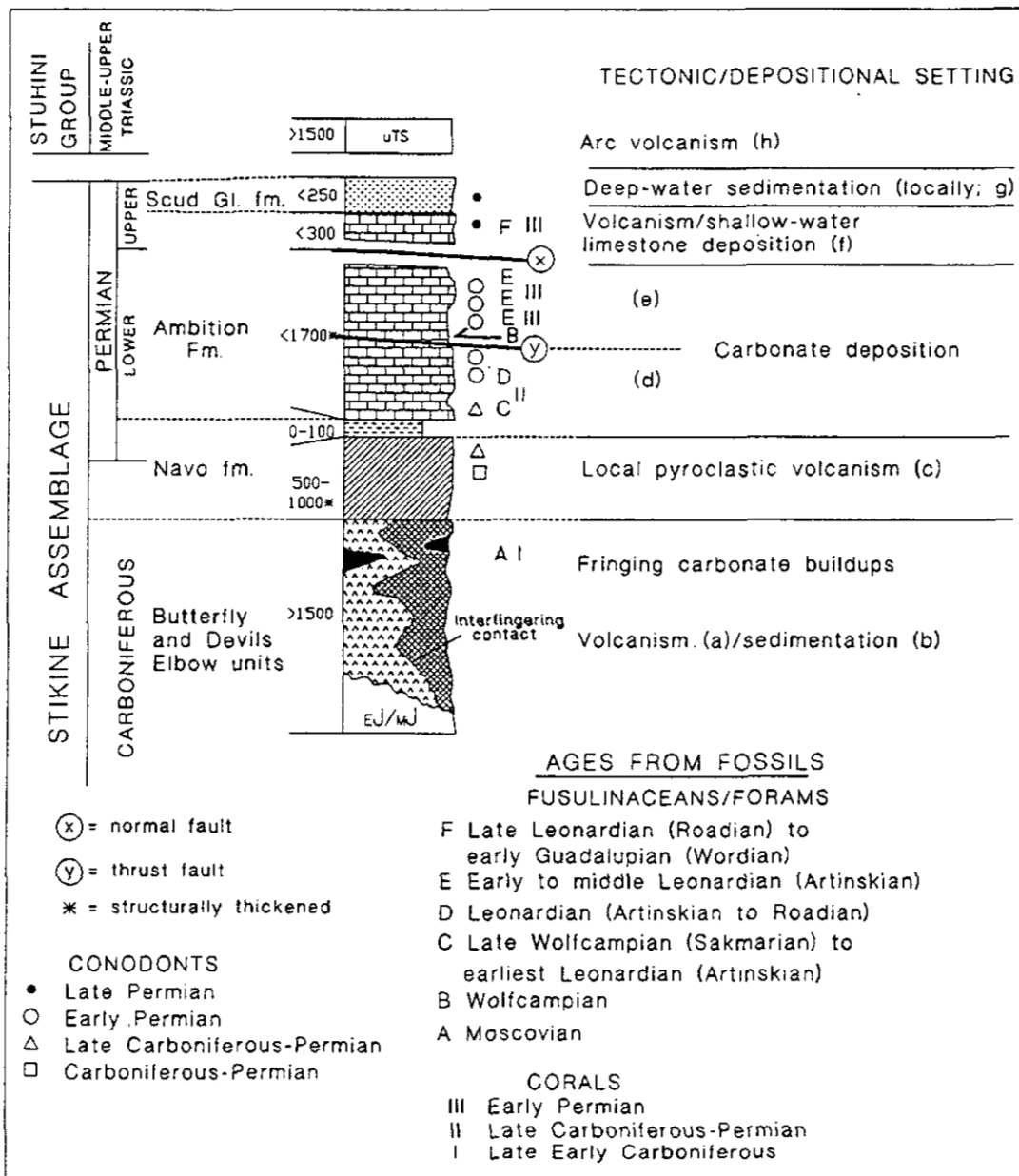


Figure 2-4. Generalized stratigraphic column and paleoenvironmental interpretations for the Stikine assemblage in the Scud River area. (a) aphanitic basalt flows and tuff; (b) graphitic argillite, phyllite, limestone; (c) felsic tuff, minor silty limestone; (d) fossiliferous limestone, minor argillite; (e) tightly folded limestone; (f) maroon fusulinid-rich limestone; (g) grey and maroon crystal-lithic tuff, radiolarian chert; (h) pyroxene crystal tuff and flows/sills.

The age of the Devils Elbow unit is poorly constrained as fossiliferous limestone is rare and fossils are deformed. The unit is assigned to the Upper Carboniferous because of the identification of poorly preserved nonfusulinid foraminifers of Moscovian or younger age (Mamet, 1991) and Late(?) Carboniferous conodonts (Appendix 3) collected north of Devils Elbow Mountain. The fossil ages overlap with a U-Pb date from the Butterfly volcanic unit (see below). A preliminary Mississippian age was reported by Kerr (1948a; F32) for a small collection of deformed corals.

BUTTERFLY UNIT (Unit uCSv)

The Butterfly unit, named for good exposures east of Butterfly Lake, extends south to the Navo Creek area (Figure 2-3). It is characterized by mafic metavolcanic rocks with subordinate interbedded sedimentary rocks. Total thickness of the unit is unknown because strata are folded and faulted, but may exceed 1000 metres.

The unit consists of faintly foliated aphanitic and rarely pyroxene-plagioclase-phyric basalt and hornblende-phyric diabase. Foliated basalt grades into thin chlorite schist zones. Foliated lapilli and block tuff contain elliptical basalt scoria and felsic volcanic fragments and are intercalated

TABLE 2.1
U-Pb AND K-Ar ISOTOPIC DATES FOR STRATIFIED ROCKS

FIELD NO.	MAP UNIT	ROCK TYPE	GROUP	DATING METHOD	MINERAL	AGE (Ma)
DBR89-471	TS	Andesite tuff	Sloko	K-Ar	Hb	48.8 ± 1.7
DBR89-376	KTS	Rhyolite tuff	Sustut	K-Ar	WR	51.6 ± 1.8
DBR89-25	KTS	Wacke	Sustut	K-Ar	Bi	85.6 ± 3.0
DBR90-162	ImJH	Andesite flow bx	Hazelton	U-Pb	Zr	185 + 7/- 1
DBR90-151	ImJH	Felsite	Hazleton	U-Pb	Zr	Indeterminate
DBR91-717	ImJH	Rhyolite	Hazelton	U-Pb	Zr	175 + 4/- 1
CGR89-217	ImJH	Andesite tuff	Hazelton	K-Ar	WR	148 ± 5
CGR89-439	ImJH	Andesite	Hazelton	K-Ar	WR	166 ± 6
MGU90-740*	uTSv	Pyroxene crystal tuff	Stuhini	U-Pb	Zr	227 ± 1
MGU90-750*	pPS	Meta.-crystal tuff	Stikine	U-Pb	Zr	311+6.2-10.4
MGU89-314	pPS	Hornblende schist	Stikine	K-Ar	Hb	155 ± 5

* = From Gunning (1993a), see Appendices 12 and 13 for analytical data and references.



Photo 2-1. Heterolithic andesitic volcanic breccia of the Stikine assemblage, Butterfly unit (uCSv) east of Butterfly Lake. Clasts include andesite, basalt and felsic tuff. The succession is dominated by massive basalt flows.

with foliated basalt flows. Thin intervals of light grey weathering-feldspar crystal rich breccia and block and lapilli tuff are distinct (Photo 2-1), though volumetrically minor. Metre-thick beds of pale green phyllite and sericitic ash tuff occur throughout the unit. The volcanic units are distinguished from lithologically similar rocks of the Stuhini Group by stratigraphic setting (*i.e.* position below Permian limestone where determinate), predominance of aphanitic flows, higher metamorphic grade and more intense deformation. Metamorphic grade and intensity of structural fabric are used as a guide to distinguish Paleozoic from Mesozoic strata, but cannot be applied exclusively because Upper Triassic strata are locally deformed and metamorphosed, as in the Scud River valley. In addition, pyroxenes tend to be unzoned, small, and less calcic compared to those in the pyroxene-rich rocks of the Stuhini Group (Gunning, 1993a).

The western, lower contact is not exposed because it is intruded by younger plutons. The eastern, upper contact is gradational with felsic tuff of the Navo formation near Navo Creek. To the north, a Mesozoic pluton intrudes the Butterfly unit, although the contact is locally faulted.

A Moscovian U-Pb date of $311.1 \pm 6.2 - 10.4$ Ma (J.K. Mortensen *in* Gunning, 1993a) obtained on zircon from a mafic crystal tuff constrains the age of these volcanic rocks to Late Carboniferous. A K-Ar date of 155 ± 5 Ma was obtained on hornblende from the same unit and is interpreted to be thermally reset. In the Navo Creek area, the unit is no younger than the Late Carboniferous to Early Permian Navo formation which overlies it.

Nine samples from the Butterfly unit and Chutine culmination were collected for geochemical analysis (Appendix 8). Only three samples were acceptable on the basis of screening criteria set out in Appendix 9. These samples exhibit too much scatter on most major and trace element diagrams to support any significant generalizations about Stikine assemblage chemistry. Some minor elements are less variable, but a detailed petrochemical characterization is not possible. Eleven mafic flows from the Butterfly Lake area are tholeiitic basalt based on the abundances of selected elements (Gunning, 1993a).

CHUTINE RIVER AREA

The core of the Chutine culmination (Figure 2-3) comprises siltstone, argillite, sericitic ash tuff, and green and maroon, phyllitic plagioclase-rich andesitic lapilli tuff, and a granitoid-bearing volcanic conglomerate. These units are correlative with the Upper Carboniferous Butterfly and Devils Elbow units to the south. Fabrics vary from schistose to unfoliated. The siltstone in the core of the Ugly antiform (Figure 2-3; along the northwestern edge of the culmination) resembles parts of the felsic tuff unit (Navo formation) that lies directly below Permian limestone in the Scud River area.

Brown-weathering pillow basalt, less than 50 metres thick, is intercalated with phyllitic sedimentary rocks and tuff near the Ugly antiform. Individual pillows are up to 2 metres long, with amygdaloidal cores, well preserved chilled margins and intrapillow micrite (Photo 2-2). Siltstone bedding is locally transposed adjacent to chlorite schist zones and discrete chlorite phyllite layers within ap-

parently undeformed siltstone illustrate the degree of inhomogeneous strain. Farther southeast, poorly sorted polymictic conglomerate contains cobble to pebble-sized clasts of limestone and siltstone, and is similar to a polymictic conglomerate east of Butterfly Lake (Figure 13 in Gunning, 1993a). The limestone clasts, up to 25 centimetres long, are unstrained. Foliated, recrystallized Permian limestone lies structurally below the conglomerate and dark grey siltstone.

The northern contact of the Barrington River culmination is inferred to be a steep, east-trending fault that places phyllite against volcanic rocks of the Stuhini Group. The southern contact with the Stuhini Group was not mapped. The eastern extent of these phyllitic rocks is poorly known.

BARRINGTON RIVER AND LITTLE TAHLTAN LAKE AREAS (Unit uCS)

Phyllitic tuff, siltstone, andesite and limestone exposed in the Barrington River valley and northwest of Little Tahltan Lake (Little Tahltan Lake culmination; Figure 2-3) are similar to rocks in the core of the Chutine culmination and in the Butterfly Lake and Devils Elbow area, based on lithology and to a lesser extent the fabric. The strata here are more phyllitic and more complexly folded than in most other areas. Their characteristic pale green, grey and maroon weathering surfaces and homogeneous, rounded outcrops contrast with the more irregular, blocky Stuhini Group exposures.

Alternating centimetre to millimetre-scale layers of green, dark grey, white and maroon rocks grade from chlorite schist to unfoliated ash and lapilli tuff, siltstone and argillite. Concordant and discordant white quartz veins and pods are restricted to rocks of the Barrington unit. A foliated, thinly layered, recrystallized grey to tan limestone, 25 metres thick, is complexly infolded with limy tuff and chlorite phyllite in the Little Tahltan Lake culmination. Farther north, a weakly foliated, dark green hornblende-plagioclase-phyric meta-andesite sill or flow occurs within the phyllitic tuff succession. In the same area, faintly foliated granodiorite dikes intrude the sequence. A foliated, recrystallized limestone layer, at least 75 metres thick, crops out in the culmination. Green and maroon chlorite phyllite, ash tuffs and silicic layers occur within and below the limestone. The pale green, grey and cream-coloured ash tuffs are thin bedded to laminated. Grey phyllitic siltstone and shaly siltstone are also common. Massive, coarse-grained pyroxene-phyric basalt dikes, interpreted to be Stuhini Group feeders, intrude the section. Similar dikes, also interpreted to be Late Triassic based on petrographic character and chemical composition, intrude correlative strata of the Devils Elbow unit in the Missusjay Mountain and Devils Elbow Mountain areas.

The southeastern contact of the Little Tahltan Lake culmination is inferred to be a steep, northeast-trending fault that places greenschist-grade, polydeformed phyllite against lower grade, less deformed, steeply dipping siltstone and volcanic rocks of the Stuhini Group. The northern contact with the Stuhini Group was not mapped. The northeastern extent of these phyllitic rocks is poorly known because of lack of outcrop.

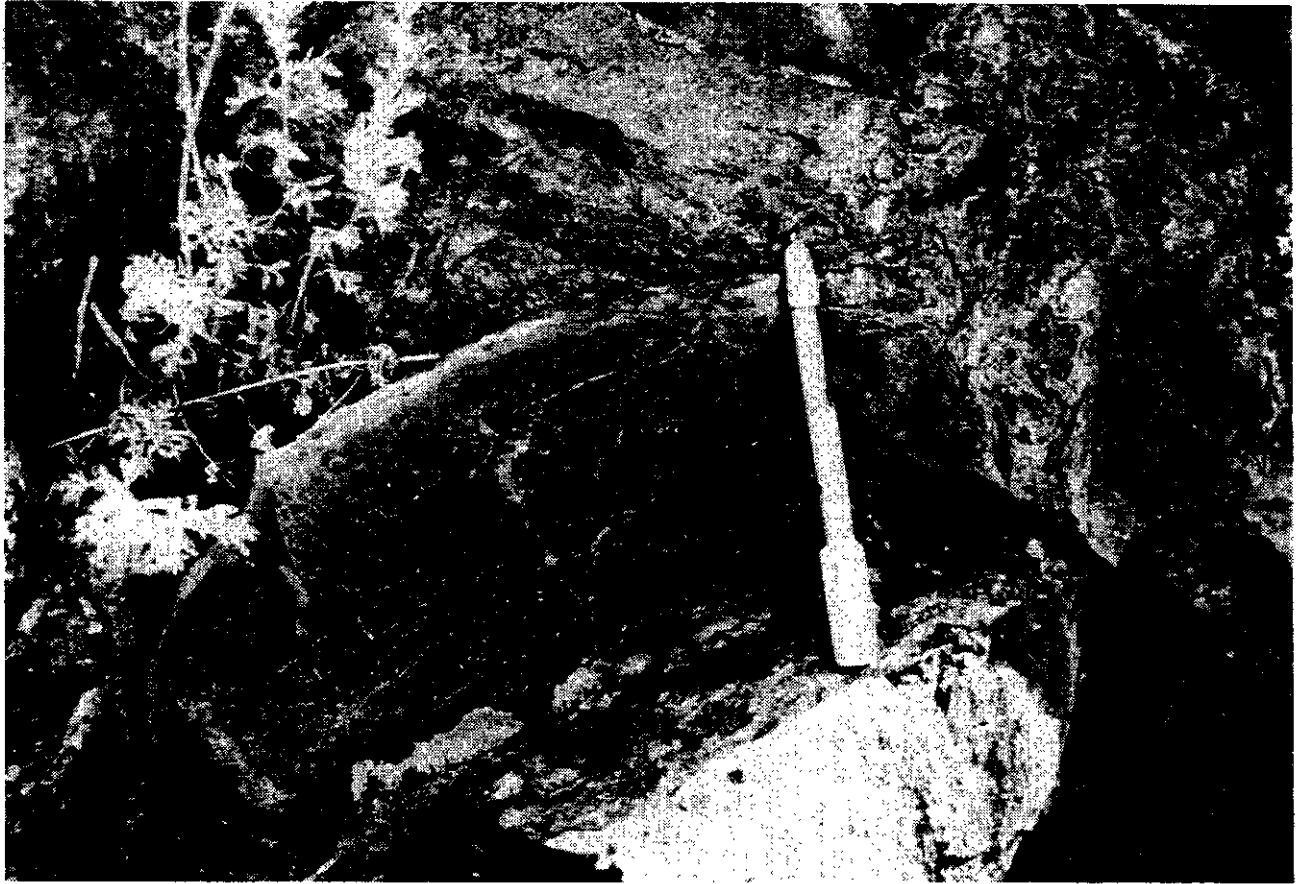


Photo 2-2. Pillow with intrapillow micrite, a rare example of pillow basalt within the Stikine assemblage in the study area, southeast of the Ugly anticline.

The age of unit uCS in the Barrington River area is uncertain. An infolded limestone in the Barrington culmination yielded a poor collection of probable Permian conodonts (Appendix 1). However, the similarity in lithologies and structural style between the Barrington area and Devils Elbow and Butterfly units is the basis for inclusion in the Carboniferous. Similar strata with similar structural style are well exposed to the northwest in the Tulsequah map area (Bradford and Brown, 1993a, b) where Carboniferous U-Pb dates have been obtained (Oliver and Gabites, 1993). Lithologically similar but undated sequences are exposed to the southwest near Triumph Creek in the Chutine map area (104F; Westcott, 1989a).

UPPER CARBONIFEROUS TO LOWER PERMIAN STRATA

NAVO FORMATION (Unit uCSf)

Felsic volcanic rocks of the Navo formation gradationally overlie volcanic rocks of the Butterfly unit between "Rugose" and Oksa creeks. The formation is tightly folded, but its estimated stratigraphic thickness is less than 500 metres (Figure 2-4).

The Navo formation is a sequence of weakly foliated to massive, light grey to pale green, fine-grained to aphanitic felsic ash tuff, lapilli tuff and tuffaceous siltstone. Lenses and layers of more recessive, dull brown weathering, silty

limestone are common. Pyrite euhedra, up to 1 centimetre across, form conspicuous rusty weathering spots in some exposures. Intercalated thin, grey to brown dolomitic limestone and argillite beds and lenses predominate toward the top of the succession. Muscovite, and lesser biotite, magnesium chlorite and calcite form a pervasive microscopic foliation. Plagioclase crystals are rare within lithic tuff. Decimetre to centimetre-scale, planar to curvilinear bedding is characteristic (Photo 2-3). Local load casts, flame structures, fining-upward sequences, crossbeds and small-scale growth faults in tuffaceous siltstone consistently indicate a right-way-up stratigraphic succession.

The basal contact is gradational with the underlying Butterfly unit, northwest of Navo Creek. The upper contact of the Navo formation is a sharp, wavy, conformable contact with argillite of the Ambition Formation, near the toe of "Rugose" glacier. However, south of the glacier and in Navo Creek, the contact is interpreted to be a fault, because steeply dipping, chevron-folded felsic tuff beds are overlain by gently dipping argillite and limestone. North of Navo Glacier, ash tuff of the Navo formation is infolded with recrystallized limestone of the Permian Ambition Formation. East of Misusjay Mountain and north of the Chutine River in the Ugly antiform, folded siltstone directly below Permian limestone resembles felsic tuff of the Navo formation. Discontinuity of the formation between Navo Creek and Devils Elbow Mountain may be related to non-deposition, post-Permian erosion or a combination of both.

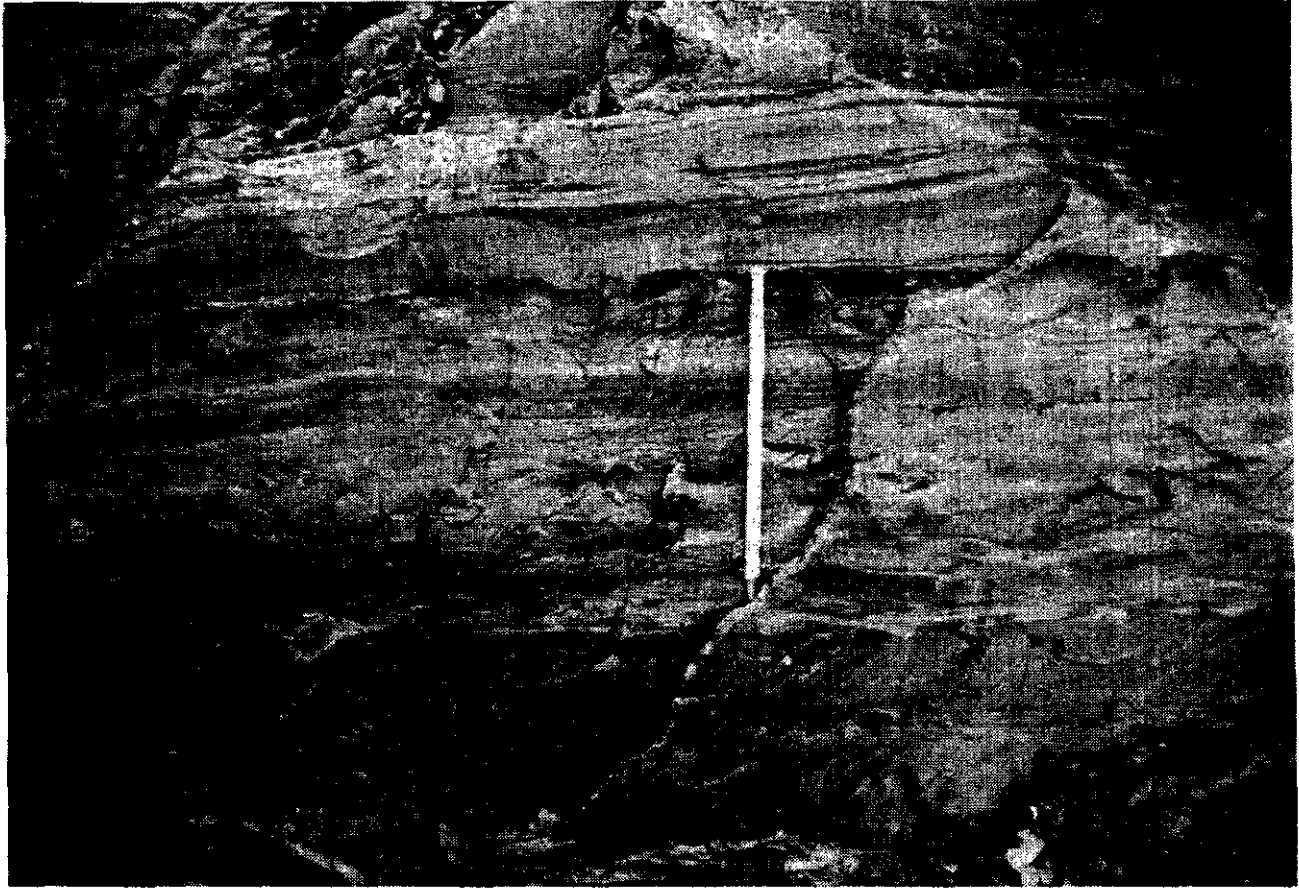


Photo 2-3. Fine-grained reworked felsic tuff (Navo formation; unit uCSf) with atypical, well preserved crossbeds. These deposits are interpreted to be turbidites. Most beds in the formation, however, are internally massive and resemble grain flows.

The age of the Navo formation is bracketed by the underlying Upper Carboniferous Butterfly Lake unit and the overlying Lower Permian limestone unit. A few poorly preserved conodonts from two thin limestone beds near the top of the succession are assigned a Late Carboniferous to Early Permian age (Appendix 3).

LOWER TO UPPER PERMIAN STRATA

AMBITION FORMATION (Unit IPS)

Extensive exposures of thick, deformed Permian limestone are the most distinctive feature of the Stikine assemblage (Monger, 1977a), especially in the project area. The Ambition Formation, named after the highest mountain in the study area, is formally defined and described in detail in Gunning *et al.* (1994). It comprises locally thick but laterally discontinuous succession of limestone (Figure 2-3). Correlation of the less extensive and commonly fault-bounded successions of limestone in the Missusjay Creek and Chutine River areas (Figure 2-3) is based on rock types, bedforms and Permian ages. The limestone is a minimum of 500 metres thick and is structurally thickened by folding and reverse faults in most areas. The type section described south of Rugose Creek is 1074 metres thick (Gunning *et al.* 1994).

Argillite Unit (Unit IPSa)

A basal argillite unit, well exposed between the Scud River and Navo Creek, forms a distinctive rusty brown weathering sequence that overlies the Navo formation and grades upward into the limestone unit. It is about 50 metres thick at the toe of Rugose Glacier, at the base of the type section for the Ambition Formation. It is dominated by massive, black to dark grey argillite with lesser thinly bedded siltstone. Bedding-parallel bands of pyrite and/or pyrrhotite are ubiquitous and comprise up to 5% of the rock. The upper contact of this unit is a 30-metre gradation into overlying dark grey micritic limestone.

Limestone Unit (Unit IPSc)

North of the Scud River, in the Rugose Glacier area (Figure 2-3), there is a homoclinal panel of Lower to Upper Permian limestone which comprises two shallowing-upward successions. Dark grey, fine to medium-grained skeletal lime mudstone and minor black argillite form the lower part of both successions (Photo 2-4). The upper succession consists of more than 300 metres of centimetre to decimetre-thick beds of well bedded grey echinoderm skeletal wackestone and brown whole-fossil rudstone which grades upward into light grey wackestone and tan, nodular and bedded chert (Photo 2-5). The chert is interpreted to have formed during limestone diagenesis.



Photo 2-4. Planar, thin to medium-bedded argillaceous limestone and limestone (unit IPSc).

The limestone is particularly fossiliferous in the type section area, near Rugose Glacier. Rugose corals up to 30 centimetres long, fusulinids, fenestrate and ramose bryozoa, tabulate corals (*syringopora* ?), brachiopods, echinoderm stem fragments, rare sponge spicules and rare gastropods constitute a locally abundant, but low diversity fossil assemblage. Intact corals throughout the lower part of the succession indicate limited transport. Many fossils are in tabular, bedding-parallel concentrations interpreted to be storm deposits.

The upper part of the formation is massive to thick-bedded, white to buff, sparry limestone that forms the top of the Permian limestone succession throughout the region. The base is locally a southwest-directed reverse fault; elsewhere the contact is poorly defined due to rugged topography and ice cover. Subordinate argillite and maroon and green andesitic tuff are characteristic of the top part of the limestone unit. The tuff forms concordant lenses and structurally disrupted discordant bodies up to 50 metres thick. Rare solitary corals and gastropods occur in metre-thick beds of buff and white sparry limestone and echinoderm-skeletal packstone in the Scud Glacier outwash valley. The highest stratigraphic unit is a mauve to maroon, tuffaceous fusulinid floatstone, exposed east of the toe of the Scud Glacier (unit uPSI).

In the Chutine culmination (Figure 2-3), the Ambition Formation comprises northeast to east-trending, complexly folded, well bedded to massive, light and dark grey, recrystallized limestone that forms conspicuous white cliffs north and south of the Chutine River. The simplified map pattern resembles an east-striking anticline. In fact, lithologic units

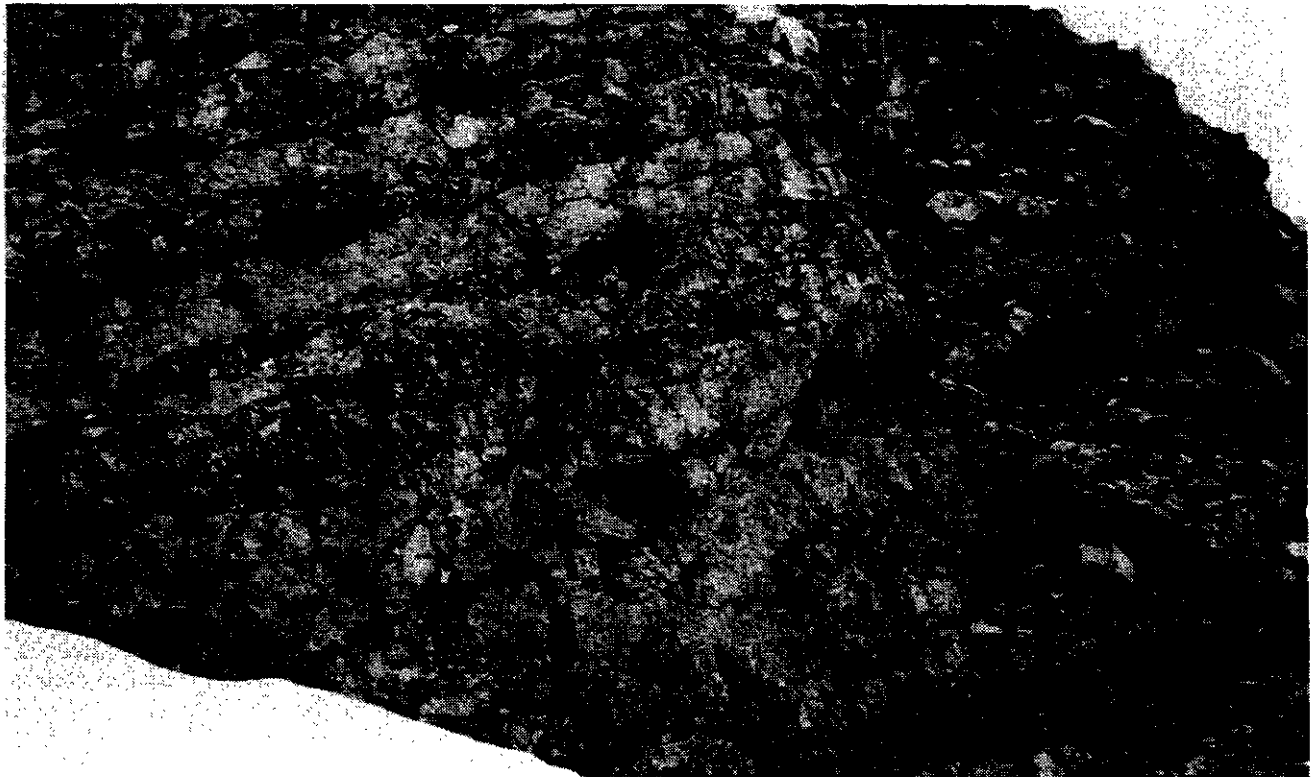


Photo 2-5. Medium-bedded limestone with chert layers and lenses (unit IPSc).

structurally above and below the limestone vary along strike, as does the thickness of the limestone itself, indicating structural and/or facies complications that were not resolved in this study. Macrofossils are much less common than in the Scud River area, but locally the limestone contains rugose corals, brachiopods, bryozoans, and echinoderm columnals (Appendices 1 and 2). Perhaps the limestone facies here was deposited in slightly deeper water and hence is less fossiliferous than in the Scud River area.

The age of the Ambition Formation is well constrained by an abundant assemblage of Permian conodonts, fusulinids and macrofossils (Appendices 1, 2, 3). The section examined south of Rugose Glacier provides the most comprehensive database for Permian limestone of the Stikine assemblage (Gunning *et al.*, 1994). Upper Wolfcampian to lowest Leonardian (Sakmarian to Artinskian) fusulinids occur in argillaceous wackestone at the base of the Ambition Formation and early Guadalupian (Wordian) fusulinids in the upper part (Appendix 2). The maroon tuffaceous limestone at the top of the succession contains uppermost Lower Permian to lowermost Upper Permian (late Leonardian to early Guadalupian) fusulinaceans (Appendix 2) and lower Upper Permian, Guadalupian conodonts (*Neogondolella cf. phosphoriensis* (Youngquist, Hawley and Miller; Appendix 3). These are the youngest age determinations for the Stikine assemblage in the study area.

The Early Permian age of the limestone delineating the Chutine culmination is based on Asselian, Sakmarian and Artinskian fusulinids (Appendix 2) and Artinskian conodonts (Appendix 3). The Permian age of the Missusjaj Mountain limestone is taken from Kerr (1948a; F30 and F31).

SCUD GLACIER FORMATION (Unit uPS)

A section of interbedded tuff, chert and argillite rest, apparently conformably (the contact is not well exposed), on maroon tuffaceous limestone at the top of the Ambition Formation, near the toe of the Scud Glacier (Figures 2-3, 2-5). The section is over 250 metres thick and is exposed only in this area. Grey, green and maroon crystal lithic tuffs, and tuffaceous mudstones are massive to flaggy. Pale grey, felsic lithic fragments predominate over mafic fragments. Local chloritic wisps may be relict fiammé. Crystal fragments include plagioclase and pyroxene. The tuffs are gradationally overlain by thin-bedded green siliceous mudstone, green radiolarian chert, thin-bedded to laminated brick-red chert and distinctive grey and green ribbon chert. The chert is overlain by strongly contorted and disharmonically folded black chert and graphitic argillite (Photo 2-6).

The age of the Scud Glacier formation is assumed to be early Late Permian, based on its stratigraphic position. The lower age bracket is the underlying Late Permian limestone at the top of the Ambition Formation. Within the formation, poorly preserved conodonts from chert yield possible Permian ages (Appendix 3). The exact position of the upper contact of the formation, the top of the Stikine assemblage, is equivocal (*i.e.* somewhere within pelagic strata; Figure 27 in Gunning, 1993a), but is assumed to be between the unit of black ribbon chert and overlying unit of green, siliceous, radiolaria-bearing mudstone that yielded Triassic

conodonts (Appendix 3). The upper age limit, Late or Middle Triassic is provided by rocks above these strata that are correlated lithologically with the "Tsaybahe Group" of Read (1984) or lowermost Stuhini Group.

REGIONAL CORRELATIONS

Early Carboniferous volcanic successions as exposed in the Tulsequah Chief (Sherlock *et al.*, 1994), Golden Bear (Bradford and Brown, 1993a) and Oweege dome areas (Greig and Gehrels, 1992) and Early Carboniferous limestone in the Iskut River region (Logan, Drobe and McClelland, in preparation; Gunning, 1993b), are apparently not present in the project area. The Butterfly Lake part of the Stikine assemblage succession is lithologically and age-equivalent to a meta-volcanic succession with discontinuous, fusulinid-bearing Moscovian limestone and other sedimentary rocks, stratigraphically above the Tulsequah Chief volcanogenic massive sulphide deposit (Nelson and Payne, 1984). Coeval rocks in the Golden Bear area include felsic phyllite that yielded U-Pb dates between 300 and 320 Ma (Oliver and Gabites, 1993). The most extensive unit is the Permian Ambition Formation limestone, extending discontinuously from the Tulsequah River area south to Terrace. The overlying chert succession may correlate with the Tsaybahe Group as mapped by Read (1984) in the Grand Canyon of the Stikine River.

PALEOENVIRONMENTAL INTERPRETATION

The pre-Permian sedimentary strata of the Stikine assemblage in the project area record pelagic sedimentation in an open-marine setting, locally in warm, shallow water within the euphotic zone. Contemporaneous, oceanic volcanism was dominated by subaqueous aphanitic basalt flows during the Late Carboniferous, accompanied by discontinuous limestone accumulation. Facies relationships indicate a subdued paleotopography, perhaps there were numerous fissure eruptions in an extensional setting (Gunning, 1993a). Proximal volcanic facies related to edifice construction have not been recognized. The Navo formation represents limited felsic volcanism and submarine turbidite deposition at the end of the Carboniferous volcanic cycle. Local emergent facies are noted to the south in the Forrest Kerr Creek area (Logan *et al.*, 1990a).

The Lower Permian in this region is represented by thick limestone deposition and a long hiatus in volcanism. The Ambition Formation records neritic carbonate sedimentation in a subtropical, open-marine setting, probably on a ramp, throughout most of the Permian (Gunning, 1993a; Gunning *et al.*, 1994). Argillite and dark grey micrite at the base of the shallowing-upward successions indicate high preservation rates of organic matter, perhaps due to high surface production and low-energy environments of deposition. Sparry, clean-washed, fusulinid rudstone in the upper part of the formation accumulated in a high-energy environment, possibly within the active wave-base. The maroon and green tuffs, sporadically deposited in the Permian, represent isolated, episodic, pyroclastic volcanism contemporaneous with limestone deposition. The maroon and green colour suggests fluctuating oxidizing and reducing conditions, either during tuff deposition in a shallow-marine to

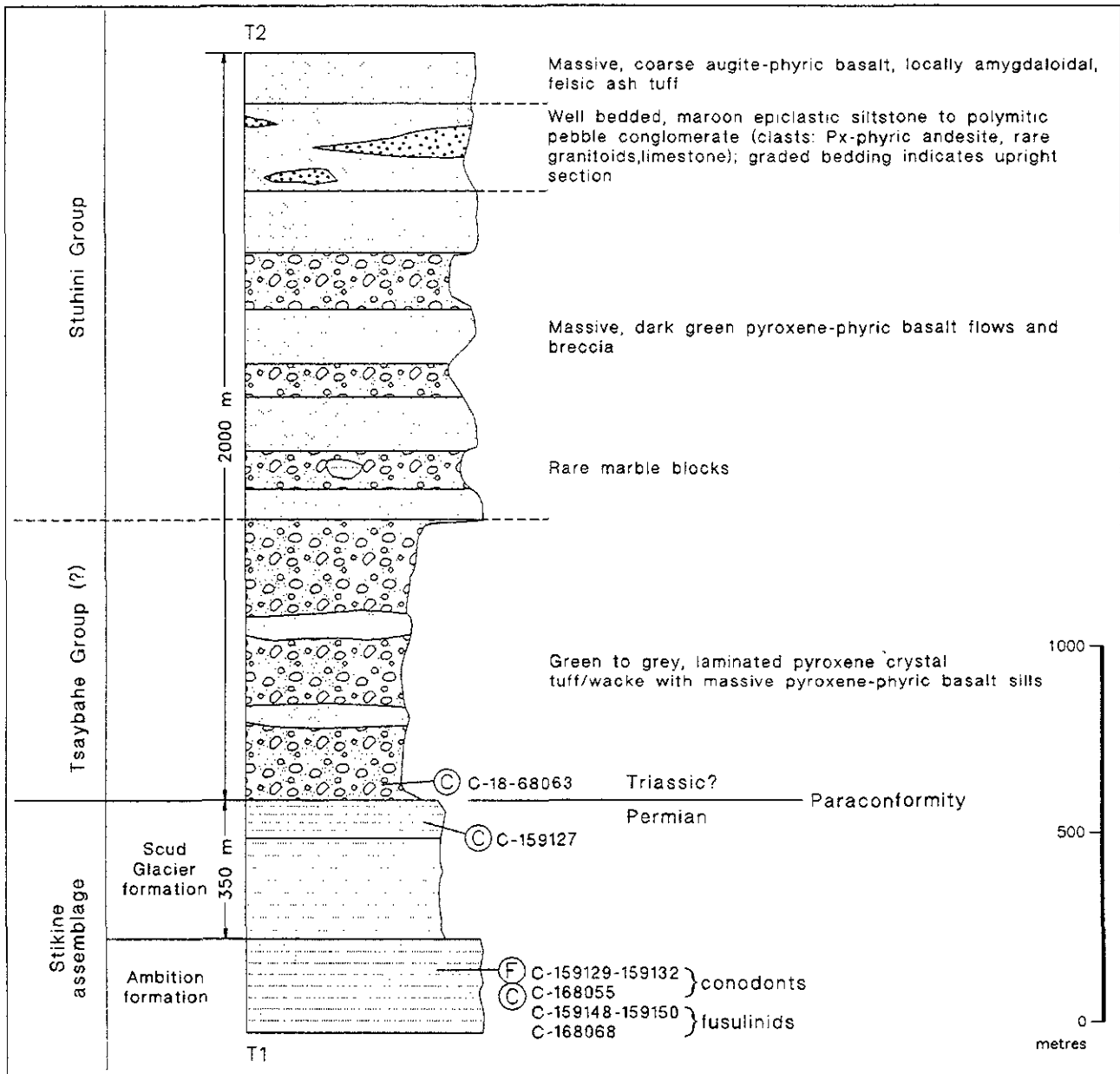


Figure 2-5. Schematic stratigraphic column near the toe of the Scud Glacier.

subaerial environment or by later diagenetic processes. The extent of the volcanism and how it relates to a larger oceanic arc is unknown. The change from maroon tuff to radiolaria-bearing siliceous mudstone and chert marks a change to open-marine, pelagic sedimentation in the Late Permian, which may have persisted until the onset of Late Triassic volcanism.

EARLY PERMIAN TO MIDDLE TRIASSIC WIMPSON UNIT (Unit mTc)

The Wimpson unit comprises buff, light to dark grey weathering chert, siliceous siltstone and green and maroon siliceous ash tuff and radiolarian chert. It crops out in four areas: near Wimpson Creek, east of Barrington River, along the Barrington road, and possibly on the southern limb of the Barrington River culmination (Figure 2-3). A maximum

structural thickness of approximately 1000 metres is exposed east of Wimpson Creek. Here the section is well bedded, with parallel, centimetre-scale beds of chert separated by thin layers of chlorite and sericite phyllite. Along the Barrington road the exposures comprise bright green and red, laminated to bedded siliceous ash tuff and chert lying structurally below white Permian limestone, perhaps due to reverse faulting. Kerr (1948a) states that the Permian limestone becomes interbedded with, and grades upward into varicoloured "quartzite" (Unit mTc), although this relationship was not observed. This relationship is similar to that near the toe of the Scud Glacier where Permian limestone grades up into crystal tuff and ash tuff (Scud Glacier formation). The more extensive Wimpson unit maybe correlative with the Scud Glacier formation, however, they differentiated here because of the apparent younger age of the former.



Photo 2-6. Ribbon chert, alternating black to grey chert and thinner argillite interbeds (unit uPS) from disharmonically folded section above less deformed tuffs and varicoloured cherts.

Some of these cherty rocks are interpreted as siliceous oozes which accumulated as pelagic sediments in an open-marine setting, below the carbonate compensation depth. Scattered sponge spicules occur in some beds near the Ugly anticline.

The Wimpson unit yielded Middle Triassic and Early Permian microfossil ages from separate areas (localities W1 and W2 on Figure 2-3). Middle Triassic (Ladinian) radiolaria and conodont species were obtained from buff chert and grey limestone respectively, east of Wimpson Creek (locality W1; Appendices 3 and 5) where they are surrounded by Upper Triassic tuffaceous wacke. Farther east along the Barrington road (locality W2), green and maroon tuffaceous chert lies structurally below Permian limestone (Ambition Formation). The chert yielded Artinskian to Kungurian radiolaria, and Permian, probably Artinskian, conodonts (Appendix 5). Both microfossil localities are included in the Wimpson unit because green and maroon siliceous tuff occur in both areas. Alternatively, they may represent distinct stratigraphic units above and within the Permian limestone (*i.e.* not structurally interleaved as currently interpreted).

An isolated, dark grey limestone pod contains Early Triassic, Smithian conodonts (Appendix 3), but is surrounded by Upper Triassic Stuhini Group tuffaceous wacke (unit uTSs1). Similar isolated limestone pods containing Early Triassic conodonts are present in the Tatsamenie Lake

area. These pods are either structural slivers or olistoliths. Early Triassic conodont ages are extremely rare in the Cordillera (M.J. Orchard, personal communication, 1993).

Contact relationships of the Wimpson unit with underlying Lower Permian limestone north of Chutine River are important, though equivocal, because they may indicate a Permo-Triassic unconformity. In addition, the nature of the upper contact of the Middle Triassic chert with the Stuhini Group in this area is complicated by structural interleaving of the units in the Kitchener fault zone. The Wimpson unit that contains the Ladinian conodonts appears to grade abruptly upward into tuffaceous wacke of the Stuhini Group. A similar relationship is present at the toe of the Scud Glacier.

PERMO-TRIASSIC CONTACT RELATIONSHIPS

Permo-Triassic unconformities are documented along the length of the Cordillera in Stikinia and Quesnellia (Read and Okulitch, 1977; Read *et al.*, 1983). In many areas there is a significant break in deposition, marked locally by angular unconformities. In places there is a contrast from foliated deformed rocks to less deformed material which implies a tectonic event at this time (*cf.* Chapter 4, Tahltanian orogeny).

Permo-Triassic contacts are poorly exposed in the map area; Permian limestone commonly is faulted against, or

overlain unconformably by, the Upper Triassic Stuhini Group. However, a few Permo-Triassic contacts have been documented; northeast of Devils Elbow Mountain, at the toe of the Scud Glacier, north of the Chutine River, and along the northern part of the Little Tahltan Lake culmination. The underlying Paleozoic and overlying Mesozoic units vary in age and character in these areas, but in general there appears to be a younging of the Triassic cover from north to southeast. This suggests a period of erosion, diachronous pelagic sedimentation and pyroclastic volcanism after Early Permian limestone accumulation and prior to the onset of Late Triassic volcanism.

Permian limestone is gradationally overlain by Upper Permian tuffaceous limestone, tuff and pelagic sedimentary rocks at the toe of the Scud Glacier (Scud Glacier formation). Perhaps correlative strata of the Wimpson unit (north of the Chutine culmination) also mark the transition from Permian limestone deposition to tuff and chert accumulation prior to the main Upper Triassic volcanic event. Collectively, strata in these two areas indicate a transition from carbonate ramp deposition to local and minor calcalkaline volcanism and pelagic chert deposition. More work is required to determine if these changes were gradational and time-transgressive or distinct events.

NORTHEAST OF DEVILS ELBOW MOUNTAIN

About 6 kilometres north of Devils Elbow Mountain variably foliated rocks of the Devils Elbow unit are unconformably overlain by massive augite-phyric Stuhini Group basalt. Lower Permian limestone exposed to the north at Missusjay Mountain and to the south at Scud River is missing, implying either an unconformity or non-deposition, or both. If there is an unconformable relationship, over 1000 metres of limestone representing most of the Permian (about 80 Ma) was removed, yet the immediately overlying Upper Triassic strata lack Permian limestone clasts or a prominent basal conglomerate.

TOE OF SCUD GLACIER

Near the toe of the Scud Glacier, fusulinid floatstone and rudstone at the top of the Ambition Formation grades up into maroon tuff assigned to the Scud Glacier formation. Late Permian limestone, maroon tuff and chert grade up into, and are broadly folded together with, tuffaceous wacke and tuff correlated with either the "Tsaybahe" or Stuhini groups. Thinly bedded Permian ribbon chert and argillite are locally disharmonically folded, unlike thicker bedded Triassic tuffaceous wacke, presumably due to competency contrast.

SOUTH OF SCUD GLACIER

South of the Scud River, Lower Permian limestone is paraconformably overlain by either *Daonella*-bearing Middle Triassic siliceous shale or by interbedded siltstone and argillite of the Stuhini Group containing Upper Triassic, Carnian conodonts (Souther, 1972; Logan and Koyanagi, 1989, 1994).

NORTH OF THE CHUTINE CULMINATION

North of the Chutine River the contact between Lower Permian limestone and Middle Triassic chert or Upper Tri-

assic tuffaceous sedimentary rocks is disrupted by the Kitchener fault zone. The contact between Lower Permian limestone and Upper Triassic volcanic rocks along the southern limb of the Chutine culmination was not observed, but is interpreted as a reverse fault.

UPPER TRIASSIC OR OLDER MAFIC METAVOLCANIC ROCKS (Unit uTSmv)

Variably metamorphosed and locally hornfelsed and altered mafic rocks, mapped as amphibolite and amphibolite gneiss by Souther (1972; his unit B), underlie areas near Endeavour Mountain, east of Middle Scud Creek, east of the Scud Glacier, and north of the Hickman Ultramafic Complex (Figure 2-6). The rocks near Endeavour Mountain are referred to here as the Endeavour complex; they were not examined in detail because they underlie a rugged, ice-covered area. Lithologies vary from biotite schist to massive or brecciated pyroxenites and metavolcanic rocks. Local layering, interpreted to be relict bedding, suggests that at least part of the unit is mafic metavolcanic material. Pyroxene-phyric basalt flows or sills are recognized in some localities.

The north-trending Endeavour complex, 12 kilometres long, is enigmatic, displaying attributes of both ultramafic bodies and metavolcanic rocks. According to Souther (1972, p. 20) euhedral leucite phenocrysts provide evidence for a volcanic protolith. Epidote-altered clinopyroxene basalt breccia from this body resembles Stuhini Group lithologies. Souther's work identified a fault contact with Permian limestone in the southwestern corner of the complex. However, an apparent intrusive contact between olivine clinopyroxene basalt and Permian limestone was observed at one locality on the flank of Ambition Mountain. The Middle Jurassic Strata Glacier and Dokdaon plutons intrude the complex on the east and west (Figure 2-6).

All observed contacts of the complex are intrusive or faults. The unit has compositional similarities with the mafic part of the Stuhini Group to which it is tentatively correlated, but it is barren of fossils (Appendix 4). A minimum age is provided by the Late Triassic and Middle Jurassic plutons which intrude it.

UPPER TRIASSIC STUHINI GROUP (Unit uTS)

The Stuhini Group was originally defined by Kerr (1948b) for rocks in the Taku River valley of Tulsequah map area. Souther (1971) included all Upper Triassic volcanic and sedimentary rocks that lie above a Middle Triassic unconformity and below the Upper Triassic (Norian) Sinwa limestone in the Stuhini Group. Correlative strata are known as the western Takla Group on the eastern side of Stikinia (Monger, 1977c) and the Lewes River Group in the Whitehorse Trough (Wheeler, 1961). In practical terms, the group is defined in the Telegraph Creek area as volcanic-dominated strata (predominantly Upper Triassic, but may include Middle Triassic rocks) that overlie Paleozoic or rare Lower and Middle Triassic strata and occur below Lower to Middle Jurassic Hazelton volcanic rocks.

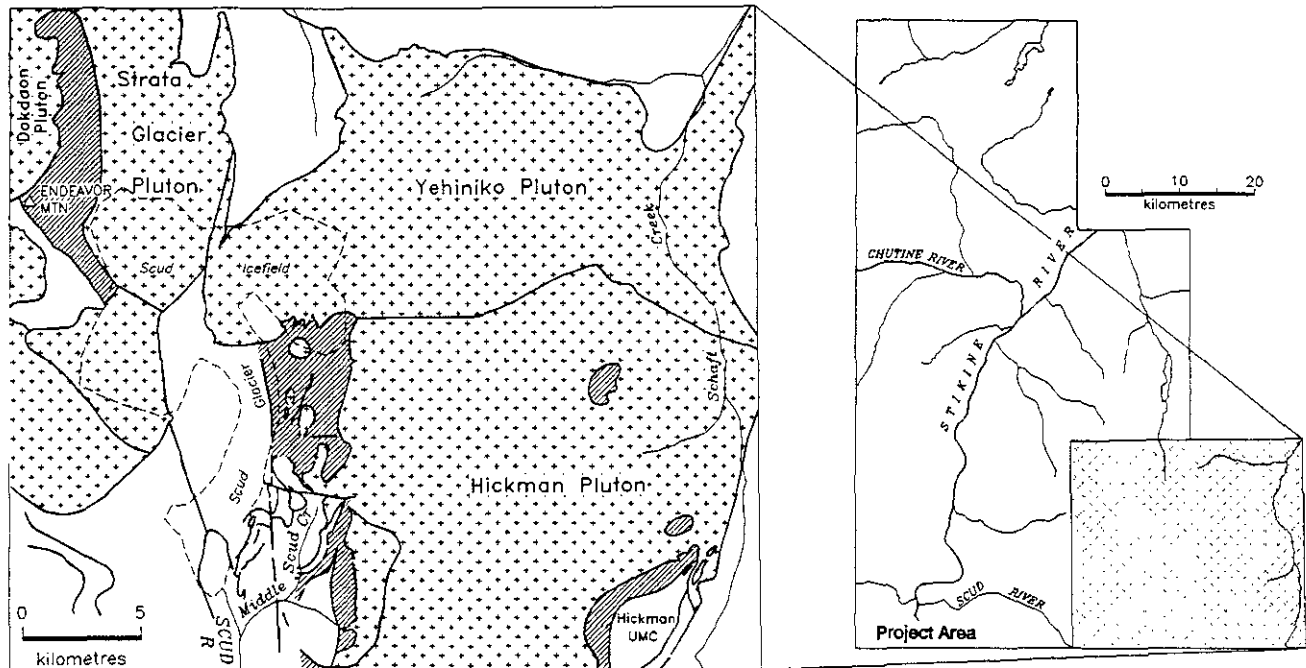


Figure 2-6. Distribution of enigmatic mafic metavolcanic rocks shown in dark grey (UMC = ultramafic complex).

The Stuhini Group is the dominant map unit north of the Kitchener fault zone; Stuhini Group rocks also extend southward to the confluence of the Chutine and Stikine rivers, and farther south on both sides of the Hickman batholith (Hickman, Yehiniko and Nightout plutons; Figure 2-7). Much of the area underlain by the Stuhini Group in the Stikine River valley is at lower elevations and covered with unconsolidated deposits and thick vegetation. The lack of marker units, the similarity in colour and weathering characteristics of constituent lithologies, and the lack of age determinations from the volcanic strata hinder subdivision of the Stuhini Group, elucidation of structural geology and reconstruction of stratigraphy. Despite these limitations, an attempt has been made to construct a composite stratigraphic column for the group, based on dominant lithology and age.

There are two sedimentary units that interfinger with various volcanic facies (Figures 2-7, 2-8). The total stratigraphic thickness is estimated to be at least 3500 metres, based on composite columns, but is poorly constrained. Sediment-dominated units are named here the Kitchener and Quattrin units (units uTSs1 and uTSs2), and include tuffaceous greywacke, siltstone, discontinuous limestone and minor shale. Volcanic-dominated facies are subdivided into mafic and intermediate flows and tuffs, tuffaceous wacke and bladed-plagioclase porphyry. Felsic volcanic rocks occur only locally. Contacts between these facies are gradational. Most of the units are believed to be submarine, based on the presence of chert and limestone interbeds, rare marine bivalves, and very rare pillows. Local epiclastic units and rare welded tuff may have been subaerial.

Stuhini Group lithologies commonly lack penetrative fabrics that characterize Paleozoic units (Photo 2-7), except in the Scud River valley. However, evidence for deforma-

tion includes highly variable bedding attitudes and recognition of rare folds in well bedded sections. Volcanic rocks of the Stuhini Group, although similar in some respects to overlying Lower to Middle Jurassic volcanic rocks, are more mafic and contain a larger component of subaqueous deposits. In addition, Upper Triassic flows, sills and beds commonly dip steeply, whereas Lower to Middle Jurassic successions are typically gently dipping. Augite-bearing volcanic rocks occur in both the Upper Triassic and Lower to Middle Jurassic packages, but are more abundant and augite rich in the Stuhini Group.

CARNIAN TO LOWER NORIAN: KITCHENER UNIT (Unit uTSs1)

An east-trending belt of well bedded to massive sedimentary rocks, the Kitchener unit, which has a maximum thickness of 1500 metres, extends from Mount Kitchener to Rugged Mountain (Figure 2-7). Poorly exposed, recessive sedimentary rocks also included in this unit occur in two belts that trend east-northeast from near the confluence of the Stikine and Chutine rivers. Other areas underlain predominantly by sedimentary rocks, but lacking age control, include the areas near Tahltan Lake, north of Little Tahltan Lake, and north of Tahltan River (Figure 2-7).

Sedimentary rocks are mainly brown weathering and composed of parallel bedded to laminated, tuffaceous siltstone, wacke and minor argillite and shale. Thinly interlayered tuffaceous wacke, siltstone and mudstone rhythmites, probably deposited as distal turbidites, are common. The Stikine and Chutine exposures include olive, mafic tuffaceous wacke and lesser brown-weathering arkosic greywacke, siltstone and shale, minor tuffaceous(?) and sandy limestone, limestone conglomerate and breccia, granitoid-bearing polymictic conglomerate and black ribbon chert.

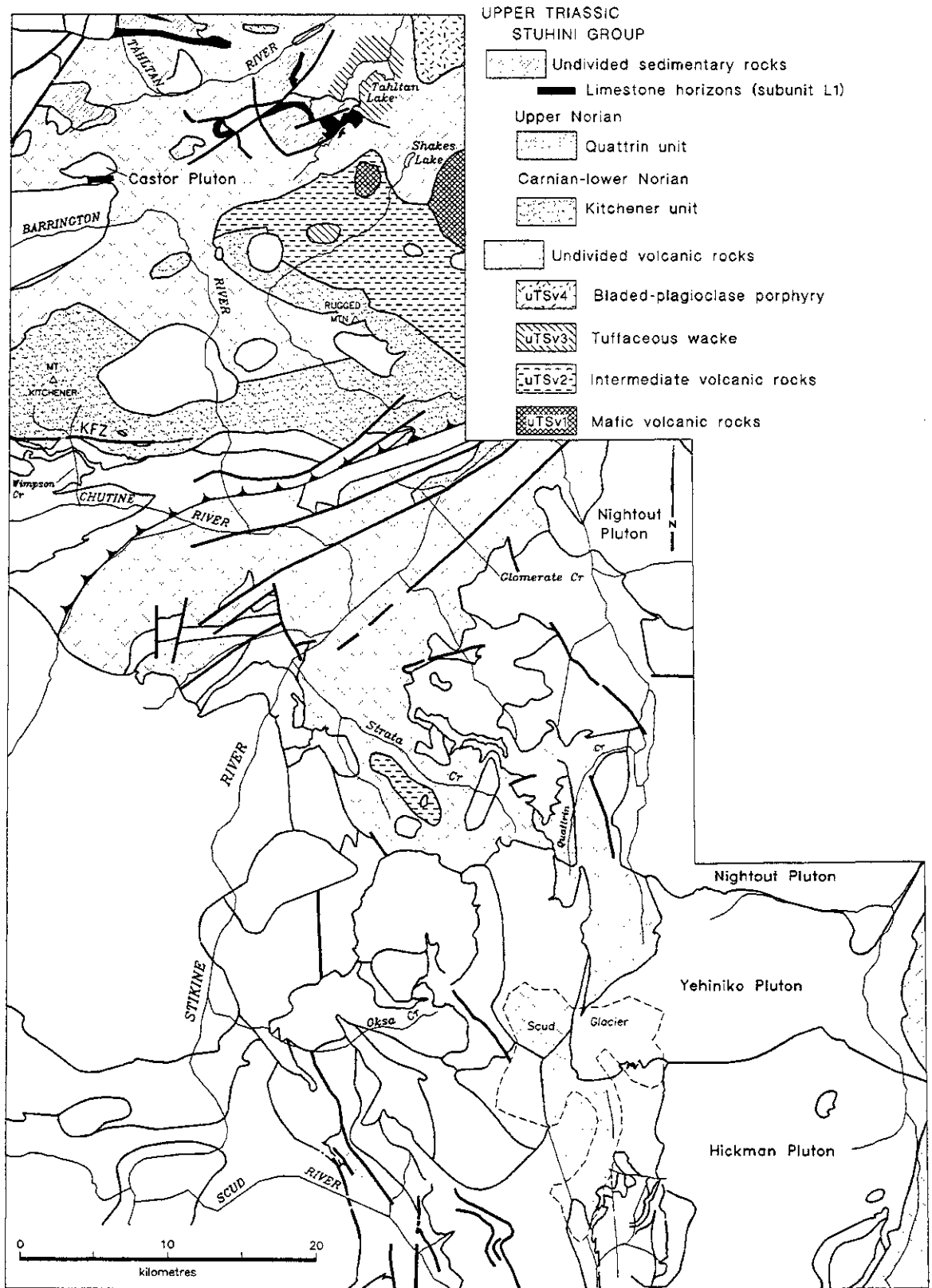


Figure 2-7. Distribution of the Upper Triassic Stuhini Group. KFZ = Kitchener fault zone.

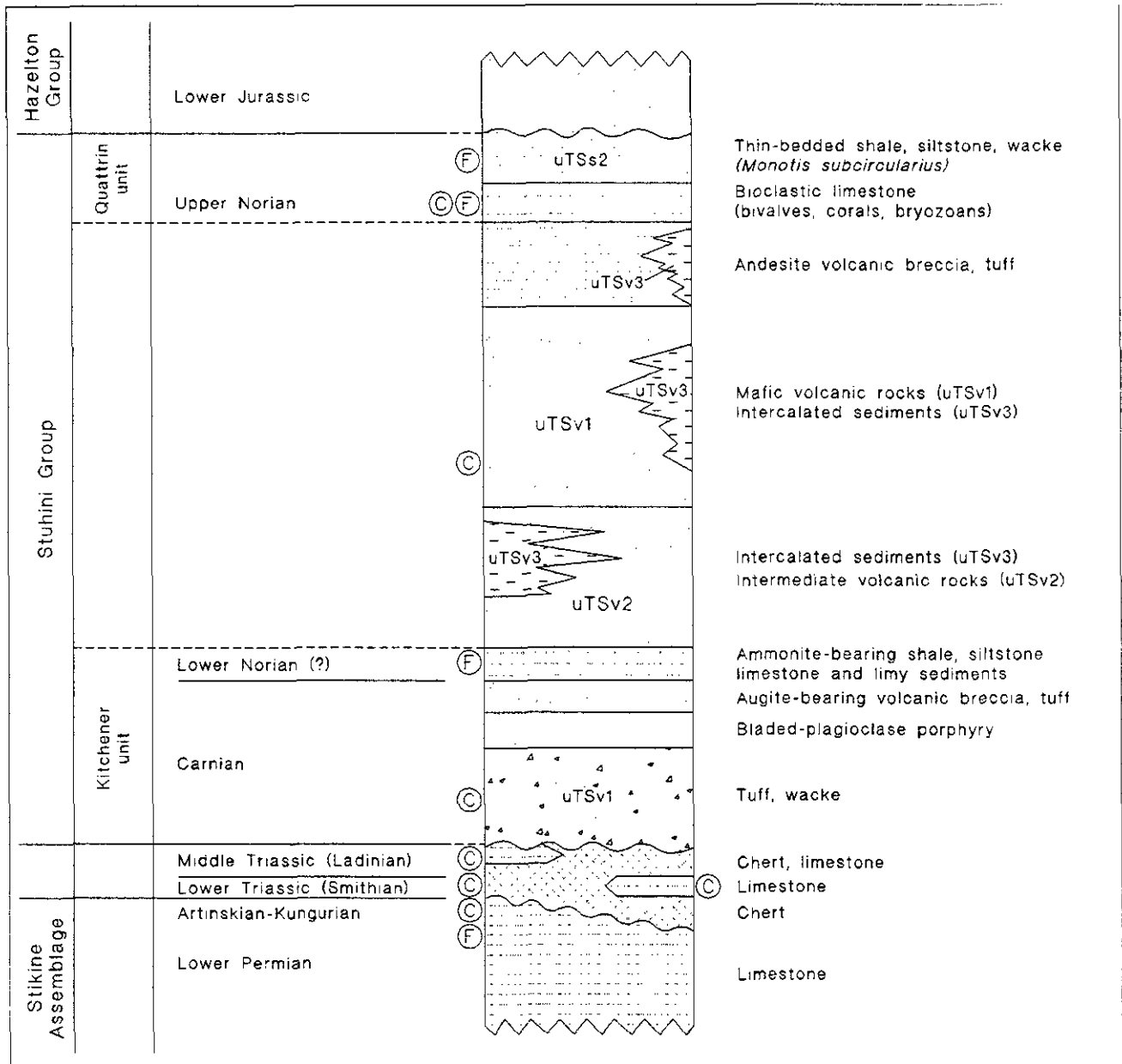


Figure 2-8. Schematic Stuhini Group stratigraphic column. C = conodont age determination, F = fusulinid age determination.

The polymictic conglomerate is matrix supported with subangular to subrounded clasts up to one metre in length. The undated, massive medium-grained diorite and granodiorite clasts resemble samples from the Late Triassic plutons and hence they are the interpreted source of the clasts. Volcanic clasts are also abundant, including augite basalt, plagioclase-phyric andesite and minor tuff. Trough cross-bedding, normal grading and fining-upward volcanoclastic sequences occur throughout (Photo 2-8a). The huge clast sizes, scour-and-fill structures, syndepositional growth faults and angular argillite rip-up clasts (Photo 2-8b) point to a paleodepositional surface with some relief. Several sections of pale grey weathering, thick-bedded to massive, micritic limestone (up to 20 m thick) occur within the unit, between Mount Barrington and Isolation Mountain. Massive pyroxene-crystal lithic lapilli tuff, green ash tuff and

cherty tuff are subordinate to the sedimentary strata. Tuffaceous wacke and crystal lithic lapilli tuff form massive, unbedded sections of the unit and increase in abundance to the east. Coarse, heterolithic pebble conglomerate contains siltstone, wacke and chert fragments and intraformational limestone clasts.

Deformation within unit uTSs1 appears largely fault-controlled and high level in a gross sense. For example, the section changes from flat-lying strata at Mount Kitchener to vertical strata within the Kitchener fault zone. Locally, however, where the unit is dominated by thinly bedded sedimentary strata and is less competent, it is recumbently folded, such as south of Damnation pluton.

The age of the unit is based on several widespread conodont and bivalve collections (from limestone layers and

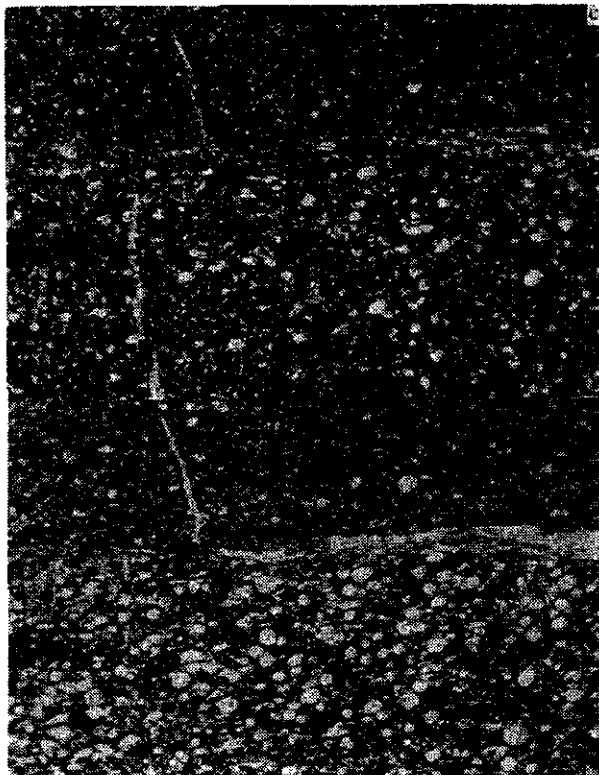
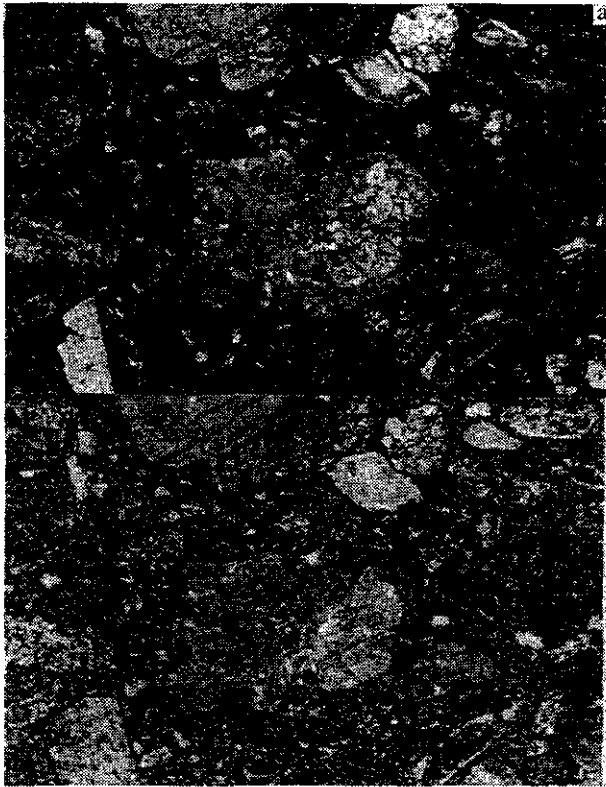


Photo 2-7. Photomicrographs of Stuhini Group rocks, showing well preserved primary textures and structures [upper = crossed nicols, lower = plane light]: (a) Amygdaloidal clinopyroxene basalt flow with quartz, chlorite and calcite-filled amygdules, 6 kilometres north of Mount Kitchener (JTI91-128), (b) Clinopyroxene-hornblende-plagioclase crystal tuff, 3 kilometres north of Limpoke Creek (DBR91-203), (c) Laminated quartz-bearing tuffaceous wacke, 6 kilometres north of Mount Kitchener (JTI91-129).

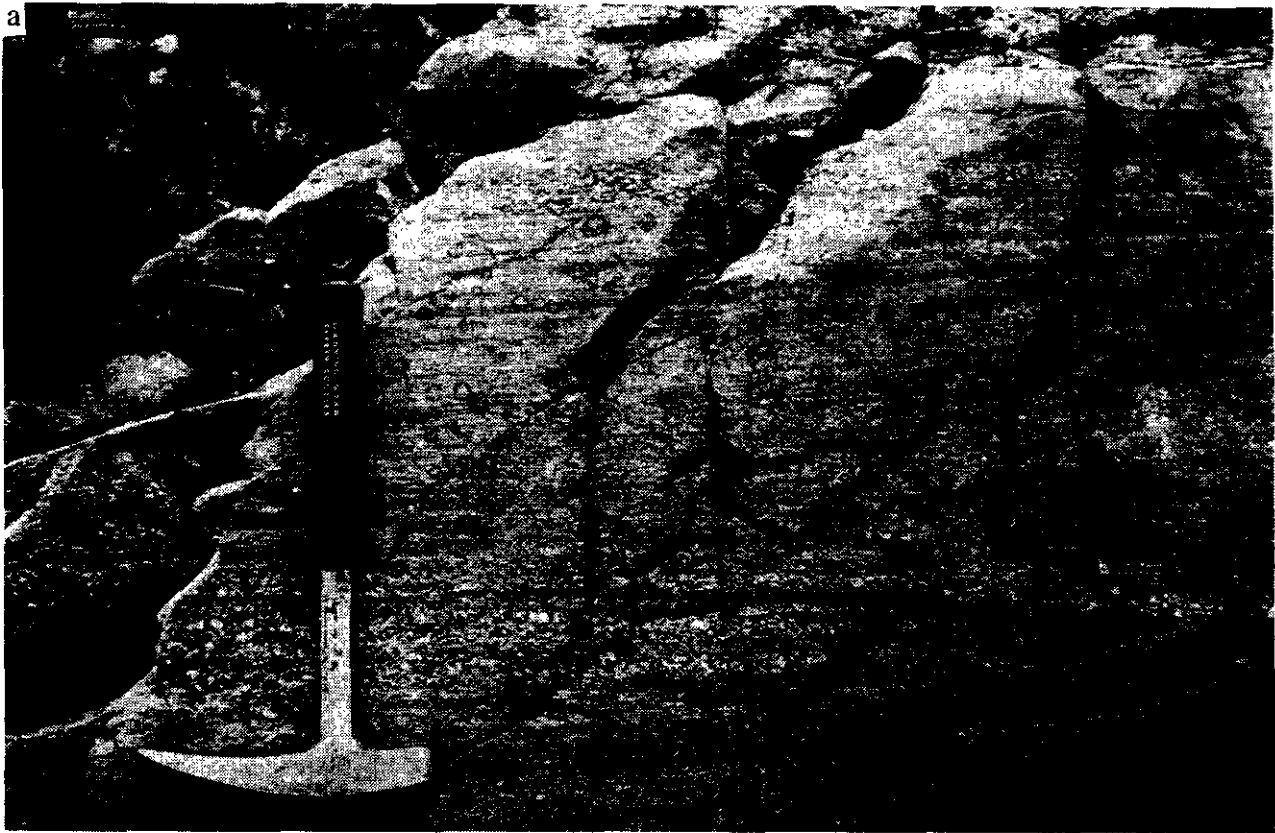


Photo 2-8. Unusually well exposed sedimentary structures in Upper Triassic tuffaceous rocks, north of Limpoke pluton (DBR91-208): (a). Well bedded, cross-stratified epiclastic rocks that indicate a southeast paleocurrent for the deposit (unit uTSs1); (b) Angular silty shale rip-up clasts supported in a well sorted tuffaceous sandstone composed of rounded, aphanitic andesite lapilli.

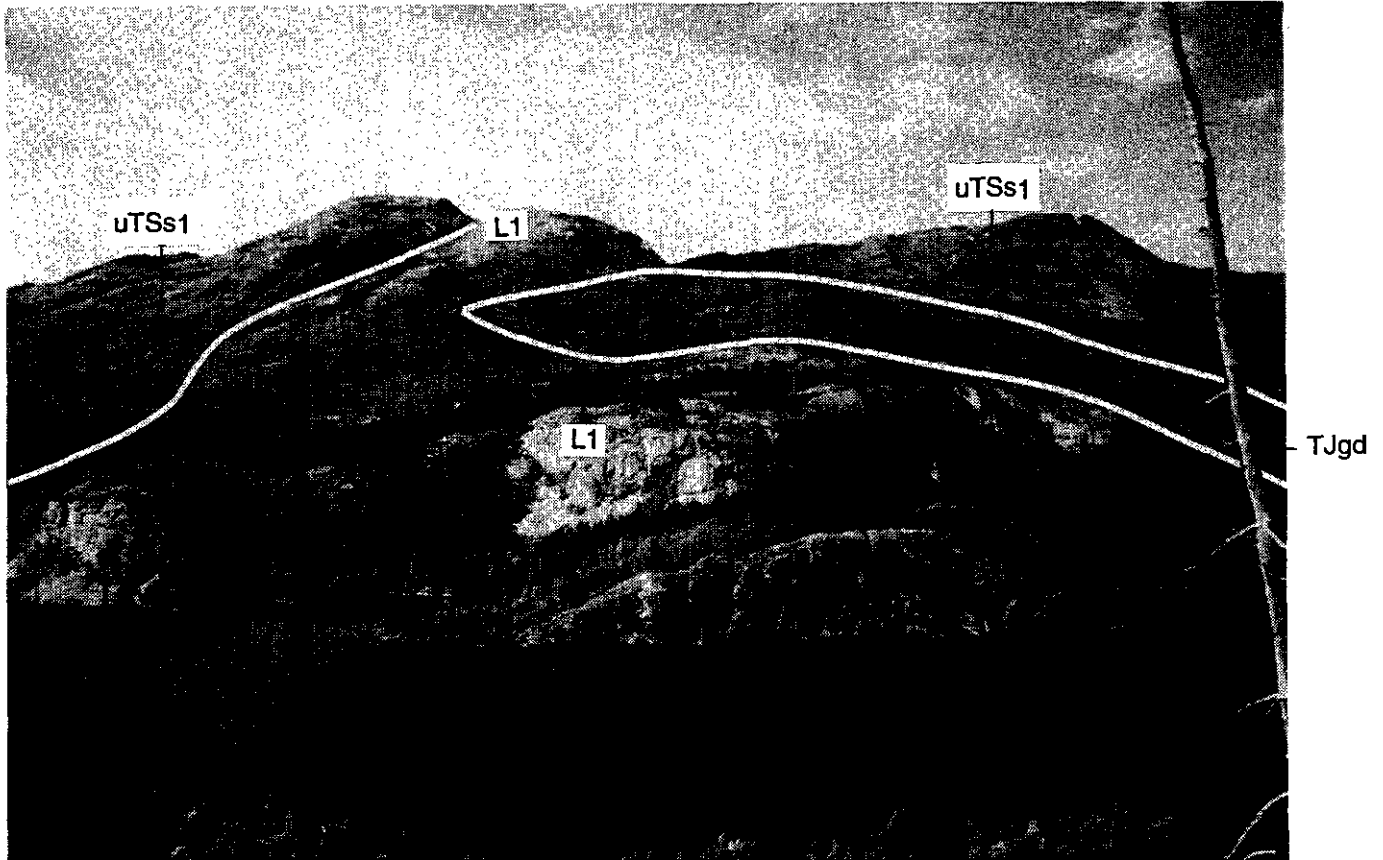


Photo 2-9. View northwest to Carnian limestone cliffs (subunit L1) southwest of Tahltan Lake; the section is unusually thick for Stuhini Group carbonate in the study area (DBR91-124).



Photo 2-10. Heterolithic breccia with angular volcanic fragments and subrounded plutonic clasts south of Glomerate Creek; plutonic clasts may have had a more distal source relative to the volcanic debris (unit uTSv; DBR89-47). The breccia was interpreted to be Jurassic by Kerr (1948a), however, a correlation to Upper Triassic Stuhini Group is suggested by our new Upper Triassic fossils (Appendix 1, DBR89-48).

shaly beds, respectively) with taxa assigned Carnian to early Norian ages (Appendices 1, 3; Figure 2-8).

LIMESTONE HORIZONS (Subunit L1)

Discontinuous fine-grained limestone units occur within both the Kitchener sedimentary and volcanic facies. They form prominent light grey outcrops in four areas: Mount Barrington - Isolation Mountain, west of Tahltan Lake (Photo 2-9), the Castor pluton area, and north of the Tahltan River (Figure 2-7). Contacts are rarely exposed but they appear to be conformable. Most limestones are less than 30 metres thick and, unlike the Permian or older carbonates, are not significantly recrystallized or foliated. West and south of Tahltan Lake, the unit is more than 100 metres thick and dips gently, whereas in most other areas beds are thinner and steeply dipping. Along the southern contact of the Castor pluton, the limestone is 25 metres thick, well bedded and has a porcellaneous texture. A small limestone pod northwest of Little Tahltan Lake has phyllitic, deformed margins adjacent to chlorite phyllite and massive Stuhini andesite. A heterolithic breccia, containing angular limestone blocks up to 8 metres across, and smaller plagioclase-porphyrific andesite and rare granitoid clasts supported in a coarse limy volcanic matrix is exposed at the top of a limestone unit north of Glomerate Creek (Photo 2-10). A feldspathic wacke and polymictic conglomerate contains subrounded clasts of

massive hornblende granodiorite up to 30 centimetres in diameter. We believe the undated clasts are derived from coeval Late Triassic plutons. This deposit is interpreted to be adjacent to a paleofault scarp and the blocks represent submarine talus material.

Most limestone bodies contain Carnian conodonts; however, the limestone 7 kilometres southwest of Tahltan Lake has late Ladinian to Carnian conodonts (Appendix 3). Early Norian ammonites and late Carnian to early Norian conodonts provide a precise age in the Stikine and Chutine rivers area (Appendices 1 and 3). In addition, two localities with fossils interpreted as Lower Jurassic by Kerr (1948a) near Glomerate and Flag creeks, yielded probable Norian macrofossils (Appendix 1). These ages suggest that the Lower Jurassic units previously mapped in the Stikine valley by Kerr, and Souther (1972), are probably Upper Triassic and part of the Kitchener unit. It is not possible to distinguish the Carnian and Norian limestones on the basis of lithology.

VOLCANIC FACIES (Unit uTSv)

In general, the Kitchener sedimentary unit between Mount Kitchener and Barrington River interfingers with, and is overlain by, mafic and intermediate volcanic rocks. The basaltic flows, breccia and tuff are also well exposed elsewhere, including northeast of Rugged Mountain, Missusjay Creek, northeast of Devils Elbow Mountain and west of the Scud Glacier. Detailed descriptions of basalt near Missusjay Creek and in the Scud River and Scud Glacier areas are found in Gunning (1993a). The bladed-plagioclase porphyry facies typically underlies areas to the north and northwest. It is dominated by mafic and intermediate volcanic rocks, although volumetrically insignificant felsic units are widespread. The following discussion of volcanic facies (uTSv1 to 4) is based on compositional affinity. Stratigraphic position of the facies varies and similar lithologies are probably repeated in successive volcanic cycles (Figure 2-8).

MAFIC VOLCANIC ROCKS (Unit uTSv1)

The most distinctive Stuhini Group lithologies are mafic volcanic rocks, including clinopyroxene-hornblende and plagioclase-phyric, locally amygdaloidal basalt or basaltic andesite flows and crystal-lithic lapilli tuffs. They are typically dark green, massive, and contain distinctive, blocky clinopyroxene and lath-shaped plagioclase phenocrysts. Composition of the tuffs is similar to flows. Lapilli to block size (2 to 75 cm) fragments are supported in a crystal-rich matrix. Monolithic amygdaloidal basalt breccia, interpreted as autobrecciated flow, occurs locally. A pyroxenite clast in a reworked(?) lapilli tuff southwest of Shakes Lake suggests that an ultramafic intrusion, perhaps the Latimer Lake body, was unroofed during the deposition of the tuff. Minor epidote-carbonate veinlets are common in the basalt. Layering in tuff units is uncommon and attitudes are generally obtained on interbedded finer grained pyroclastic or volcanoclastic units. Pillowed basalt flows were recognized only locally, for example, northeast of the confluence of the Stikine and Chutine rivers.

Basaltic flows and tuffs of unit uTSv1 are clinopyroxene rich and lack orthopyroxene, suggesting a possible

petrochemical link to spatially associated Alaskan-type ultramafic intrusive bodies. This is discussed in Chapter 3.

A fault-bounded panel of mafic tuff and argillite correlated with strata north of Missusjay Creek and with other mafic Stuhini volcanic rocks yielded a 227 ± 1 Ma U-Pb zircon date (Carnian; J.K. Mortensen *in* Gunning, 1993a). The date suggests the strata are coeval with the Kitchener unit.

INTERMEDIATE VOLCANIC ROCKS (Unit uTSv2)

Massive, plagioclase-rich, andesitic block-tuffs, tuffs and flows predominate in the area south of Shakes Lakes and on the ridges immediately south of Strata Creek (Figures 2-7, 2-8). Green and maroon, plagioclase-porphyrific andesite fragments are characteristic components. An andesitic composition is inferred for the flows, from the coexistence of plagioclase and hornblende; locally, embayed volcanic quartz crystals occur within lapilli tuff. The unit is lithologically similar to part of the Lower Jurassic Unuk River Formation (Hazelton Group), south of the Iskut River, however, diagnostic pyroxene-rich flows of the Stuhini Group overlie it, so it is included in the Stuhini Group. Mappable subunits include maroon volcanic rocks (uTSv2m; c) and distinctive beds of white to light grey, well bedded, hornblende-rich epiclastic rocks exposed on a ridge northwest of the Brewery pluton (uTSv2m). The distribution of the distinctive hornblende-rich tuffaceous wacke suggests a subhorizontal attitude for the massive strata of this area. The maroon rocks that overlie dark grey siltstone and shale are brick-red, poorly sorted, heterolithic volcanic conglomerates, which contain abundant limestone clasts and boulders, some measuring up to 10 metres in diameter (Photo 2-11). The limestone olistoliths indicate a high-energy environment, and contact relations with marine siltstone and shale indicate transport from a high to low-energy setting. The maroon rocks are interpreted to be debris flows (lahars) which incorporated reefoidal limestone blocks as they flowed down the flank of an Upper Triassic volcanic edifice.

TUFFACEOUS WACKE (Unit uTSv3)

Olive-green medium-grained plagioclase-rich tuffaceous wacke forms massive outcrops north and southwest of Shakes Lake (Figures 2-7, 2-8). Like unit uTSv2, it is rarely bedded, but lacks large fragments. It grades into intermediate volcanic rocks of unit uTSv2 and may represent a more distal facies.

BLADED-PLAGIOCLASE PORPHYRY (Unit uTSv4)

Brown-weathering bladed-plagioclase phyric basalt or basaltic andesite flows predominate northeast of Tahltan Lake and form isolated exposures north of Tahltan River (Figure 2-7). Series of flows are at least 150 metres thick, although individual thicknesses are unknown. A bladed porphyry unit, 25 metres thick, interpreted to be a sill, is exposed on a cliff face 1 kilometre south of Tahltan Lake.

VOLCANIC SUBUNITS

Felsic Volcanic Facies (Subunit uTSvf)

Pale green to dark grey, pyritic, laminated siliceous ash tuffs are most common, but siliceous lithic lapilli tuff and



Photo 2-11. Large, angular limestone boulder, 3.5 metres in diameter, in maroon volcanic conglomerate (unit lbx), a coarse facies of unit uTSv2, southwest of Brewery pluton. This boulder, too large to be transported by fluvial processes, must have been carried by a debris flow that incorporated limestone. Such deposits indicate a high-energy, unstable and cannibalistic setting, possibly eroding the limestone from the flank of a stratovolcano.

welded to unwelded ignimbrite occur locally (Photo 2-12). Pale green to grey, fine-grained to aphanitic silicic and felsic tuffs north of Schaft Creek are interpreted to be waterlain ash tuffs. In places, mafic crystal-lithic tuff and tuff-breccia contain rare felsic clasts. Compositions of the flows and fragments in pyroclastic and volcanoclastic rocks span the mafic to felsic spectrum, but are dominantly mafic to intermediate.

Polymictic Conglomerate (Subunit hcgl)

A mappable subunit of polymictic conglomerate (does not include the isolated exposures previously mentioned) with abundant granitoid clasts is exposed in three areas: the headwaters of Strata Creek, along the western margin of the glacier at the headwaters of Quattrin Creek, and on both sides of the Scud Glacier (Figure 2-7). The conglomerates vary from matrix to framework supported and contain prominent clasts of light grey granitic rocks, together with variably epidotized volcanic rocks, dark green augite basalt, and rarely, amphibolite, limestone and ultramafite (Photo 2-13). Cobble to pebble sized clasts are rounded to sub-rounded. The conglomerates are distinguished from the granitoid-bearing conglomerates in units uTSs1 and L1 by their position within volcanic-dominated successions, by the greater portion of plutonic clasts (10 to 35%) and by their

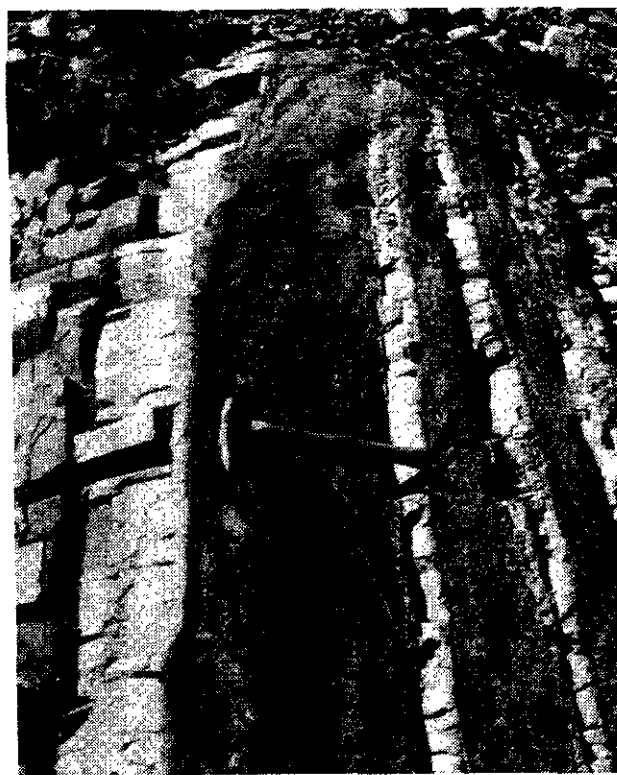


Photo 2-12. Light grey weathering dacitic lapilli tuff (recessive) and ash tuff (resistant) beds (unit uTSvf), north of Conover Creek. Lithic fragments of similar lithology occur in mafic augite crystal tuff elsewhere in the succession.

spatial association with the Hickman batholith. The plutonic clasts are hornblende granodiorite to quartz monzonite and are interpreted to be derived from the Late Triassic plutons. Another possible source is the Devonian Forrest Kerr pluton (Logan *et al.*, 1993a), however, its granite and diorite compositions are dissimilar to the clasts in the conglomerate.

The conglomerates indicate that significant unroofing of plutonic rocks occurred during Stuhini volcanism. A modern analogue may be the 2 Ma Takidani granodiorite in the Japan Alps, which has already been unroofed (Harayama, 1992).

UPPER NORIAN: QUATTRIN UNIT (Unit uTSs2)

The Quattrin unit includes the youngest rocks assigned to Stuhini Group and occurs in a disrupted clastic and pyroclastic succession exposed between Strata and Quattrin creeks (Figures 2-7, 2-9). Several subunits of pale grey weathering, thick-bedded to massive, micritic and bioclastic limestone up to 20 metres thick occur at the transition with stratigraphically lower, massive flows and breccias to the southwest (unit uTSv). Dark grey to black siltstone, green and pale grey arkose and black shale overlie the limestone. Maroon, mauve and brick-red massive lapilli tuff, tuffaceous mudstone and lesser laminated limy ash tuff overlie the sedimentary rocks. A similar unit forms a narrow east-trending belt which crosses Helveker Creek (Photo 2-14). There, large lenses of steeply south dipping, thick-bedded



Photo 2-13. Stuhini Group heterolithic breccia/conglomerate composed of volcanic and plutonic fragments (unit hcgl), along the east and west sides of Scud Glacier (DBR88-299). Volcanic blocks are coarse augite-phyric basalt and finer grained andesite. Plutonic clasts, up to a metre in diameter, are hornblende monzonite, believed to be derived from the nearby Hickman pluton.

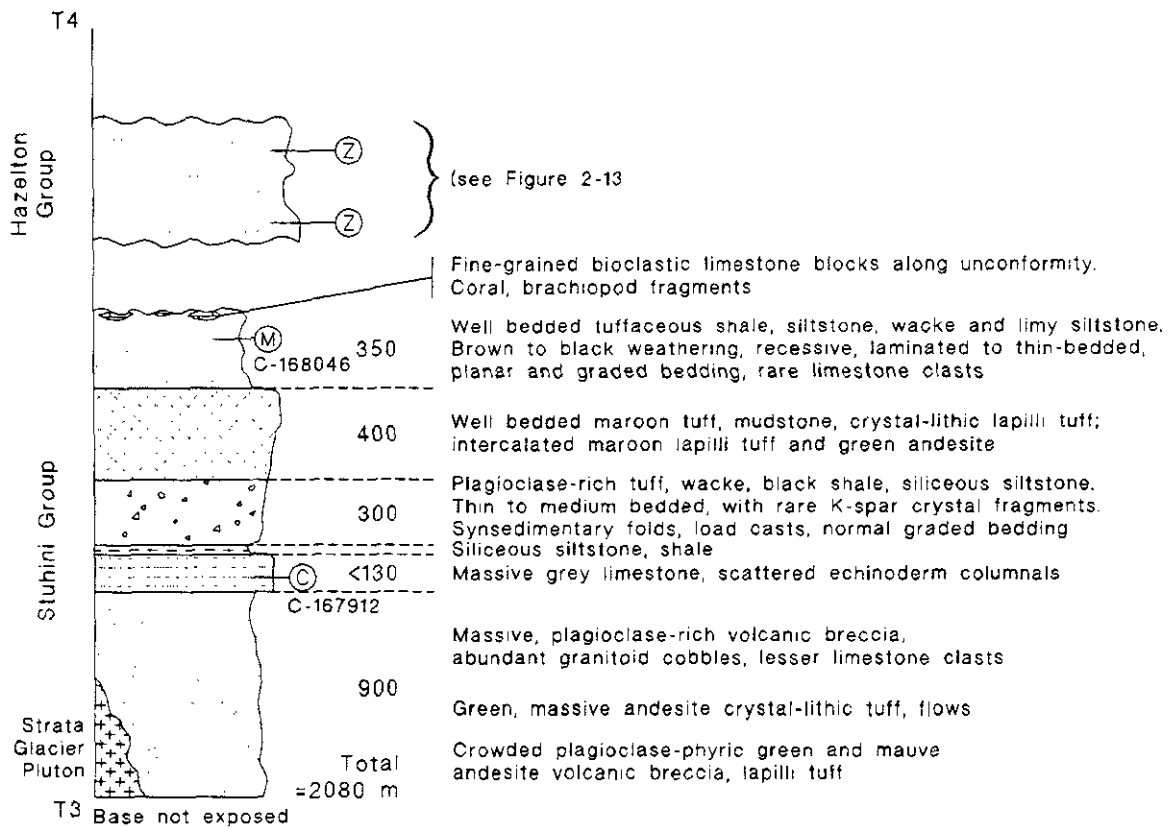


Figure 2-9. Schematic Stuhini Group stratigraphic column from the headwaters of Strata Creek.

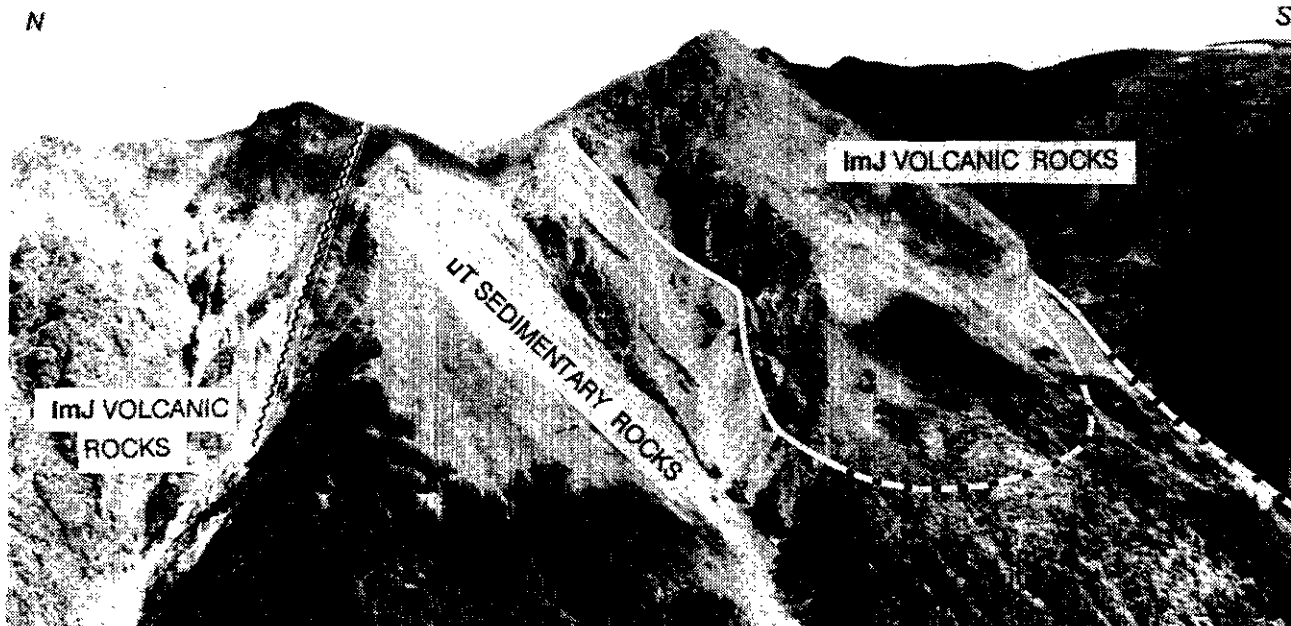


Photo 2-14. Unconformable contact of Stuhini Group sedimentary rocks (unit uTSs2) with overlying Jurassic volcanic rocks (unit ImJHv), Helveker Creek valley. The erosional surface has high relief but no basal conglomerate is evident in this area.

to massive limestone and minor thin-bedded, light grey chert, grade upward into well bedded, dark grey siltstone and green sandstone. A few coalified plant fragments were found at one locality.

Fossil control for the sedimentary unit is provided by occurrences of the late Norian macrofossil, *Monotis subcircularis*, reported by Souther (1972; Figure 2-9; Appendix 1). Late Norian conodonts were also collected from a limestone unit directly below the clastic rocks (Figure 2-9; Appendix 3).

CHEMISTRY AND TECTONIC SETTING OF THE STUHINI GROUP

Major and trace element geochemical data for 32 samples from the Stuhini Group are tabulated in Appendix 8. Data from 18 samples of flows or sills were plotted after applying criteria to filter out altered samples (Appendix 9). Two additional samples of probable Stuhini Group were included in this data set (MGU89-215, MGU89-239). Most samples in the relatively unaltered subset have undergone some alteration and contain small veinlets and patches of chlorite, carbonate and other secondary minerals. Effects of alteration were minimized by avoiding obvious veining, brecciation and alteration during sampling, but some alkali mobility can be expected in weakly chloritic or carbonate-altered samples. Petrological characterizations based on major element plots are supported by petrogenetic plots which use relatively immobile trace elements. All samples are pyroxene or plagioclase and pyroxene-phyric. Metamorphic grade ranges from zeolite to lower greenschist facies.

The Stuhini Group includes tholeiitic to calcalkaline (Figure 2-10a) basalts, basaltic andesites, trachybasalts and basaltic trachyandesites (Figure 2-10b). The suite straddles the subalkaline-alkaline boundary on the alkali-silica plot (Figure 2-10c), with five of the samples plotting in the al-

kaline field. Pyroxene-porphyrific flows and breccia from the lower part of Stuhini Group in the southern part of the project area are mainly basalt with less abundant absarokite (Gunning, 1993a). They have similar characteristics to the samples discussed above, falling along the alkaline-subalkaline field boundaries. All of the samples are medium to high-potassium basalts (Figure 2-10d), with half of the samples in the high-potassium basalt category. Eight samples have shoshonitic affinities, with K_2O greater than 1.8%, K_2O/Na_2O greater than 0.6, TiO_2 less than 1.3%, near silica saturation, and low iron enrichment (Morrison, 1980; de Rosen Spence, 1985; Gill and Whelan, 1989). One sample, excluded in accordance with one of the alteration criteria ($K_2O/Na_2O > 2.0\%$), may be part of the shoshonitic association.

Trace element plots support characterization of the Stuhini Group as an arc-related volcanic succession, an interpretation compatible with regional tectonic relationships (e.g. Souther, 1977), the dominantly calcalkaline composition of the volcanic rocks, and the abundance of porphyritic flows and pyroclastic rocks. The suite clusters in the island arc field on Shervais' (1982) Ti-V plot (Figure 2-11a). Mullen's (1983) TiO_2 -MnO- P_2O_5 plot shows the Stuhini Group as dominantly calcalkaline basalt (Figure 2-10e). An arc interpretation is also supported by Pearce and Cann's (1973) Ti-Zr-Sr plot (Figure 2-11b), where the samples cluster near the calcalkaline island-arc basalt boundary. The linear cluster points toward the strontium apex, suggesting either strontium metasomatism during regional metamorphism or plagioclase fractionation.

Ten samples plotted on mid-ocean ridge basalt normalized spidergrams (Figure 2-11c) display a signature typical of subduction-generated calcalkaline and shoshonitic volcanic arc basalts, with strong enrichments in lithophile elements (Sr, K, Rb and Ba) and flat Nb, Zr, Ti and Y trends

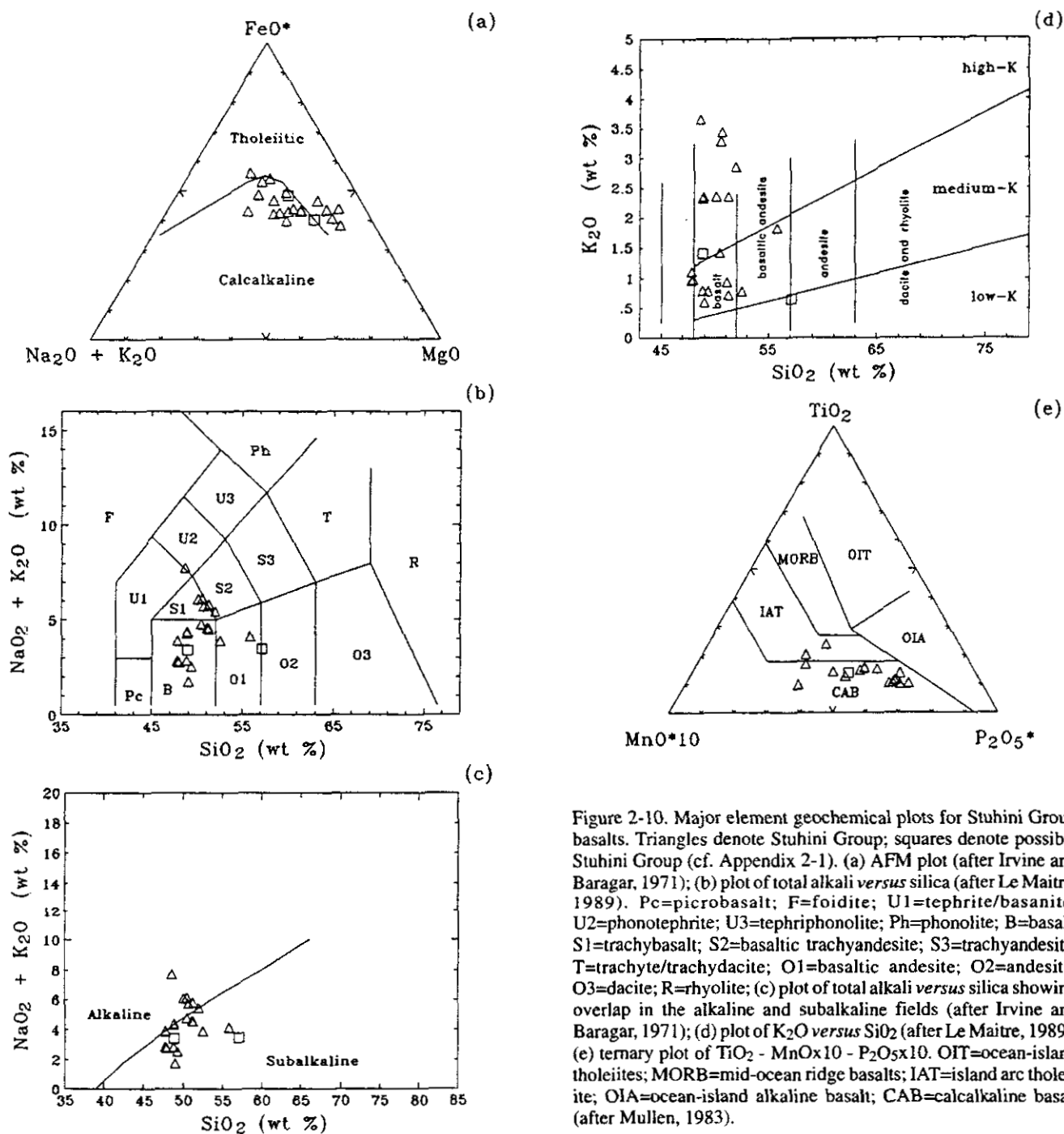


Figure 2-10. Major element geochemical plots for Stuhini Group basalts. Triangles denote Stuhini Group; squares denote possible Stuhini Group (cf. Appendix 2-1). (a) AFM plot (after Irvine and Baragar, 1971); (b) plot of total alkali versus silica (after Le Maitre, 1989). Pc=picrobasalt; F=foiidite; U1=tephrite/basanite; U2=phonotephrite; U3=tephriphonolite; Ph=phonolite; B=basalt; S1=trachybasalt; S2=basaltic trachyandesite; S3=trachyandesite; T=trachyte/trachydacite; O1=basaltic andesite; O2=andesite; O3=dacite; R=rhyolite; (c) plot of total alkali versus silica showing overlap in the alkaline and subalkaline fields (after Irvine and Baragar, 1971); (d) plot of K_2O versus SiO_2 (after Le Maitre, 1989); (e) ternary plot of TiO_2 - $\text{MnO} \times 10$ - $\text{P}_2\text{O}_5 \times 10$. OIT=ocean-island tholeiites; MORB=mid-ocean ridge basalts; IAT=island arc tholeiite; OIA=ocean-island alkaline basalt; CAB=calcalkaline basalt (after Mullen, 1983).

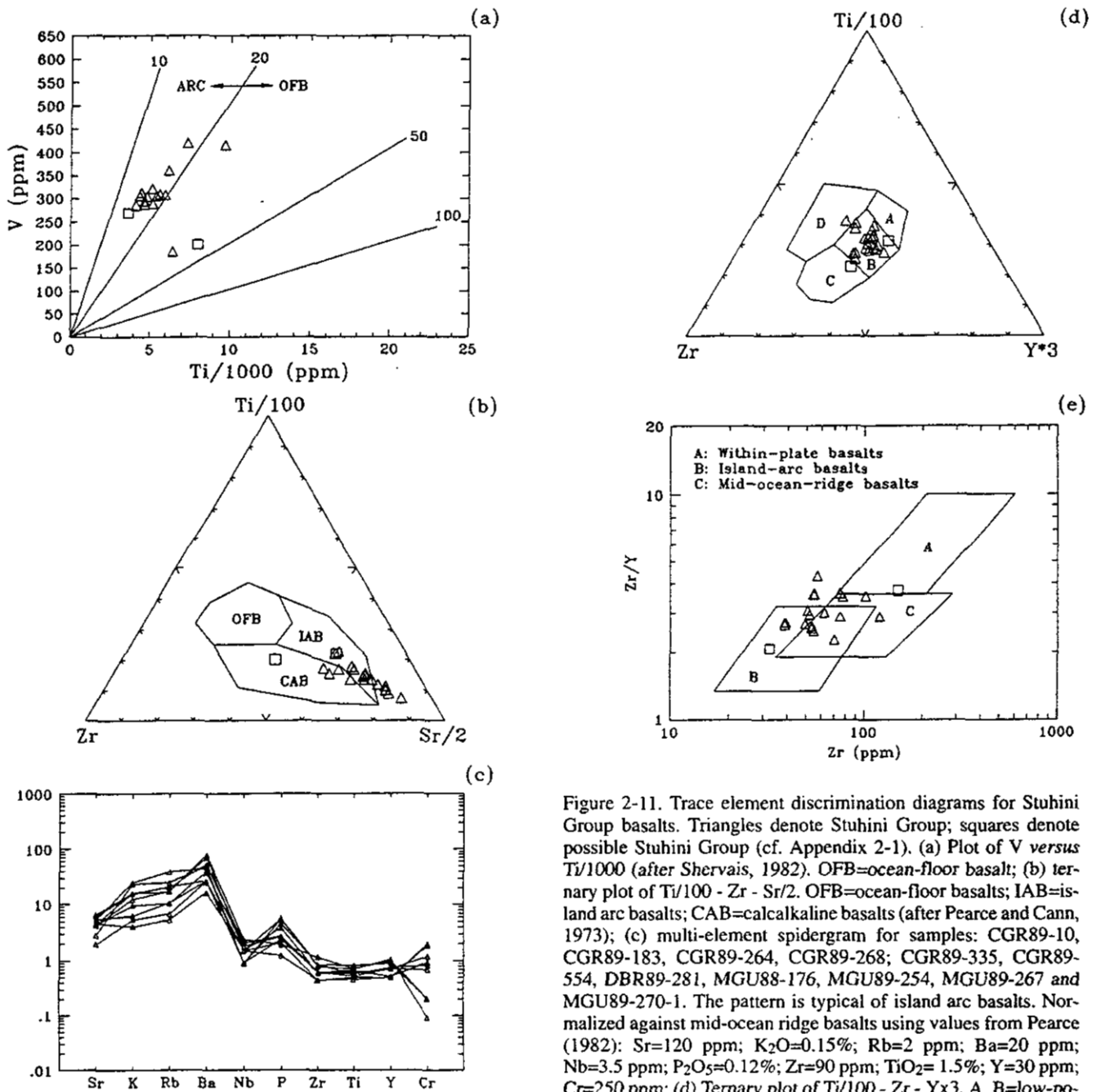


Figure 2-11. Trace element discrimination diagrams for Stuhini Group basalts. Triangles denote Stuhini Group; squares denote possible Stuhini Group (cf. Appendix 2-1). (a) Plot of V versus Ti/1000 (after Shervais, 1982). OFB=ocean-floor basalt; (b) ternary plot of Ti/100 - Zr - Sr/2. OFB=ocean-floor basalts; IAB=island arc basalts; CAB=calcalkaline basalts (after Pearce and Cann, 1973); (c) multi-element spidergram for samples: CGR89-10, CGR89-183, CGR89-264, CGR89-268; CGR89-335, CGR89-554, DBR89-281, MGU88-176, MGU89-254, MGU89-267 and MGU89-270-1. The pattern is typical of island arc basalts. Normalized against mid-ocean ridge basalts using values from Pearce (1982): Sr=120 ppm; K₂O=0.15%; Rb=2 ppm; Ba=20 ppm; Nb=3.5 ppm; P₂O₅=0.12%; Zr=90 ppm; TiO₂= 1.5%; Y=30 ppm; Cr=250 ppm; (d) Ternary plot of Ti/100 - Zr - Yx3. A, B=low-potassium tholeiites; B=ocean-floor basalts; B, C=calcalkaline basalts; D=within-plate basalts (after Pearce and Cann, 1973); (e) plot of log (Zr/Y) versus log Zr (after Pearce and Norry, 1979). Pearce (1983) uses this diagram to distinguish arc volcanics erupted on oceanic crust from those erupted on continental crust, with continental arcs above Zr/Y = 3.

(Pearce, 1983). The slight enrichment in niobium and higher average concentration of niobium relative to zirconium suggest a weak within-plate signature typical of alkalic ocean-island basalts. Zirconium/yttrium ratios are also indicators of within-plate enrichments. A few samples plot in or near the within-plate field on the Ti-Zr-Y plot (Figure 2-11d), while on a Zr versus Zr/Y plot (Figure 2-11e), several samples plot outside the oceanic-arc field toward higher Zr/Y values. Similar weak, within-plate signatures are sometimes seen in arcs along continental margins, where subcontinental lithosphere undergoes melting (Pearce, 1983).

DEPOSITIONAL ENVIRONMENTS

The following is a synopsis of Triassic stratigraphic evolution in the project area. The rock record for the Lower Triassic is poor, as it is elsewhere in the Cordillera. The Early Triassic black micritic limestone pod surrounded by Carnian tuffaceous wacke of the Stuhini Group suggests that the pod may be an olistostrome. The paucity of coeval Early Triassic strata may be due to limited primary deposition, to erosion or to lack of data.

By the Middle Triassic, deep-water chert was deposited unconformably on Lower Permian limestone and older strata in the Wimpson Creek area (Figure 2-8), its areal distribution was limited, possibly by arc topography. An influx of fine tuffaceous material, probably from distal volcanic centres, gradually overwhelmed chert deposition in Carnian time (Kitchener unit). Interpretations based on facies trends are hindered here because the polarity of the arc remains unknown. However, thick tuffaceous sediments continued

to accumulate in the west (relative to present orientation of Stikinia), whereas in the east, interfingering basalt and andesite flows were an important component. As the volcanic pile thickened, there was local carbonate accumulation, possibly as fringing reefs. Eventually the proximal eastern facies of flows, volcanic breccia and tuff prograded westward over the distal facies. The western migration of volcanism may have coincided with emergence of some of the volcanic edifices. Rare, welded dacite tuff and maroon fluvial epiclastic rocks containing polymictic subrounded granitic and carbonate clasts indicate local subaerial conditions. The coarse conglomerate/breccia unit required a high-energy system, probably reflecting significant relief, to transport the clasts. Clast compositions indicate that unroofing of Hickman suite plutons was synchronous with deposition of the upper part of the Upper Triassic volcanic pile. Carnian limestone deposition north of the Tahltan River occurred at a transition from volcanic to sediment-dominated settings. Distal turbidites of the late Norian Quattrin unit represent the final record of Triassic, low-energy submarine deposition in the map area.

LOWER TO MIDDLE JURASSIC HAZELTON GROUP (Unit ImJH)

Lower to Middle Jurassic volcanic and minor sedimentary rocks underlie a 100 square kilometre outlier centred around Helveker Creek, and also outcrop northeast of Yehiniko Lake, where they were mapped as Stuhini Group by Souther (1972; Figure 2-12). They represent the northwestern-most extent of the Hazelton Group yet recognized. A

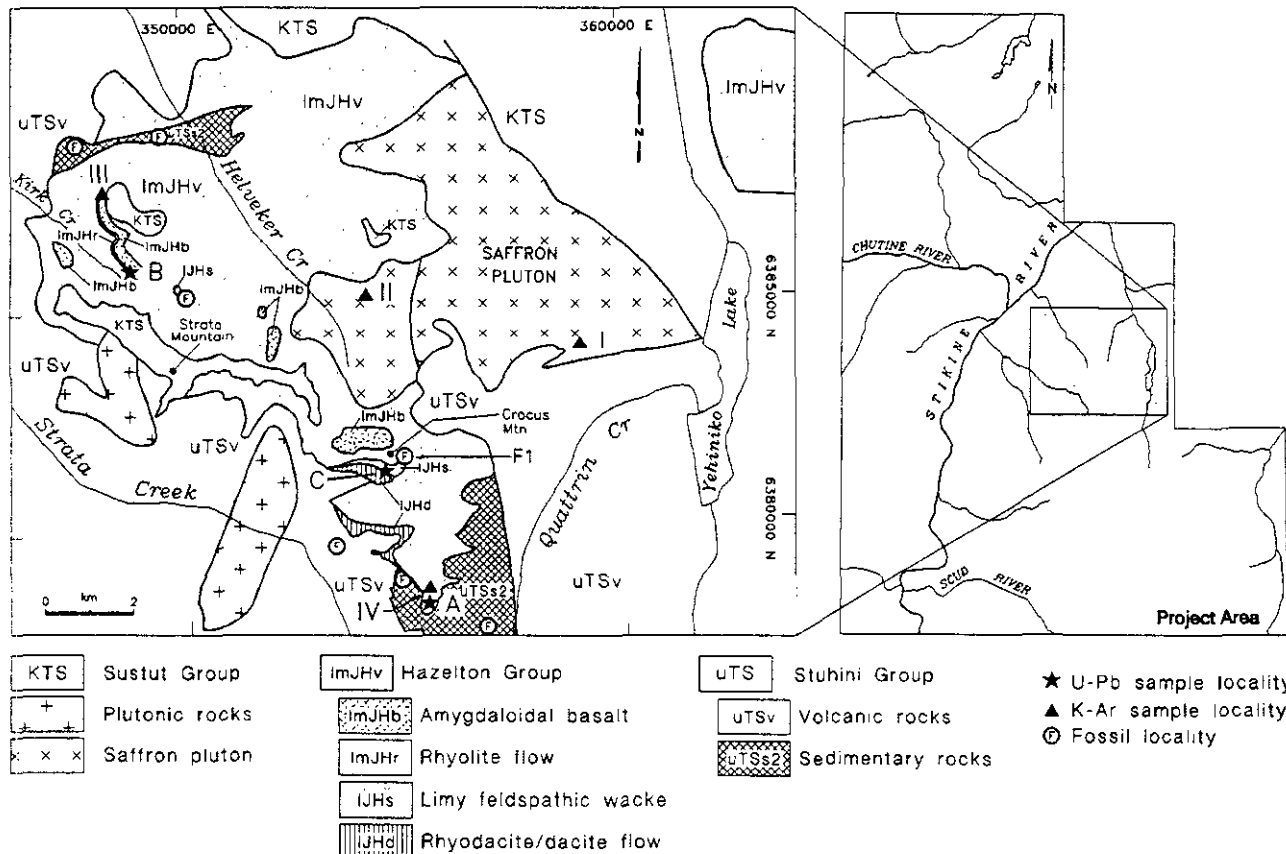


Figure 2-12. Distribution of Lower to Middle Jurassic Hazelton Group. Potassium-argon dates: I = 162±7 Ma, II = 162±7 Ma, III = 166±6 Ma, IV = 148±5 Ma. Uranium-lead dates: A = 185±7-1 Ma, B = 175±4-1 Ma, C = indeterminate.

composite stratigraphic column (Figure 2-13) is based on three well exposed areas: Crocus Mountain, the ridge between Strata and Quattrin creeks and a prominent cirque in the headwaters of Kirk Creek, where a paleomagnetic study was conducted (Vandall *et al.*, 1992).

The composite Jurassic section is over 1000 metres thick and is characterized by gently dipping, massive plagioclase-rich andesite flows and tuffs with maroon or purple hues (unit ImJHv; Photo 2-15) and is typified by exposures between Kirk Creek and the ridge south of Crocus Mountain. The section is subdivided into five units: a local basalt dacite flow or sill (unit IJHd; Figures 2-12, 2-14), a discontinuous limestone and fossiliferous limy arkosic wacke (unit IJHs), extensive andesite flows and breccia (unit ImJHv),

pink rhyolite (unit ImJHr), and an uppermost basalt flow breccia with local pillow fragments and discontinuous limestone lenses (unit ImJHb).

DACITE UNIT (Unit IJHd)

Buff to rusty weathering aphanitic dacite (up to 300 m thick) is exposed at the base of the section and has been traced southward from Crocus Mountain for about 3 kilometres (Photo 2-16; Figure 2-13). Its keel shape with a flat top somewhat resembles a laccolith, however, its tongue-like distribution over Stuhini volcanic and sedimentary rocks is more akin to a felsic flow. These features are enigmatic and it remains uncertain whether the unit is a flow or a sill.

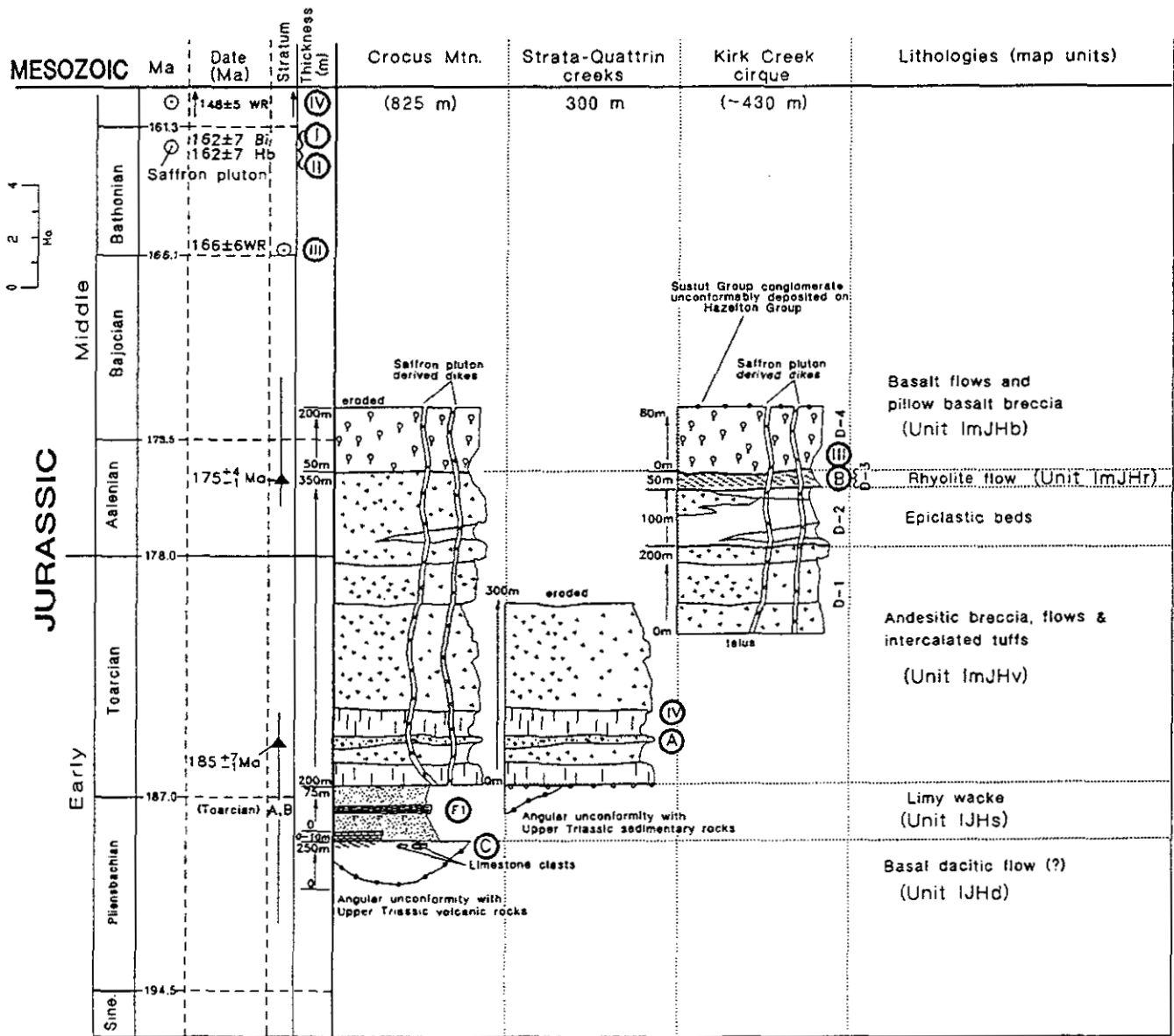


Figure 2-13. Schematic stratigraphic column of the Hazleton Group near Crocus Mountain with approximate location of U-Pb, K-Ar and fossil dates indicated. Dating method depicted by: open circle = K-Ar, and solid triangle = U-Pb. Fossil dates; A = ammonoids, B = bivalves, C = conodonts.

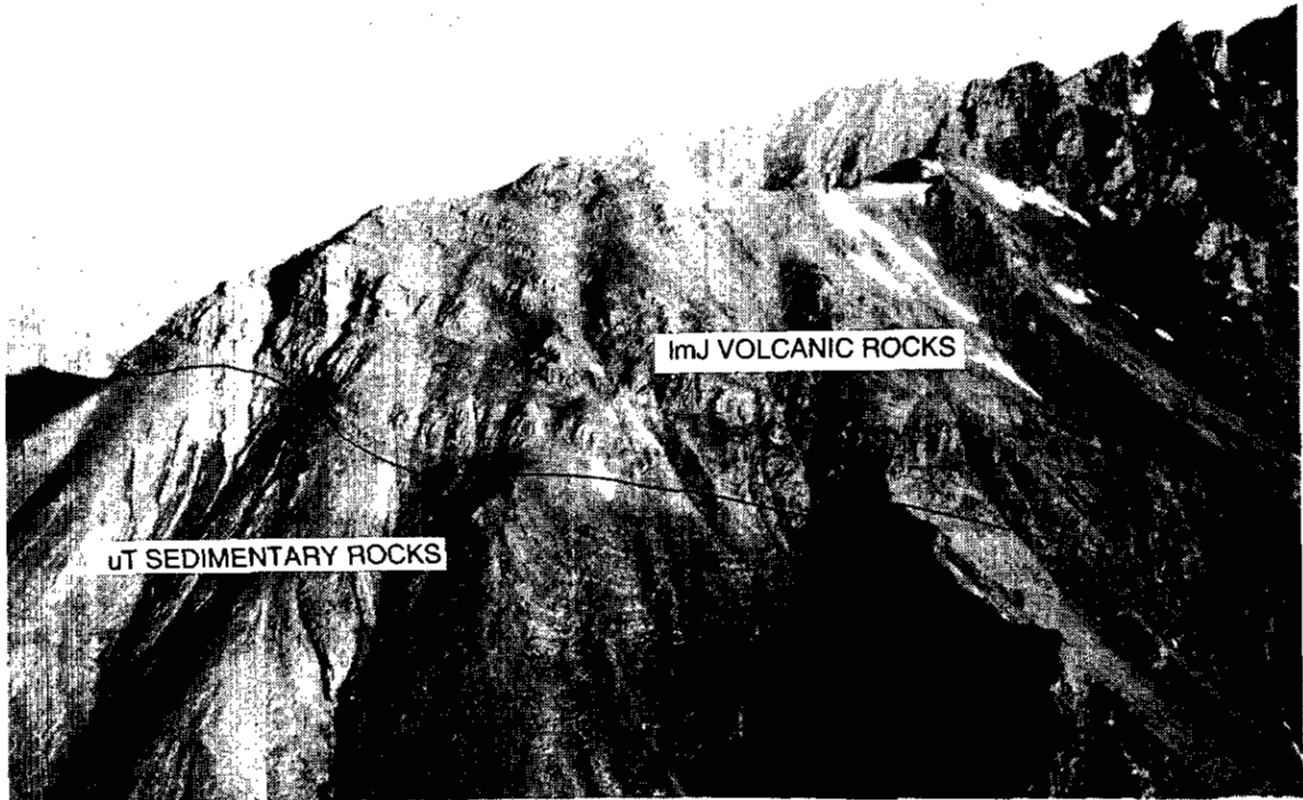


Photo 2-15. View northwest to prominent angular unconformity separating folded (steeply dipping, northeast-verging overturned beds) and faulted Upper Triassic (Norian) Stuhini Group siltstone and sandstone (unit uTSs2) from gently dipping Lower to Middle Jurassic Hazelton Group volcanoclastic rocks and flows (unit lmJHv); ridge between Strata and Quattrin creeks. U-Pb sample location shown by "x" on photograph, the 185 ± 7-1 Ma date constrains deformation as pre-Toarcian. Note the relatively flat contact (subdued relief) relative to the high relief shown in Photo 2-14, 12 kilometres north-northwest.

The massive and locally flow banded, fragmental dacite contains scattered very fine grained plagioclase phenocrysts altered to calcite. The uppermost part of the dacite unit, exposed directly south of Crocus Mountain, is a green-weathering, plagioclase-rich, crystal lithic tuff that is locally welded. This tuff yielded too few zircons to obtain a meaningful U-Pb date (J.K. Mortensen, written communication, 1992). The tuff contains limestone fragments that have similar textures to an overlying limestone unit 10 metres thick. The creamy grey weathering limestone is massive to thickly bedded with bivalve fragments throughout. Tuffaceous wacke (unit lJHs) above the limestone interfingers with lesser, brown-weathering amygdaloidal andesite flows.

LIMY WACKE (Unit lJHs)

The recessive, poorly exposed buff-weathering limy wacke forms a discontinuous horizon immediately south of Crocus Mountain. The recessive nature of these sedimentary rocks may mean they are more extensive than currently mapped. The unit comprises limy wacke, turbiditic ash tuff and minor lithic lapilli tuff. Rare, black silty shale lenses were processed unsuccessfully for radiolaria (Appendix 4). Dark purple to maroon pyroxene and plagioclase-phyric andesite flows of unit lmJHv overlie the wacke horizon.

The volcanic rocks above the limestone appear to be submarine based on their predominant green colour, lapilli tuff with glauconite-rich matrix and intercalated limy beds bearing marine bivalve fragments.

The wacke contains ammonite and *Weyla* fragments, belemnites, abundant terebratulid brachiopods and scarce bivalves. The ammonite fragment suggests a Toarcian age (Tipper, 1989; locality F1 on Figure 2-12; Appendix 1).

ANDESITE FLOWS AND TUFF (Unit lmJHv)

Most of the section between Strata and Quattrin creeks consists of a series of andesite tuffs, breccias and flows. The thick flows (up to tens of metres) occur in subequal quantities with tuffs. Crystal-lithic andesite tuff-breccia (Photo 2-17) and lapilli tuff are commonly maroon to brick red and less typically grey-green to mottled maroon and green. They contain angular volcanic country rock fragments up to 1 metre in diameter. Thin to thick-bedded units of poorly indurated, flaggy, maroon, mauve and pale green ash and fine-grained lapilli tuff are commonly interbedded with coarse-grained tuffaceous rocks. Pale grey grit and maroon tuffaceous grit, probably derived from underlying plutonic rocks, crop out northeast of Yehiniko Lake and on Mount Kirk. The most common flows are pyroxene and plagioclase-phyric andesite. They are typically grey-green with a faint dark purple or maroon hue and are locally flow banded and amygdaloidal (zeolite, calcite, chlorite, epidote, quartz, pyrite). The intervening plagioclase crystal lithic lapilli tuff is locally weakly welded.

The Kirk Creek section comprises about 150 metres of flows and tuffs (not studied) overlain by 100 metres of aphyric, amygdaloidal basalt flows and mauve to red vol-

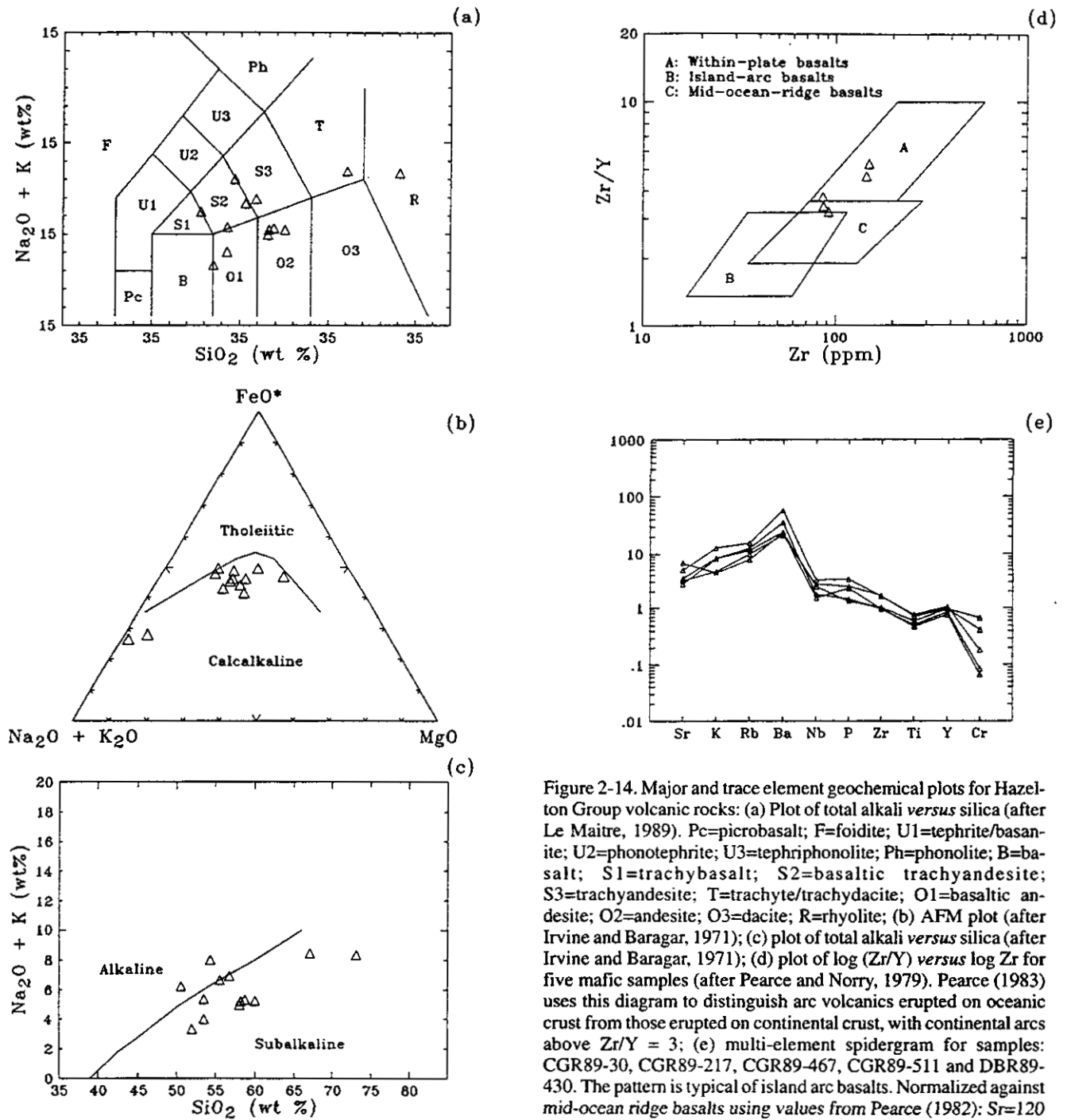


Figure 2-14. Major and trace element geochemical plots for Hazelton Group volcanic rocks: (a) Plot of total alkali versus silica (after Le Maitre, 1989). Pc=picrobasalt; F=foiidite; U1=tephrite/basanite; U2=phonotephrite; U3=tephriphonolite; Ph=phonolite; B=basalt; S1=trachybasalt; S2=basaltic trachyandesite; S3=trachyandesite; T=trachyte/trachydacite; O1=basaltic andesite; O2=andesite; O3=dacite; R=rhyolite; (b) AFM plot (after Irvine and Baragar, 1971); (c) plot of total alkali versus silica (after Irvine and Baragar, 1971); (d) plot of log (Zr/Y) versus log Zr for five mafic samples (after Pearce and Norry, 1979). Pearce (1983) uses this diagram to distinguish arc volcanics erupted on oceanic crust from those erupted on continental crust, with continental arcs above Zr/Y = 3; (e) multi-element spidergram for samples: CGR89-30, CGR89-217, CGR89-467, CGR89-511 and DBR89-430. The pattern is typical of island arc basalts. Normalized against mid-ocean ridge basalts using values from Pearce (1982): Sr=120 ppm; K₂O=0.15%; Rb=2 ppm; Ba=20 ppm; Nb=3.5 ppm; P₂O₅=0.12%; Zr=90 ppm; TiO₂=1.5%; Y=30 ppm; Cr=250 ppm.

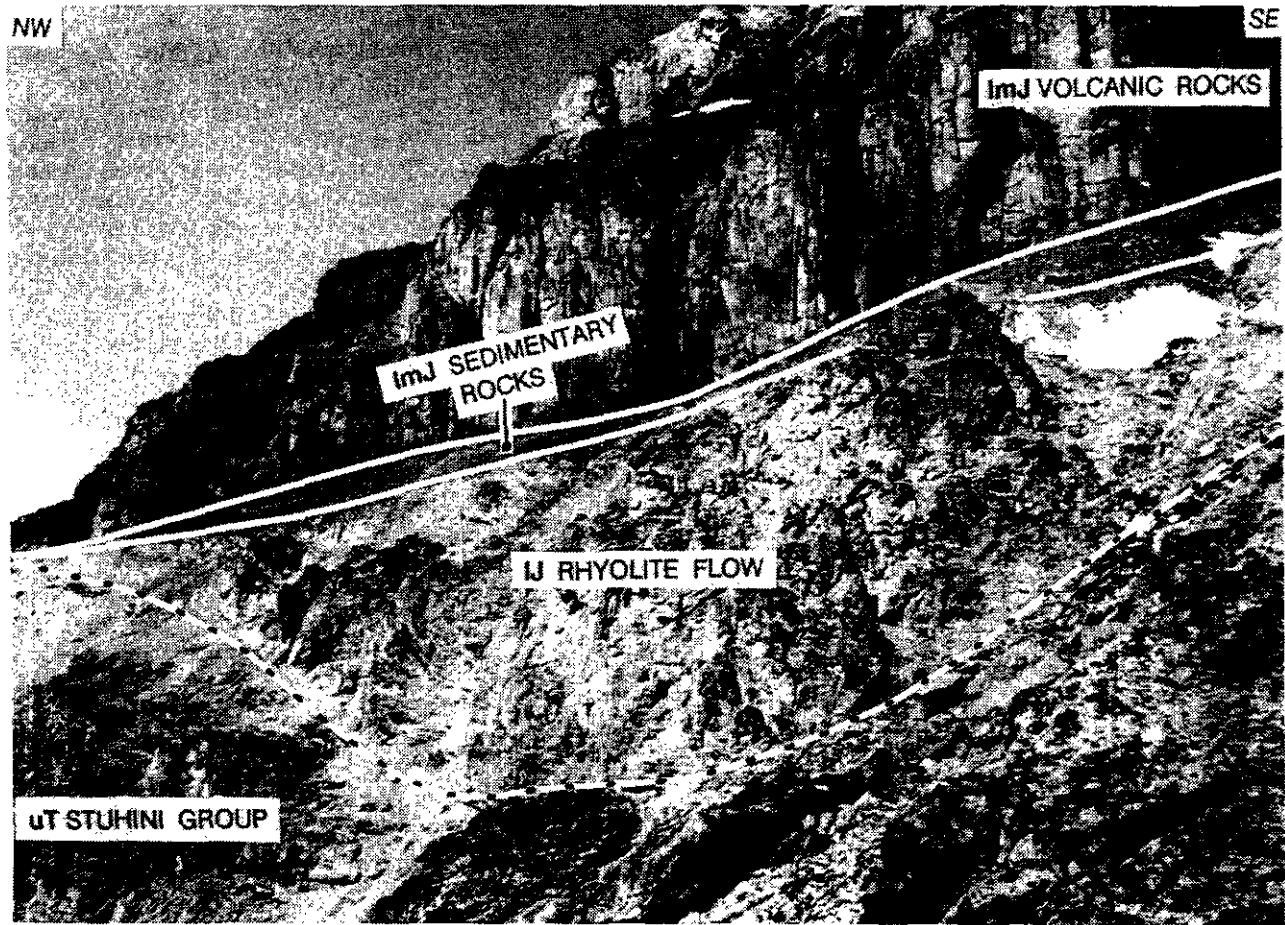


Photo 2-16. View northeast to Stuhini Group rocks (unit uTSv) overlain unconformably by pale-weathering rhyolite flow (unit IJHd) which is in turn conformably overlain by a relatively thin layer of gently dipping Toarcian sedimentary rocks (unit IJHs) and by prominent cliffs of columnar jointed Lower to Middle Jurassic basaltic andesite flows (unit ImJHv) northeast of Strata Creek.

caniclastic rocks (Divisions D-1 and D-2 on Photo 2-18, Figure 2-13). The flows, up to 5 metres thick, are dark brown to faintly maroon, with characteristic abundant and large amygdules (filled with calcite, chlorite and zeolites). Flow margins are commonly brick red, finer grained (chilled) and locally brecciated (flow-top breccia). They are intercalated with and overlain by mauve epiclastic tuffs. The flows and tuffs thicken to the northeast. The well bedded, medium to coarse-grained epiclastic rocks display normal grading, therefore the section is right way up. The epiclastic beds are overlain abruptly by the rhyolite flow (unit ImJHr on Figures 2-12, 2-13; division D-3 on Photo 2-18).

RHYOLITE (Unit ImJHr)

Distinctive pink to brick-red weathering, hematitic flow-banded rhyolite overlies epiclastic rocks in the Kirk Creek cirque and overlies andesite flows west of Mount Kirk (unit ImJHr on Figures 2-12, 2-13; division 3 on Photo 2-18). The crudely columnar jointed flow attains a maximum thickness of 50 metres and was traced over 2 kilometres along strike, making it an important local marker (Figure 2-12). Northwest-striking flow banding varies in northeast dip between 20° and 50° and locally forms spectacular root-

less flow-folds. The rhyolite is aphanitic, to locally auto-brecciated, with rare spherical vesicles lined with silica. Flow banding and local welding, and the tongue-like geometry suggest that it may represent an ignimbrite deposit. Rhyolite is overlain by coarse, heterolithic volcanic breccia, presumably debris-flow deposits.

BASALT (Unit ImJHb)

The highest units in the Kirk Creek section include dark grey to dark green plagioclase and coarse pyroxene-porphyrific flows that form the resistant ridge (division D-4 on Photo 2-18). Flows are thicker and epiclastic beds are absent in this part of the section, in contrast to division 2. Dark green and lesser maroon, carbonate-cemented amygdaloidal olivine basalt pillow breccia (Photo 2-19) and rare bioclastic limestone lenses comprise the highest unit farther southeast, north of Crocus Mountain.

The uppermost Kirk Creek flows have clinopyroxene phenocrysts with smaller inclusions of phlogopite, indicating their high-potassium, alkaline affinity. Basalt flows north of Crocus Mountain contain olivine (about 5%) altered to serpentine and chlorite, and veinlets and amygdules are filled with chlorite, albite and calcite.



Photo 2-17. Maroon plagioclase crystal rich, lithic lapilli tuff with angular lapilli and blocks of andesite (CGR89-217; unit lmJHv). The dominant lithology along the ridge between Strata and Quatrin creeks, forming most of unit lmJHv.

CHEMISTRY

Twenty-one samples of flows and sills were analyzed for major and trace elements, with eight of these being discarded for classification purposes in accordance with the alteration screening criteria set out in Appendix 9. The thirteen relatively unaltered samples span a wide compositional range, including basaltic andesites, andesites, basaltic trachyandesites, trachyandesite, trachyte and rhyolite (Figure 2-14a). The suite is dominantly subalkaline, with two samples from division 4 (unit lmJHb) on the Kirk Creek section plotting in the alkaline field (Figure 2-14c). All are calcalkaline on the AFM plot (Figure 2-14b). The broad compositional range and lack of rocks of shoshonitic affinity distinguish the Hazelton Group from Stuhini Group.

A trace element spidergram of five of the most mafic samples, normalized to mid-ocean ridge basalt, exhibits a profile very similar to the Stuhini Group, but with slightly higher niobium and zirconium concentrations and a lower phosphorus spike (Figure 2-14e). The strong lithophile element enrichments are probably related to subduction in an arc setting (Pearce, 1983; Marsden and Thorkelson, 1992), while the slight niobium enrichment and relative concentrations of niobium, zirconium and yttrium establish a subtle within-plate signature (Pearce, 1983). This suite plots above the oceanic-arc field on the Zr versus Zr/Y plot (Figure 2-14d), with three samples in the within-plate field. These chemical signatures are compatible with a variety of tectonic scenarios. In addition, the process of eruption through two older volcanic successions (Stikine assemblage and Stuhini Group) may have had the effect of increasing incompatible element enrichments through crustal contamination. The

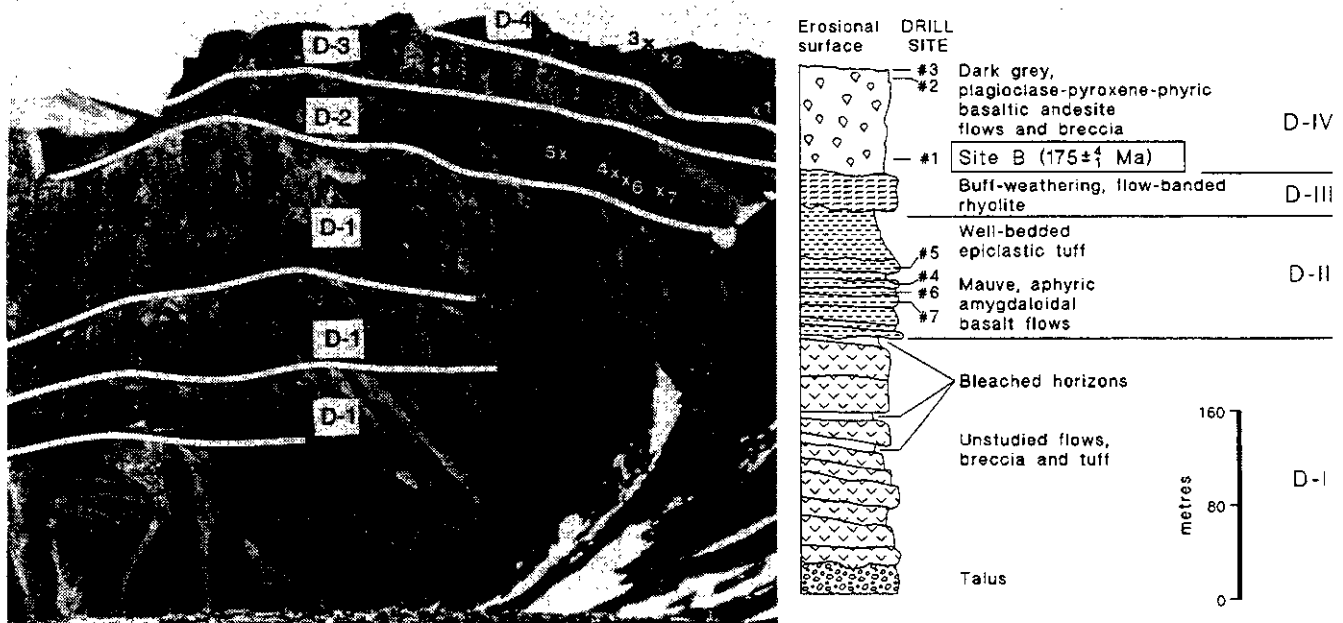


Photo 2-18. View northeast to nearly flat lying lava flows and volcaniclastic rocks characteristic of the Jurassic succession (unit lmJHv), 3 kilometres south of Mount Kirk. The rhyolite flow (unit lmJHr) that was sampled for U-Pb dating is identified as Site B. Paleomagnetic drill sites shown in the right-hand column are described in Vandall *et al.* (1992).



Photo 2-19. Basalt fragment displaying bread-crust texture (unit lmJHb; DBR89-430), possibly a bomb, immediately northwest of Crocus Mountain. Most of the basalts found at the top of the Hazelton succession are massive.

discrimination among possible tectonic settings based on the composition of rocks is therefore ambiguous.

CONTACT RELATIONSHIPS BETWEEN JURASSIC AND TRIASSIC UNITS

In most places Lower to Middle Jurassic rocks rest with angular unconformity on older rocks. The unconformity is particularly well exposed 3 kilometres southeast of Crocus Mountain, where the angular relationship between overlying Jurassic tuffaceous rocks and underlying upper Norian turbidites approaches 90°. Isolated limestone pods distributed along the contact are interpreted to represent remnants of Triassic limestones. The unconformity is locally marked by a maroon polymictic boulder conglomerate, west of Mount Kirk (Photo 2-20) and east-southeast of Crocus Mountain. Relief on the unconformity is variable (Photos 2-15; 2-16), but locally appears to be as much as 500 metres over short (1000 m) distances (Photo 2-14). Northeast of Yehiniko Lake, maroon tuff and minor tuffaceous grit rest nonconformably on the Nightout pluton. The schematic relationship is shown in Figure 2-15.

An angular unconformity between moderate to steeply dipping Stuhini Group volcanic rocks and gently dipping Lower Jurassic (Logan and Drobe, 1993a) polymictic conglomerate is exposed along the eastern edge of the map area.

AGE AND CORRELATION

The age of the volcanic rocks is based on two zircon U-Pb dates, macrofossil ages, and on intrusive relationships with the Saffron pluton (Table 2-1). A U-Pb zircon age of $185 \pm 7/-1$ Ma, Toarcian (M.L. Bevier *in* Brown *et al.*, 1992c, "Sample A"), from an andesite flow breccia (unit lmJHv) constrains the age of this unit. A whole-rock K-Ar date of 148 ± 5 Ma from an equivalent stratigraphic level, most likely is partially reset. A U-Pb zircon date of $175 \pm 4/-1$ Ma, Aalenian (W.C. McClelland *in* Brown *et al.*, 1992c, sample B), was obtained from pink flow-banded rhyolite (unit lmJHr) where a whole-rock K-Ar date of 166 ± 6 Ma from an andesite directly above the rhyolite is reset, and not surprisingly, is concordant with K-Ar dates obtained from the Saffron pluton. A third sample of flow-banded dacite (unit lmJHd; sample C on Figures 2-12, 2-13) yielded an indeterminate U-Pb date (J.K. Mortensen, written communication, 1992). Biotite from granite and hornblende from quartz monzodiorite of the Saffron pluton yield concordant K-Ar ages of 162 ± 7 Ma (localities I and II, Figure 2-12).

Ammonite fragments, belemnites, brachiopods and scarce bivalves from three new fossil localities have been assigned Toarcian ages (H.W. Tipper *in* Appendix 1). Prior to this study, fossils from one locality near Mount Kirk were interpreted to be Jurassic by Kerr (locality F28 of Kerr, 1948a) and his locality F29 may be within the same unit.

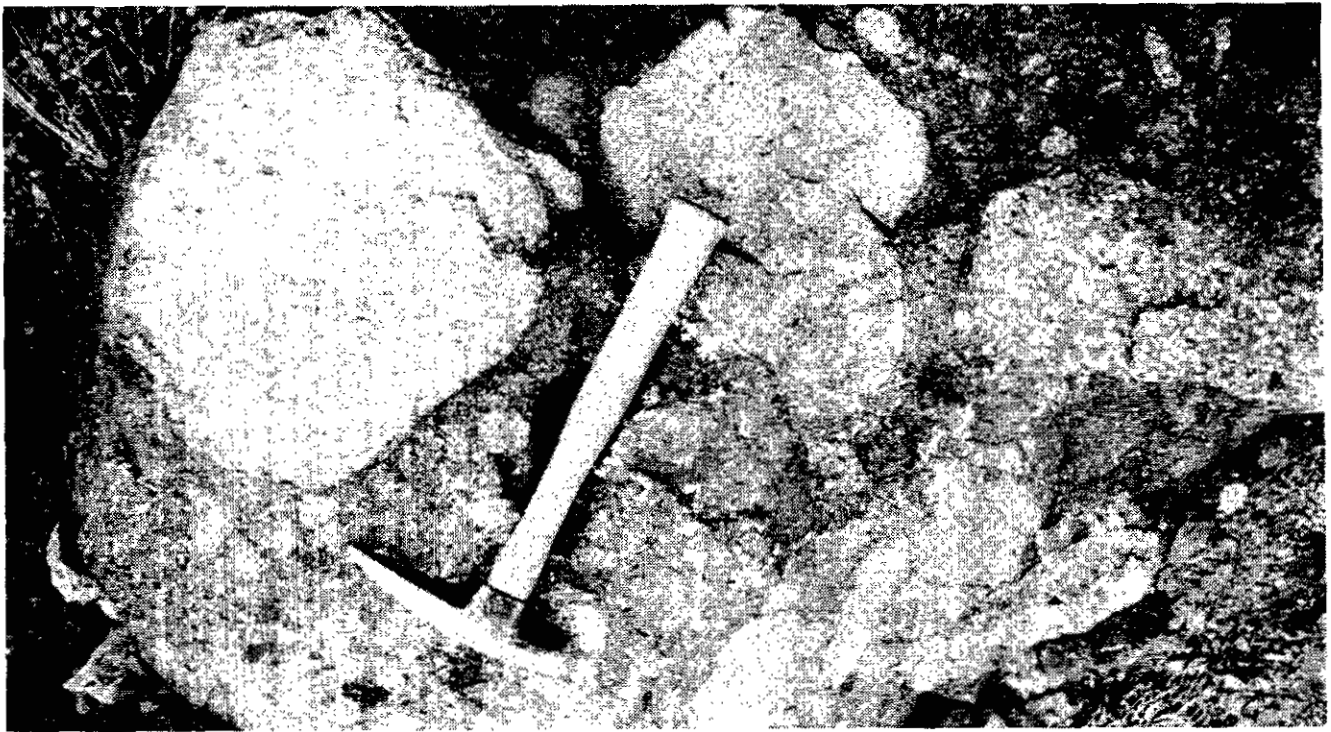


Photo 2-20. Lower Jurassic tuff-breccia (unit ImJHv) supporting accidental lithic fragments of bladed-plagioclase porphyritic basalt (probably from unit uTSv-p), north of Helveker Creek (CGR89-173).

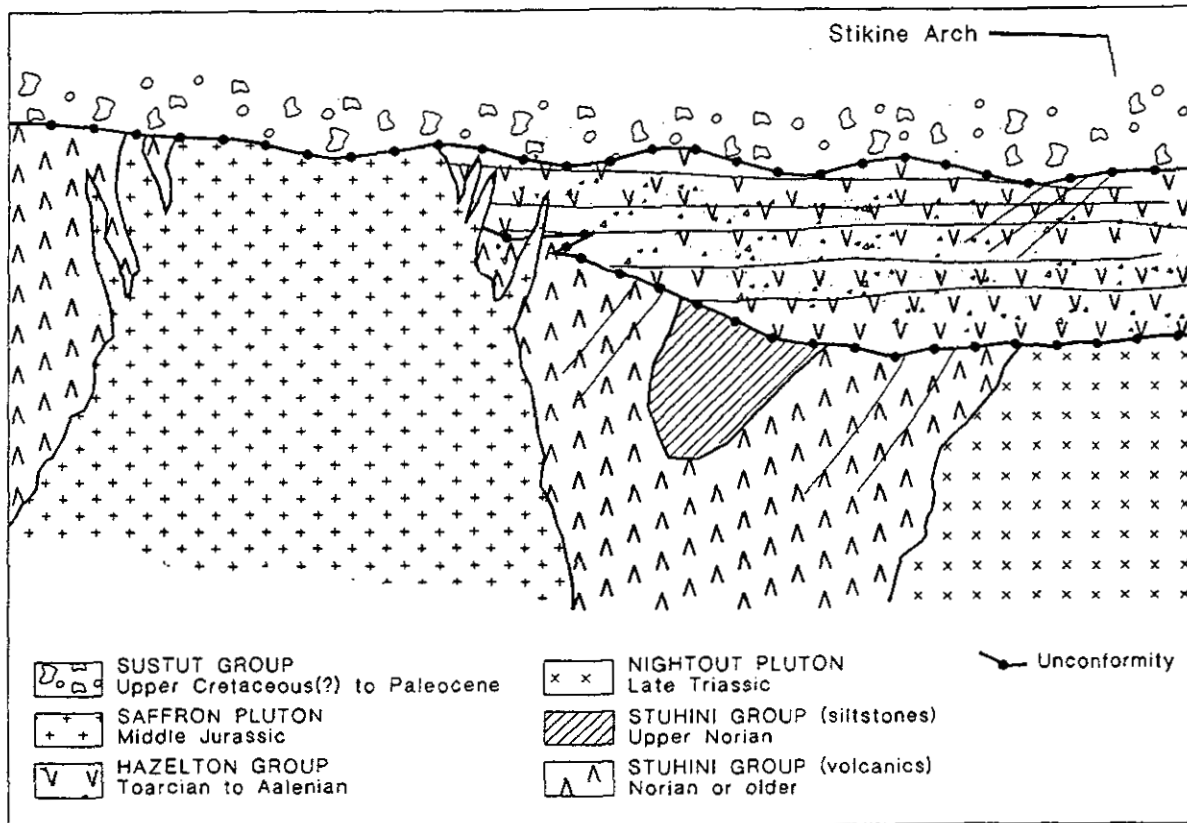


Figure 2-15. Schematic diagram illustrates unconformable relationships between the Upper Triassic Stuhini Group, Jurassic Hazelton Group and Upper Cretaceous to Paleocene Sustut Group, and their relation to the Late Triassic Nightout and Middle Jurassic plutons. Rocks of the Hazelton outlier are intruded by the Saffron pluton which is in turn unconformably overlain by conglomerate of the Sustut Group. These relationships are similar to that for the Stikine Arch about 100 kilometres to the east (cf. Thomson *et al.*, 1986).

Based on lithology and age, the limy wacke (unit IJHs) correlates with the lower member of Salmon River Formation, of Anderson and Thorkelson (1990), in the Iskut River area, and overlying strata with the upper member.

DEPOSITIONAL ENVIRONMENT

Rapid facies changes within the Hazelton Group suggest that subaerial and marine deposition were contemporaneous. For example, on the ridge 1.5 kilometres north of Strata Mountain, a southwest to northeast facies transition occurs between maroon (subaerial) andesite flows and tuff-breccia, and pale green (subaqueous) andesite ash and dust tuff, green andesite flows with interbedded dark green siltstone and arkosic greywacke containing belemnites, bivalves and rare ammonites. In turn, the marine rocks grade vertically and laterally (farther to the northeast) into maroon tuff-breccia. This suggests that contemporaneous subaerial and marine deposition occurred in an emergent island setting. The flow-banded rhyolite and maroon andesite flow tops and bottoms are interpreted as subaerial features. Overall, subaerial rocks appear to dominate the Jurassic package, but marine rocks are also exposed southeast of Strata Mountain (argillite, siltstone, fossiliferous greywacke, carbonate-cemented amygdaloidal basalt pillow-breccia and rare bioclastic limestone lenses), north of Mount Kirk (mauve lapilli tuff with limestone lenses) and northwest of Mount Kirk (green, carbonate-cemented arenaceous sandstone, siltstone and polymictic cobble conglomerate, and pale grey massive limestone).

UPPER CRETACEOUS(?) TO PALEOCENE SUSTUT GROUP (Unit KTS)

Coarse-grained clastic and subordinate fine-grained tuffaceous rocks, correlated on a lithologic basis with the Brothers Peak Formation of the Sustut Group (Souther, 1972; Eisbacher, 1974), are exposed in a belt that trends northwest from near Yehiniko Lake to Mount Helveker, and in outliers southwest of the belt at Mount Kirk and Strata Mountain (Figure 2-16; Photo 2-21). At Mount Helveker, a nearly complete section is up to 500 metres thick. Kerr (1948a) mentions an exposure of the basal contact at this locality but it was not found. Most of Yehiniko valley appears to be underlain by Sustut Group sediments, but they are poorly exposed. Prior to Quaternary or late Tertiary erosion, the group would have formed a continuous unit, from Strata Mountain to Yehiniko Creek (Figure 2-16), forming a basin at least 20 kilometres wide.

Very poorly indurated, matrix-supported polymictic cobble to boulder conglomerate, in places resembling Quaternary glaciofluvial deposits, characterize the Sustut Group in the project area. Feldspathic greywacke, siltstone and rare shale and conspicuous pale-coloured rhyolite tuff are subordinate. Basalt flows are rare. Brick-red, brown and grey conglomerates are massive to moderately well bedded and locally contain crossbeds and foreset beds (Photo 2-22). They are poorly sorted but clasts are well rounded, except in Yehiniko Creek valley, where clasts, locally up to 3 metres in diameter, vary from well rounded to subangular. Clasts are derived from older stratified and plutonic rocks, and on Mount Kirk include distinctive pink flow-banded rhyolite derived from immediately underlying Aalenian volcanic rocks. The conspicuous white bull quartz clasts (up to 10%) are of unknown provenance. Granitic clasts resemble Ye-

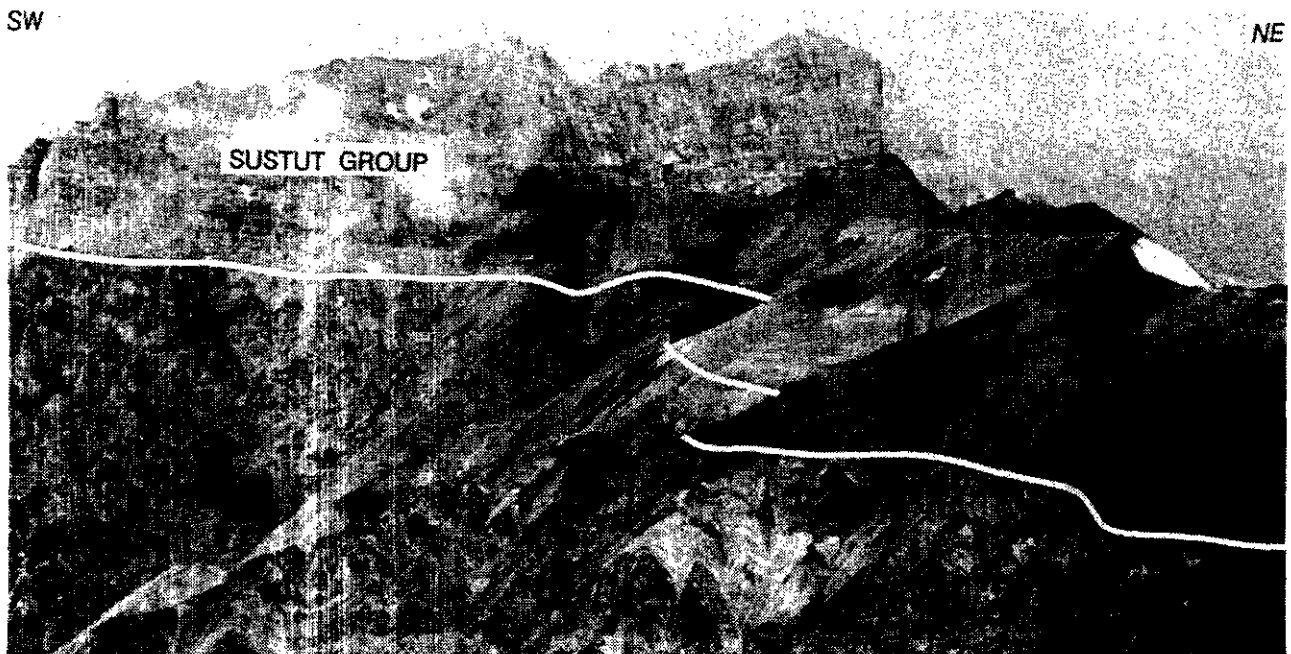


Photo 2-21. View northwest to Strata Mountain which comprises Sustut Group conglomerate and sandstone (unit KTS) unconformably deposited on altered Lower to Middle Jurassic volcanic rocks (unit ImJHv) and Middle Jurassic (?) dikes. The light coloured areas below the unconformity are limonitic, altered volcanic rocks and dikes.

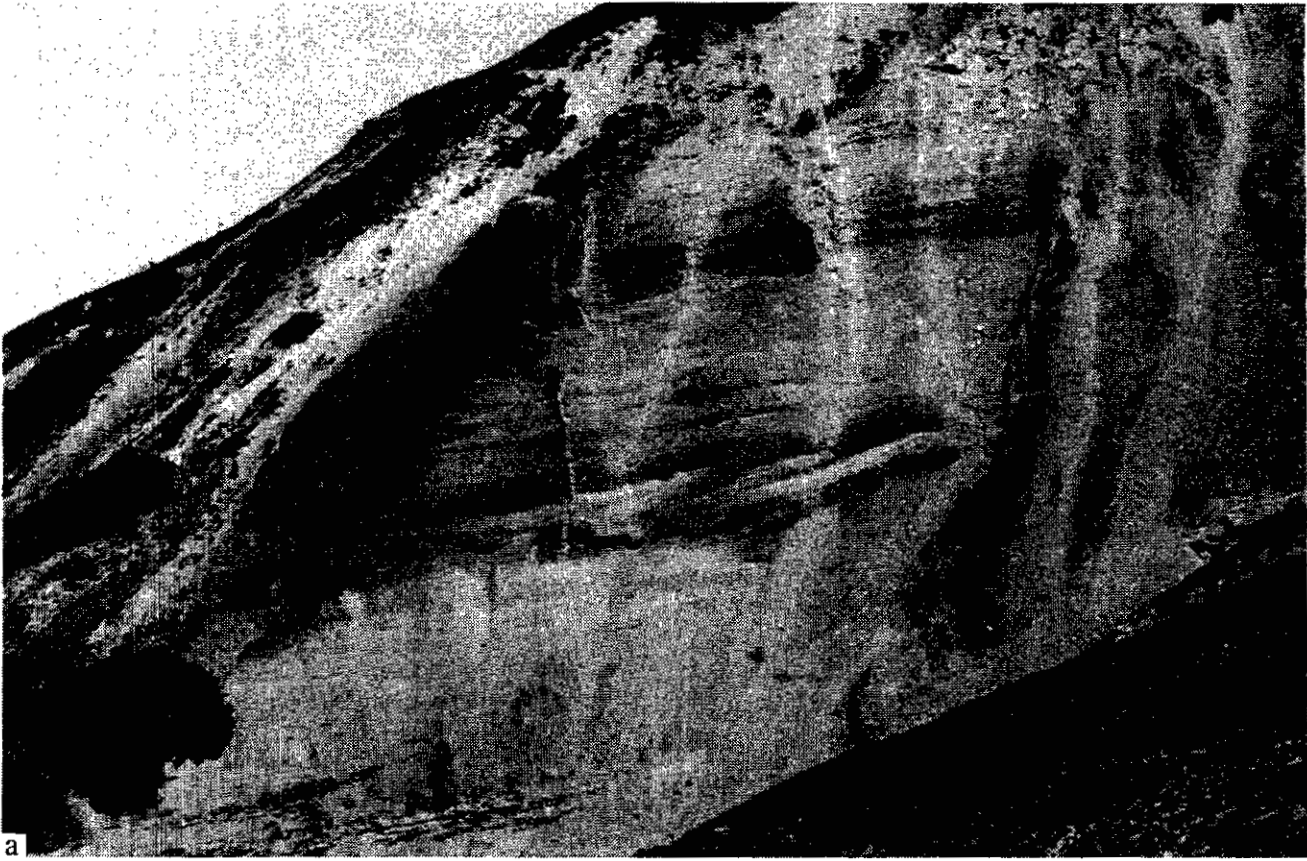


Photo 2.22 (a)



Photo 2-22 (b).



Photo 2-22. Typical conglomerates that dominate the Upper Cretaceous to Paleocene Sustut Group in the Mount Helveker and Yehiniko valley area: (a) View northeast to medium to thick-bedded polymictic conglomerate (unit KTS) with rare interbeds of rhyolite tuff, on north flank of Mount Helveker. Foreset beds in centre of photograph indicate north to northeast paleocurrents. Narrow dacite and basalt dikes, feeders to overlying Sloko volcanic rocks, cut conglomerate. (b) Polymictic conglomerate intruded by basalt dikes on the southern flank of Mount Helveker (DBR89-3). (c) Typical poorly sorted, poorly indurated, matrix-supported polymictic conglomerate showing weak imbrication of clasts, southeast flank of Mount Helveker.

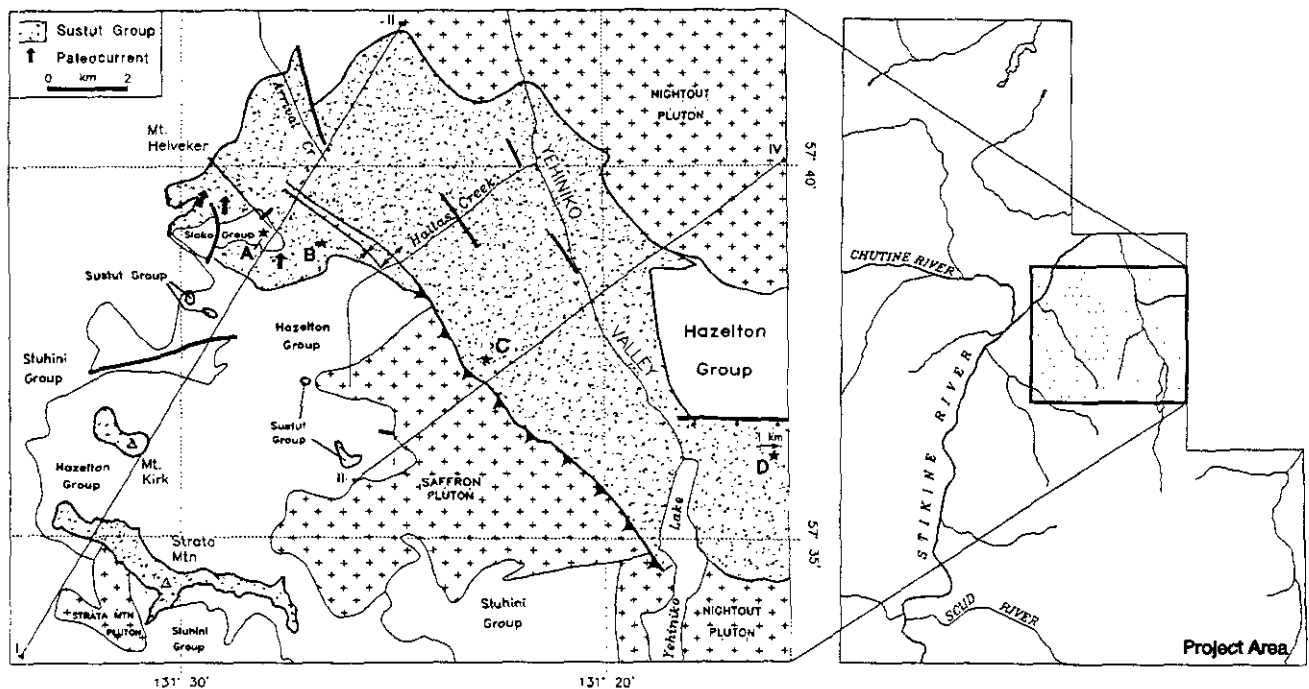


Figure 2-16. Distribution of Sustut Group, paleocurrent directions and age constraints. The key areas discussed in text are indicated. A = 43.8 ± 1.7 Ma hornblende K-Ar date; B = 51.6 ± 1.8 Ma whole-rock K-Ar date; C = 85.6 ± 3.0 Ma biotite K-Ar date; D = Paleocene palymorphs.

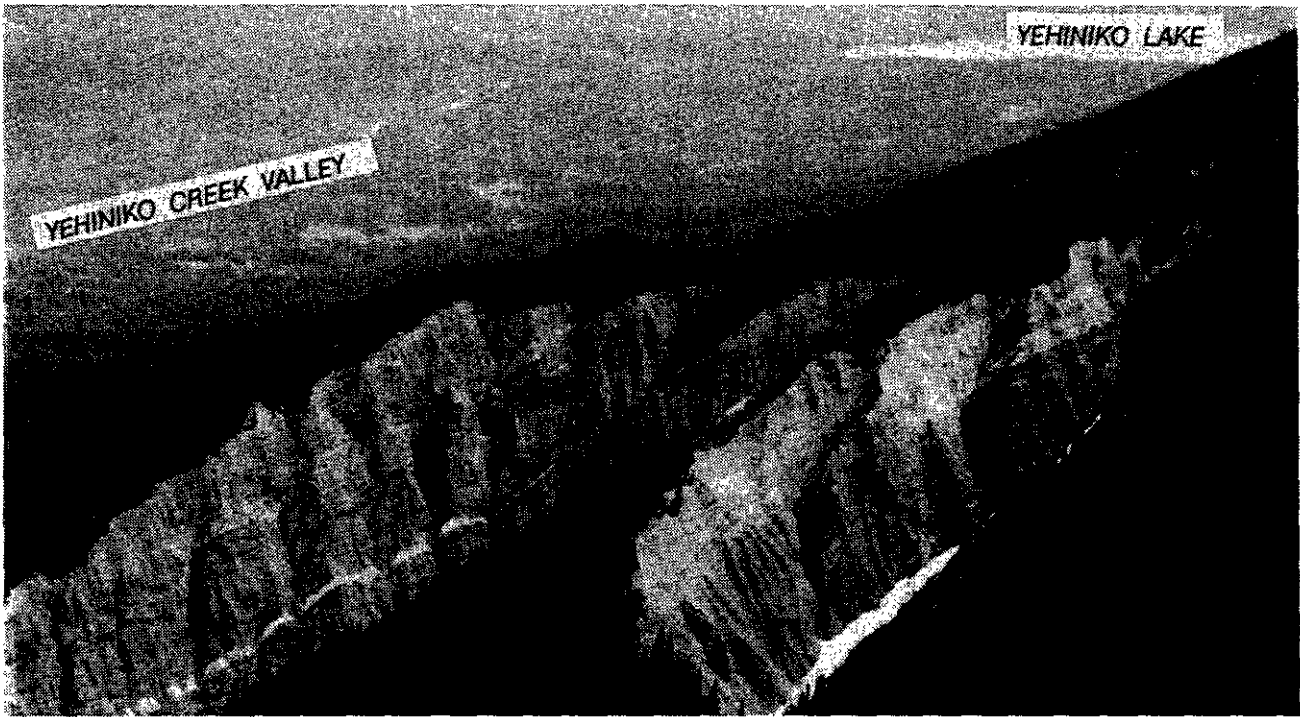


Photo 2-23. View southeast to bedded Sustut Group conglomerate (unit KTS) with a prominent layer of white rhyolite tuff (subunit t; DBR89-24 area; see Figure 2-17 for detailed stratigraphy).

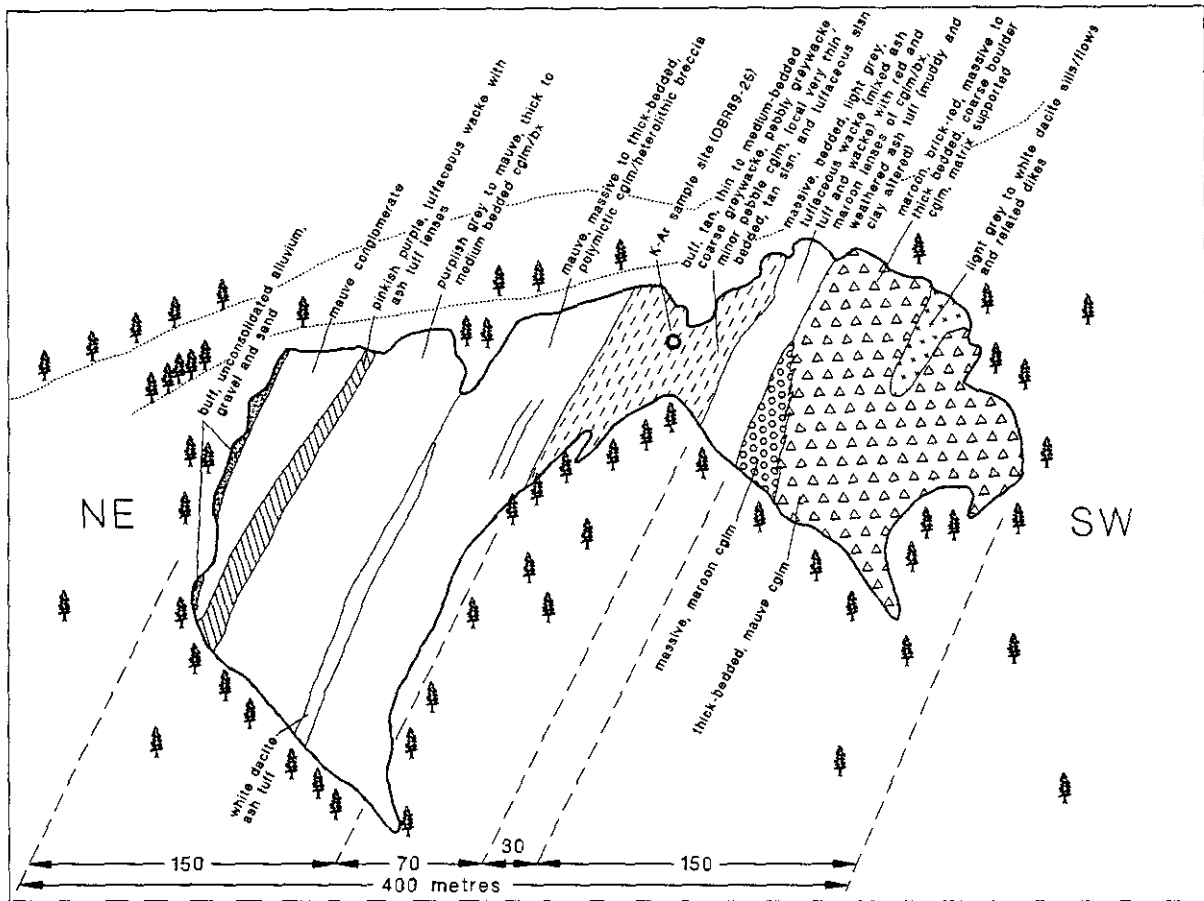


Figure 2-17. Schematic sketch of key exposure of the Sustut Group northwest of Yehiniko Lake, location C on Figure 2-16 (see Photo 2-23).

hiniko, Saffron and Sawback plutons. If clasts of the Sawback pluton are present, it restricts the age range of the conglomerates to post-Eocene. Clasts are commonly surrounded by a rim of maroon, oxidized material. Coaly plant stems, deciduous leaves and wood fragments occur locally. Sandstone lenses and beds are buff, brown, pale green, grey, maroon and olive, and locally contain fresh biotite. Thin but prominent, white, mauve and pale green, biotite quartz-eye rhyolite to rhyodacite ash to lapilli tuff units, up to 10 metres thick and locally welded, are in places interbedded with conglomerate (Photo 2-23; Figure 2-17).

Sustut Group rocks on Strata Mountain, so named for its prominent horizontal beds of laterally continuous, massive to thick bedded greywacke and polymictic conglomerate, have slightly different characteristics from west to east. The western facies, forming a rugged ridge, is more resistant, thick to medium-bedded, dull brown weathering, coarse greywacke and cobble conglomerate, with rare dacite sills and/or flows. The basal beds were described by Kerr (1948a) as red sandstone and arenaceous shale deposited on a strongly weathered red erosional surface, possibly a preserved regolith. The eastern facies, forming a rounded ridge profile, is coarser, poorly indurated, maroon, matrix-supported cobble conglomerate. According to Kerr and in accord with our observations, the lower beds are dominated by Stikine assemblage pebbles, whereas the top of the section is largely plutonic material.

The Kirk Mountain outlier is dominated by maroon, matrix-supported cobble to boulder conglomerate. Polymictic conglomerate contains unique pink, flow-banded rhyolite clasts derived from immediately underlying Hazelton Group rocks. Its southeast flank is cut by plagioclase-porphyrific dacite dikes.

The Mount Helveker section comprises a lower maroon to mauve, volcanic-rich cobble conglomerate overlain by buff weathering conglomerate with predominant plutonic clasts (Salat and Noakes, 1979). Conglomerates are poorly sorted, poorly indurated, massive to medium-bedded and matrix supported. The lower conglomerate contains clasts of volcanic rocks, with lesser plutonic, quartz and sedimentary rocks. Clasts in the upper conglomerate are hornblende biotite granodiorite, hornblende biotite granite, pink potassium feldspar megacrystic granite (totalling approximately 85%), with the remainder comprising volcanic rocks, feldspathic greywacke and siltstone. The megacrystic granite clasts resemble Eocene granite from the Coast Belt. In general the section is a poorly sorted, coarsening-upward sequence with low-angle bedding, indicated by discontinuous feldspathic greywacke lenses. Bedding steepens to over 75° on the north flank of the mountain. A northeast-directed paleocurrent is presumed, however, this is based on only a few measurements of imbricated clasts and foreset beds. Salat and Noakes (1979) also indicate an east-northeast paleocurrent direction in both basal and upper conglomerate units. Local greywacke beds display eroded channels filled with cobble conglomerate. Chalky white to greenish grey, flaggy and friable crystal vitric rhyolite ash tuff beds, less than 4 metres thick but laterally continuous, are preserved between cobble conglomerate beds. The tuff contains fresh, black biotite crystal fragments, aligned parallel to bedding, very

fine grained relict glass shards, quartz and lithic fragments. Fine-grained hornblende dacite flows (or sills) and maroon plagioclase crystal lithic tuff are locally present. Basalt dikes, believed to be feeders to younger flows, cut the conglomerate and display red and maroon reaction fronts up to 2 metres from their contacts.

The headwaters of Hallas Creek are underlain by red to brick-red, poorly sorted polymictic conglomerate, both matrix and clast supported. Imbricated clasts indicate an east-northeast paleocurrent direction. Midway down Hallas Creek, well bedded greywacke with rare coalified tree trunk fragments, and columnar jointed rhyodacite flows and tuff overlie deposits of coarse angular volcanic fragments supported in a muddy matrix; fragments are up to 3 metres in diameter. The deposits are interpreted to be debris flows. Four kilometres farther to the northwest, in Arrival Creek, dull green plagioclase-porphyrific andesite flows and biotite quartz crystal lithic rhyolite tuff are interbedded with polymictic cobble conglomerate. Weakly welded crystal (biotite, plagioclase, quartz) vitric tuff contains relict glass shards.

Northwest of Yehiniko Lake, the Sustut Group sediments are well exposed in two parallel gullies (Photo 2-23; Figure 2-17). The steeply northeast dipping succession comprises red to maroon, polymictic cobble conglomerate and breccia overlain by buff-weathering, coarse sandstone and maroon conglomerate/breccia. Buff-weathering greywacke and cobble conglomerate are thick-bedded, laterally continuous deposits with graded bedding that indicates the succession is right way up.

Two kilometres to the northwest, clast imbrication suggests paleocurrents were to the northeast. Here, the sediments are also predominantly matrix-supported, dull brown, cobble to boulder conglomerate with rare pebbly sandstone interbeds. Clasts, in order of abundance, are biotite granite, green andesite, maroon plagioclase-porphyrific andesite, biotite hornblende granodiorite, foliated hornblende diorite, basalt and rare siltstone and quartz. Dacite clasts, lithologically and texturally similar to flows and sills within the Sustut Group itself, are also present. A light grey to pale green dacite lapilli tuff unit, up to 5 metres thick, lies between cobble conglomerate beds.

CHEMISTRY

Geochemical analyses for two possible flows and a volcanoclastic sample are tabulated in Appendix 8. Only one unaltered flow sample was plotted on Figure 2-18 together with samples of Sloko Group and Miocene basalt. It falls on the border of the andesite and basaltic andesite fields (Figure 2-18a). It is a calcalkaline, subalkaline rock on the AFM and alkali-silica plots (Figures 2-18c and b), and plots in the within-plate field on the Zr versus Zr/Y plot (Figure 2-18d).

CONTACT RELATIONSHIPS

The Sustut Group rests with angular unconformity on a pediment of Upper Triassic and Lower Jurassic volcanic rocks on Strata Mountain and Mount Helveker and on Lower Jurassic volcanic rocks on Mount Kirk (Photo 2-24; Figures 2-15, 2-16). An irregular, ankeritic or iron-manganese oxide weathered surface is described by Salat and

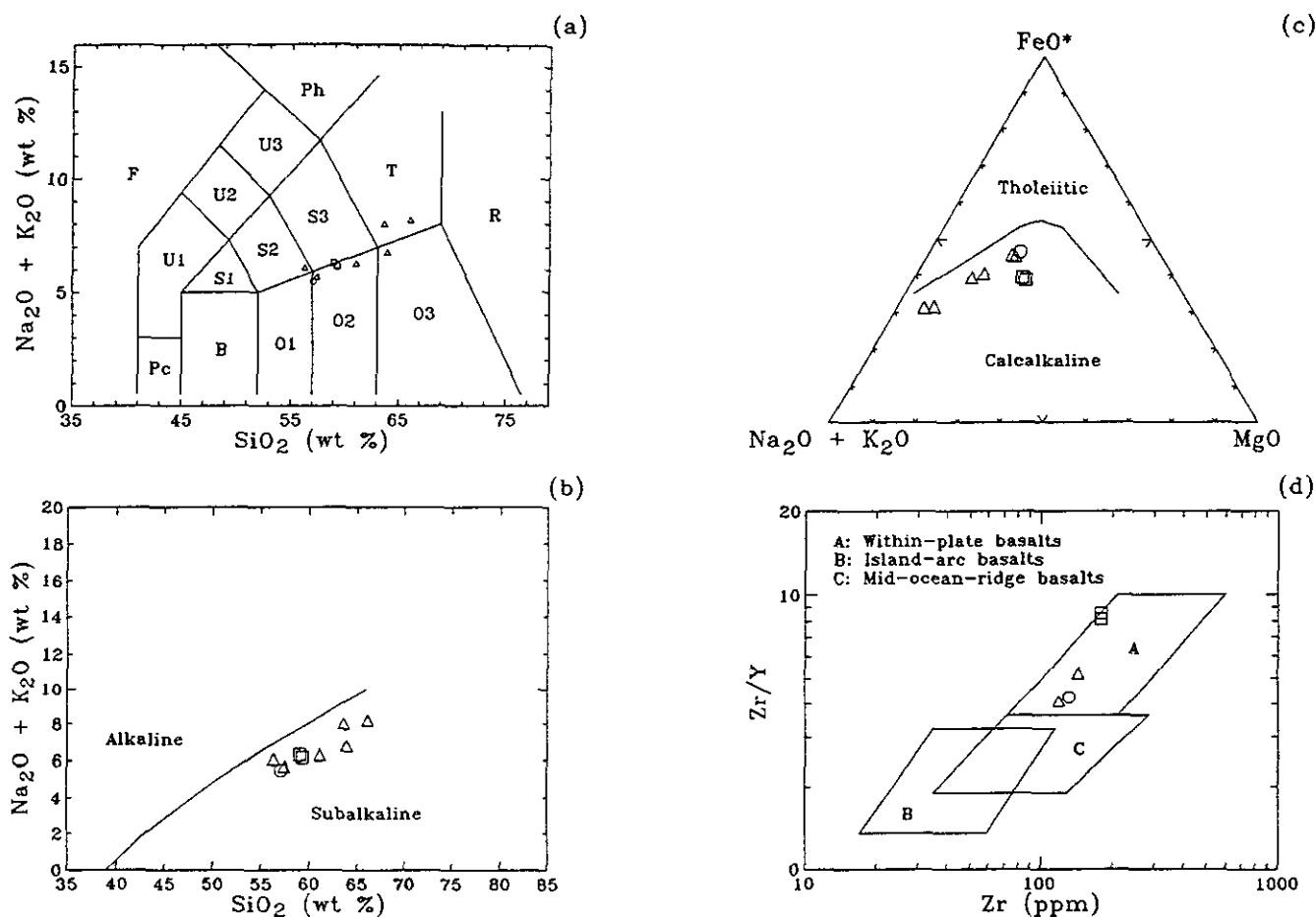


Figure 2-18. Major and trace element geochemical plots for Sustut Group (circles), Sloko Group (triangles) and Miocene (?) volcanics (squares): (a) plot of total alkali versus silica (after Le Maitre, 1989). Pc=picrobasalt; F=foiidite; U1=tephrite/basanite; U2=phonotephrite; U3=tephriphonolite; Ph=phonolite; B=basalt; S1=trachybasalt; S2=basaltic trachyandesite; S3=trachyandesite; T=trachyte/trachydacite; O1=basaltic andesite; O2=andesite; O3=dacite; R=rhyolite; (b) plot of total alkali versus silica (after Irvine and Baragar, 1971); (c) AFM plot (after Irvine and Baragar, 1971); (d) plot of $\log(Zr/Y)$ versus $\log Zr$ (after Pearce and Norry, 1979). Pearce (1983) uses this diagram to distinguish arc volcanics erupted on oceanic crust from those erupted on continental crust, with continental arcs above $Zr/Y = 3$.

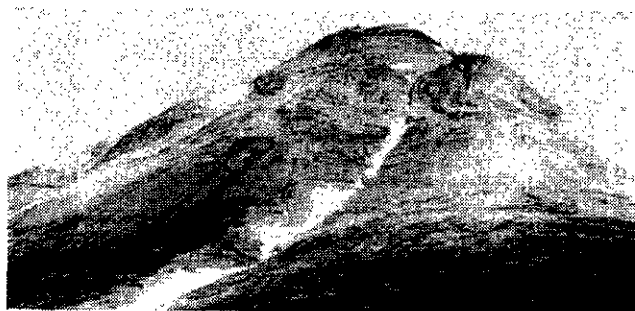


Photo 2-24. View northwest to Sloko volcanic rocks (unit TS) capping Mount Helveker. Uranium-bearing coalified wood fragments located in Sustut conglomerate (unit KTS), crop out in the snow-filled gully. Basalt dikes, feeders to the Sloko Group, can be seen cutting the Sustut Group conglomerate near the break in slope (see Photo 2-22b).

Noakes (1979) on the north flank of Mount Helveker. The estimated total stratigraphic thickness varies from 300 to 700 metres from the south to north flank of the mountain. The depositional surface as exposed on Strata Mountain is essentially flat from east to west (*i.e.* mature). The basal contact is 350 to 450 metres higher in elevation at Strata Mountain than on the southern flank of Mount Helveker (7.5 km farther north); the present slope of the basal contact is about 3°. East of Yehiniko Lake, subhorizontal conglomerate rests unconformably on the Nightout pluton.

Northeast of Yehiniko lake, Sustut Group sedimentary rocks are in contact with altered intrusive rocks and Hazelton volcanic rocks. Northwest of Yehiniko Lake, steeply northeast dipping strata of the Sustut Group are inferred to be faulted against the Yehiniko pluton. In the Mount Helveker area, basalt and felsite dikes, believed to be Sloko Group feeders, intrude the sediments with striking thermal

effects; conglomerate up to 2 metres from the basalt dikes is red and oxidized (Photo 2-22a). Sloko Group welded tuff sits unconformably on limonitic Sustut conglomerate.

AGE AND CORRELATION

Palynomorphs, extracted from a sample collected 4 kilometres east of the map boundary, suggest an Early Paleocene age, which is younger than the Brothers Peak Formation in its type area (Appendix 7). An additional ten samples were processed for palynomorphs but were unproductive. Fossil leaves of *Aspidiophyllum trilobatum* collected from exposures of possibly correlative strata 28 kilometres northeast of Mount Helveker, on Kunishina Creek, suggest a Late Cretaceous age (Kerr, 1948a). A Late Cretaceous biotite K-Ar date of 85.6 ± 3.0 Ma (Table 2-1) for a biotite-bearing wacke supports the Brothers Peak Formation correlation (*sensu stricto*). However, the biotite flakes have two possible sources: the Middle Jurassic Saffron pluton, or a primary volcanic origin. The unaltered crystals suggest a volcanic origin rather than erosion from a pluton and therefore the date is interpreted to reflect the time of deposition of the wacke. An Eocene whole-rock K-Ar date of 51.6 ± 1.8 Ma was obtained from biotite-bearing vitric rhyolite ash tuff (Table 2-1). The date is younger than expected, and may be the age of zeolite grade metamorphism related to Sloko Group volcanism. Eisbacher (1974) advocated that the Brothers Peak deposition continued into the Eocene after obtaining similar K-Ar results, however, these ages are interpreted here to be reset. If they represent depositional ages, then the rocks are correlative with Eocene sedimentary rocks of the "Tanzilla Canyon formation" exposed near Tuya River and Tanzilla Canyon (Read, 1984), and would be tentatively assigned to the Sifton assemblage (Gabrielse *et al.*, 1991b). Souther (1972) included beds at the summit of Strata Mountain with the Sloko Group because of the presence of primary felsic volcanic material. However, it is now apparent that these rocks are correlative with the Sustut Group, as originally advocated by Kerr (1948a). As presently interpreted, it is unlikely that some of the granitic clasts are derived from plutons as young as Eocene; however, closer examination of the clasts and U-Pb dating could confirm this.

DEPOSITIONAL ENVIRONMENT

A high-energy alluvial fan setting with rapid sediment input from areas of high relief is envisioned for the Sustut Group. A system of coalescing alluvial fans, and probably braided streams, received intermittent pyroclastic deposits and rare flows. It is inferred that a transverse drainage system was developed, where streams flowed directly from the uplifted source (Miall, 1981). The laterally continuous, thin white tuff horizons are believed to be episodic airfall deposits, preserved due to rapid burial by prograding alluvial fan sediments. The basin may have been fault controlled, as are numerous modern alluvial fans (Miall, 1981). Imbricated clasts and foreset beds at several localities suggest north to northeastward-directed paleocurrents, in accord with Kerr's (1948a) observation that clast size decreases to the northeast. Fossil wood fragments and deciduous leaf imprints indicate vegetated areas in a temperate climate, probably on

and adjacent to the fans. The progression from volcanic to plutonic-dominated clast compositions in conglomerates at Mount Helveker suggests initial erosion of Mesozoic volcanic strata and subsequently their related plutons, as advocated by Kerr (1948a). The large clast sizes and coarse greywacke interbeds indicate most of the sediments accumulated in the proximal alluvial fan facies. The red to maroon clast rims signify subaerial deposition.

Regionally, the deposition of the coarse clastic blanket suggests a tectonic event (development of the Coast Belt) that uplifted Stikine Terrane to the west (present Coast Belt), eroded older strata and plutons, formed a major erosional surface, and deposited coarse clastic material in the map area. The sediments represent late to postorogenic intermontane molasse deposition (Miall, 1978), in a basin that may have been related to strike-slip faulting in either compressional or tensional stress regimes, based on plate models for the Cordillera in Late Cretaceous to Paleocene time (Gabrielse, 1985). The preservation and distribution of the sediments mimics those at the mouth of Mess Creek (Souther, 1972) and southwest of the Grand Canyon of the Stikine River (Read, 1983, 1984). If this correlation is correct, then it implies that there was significant transtension west of the right-lateral related strain documented by Gabrielse (1985) for the Dease Lake area.

EOCENE SLOKO GROUP (Unit TS)

Eocene stratified rocks in the map area are characterized by chalky white, poorly indurated intermediate tuff, exposed only near the summit of Mount Helveker (Figures 2-19, 2-20; Photo 2-24). The well exposed section is between 150 and 275 metres thick and comprises a basal, gently dipping welded dacite tuff and breccia, overlain by porphyritic basaltic andesite flows (or sills?) and capped by hornblende-rich andesite breccia.

The basal white, grey and pale green, quartz-biotite crystal ash to lapilli dacite tuffs and ignimbrite are both welded and unwelded. Locally, prominent eutaxitic textures are defined by flattened fiammé. Individual cooling units are difficult to define. Intercalated pale green plagioclase-porphyritic dacite flows and flow breccias have irregular fractures and are locally columnar jointed. On the west side of Mount Helveker, welded tuff is overlain by brick-red volcanic breccia and well bedded lithic lapilli tuff, interpreted to be pyroclastic surge and flow deposits. They are overlain by light grey weathering hornblende and plagioclase-phyric dacite flows and sills. Lithologically similar dikes cut Sustut Group rocks on Mount Kirk, 6 kilometres to the southwest.

Overlying the dacite flows near the top of the south side of Mount Helveker are distinctive dull brown weathering, resistant, columnar jointed, pyroxene-plagioclase-porphyritic andesite flows and monolithic flow breccia. The cumulative thickness of the subhorizontal flows is about 75 metres, individual flows or sills are 2 to 5 metres thick (Photo 2-25). The top of Mount Helveker is capped by poorly indurated, recessive, light grey, pale to olive-green weathering, andesitic volcanic breccia and hornblende crystal lithic lapilli tuff. Hornblende crystals in the matrix and

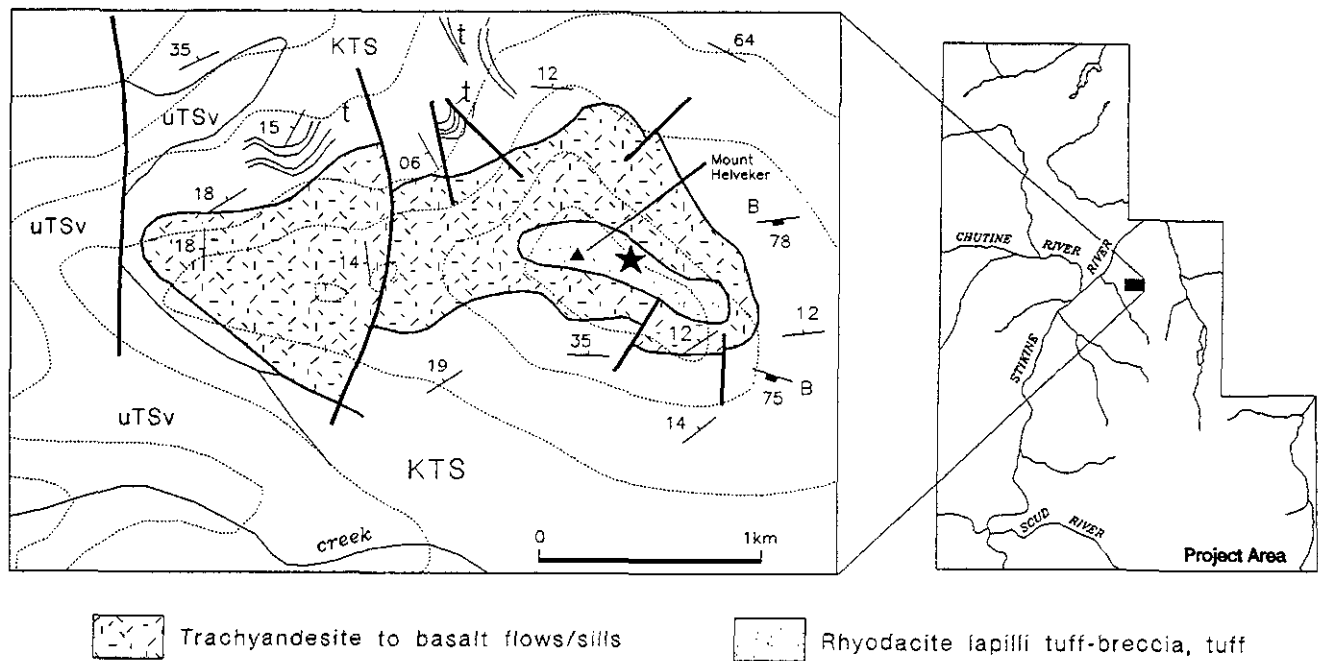


Figure 2-19. Distribution of Sloko volcanic rocks at Mount Helveker. Star depicts K-Ar sample locality.

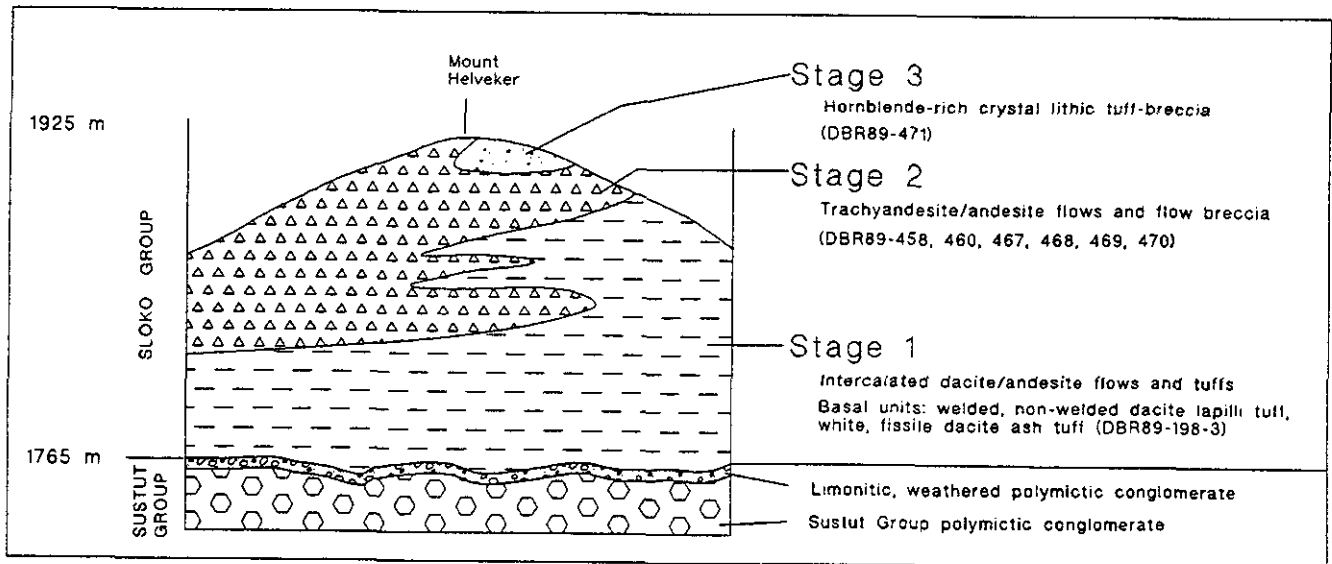


Figure 2-20. Schematic Sloko Group stratigraphic column based on the erosional remnant preserved at Mount Helveker. Sample numbers correspond to lithochemical samples in Appendix 8. Progression of Sloko Group volcanism at Mount Helveker is indicated by stages 1 to 3.

lithic fragments are unaltered, however, plagioclase grains and the matrix are clay-altered (Photo 2-26).

CHEMISTRY

Nine chemical analyses of Sloko rocks are given in Appendix 8, with two altered samples and one volcanoclastic sample being discarded from the suite used for chemical classification. The six remaining samples include rocks of andesitic to dacitic compositions (Figure 2-18a), with sub-

alkaline, calcalkaline affinities (Figure 2-18b, c). Two of the more mafic samples plot in the within-plate field on the Zr versus Zr/Y plot (Figure 2-18d).

On Mount Helveker, the lowermost dacitic to andesitic unit (stage 1: Figure 2-20) includes a basal trachytic or trachydacitic ash tuff. The middle unit (stage 2) is mainly andesitic, with one dacite sample and one basaltic trachyandesite. The andesitic rocks cluster near the boundary of the trachyandesite field, and may be characterized as medium

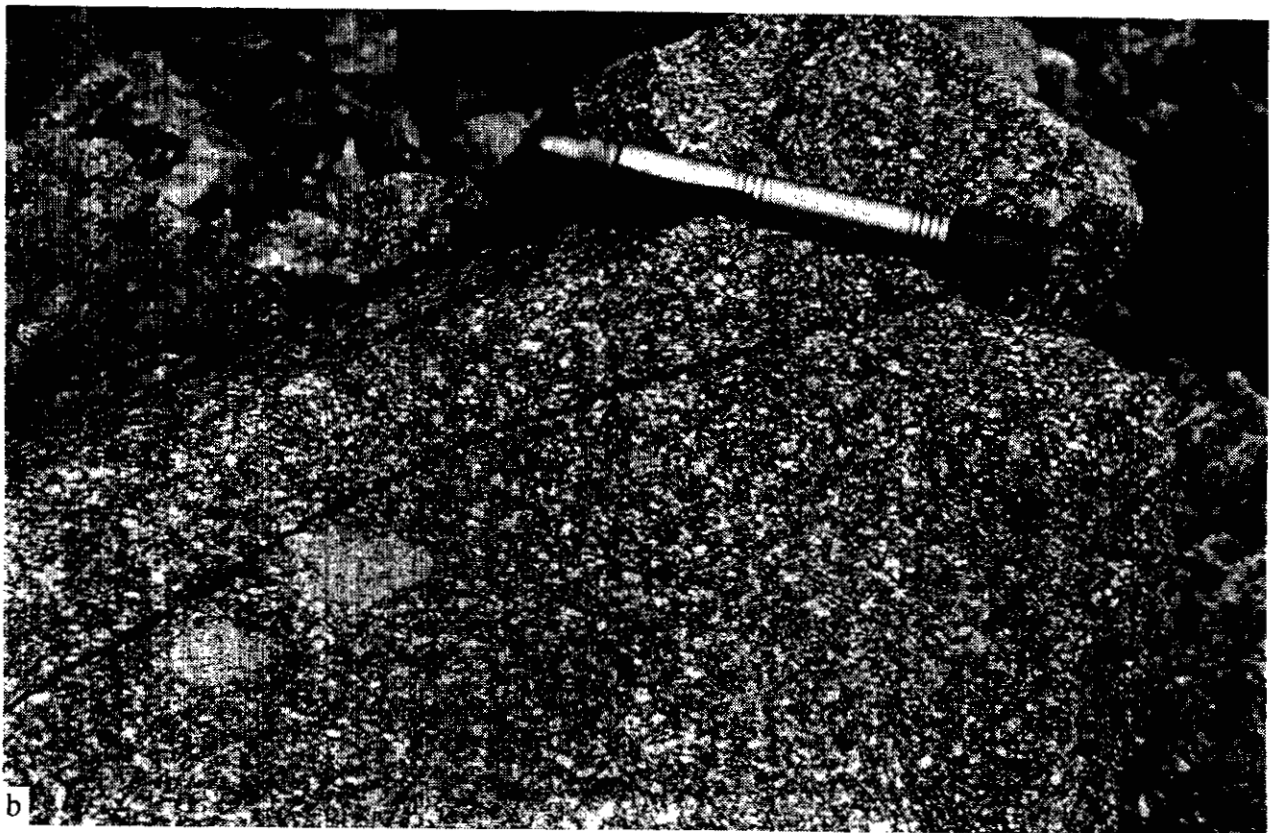


Photo 2-25. Trachyandesite flows dominate the upper half of the Sloko Group succession on the southern flank of Mount Helveker (unit TSb): (a) view north to subhorizontal, columnar jointed flows over 6 metres thick (DBR89-468); and (b) prominent, white plagioclase phenocrysts in a brown aphanitic groundmass (DBR89-469).



Photo 2-26. The top of Mount Helveker is andesitic hornblende-rich crystal lithic lapilli tuff-breccia (included in unit TSd), from which an Eocene K-Ar date was obtained (DBR89-371; Appendix 3-2).



Photo 2-27. View southeast to flat-lying, columnar jointed basalt flow (unit Mb), about 6 metres thick, 1.6 kilometres south of Latimer Lake. The undated flows are tentatively correlated with the Level Mountain flood basalts.

to high-potassium andesites. The upper hornblende-rich crystal lithic tuff-breccia (stage 3) is trachytic or trachydacitic in composition.

Overall there is a subtle angular discordance (10°) between essentially flat-lying Sloko Group volcanic rocks and underlying weathered, limonitic, gently dipping Sustut Group conglomerate (Photo 2-24), however, beds are locally conformable.

AGE AND CORRELATION

Kerr (1948a) referred to these rocks as "Helveker volcanics" (which he believed were Late Cretaceous; his unit 1). Souther (1972) first correlated the rocks with the Eocene Sloko Group (his unit 24). New K-Ar dates reported here indicate Sloko Group volcanism was coeval with Coast Belt plutonism in the map area. Fresh hornblende crystals from grey to olive lithic fragments and matrix yielded a K-Ar date of 48.8 ± 1.7 Ma (Table 2-1; Photo 2-26). There are no younger thermal events recognized in the area, and this result is considered an extrusive age. Regionally the age of the group ranges from 45 to 55 Ma (Souther, 1977; Lambert, 1974).

DEPOSITIONAL ENVIRONMENT

The basal contact of the Sloko Group with the Sustut Group marks a change from high-energy, alluvial fan and fluvial deposition with minor intermittent rhyolitic volcanism, to extensive, explosive subaerial dacitic to andesitic volcanism. The combination of lava flows and pyroclastic flows suggests Mount Helveker was close to a composite volcano, but not directly within the vent facies, as most tuffaceous material is lapilli to ash size. Exposures are remnants of what must have been a much more extensive volcanic pile. More extensive erosional remnants, preserved within grabens, occur to the northwest in the Tulsequah map area (Souther, 1971; Bradford and Brown, 1993b).

MIOCENE OR YOUNGER (?) FLOWS (Unit Mb)

Previously unmapped, flat-lying columnar jointed potassic andesite flows form isolated, cliff-face exposures (Photo 2-27) and benches in a densely forested area 1.6 kilometres south of Latimer Lake. The brown-weathering, amygdaloidal flows contain unaltered biotite and clinopyroxene phenocrysts set in a groundmass containing green-brown plagioclase microlites. Amphibole and clinopyroxene also occur as xenocrysts. Amygdules of intergrown quartz and calcite comprise 10% of the rock. The series of flows, over 330 metres thick, is intermittently exposed from 670 to 1000 metres elevation. Individual flows are 4 to 6 metres thick. Local red-brown interflow conglomerate suggests fluvial reworking of some lava flows.

CHEMISTRY

Three individual flow samples were collected from the same outcrop for chemical characterization of this unit. One sample with a loss on ignition value greater than 4% was discarded. The flow is andesitic and has calcalkaline, subalkaline affinities (Figures 2-18a, b, c). Chrome values are an order of magnitude greater than those from andesites of the Hazelton, Sustut and Sloko groups. The Zr versus Zr/Y plot shows a trend toward higher Zr/Y values from Sloko and Sustut Groups to the Miocene (?) volcanics (Figure 2-18d), with the latter displaying a strong within-plate signature.

Neogene volcanism in the Stikine belt includes both alkaline basalt and peralkaline sialic suites, which occur in an echelon segments controlled by extensional structures. The controlling structures may be wrench faults related to larger scale dextral transcurrent structures (Souther, 1992).

AGE AND CORRELATION

The Latimer Lake flows may be correlative with flows 20 kilometres to the east, where basalt remnants derived from the Mount Edziza area rest on river gravels in the Stikine River valley (Kerr, 1948a; Souther, 1972, 1992). Alternatively, they may correlate with flows that emanate from Level Mountain, a shield volcano 33 kilometres to the north-northwest (Hamilton, 1981). The source of the Latimer Lake flows is unknown and they remain undated.

QUATERNARY (Unit Qal)

Examination of Quaternary features was not the focus of the project but some relevant observations are included here to stimulate further research. Orientation of glacial striations suggests at least three episodes of ice transport in the Tahltan Lake map area. A north-northwest or south-southeast ice movement above 1300 metres elevation contrasts with a north-northeast direction evident over the lower, rolling hills west of Shakes Lake. Large granite erratics, similar to the Sawback pluton to the south, lie on a plateau at 1700 metres elevation and are probably the product of this northeasterly directed ice movement. In addition, Sustut Group polymictic conglomerate boulders occur on Isolation Mountain (DBR91-245) and assuming their source was the Strata Mountain - Yehiniko Valley area, then ice movement must have been to the north. In contrast, erratics south of Tahltan Lake, at 1000 metres elevation, point to a period of southward-directed ice movement.

Broad, U-shaped glaciated valleys commonly display misfit drainages, such as along the upper reaches of the Tahltan River, and demonstrate how Pleistocene glaciation has partially controlled the present drainage system. Clearly, more work is required to resolve the timing and limits of each ice advance and its Quaternary deposits. A study of the Quaternary geology and climate change of Mount Edziza and Telegraph Creek area has recently been completed by Spooner (1994).

CHAPTER 3 INTRUSIVE ROCKS

REGIONAL OVERVIEW

Plutonic rocks of northern British Columbia represent at least seven intrusive episodes: Late Devonian, Middle (?) to Late Triassic, Late Triassic, Early Jurassic, late Early Jurassic, Middle Jurassic, and Eocene (Figure 3-1; Anderson, 1993; Bevier and Anderson, 1991; Logan *et al.*, 1992a; Woodsworth *et al.*, 1991). There are no known Cretaceous plutons, which is in sharp contrast to the areas to the north near Atlin and south of Bowser Basin. Plutonic rocks related to individual episodes have been assigned to separate suites, most of which are distinctive enough to be recognized at the property scale.

The Forrest Kerr pluton, southeast of the project area, is the only known representative of the oldest suite; it intrudes Devonian strata and is overlain nonconformably by Early Carboniferous limestone (Logan *et al.*, 1993c; Drobe *et al.*, 1992). Middle(?) to Late Triassic plutons fall into two groups: small, Alaskan-type ultramafic bodies and larger calcalkaline plutons. Both intruded at shallow levels and are coeval with Stuhini Group volcanism (Woodsworth *et al.*, 1991). The ultramafic suite, known as the Polaris suite (Woodsworth *et al.*, 1991), includes the Gnat Lakes Complex (Nixon *et al.*, 1989), the Mount Hickman Ultramafic Complex and two smaller bodies discovered in the course of this study. However, new isotopic data for the Polaris

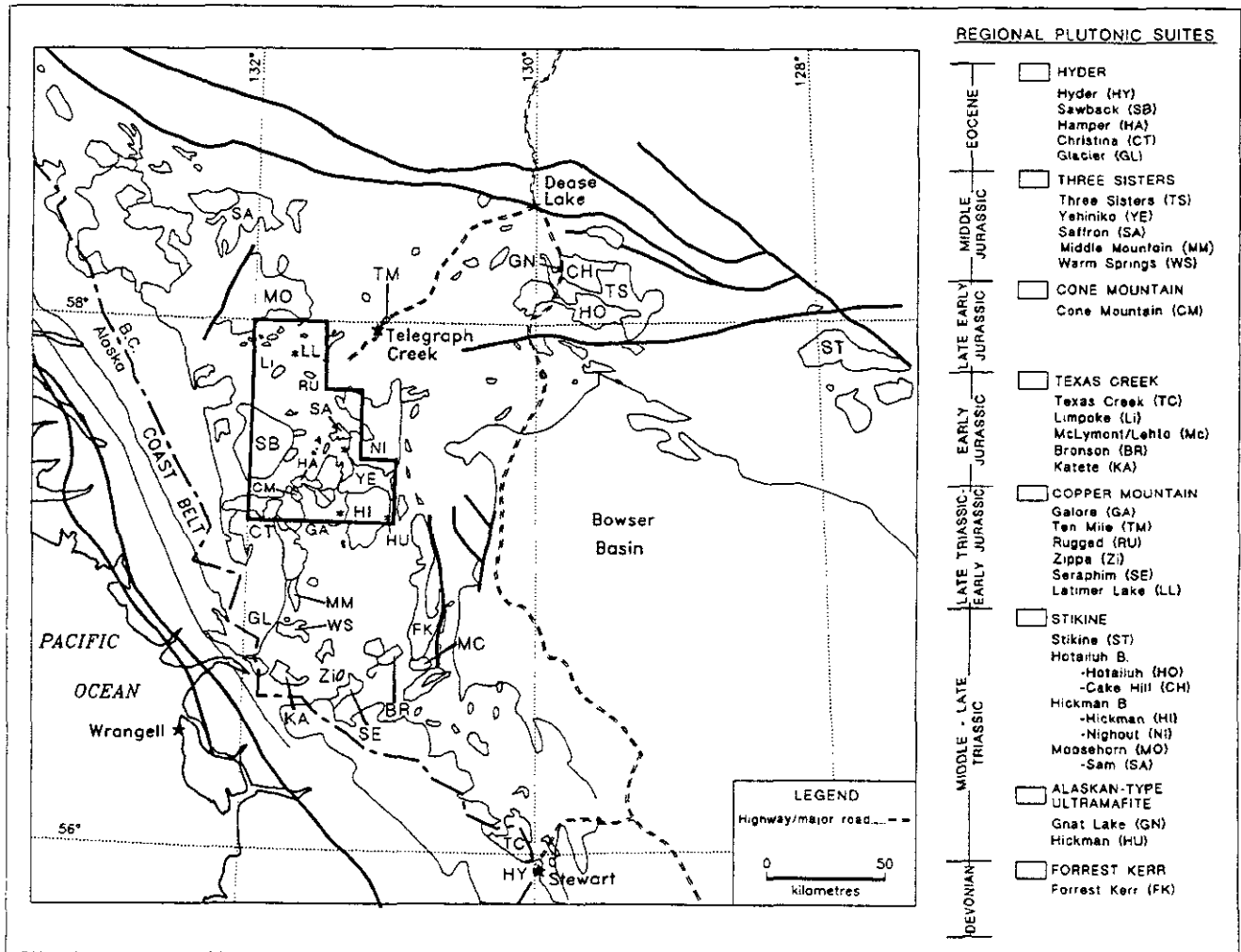


Figure 3-1. Distribution of plutonic rocks, outline of Bowser Basin and Skeena fold belt between Stewart and Dease Lake (modified from Wheeler and McFeely, 1991). Selected plutons are labelled; details of the Stikine project area (outlined) are shown in Figure 3-2.

TABLE 3-1
CHARACTERISTICS OF INTRUSIVE ROCKS

Age/ Plutonic Suite	Pluton name	Rock type	Accessory Minerals	Contact Relations
Eocene (51-55 Ma) HYDER	Sawback, Christina, Hamper	Bio granite, Bio granodiorite	Trace Mag	Intrudes all older units
Tertiary ??	Scud	Pro. alt. granodiorite		Intrudes Stikine assem.
Middle Jurassic (170-177 Ma) THREE SISTERS	Yehiniko, Saffron, Niko, Conover	Hb-Bio granite	Mag, Trace ti	Intrudes Stuhini Gp., Hazelton Gp. & Stikine suite
Late Early Jurassic (180-187 Ma) CONE MOUNTAIN	Cone Mtn., Navo, Strata Glacier, Dokdaon, Devils Elbow, Jacksons, Strata Mtn., Shebou	Bio-Hb granodiorite		Intrudes Stikine assemblage & Copper Mtn. suite
Early Jurassic (?) DIORITE	Geology Ridge, Navo	Bio-Hb diorite to Qtz diorite		Intrudes Stikine assemblage & Copper Mtn. suite Intruded by Cone Mtn & Hyder suites
Early Jurassic (189-195 Ma) TEXAS CREEK	Limpoke, Poque, Brewery Pereleshin, Oksa Ck.	Hb Qtz monzonite	Ti, trace mag.	Intrudes Stikine assemblage & Stuhuni Gp.
Late Triassic to Early Jurassic (210-195 Ma) COPPER MOUNTAIN	Rugged Mtn., Butterfly Latimer L., Damnation,	Syenite, monzonite Quartz monzonite Bio mt clinopyroxenite	Gnt., Ti., apt., mag. Ti, apt.	Intrudes Stikine assemblage & Stuhini Gp.
Middle to Late Triassic (220-228 Ma) STIKINE	Hickman , Nightout, Tahltan Lake, Castor, Little Tahltan Lake, Tahltan River, Half Moon	Hb-Bio granodiorite to Qtz monzonite	Py, mag.	Intrudes Polaris suite, Stuhini Gp., uncon. overlain by Hazelton Gp.
Middle to Late Triassic ALASKAN-TYPE ULTRAMAFITES	Middle Scud, Mt. Hickman Complex, Yehiniko	Clinopyroxenite dunite	Ol, mag., cr	Intruded by Hickman pluton

Note: Hickman batholith = Hickman pluton, Yehiniko pluton, Nightout pluton. Abbreviations: Apt = apatite; Bio = biotite; Cr = chromite; Gd = granodiorite; Gnt = melanite garnet; Hb = hornblende; Megacr = megacrystic; Mag = magnetite; Ol = Olivine; Pro. alt. = prophylically altered; Qtz = quartz; Sy = syenite; Ti = titanite; UM = ultramafite; uncon = unconformably.

Complex (Nixon *et al.*, 1993) suggest that it is younger than most of the ultramafic complexes in the project area which are referred to here as Alaskan-type ultramafic plutons. The Stikine calcalkaline suite of plutons is the most extensive in the area. It includes the Stikine, Hotailuh, Hickman and Moosehorn batholiths (Figure 3-1). Late Triassic to Early Jurassic alkaline plutons of the Copper Mountain suite are commonly associated with porphyry copper-gold deposits throughout British Columbia (Woodsworth *et al.*, 1991). The Rugged Mountain pluton and Butterfly pluton in the study area and the Galore Creek intrusions immediately to the south, are correlative with the Copper Mountain suite. Commonly, the plutons are bimodal, with ultramafic and syenite phases. The Early Jurassic event, genetically related to important vein deposits in the Stewart-Iskut area, comprises the Texas Creek suite with large, calcalkaline heterogeneous plutons. Late Early Jurassic intrusions have been added to these suites based on new data for the Cone Mountain pluton. Middle Jurassic plutons are included in the Three Sisters suite, described by Anderson (1983a,b). Extensive Eocene plutons of the Hyder suite commonly underlie the eastern part of the Coast Belt.

Plutonic rocks underlie about 40% (1500 km²) of the map area, mainly in the south (Figure 3-2). Field relationships, compositional, mineralogical and textural data, combined with radiometric dates, were used to define suites of

intrusions (Table 3-1). Compositions of intrusive rocks were determined by examining hand specimens stained for potassium feldspar and studying thin sections. Intrusive rocks were named using the classification schemes of Streckeisen (1976) and Le Maitre (1989). Whole-rock major and trace element analyses of 65 samples were used to classify rock types and discriminate among possible tectonic settings. Geochemical data and a description of analytical techniques are in Appendix 11. Table 3-2 provides a summary of radiometric dates. Analytical data for new dates are in Appendices 12 and 13. All previously published K-Ar isotopic dates were recalculated using the decay constants of Steiger and Jäger (1977); one sigma errors are reported.

MIDDLE (?) TO LATE TRIASSIC PLUTONS (228-220 Ma)

Triassic plutons are well represented in the study area and fall into two main groups: small, Alaskan-type ultramafic plutons, and more extensive tholeiitic to calcalkaline diorite to granodiorite stocks. They correspond roughly to the Polaris and Stikine suites of Woodsworth *et al.* (1991).

ALASKAN-TYPE ULTRAMAFITES

Alaskan-type ultramafite bodies underlie Mount Hickman, "Middle Scud" Creek, and an area southwest of Yehiniko Lake (Figure 3-3). They are typically dull brown to

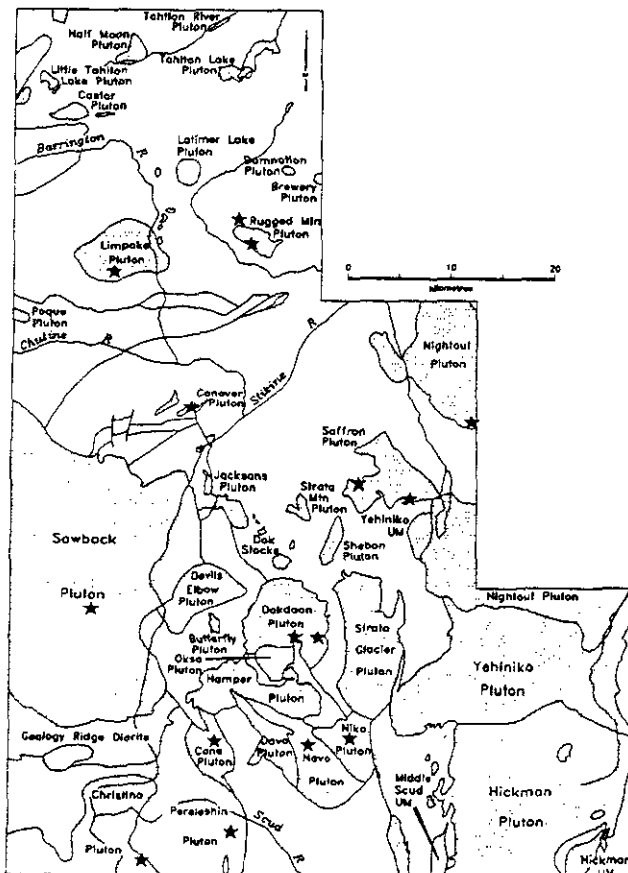


Figure 3-2. Distribution of plutons in the project area, showing isotopic age determination sample localities.

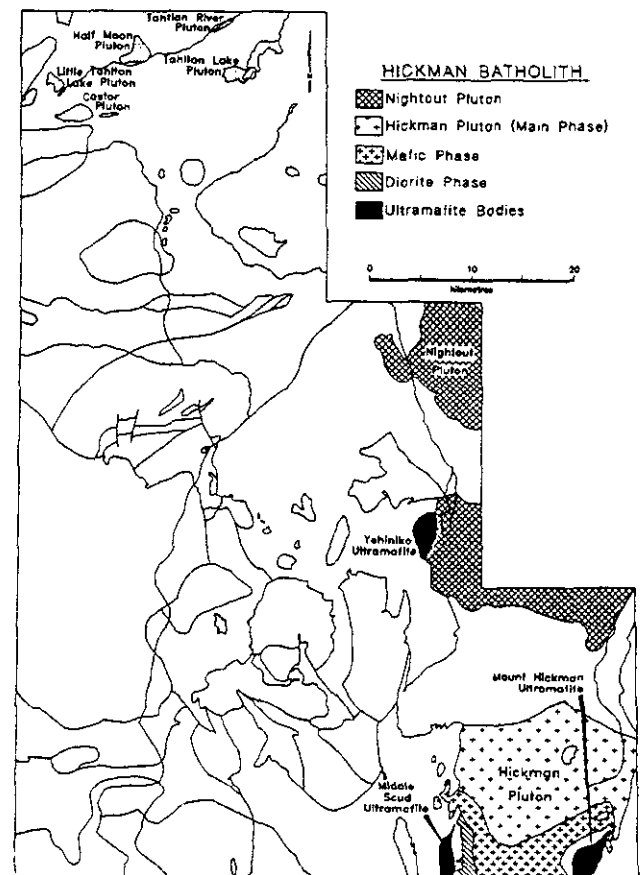


Figure 3-3. Distribution of the Middle to Late Triassic Stikine and Mount Hickman Plutonic Suites.

TABLE 3-2
SUMMARY OF ISOTOPIC DATES FOR PLUTONIC ROCKS

FIELD NO.	MAP UNIT	ROCK TYPE	PLUTONIC SUITE	PLUTON	DATING METHOD	MINERAL	AGE (Ma)	REF.
DBR88-290-2	E	Felsite dike	Hyder	Dike	K-Ar	Bi	49.7 ± 1.7	3a
MGU88-48	Egd	Granodiorite	Hyder	Christina	K-Ar	Bi	54.2 ± 1.7	3a
MGU88-48	Egd	Granodiorite	Hyder	Christina	K-Ar	Hb	56.1 ± 2.0	3a
GC 66-6	Egd	Quartz monzonite	Hyder	Christina	K-Ar	Bi	45.1 ± 2	2
MGU88-76	Egn	Biotite granite	Hyder	Sawback	K-Ar	Bi	48.0 ± 1.7	3a
CGR89-495	mJgn	Granite	Three Sisters	Saffron	K-Ar	Bi	162 ± 7	3a
CGR89-517	mJgn	Monzodiorite	Three Sisters	Saffron	K-Ar	Hb	162 ± 7	3a
81-HA19a	mJgn	Quartz monzonite	Three Sisters	Yehiniko	Rb-Sr	Bi	170 ± 16	1
81-HA19a	mJgn	Quartz monzonite	Three Sisters	Yehiniko	K-Ar	Bi	172 ± 6	1
81-HA19a	mJgn	Quartz monzonite	Three Sisters	Yehiniko	Rb-Sr	WR	178 ± 11	1
DBR88-328	mJgd	Pink granite	Three Sisters	Niko	K-Ar	Bi	177 ± 7	3a
CGR89-546	eJm	Monzonite	Three Sisters	Conover	K-Ar	Hb	177 ± 6	3a
DBR90-40	leJgd	Granodiorite	Cone Mtn.	Cone Mtn.	U-Pb	Zr	184.7 ± 0.6	3c
DBR88-331	leJgd	Granodiorite	Cone Mtn.	Dokdaon	K-Ar	Hb	158 ± 6	3a
DBR88-329	leJgd	Granodiorite	Cone Mtn.	Navo	K-Ar	Bi	163 ± 6	3a
DBR88-329	leJgd	Granodiorite	Cone Mtn.	Navo	K-Ar	Hb	182 ± 7	3a
DBR91-723	eJm	Monzonite	Texas Creek	Limpoke	U-Pb	Zr	194 ± 2	3c
DBR91-723	eJm	Monzonite	Texas Creek	Limpoke	K-Ar	Hb	182 ± 5	3a
MGU88-102	eJqm	Quartz monzonite	Texas Creek	Pereleshin	K-Ar	Hb	204 ± 7	3a
INE91-119	ITs	Bi-cpx syenite	Copper Mtn.	Rugged Mtn.	Ar-Ar	Bi	195 ± 3	3b
DBR91-725	ITs	Bi syenite	Copper Mtn.	Rugged Mtn.	U-Pb	Zr	>189.4 ± 0.6	3d
MGU90-743	ITs	Hornblende syenite	Copper Mtn.	Butterfly	Ar-Ar	Hb	204.1 ± 2.0	4
CGR89-78	ITgd	Monzonite	Stikine	Nightout	K-Ar	Hb	200 ± 7	3a
81-HA17a	ITgd	Hb-Bi granodiorite	Stikine	Nightout	K-Ar	Hb	228 ± 8	1
81-HA17a	ITgd	Hb-Bi granodiorite	Stikine	Nightout	Rb-Sr	Bi	232 ± 5	1
81-HA17a	ITgd	Hb-Bi granodiorite	Stikine	Nightout	K-Ar	Bi	236 ± 9	1
81-HA10a	ITm	Bi-Hb granodiorite	Stikine	Hickman	K-Ar	Bi	209 ± 15	1
81-HA10a	ITm	Bi-Hb granodiorite	Stikine	Hickman	Rb-Sr	Bi	216 ± 4	1
81-HA10a	ITm	Bi-Hb granodiorite	Stikine	Hickman	K-Ar	Hb	221 ± 8	1
81-HA10a	ITm	Bi-Hb granodiorite	Stikine	Hickman	Rb-Sr	WR	233 ± 23	1

One sigma errors for K-Ar and Rb-Sr dates, and two sigma errors for U-Pb dates are reported, see Appendices 12 and 13 for analytical data. References: 1 = Holbek (1988); 2 = White *et al.* (1968); 3 = this report, a = Harakal, b = Reynolds, c = McClelland, d = Mortenson); 4 = M.H. Gunning *in* Hunt and Roddick (1994, sample GSC94-41, pages 139-140).

black weathering, orthopyroxene-free clinopyroxenites which contain abundant magnetite. They intrude and hornfels mafic metavolcanic hostrocks. The body at Mount Hickman has a dunite core and a clinopyroxenite margin, suggesting an Alaskan-type affinity (*cf.* Nixon and Rublee, 1988). The ultramafites may be feeders to parts of the Stuhini Group. Other ultramafic bodies are associated with megacrystic syenite and have been included in the younger Copper Mountain suite.

MOUNT HICKMAN COMPLEX

The best exposed and studied member of the Middle to Late Triassic ultramafites is the Mount Hickman body, an oblong, northeast-trending intrusion about 3 by 5 kilometres in surface area. This study represents the body as a distinct entity rather than including it within the Hickman pluton (*cf.* Souther, 1972). Detailed descriptions of the body are given by Nixon *et al.* (1989). It comprises mainly medium-grained, equigranular, black to tan-weathering clinopyroxenite and olivine clinopyroxenite containing 10 to 15% fractured, serpentinized olivine and 3 to 5% euhedral chromite and magnetite. Part of the core is a small dunite body with serpentinized and fresh olivine. The body produces prominent magnetic highs on aeromagnetic maps (Map 9238G; Map NTS 104G; Map NO-09-M).

The ultramafite intrudes and metamorphoses a roof pendant of plagioclase-phyric andesite flows and tuffs correlative with the Carnian to Norian Stuhini Group, but is itself intruded by, and is found as xenoliths within, the main phase of the Hickman pluton. The southwest contact of the complex is hornfelsed Stuhini volcanic rocks and therefore believed to be intrusive. A limonitic zone in this area may mark the northeastward extension of a fault mapped to the south by Logan *et al.* (1993a).

MIDDLE SCUD ULTRAMAFITE

The Middle Scud ultramafite, named after the creek to the northwest, comprises a 4 square kilometre, variably serpentinized, medium to fine-grained clinopyroxenite. It intrudes mafic metavolcanic rocks (biotite schist) correlated with the Stuhini Group. Anomalously high amphibolite facies metamorphic grade attained by rocks in this area may, in part, be due to the emplacement of the ultramafic rocks. The southeast corner of the ultramafite is intruded by megacrystic quartz diorite of the Hickman pluton. Serpentine-rich shears and north-trending faults cut the ultramafite and extend north to the Yehiniko ultramafite. The Middle Scud and Yehiniko ultramafites lack the prominent aeromagnetic signatures which characterize the Mount Hickman complex.

YEHINIKO ULTRAMAFITE

An ultramafic body southwest of Yehiniko Lake was discovered during the course of this project. It shares attributes of the Middle Scud body in that it lies along north-trending faults, is sheared, is peripheral to a Late Triassic pluton, and is difficult to distinguish from mafic metavolcanic rocks correlated with the Stuhini Group. The high magnesia and chrome oxide and low silica geochemical signature was used to distinguish this body from mafic metavolcanic rocks of the adjacent Stuhini Group (Figure 3-10; Appendix 11).

The body displays faint magmatic layering developed in fine-grained, locally foliated, dull brown weathering clinopyroxenite. Granodiorite dikes, believed to be related to the Nightout pluton, cut the ultramafite. Anomalous nickel and cobalt Regional Geochemical Survey values in Saffron Creek may be derived from this body.

HICKMAN BATHOLITH

Collectively, the Stikine suite of plutons delineates the Stikine Arch. The north-trending Hickman batholith, about 65 kilometres long by 17 kilometres wide, is the southernmost body of the suite. It underlies an area of about 1200 square kilometres in the eastern part of the map area. The batholith is composed of three plutons: the Middle(?) to Late Triassic Hickman and Nightout plutons and the Middle Jurassic Yehiniko pluton (Figure 3-1; Souther, 1972; Holbek, 1988). Souther's "Hickman batholith" is a restricted circular pluton east of Schaft Creek and north of Mount Hickman and is now referred to as the Hickman pluton. The Triassic plutons are believed to be subvolcanic intrusions of the Stuhini Group, as documented for the Hotailuh batholith (Anderson, 1983a). Locally, granitoid-bearing intravolcanic conglomerates indicate denudation of parts of these plutons during Stuhini Group volcanism.

HICKMAN PLUTON

The Hickman pluton, consisting of three distinctive phases, underlies an area of 300 square kilometres in the southern corner of the map area, near Vanishing Lake. The heterogeneous **main phase** is the most extensive and is dominated by massive to faintly foliated, medium-grained, equigranular, dull grey hornblende biotite granodiorite to quartz monzodiorite. Tonalite and quartz diorite are subordinate and their relationship to the main body is uncertain. Magnetite and rare titanite are accessory minerals. The main phase intrudes the mafic phase on the south, Stuhini Group volcanic rocks and Mount Hickman complex on the east, and Permian and Upper Triassic sediments on the west. Late Triassic dates of 209 ± 15 Ma (K-Ar biotite), 221 ± 8 Ma (K-Ar hornblende), 216 ± 4 Ma (Rb-Sr biotite) and 233 ± 23 Ma (Rb-Sr whole rock; Holbek, 1988; Table 3-2) were obtained for the main phase east of Vanishing Lake. The main phase is lithologically similar and coeval with the Nightout pluton, a larger but locally more strongly foliated body exposed 10 kilometres to the north.

The **mafic phase** forms the southern border of the batholith and extends south into the area mapped by Logan and Koyanagi (1989). It comprises medium-grained, equigranular, hornblende gabbro and plagioclase-bearing hornblendite. The contact with the main phase is locally gradational and mafic xenoliths are found within the main phase.

The **diorite phase** comprises megacrystic quartz diorite and underlies a 12 square kilometre area on the west margin of the Hickman pluton. The pluton outwardly resembles potassium feldspar megacrystic quartz monzonite of the Late Triassic to Early Jurassic Pereleshin pluton (*see below*). However, as Souther (1972) noted, the rectangular megacrysts, which are up to 5 centimetres long, are plagioclase, not potassium feldspar. Quartz and hornblende,

chloritized biotite and accessory magnetite comprise the groundmass to the plagioclase megacrysts. Diorite intrudes the Middle Scud ultramafite along its western contact; the character of the eastern contact is uncertain. The diorite is spatially associated with the Hickman pluton and, at one locality, has a poorly defined gradational contact with the main phase. At another locality, the diorite phase intrudes the mafic phase. These relationships indicate that it is younger than the mafic phase and possibly coeval with the main phase. A prominent aeromagnetic anomaly that extends south along the southwest border of the Hickman pluton may outline the diorite phase.

NIGHTOUT PLUTON

The Nightout pluton (Holbek, 1988) underlies about 275 square kilometres. Its distribution has been modified from that of previous workers (Souther, 1972; Holbek, 1988) by including a phase north of Boomerang Creek which had been grouped with the Yehiniko pluton. The pluton consists of foliated to massive, medium-grained, biotite hornblende granodiorite that grades locally to tonalite, quartz monzonite, monzodiorite and diorite. Titanite is a common, locally medium-grained accessory mineral. Mafic inclusions are common along the margins. Near Lingwell Creek, the pluton is characterized by a widespread magmatic foliation and by coarse-grained (up to 2 cm) poikilitic potassium feldspar grains.

The Nightout pluton intrudes Stuhini mafic volcanic rocks on its west and northwest margins, and foliated Stikine assemblage rocks on its northern margin. Foliation in the pluton parallels the contact and the foliation in the country rocks. In Yehiniko Creek canyon, Kerr (1948a) described a thick sill-like geometry for the western part of the pluton which he referred to as the "Yehiniko mass". He suggested it was the source of arkosic sedimentary rocks in Glomerate Creek. Near the headwaters of Boomerang Creek, the Nightout pluton is overlain nonconformably by Lower Jurassic volcanic rocks of the Hazelton Group and by Upper Cretaceous to Paleocene(?) conglomerate of the Sustut Group. Along the southwest side of Yehiniko Lake and farther south, unfoliated, medium-grained equigranular (biotite) hornblende tonalite, possibly a marginal phase of the Nightout pluton, intrudes and hornfelses the Stuhini Group and the Yehiniko ultramafite.

Potassium-argon isotopic dates of 236 ± 9 Ma (K-Ar biotite), 228 ± 8 Ma (K-Ar hornblende), and 232 ± 5 Ma (Rb-Sr biotite; Holbek, 1988; Table 3-2) suggest a Middle to Late Triassic age for the southern part of the pluton. Farther north, near Boomerang Creek, a sample of biotite hornblende granodiorite collected near the pre-Lower Jurassic unconformity yielded a hornblende K-Ar date of 200 ± 7 Ma (Table 3-2; Appendix 12); this may be a partially reset age, perhaps reset during intrusion of a nearby east-striking dike swarm possibly associated with the Middle Jurassic Saffron pluton. However, in contrast to most of the Nightout pluton to the north, which is foliated, the dated sample was collected from an unfoliated phase, which may be younger (Souther, 1972).

OTHER STIKINE SUITE PLUTONS

Five undated plutons in the northern part of the map area are tentatively included in the Stikine suite: the Tahltan Lake, Castor, Little Tahltan Lake, Tahltan River and Half Moon plutons (Figure 3-3). All are small (each less than 4 km^2) and intrude Stuhini Group rocks. They lie immediately southeast of the extensive Moosehorn pluton which is believed to be Late Triassic in age (*cf.* Bradford and Brown, 1993b).

The Tahltan Lake pluton underlies a 3.5 square kilometre area immediately west of Tahltan Lake. Hornblende quartz monzodiorite dominates in the northern and western sectors of the intrusion, while the eastern half is characterized by hornblende quartz diorite. Though compositionally varied, the fine to medium-grained, equigranular rocks are texturally homogeneous. Poikilitic hornblende is relatively unaltered and occurs as subhedral to euhedral prismatic grains which enclose equant plagioclase crystals. Colour index ranges from 18 in the quartz monzodiorite to 30 in the quartz diorite. Oscillatory zoned plagioclase crystals are invariably saussuritized, giving a grey to greenish cast to the rocks. Accessory minerals include magnetite, apatite and zircon.

The Castor pluton is an eye-shaped, bimodal intrusion exposed over about 6 square kilometres southeast of Little Tahltan Lake. It is dominated by fine to medium-grained equigranular biotite hornblende granodiorite. Along the eastern margin, the border phase is characterized by fine to medium-grained hornblende quartz diorite; to the west it is represented by fine-grained equigranular tonalite. The colour index ranges from 10 to 30 and plagioclase is weakly to moderately saussuritized. Potassium-feldspar megacrystic syenite felsenmeer is associated with the western part of the pluton.

The Little Tahltan Lake plutons comprise 4 square kilometres of predominantly medium-grained, inequigranular hornblende granodiorite; most have medium to fine-grained quartz monzodiorite to hornblende diorite border phases. The colour index of the intrusion directly northwest of Little Tahltan Lake ranges from 10 to 30. Hornblende is the dominant mafic mineral and accessory minerals include magnetite and titanite. Hornblende is altered to chlorite and epidote while turbid, interlocking plagioclase laths and potassic feldspar crystals are completely replaced by carbonate and sericite. There is a poorly developed foliation within the intrusion along its western margin.

The Tahltan River pluton is a narrow, elliptical body, less than 2 square kilometres in area, that is poorly exposed along the banks of the Tahltan River northwest of Tahltan Lake. It is a predominantly leucocratic (colour index = 10), medium-grained equigranular hornblende to biotite hornblende quartz monzodiorite. Hornblende, the dominant mafic mineral, occasionally encloses crystals of plagioclase. Quartz and potassic feldspar are interstitial. Alteration is moderate, producing bleached, pale grey to white-weathering outcrops. Hornblende is partially altered to chlorite; zeolites are present along joint surfaces and quartz-epidote veinlets are common.

The Half Moon pluton is a 4 square kilometre, crescent-shaped body outcropping north of Tahltan River. The centre of the pluton consists of equigranular medium to coarse-grained hornblende quartz monzodiorite. The border phase is equigranular to inequigranular fine to medium-grained hornblende biotite quartz diorite. Mafic mineral contents range from 15 to 25%. Plagioclase is saussuritized and chlorite alteration is pervasive though weak.

LATE TRIASSIC TO EARLY JURASSIC - COPPER MOUNTAIN PLUTONIC SUITE (210-195 Ma)

The dominantly alkaline Copper Mountain suite consists of small intrusions and dikes (Figure 3-4) which range in composition from syenite to quartz monzonite. They are commonly associated with copper-gold mineralization, as exemplified by the Galore Creek deposit south of the study area. The Rugged Mountain pluton and Butterfly pluton (Gunning, 1993a) best illustrate the characteristic features of this suite in the project area, namely: abundant potassium feldspar megacrysts, aegirine-augite, biotite and melanite garnet (Neill, 1992; Neill and Russell, 1993). The alkaline intrusions and their commonly associated ultramafite phases tend to be magnetite rich and therefore produce prominent aeromagnetic anomalies. Similar syenite stocks with marginal pyroxenite complexes occur regionally and

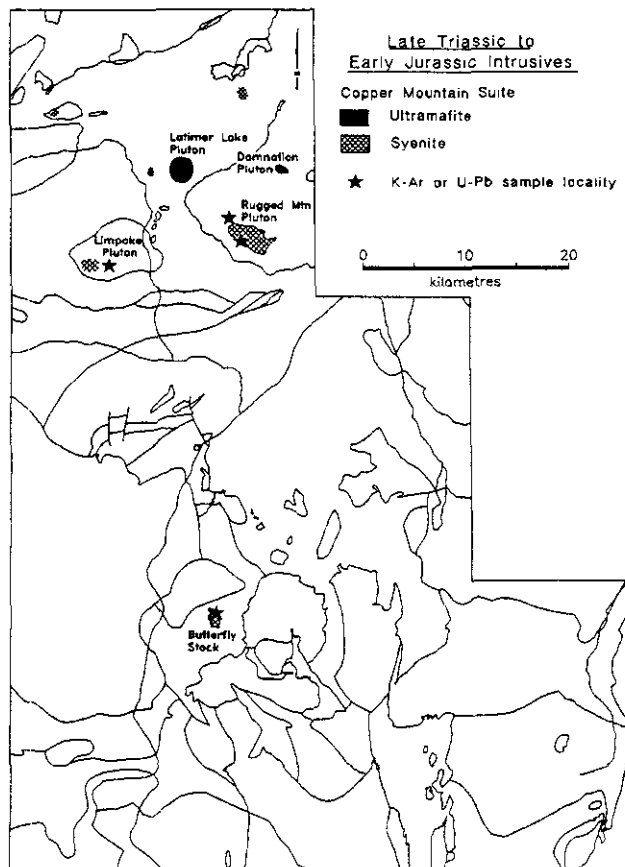


Figure 3-4. Distribution of the Late Triassic to Early Jurassic Copper Mountain Plutonic Suite.

include Galore Creek, the Ten Mile Creek body (Morgan, 1976), and the Zippa Mountain pluton (Bevier and Anderson, 1991; Lueck and Russell, 1994; Figure 3-1). The Ten Mile Creek intrusion has a well preserved clinopyroxenite border phase around a syenite core. This complex yields Late Triassic K-Ar dates [209 ± 7 Ma, recalculated from dates of Morgan (1976) using decay constants of Steiger and Jäger (1977)]. Stevens *et al.* (1982) reported an Early Jurassic biotite K-Ar date of 202 ± 7 Ma from a biotite clinopyroxenite of the Tahltan syenite stock in Stikine Canyon, presumed to be the same body as the Ten Mile Creek intrusion.

BUTTERFLY PLUTON

The Butterfly pluton, referred to as the "Butterfly Creek mass" by Kerr (1948a), intrudes Carboniferous volcanic rocks of the Stikine assemblage and volcanic rocks of uncertain age, at Butterfly Lake. Detailed descriptions of the pluton are provided by Gunning (1993a). The stock is an elongate body, less than 2 kilometres wide and 3 kilometres long. The composite, multiphase body (4 phases) comprises pyroxene-rich syenite in the southwest, and potassium feldspar megacrystic syenite to quartz monzonite in the northeast. The central part of the body is mainly hornblende syenite and lesser potassium feldspar megacrystic syenite. Black to dark green pyroxenite and pyroxene syenite is medium to coarse grained, with abundant biotite, augite, hornblende and magnetite. Distinctive flow-aligned potassium feldspar megacrysts up to 5 centimetres long comprise up to 70% of orange-brown weathering syenite to quartz monzonite. Epidotized and chloritized hornblende comprises less than 5% of the rock. Aegirine-augite, colourless garnet and biotite flakes were noted by Kerr (1948a). Disseminated pyrite and magnetite are common accessory minerals. Textures vary from coarse megacrystic to medium grained. Hornblende is the dominant mafic mineral in contrast to pyroxene in the older syenite phase. Hornblende syenite dikes with pyroxene syenite xenoliths intrude the megacrystic syenite. The eastern margin of the pluton is marked by chloritic metavolcanic phyllite and there is local biotite hornfels. Small irregular bodies of hornblende quartz monzodiorite and diorite which intrude the syenite west and south of Butterfly Lake may be related to a younger plutonic episode.

A buff-weathering, northeast-striking heterolithic intrusive syenite breccia dike intrudes siliceous siltstone on the northeast side of Butterfly Lake. Another irregular intrusive breccia is exposed in the south-central part of the pluton. The breccias contain fragments of megacrystic syenite, and lesser green, grey and black siliceous rock, granitoids, rare aphanitic basalt fragments and potassium feldspar crystals in a dark green, chloritic groundmass.

The Butterfly pluton is correlated with the Copper Mountain suite on the basis of megacrystic texture, mineralogy, composition and a 204.1 ± 2 Ma hornblende $^{40}\text{Ar}-^{39}\text{Ar}$ age (Gunning, in Hunt and Roddick, 1994).

RUGGED MOUNTAIN PLUTON

The aptly named Rugged Mountain pluton (Photo 3-1), exposed on the southern flank of Rugged Mountain, covers

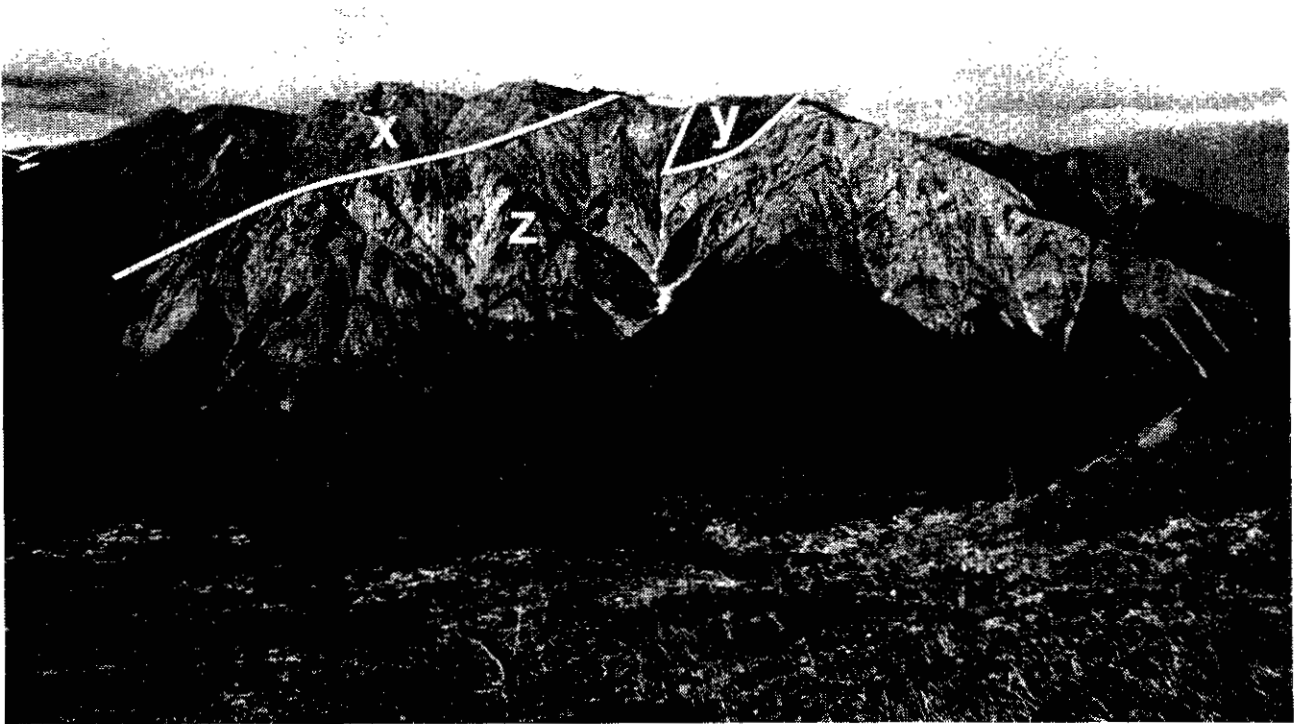


Photo 3-1. View northeast to the Rugged Mountain syenite complex (z), dark mafic border phase (y) along the northern contact of the pluton, intrudes Stuhini Group rocks (x).



Photo 3-2. Late-phase trachytic potassium, feldspar megacrystic dike of the Rugged Mountain complex.

an area of about 14 square kilometres. A detailed mapping, petrographic and mineral chemistry study of the pluton by Neill (1992) undertaken in conjunction with this project, provides the basis for much of the following description.

The pluton is a composite (3 phases and dikes), pink to light grey alkaline syenite body, which intrudes Stuhini Group tuffaceous siltstone, shale, limestone and ash tuff. The complex has a pyroxenite phase along its northern margin and most contacts between syenite and pyroxenite are sharp, but locally, an intrusive breccia is formed, with pyroxenite blocks in a syenite groundmass. This relationship is similar to the Butterfly pluton. Late-phase, leucocratic, potassium feldspar megacrystic dikes cut all phases and the country rocks (Photo 3-2). Kerr (1948a) referred to the complex as the "Shakes Creek mass".

Four main rock types were differentiated by Neill (1992), based largely on mafic mineral content: clinopyroxenite, hybrid syenite and clinopyroxenite, syenite and syenite/monzonite dikes. All rock types contain potassium-feldspar, biotite, aegirine-augite, melanite garnet, magnetite, titanite and apatite. Pyroxene is relatively unaltered but feldspars show some sericite and chlorite alteration. Garnet occurs as dark red crystals and light brown grains surrounding other accessory minerals. The garnet is a high-titanium variety of andradite that typically occurs in soda-rich igneous rocks (Kerr, 1959). The hybrid phase of the Rugged Mountain complex yielded an ^{39}Ar - ^{40}Ar biotite plateau date of 195 ± 3 Ma (P. Reynolds, written communication, 1993), which is concordant with the Limpoke pluton of the Texas Creek suite (Figure 3-5; Table 3-2).

CLINOPYROXENITE PHASE

The partially preserved biotite clinopyroxenite border phase is up to 100 metres wide and 2.5 kilometres long, and forms the steeply dipping northern contact of the complex (Photo 3-1). The contact between pyroxenite and syenite is sharp. The recessive pyroxenite weathers black to dark green and contains unaltered pyroxene and biotite. Smaller pyroxenite bodies have also been mapped along the north-east and southeast borders of the pluton.

Aegirine-augite, magnetite and apatite comprise the bulk of the rock, with lesser titanite, biotite and rare melanite

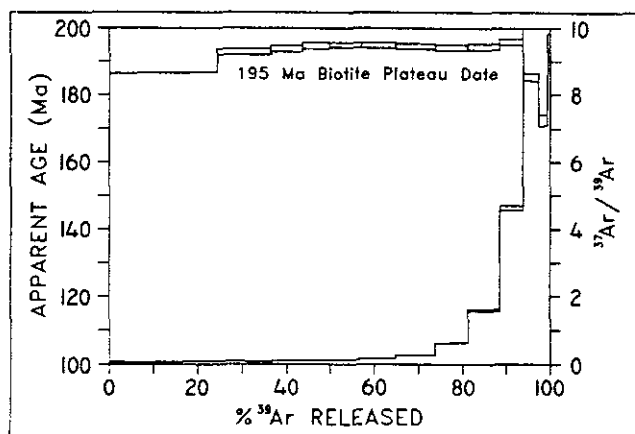


Figure 3-5. Biotite $^{37}\text{Ar}/^{39}\text{Ar}$ plateau date for the Rugged Mountain pluton (analyses by P. Reynolds, 1993).

garnet. Pyroxene of variable compositions and apatite crystals are subaligned and may represent cumulate minerals. Secondary minerals in fracture fillings include chlorite, calcite and garnet.

SYENITE PHASE

Pink, medium-grained alkali-feldspar syenite containing less than 60% mafic minerals is the predominant phase of the complex. Potassium feldspar occurs as interstitial grains and locally as megacrysts up to 2 centimetres long. Other primary minerals include melanite garnet, biotite, apatite, titanite and magnetite. Aegirine-augite commonly occurs as small, fractured cores with secondary hornblende rims. Primary hornblende is a minor component.

HYBRID PHASE

The hybrid phase has similar mineralogical features to the syenite phase but contains more than 60% pyroxene and biotite. The syenite and hybrid phases were not differentiated on the map (in pocket).

ALKALINE DIKE SWARM

West-striking syenite dike swarms are well exposed 1.5 kilometres north and 4.0 kilometres southwest of Rugged Mountain. The texturally variable dikes include both trachytic to sub-trachytic potassium feldspar megacrystic (up to 7 cm long) varieties, and trachytic albite-megacrystic varieties. Pyroxene is rare and, where present, is replaced by hornblende; otherwise the mineralogy is similar to the syenite phase. A potassium feldspar megacrystic dike on the west flank of Rugged Mountain yielded a imprecise U-Pb date, interpreted to be older than the ^{206}U - ^{238}Pb age of 189.4 ± 0.6 Ma (J.K. Mortensen, written communication, 1994; Figure 3-5; Table 3-2). Dike swarms in Barrington River canyon and on the eastern flank of Isolation Mountain are possibly related. Together the dike swarms radiate from an area outlined by a prominent aeromagnetic anomaly centred on Latimer Lake, and may be related to a blind intrusion.

LATIMER LAKE AND DAMNATION PLUTONS

Discrete ultramafite bodies without appreciable syenite underlie the Latimer Lake and Damnation Creek areas (Figure 3-4). They are included in the Copper Mountain suite because they have similar textures and compositions to clinopyroxenite phases of the suite.

The three small ultramafic plutons, underlying less than 7 square kilometres in total, intrude and hornfels Stuhini Group tuffaceous siltstone along an easterly trend, 4 kilometres north and east of Latimer Lake. Two of the intrusions had not been mapped previously. Their characteristics are well represented by the Latimer Lake pluton, which underlies a forested area and is poorly exposed. Partially caved bulldozer trenches, remaining after iron exploration on the Shakes iron deposit in the 1960s, provide most of the exposures of the pluton; however, it generates a prominent high on aeromagnetic maps (Map 9250G; NTS Map 104G).

The Latimer Lake pluton is composed of black, granular, medium to fine-grained biotite magnetite clinopyroxenite. Cumulate clinopyroxene and unaltered biotite display faint millimetre-scale layering in thin section. Bi-

otite also forms an intercumulate phase with magnetite, which was the target of iron exploration (McIntyre, 1966). Clinopyroxenite is locally brecciated and the space between fragments is filled with potassium feldspar and coarse biotite. Part of the western flank of the pluton includes intrusive breccia, consisting of pyroxenite fragments supported in hornblende diorite. Porphyritic syenite around the periphery of the body, noted by Souther (1972), was not seen during our mapping. An unnamed satellitic ultramafic body of unknown extent lies 2 kilometres farther west. The third body, the Damnation pluton, 10 kilometres to the east, shares most features of the Latimer Lake pluton but lacks syenite. It intrudes and hornfelses Stuhini Group tuff.

EARLY JURASSIC TEXAS CREEK PLUTONIC SUITE (189-195 Ma)

The Early Jurassic Texas Creek plutonic suite includes calcalkaline plutons associated with economically important precious and base metal vein deposits, like the Premier mine and Sulphurets deposits in the Stewart-Iskut area (Figure 3-1; Anderson and Thorkelson, 1990). The Texas Creek granodiorite, near Stewart, is an irregular-shaped pluton with comagmatic potassium feldspar megacrystic dikes and sills ("Premier porphyry"; Brown, 1987). The Limpoke pluton (Figure 3-6) is included in this suite on the basis of an Early Jurassic U-Pb zircon date (194 ± 2 Ma; Brown *et al.*, 1992c; Appendix 13) and on the basis of its composition and its associated copper and gold showings. A K-Ar hornblende date of 182 ± 5 Ma (Appendix 12) for the Limpoke pluton may represent a cooling age. Two smaller bodies, the Pogue and Brewery plutons, are also included in this suite.

LIMPOKE PLUTON

The Limpoke pluton, an elongate body approximately 8 kilometres long, underlies an area of 27 square kilometres immediately south of Limpoke Creek. This two-phase, texturally heterogeneous stock is dominated by an outer phase of pale grey, medium to fine-grained, equigranular biotite-hornblende quartz monzonite. The centre of the intrusion consists mainly of coarse to medium-grained plagioclase-megacrystic biotite hornblende monzodiorite with plagioclase phenocrysts, 1 to 2 centimetres in length, set in a fine-grained groundmass of potassium feldspar. The percentage of mafic minerals increases toward the outer margins of the pluton, with the colour index ranging from about 18 to 40. Hornblende is the dominant mafic mineral, but dark brown biotite locally coexists with dark green hornblende. Clinopyroxene occurs with hornblende and biotite in one locality. The intrusion contains magnetite as fine-grained granules, and they probably contribute to the significant anomaly apparent on aeromagnetic maps (Map NTS 104G). Apatite is a common accessory mineral.

Leucocratic, potassium feldspar megacrystic syenite dikes intrude the eastern and western borders of the pluton and surrounding Upper Triassic sedimentary and volcanic rocks. The dikes are similar to syenite and alkali feldspar syenite dikes northwest of the Rugged Mountain pluton. They are characterized by tabular, trachytic potassium feldspar phenocrysts 1 to 2 centimetres long, and smaller pla-

gioclase laths, all set in a groundmass of potassium feldspar. Hornblende and pyroxene occur as subhedral to euhedral prismatic grains and account for 2 to 10% of the rock.

POGUE AND BREWERY PLUTONS

The Pogue pluton, a poorly exposed body less than 3 square kilometres in area, crops out 10 kilometres southwest of the Limpoke pluton. It is composed of fine-grained, equigranular hornblende to biotite hornblende monzodiorite; biotite and hornblende comprise 20% of the rock. A subtrachytic texture defined by flow-aligned plagioclase is developed at its eastern contact. The Brewery pluton consists of pink hornblende quartz monzodiorite with about 25% mafic minerals. It is exposed only along an isolated ridge 20 kilometres northeast of the Limpoke pluton, but may extend to the east.

PERELESHIN AND OKSA CREEK PLUTONS

Potassium feldspar megacrystic quartz monzonite intrusions, the Pereleshin pluton and Oksa Creek stock, are included in the Texas Creek suite because of their similar composition. The Pereleshin pluton underlies about 180 square kilometres, from Mount Pereleshin northwest across the Stikine River into the Coast Range; its extent is greater

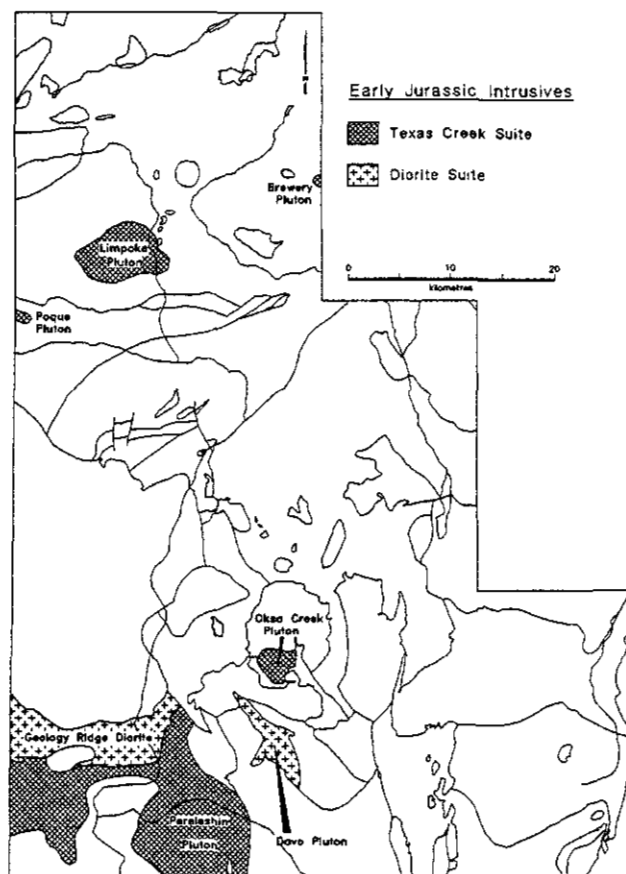


Figure 3-6. Distribution of Early Jurassic Texas Creek Plutonic Suite and Early Jurassic diorites.

than that mapped by Brown and Gunning (1989b). It is composed of grey, medium-grained, porphyritic hornblende quartz monzonite to granite. Potassium feldspar megacrysts account for 20 to 40% of the rock and anhedral quartz 10 to 25%. Mafic minerals, euhedral black hornblende and trace biotite, comprise 10 to 20%. Large titanite crystals, magnetite and apatite are accessory minerals.

A hornblende K-Ar date of 204 ± 7 Ma was obtained from this body and is interpreted as the minimum age of emplacement (Appendix 12). A Tertiary hornblende biotite granodiorite, the Christina pluton, intrudes the Pereleshin body west of Mount Pereleshin.

The Oksa Creek pluton, which is about 3 kilometres in diameter, is exposed near the headwaters of Oksa Creek. It is massive, coarse to medium-grained, crowded megacrystic quartz monzonite containing potassium feldspar megacrysts (up to 60%), hornblende (up to 25%), and distinctive coarse-grained titanite (up to 2 cm long) and secondary epidote.

EARLY JURASSIC(?) DIORITE INTRUSIONS

The Geology Ridge and Davo plutons are two distinct, undated, bodies of diorite (Figure 3-6). The east-trending Geology Ridge pluton consists of conspicuous, black to dark grey, medium-grained, equigranular, biotite hornblende diorite to monzodiorite. It was described as a "mafic migmatite" by Souther (1971). It is indeed texturally heterogeneous, with mafic pegmatites and hornblendites characterized by irregular dark patches of coarse-grained acicular hornblende up to 3 centimetres long and interstitial quartz, plagioclase and potassium feldspar.

The northwest-trending Davo pluton ranges from quartz monzodiorite to hornblende diorite in composition and underlies an area of about 15 square kilometres. It intrudes Permian limestone and underlying strata. Its western border, near the headwaters of Navo Creek, consists of a zone of vertical diorite schlieren, 50 metres wide, adjacent to recrystallized Permian limestone (*cf.* Photo 4-14). Here hostrocks contain layers and pods of garnet and garnet-diopside skarn up to 75 metres from the contact. No other plutons in the area have this strong, syn-emplacement (?) vertical fabric developed at their margins.

LATE EARLY JURASSIC CONE MOUNTAIN INTRUSIONS (187-180 Ma)

The Cone Mountain intrusions, a group of eight granodioritic plutons, are spatially associated with and contain abundant angular xenoliths of the Early(?) Jurassic Geology Ridge and Davo diorites. They are the principal intrusions north of the Scud River and include the Cone Mountain, Navo, Dokdaon, Strata Glacier, Devils Elbow, Jacksons, Strata Mountain and Shebou plutons (Figure 3-7). The Cone Mountain suite (an informal name used here because plutons of this age were previously unrecognized in the region) is characterized by leucocratic (colour index 15) biotite hornblende granodiorite. Ubiquitous angular to rounded mafic xenoliths range from less than a metre to tens of metres in diameter (*see* Photo 1c in Gunning, 1993a), and are com-

monly in complex agmatite zones of diorite, granodiorite and aplite. Locally, Cone Mountain granodiorite intrudes along joints of Early Jurassic diorite plutons.

The Cone Mountain pluton, centred on Cone Mountain, underlies an area of 30 square kilometres and intrudes the Stikine assemblage. Its eastern contact, the Cone Mountain fault, is a mylonite zone 500 metres wide (*cf.* Chapter 4: Structure and Metamorphism).

A U-Pb zircon date of 184.7 ± 0.6 Ma (Brown *et al.*, 1992c; Appendix 13) for the Cone Mountain pluton is interpreted to represent the age of emplacement of the suite. It may be coeval with Hazelton Group volcanic rocks west of Yehiniko Lake (*cf.* U-Pb date for volcanic strata; Chapter 2). Discordant mineral pair and single mineral K-Ar dates for Cone Mountain suite plutons range from Early to Middle Jurassic. The Navo pluton yielded K-Ar dates of 182 ± 7 Ma for hornblende and 163 ± 6 Ma for biotite; the Dokdaon pluton yielded a hornblende K-Ar date of 158 ± 6 Ma (Appendix 12). The hornblende date for the Navo pluton is concordant with the Cone Mountain pluton U-Pb date; the other K-Ar dates are considered to be partially reset.

The Strata Glacier, Dokdaon and Devils Elbow plutons are the largest intrusions of the Cone Mountain suite. They underlie an area of approximately 165 square kilometres, from the headwaters of Strata Creek west to Devils Elbow. They are unfoliated, medium-grained (biotite) hornblende

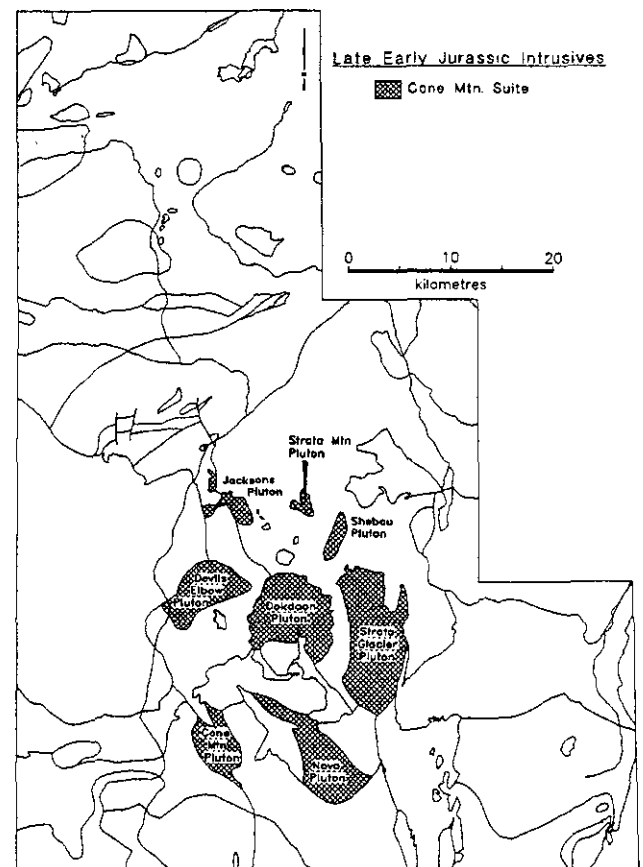


Figure 3-7. Distribution of late Early Jurassic Cone Mountain plutonic suite.

granodiorite to quartz monzodiorite which intrudes rocks of the Stuhini Group and Stikine assemblage. Titanite is a ubiquitous accessory mineral.

The Jacksons pluton is an irregular body of granodiorite which intrudes Carboniferous and Upper Triassic rocks 5 kilometres south of the confluence of Stikine River and Strata Creek. It contains numerous pendants of metavolcanic rocks adjacent to its contacts. Two kilometres west of Strata Mountain, a broad V-shaped body of medium-grained biotite-hornblende quartz monzodiorite comprises the Strata Mountain pluton. It intrudes rocks of the Stuhini Group but contact relationships with Lower Jurassic volcanic rocks to the north are uncertain. The Shebou pluton, 4 kilometres southeast of Strata Mountain, consists of texturally heterogeneous hornblende diorite and subordinate leucodiorite. On the south side of Strata Creek, this intrusion varies from fine to coarse grained, is locally foliated and rarely gneissic. On the steep slopes north of Strata Creek, the pluton is intensely altered and intruded by numerous pink, fine to medium-grained (biotite) hornblende granite to syenite dikes, thought to be comagmatic with the Middle Jurassic Saffron pluton; consequently, the contact relations with Lower Jurassic rocks to the north are uncertain.

MIDDLE JURASSIC THREE SISTERS PLUTONIC SUITE (177-170 Ma)

The Yehiniko, Niko and Saffron plutons are included in the Three Sisters suite, the younger phase of the Hotailuh batholith (cf. Anderson, 1983a; Figure 3-8).

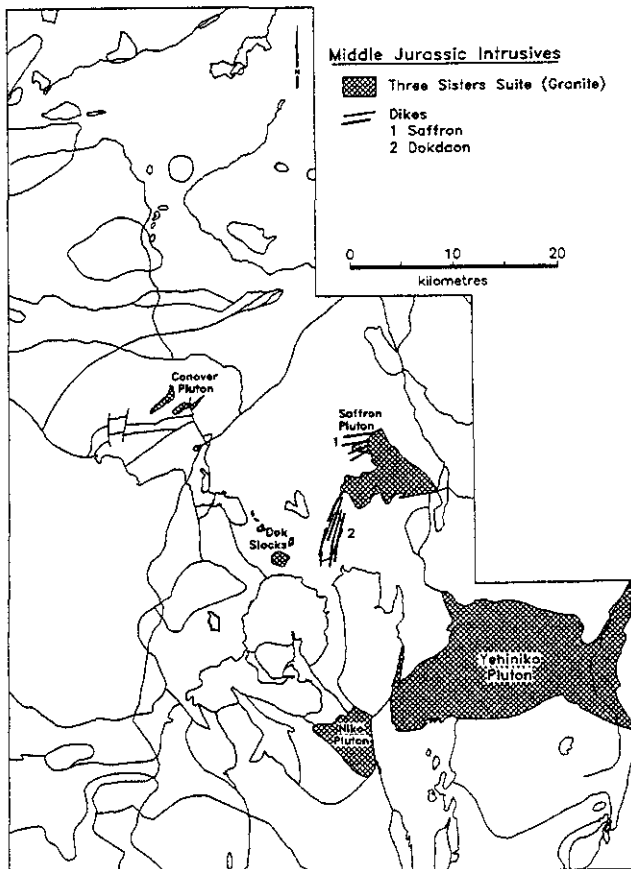


Figure 3-8. Distribution of Middle Jurassic Three Sisters Plutonic Suite.

YEHINIKO PLUTON

The Yehiniko pluton crops out over an area of about 200 square kilometres. It is composed of distinctive flesh to salmon-pink, medium-grained, equigranular biotite hornblende granite. It is distinguished from granite of the Eocene Sawback pluton by its colour, higher mafic content (colour index = 10-15) and presence of hornblende. Plagioclase is moderately saussuritized, unlike in the younger Sawback pluton, where it is generally unaltered. Magnetite and subordinate titanite are ubiquitous. Along the Scud Glacier, the pluton intrudes pyroxene-phyric Stuhini volcanic rocks on the east and the Nightout and Hickman plutons to the north and south, respectively. The Yehiniko pluton is interpreted to have been emplaced in the Middle Jurassic based on a biotite K-Ar date of 172 ± 6 Ma, and biotite and whole-rock Rb-Sr dates of 170 ± 16 Ma and 178 ± 11 Ma (Holbek, 1988).

NIKO PLUTON

The Niko pluton, west of the Scud Glacier, shares all the features of the Yehiniko pluton and is included in the Three Sisters suite. It yielded a biotite K-Ar date of 177 ± 7 Ma, which is concordant with dates from the Yehiniko pluton, and which is interpreted to represent the minimum age of emplacement (Appendix 12).

SAFFRON PLUTON

West of Yehiniko Lake, distinctive pink, medium and locally fine-grained hornblende biotite granite to quartz monzonite underlies an area of about 30 square kilometres and comprises the Saffron pluton. Northwest of Saffron Creek, distinctive orange to brown-weathering outcrops and regolith delineate the extent of this stock. Subordinate pale grey quartz monzodiorite, quartz monzonite and hornblende diorite comprise the southwest and southern parts of the pluton. The diorite is intruded by granite and quartz monzonite apophyses of the Saffron pluton and is therefore slightly older. The intrusion is more heterogeneous in both composition and texture than the Yehiniko pluton.

On the northeast margin of the Saffron pluton the steep contact with conglomerate of the Sustut Group is interpreted to be a fault. Contacts with Upper Triassic volcanic rocks and post-Late Triassic hornblende diorite on the south, and with Lower Jurassic volcanic rocks on the west, are intrusive and country rocks are strongly hornfelsed. Concordant hornblende and biotite K-Ar dates of 162 ± 6 Ma from the border phase monzonite and granite (Appendix 12), respectively, are interpreted to represent a minimum emplacement age for the Saffron pluton.

CONOVER PLUTON

West of the confluence of the Stikine and Chutine rivers, Stuhini Group rocks are intruded by distinctive seriate to crowded plagioclase-porphyrific hornblende monzonite to monzodiorite bodies. The intrusions, including the Conover pluton (about 2 km^2) and numerous associated sills, are texturally heterogeneous, but typically contain blocky to lath-shaped, locally trachytic plagioclase phenocrysts, 3 to 5 millimetres long, in a groundmass of hornblende, potassium feldspar, plagioclase and quartz. The

Conover intrusions have compositional, geochemical and textural similarities to the Pereleshin pluton. However, hornblende yielded a 177 ± 6 Ma K-Ar date (Appendix 12), therefore, they are included with the Three Sisters suite.

MIDDLE JURASSIC DIKE SWARMS AND DOK STOCKS

Abundant and distinctive pink dikes of biotite-hornblende-plagioclase (rarely potassium feldspar) porphyritic (quartz) syenite, granite and (quartz) monzonite are exposed near the west and southwest contacts of the Saffron pluton. They intrude Lower Jurassic and Upper Triassic rocks within an irregular north-northeast to northeast-trending zone marked by rusty, limonitic and clay-altered rocks. This suggests that the dikes, and in part, the alteration, are genetically related to the Saffron pluton and, together with the prominent hornfels zone around it, suggest that it is epizonal. Farther southwest along the trend of this zone, on the ridge between Dokdaon and Strata creeks, hornblende granite to quartz monzonite stocks and hornblende-plagioclase-porphyritic (quartz) syenite and (quartz) monzonite dikes are also tentatively correlated with the Saffron pluton. The stocks are associated with porphyry copper mineralization on the Dok claims (Ulrich, 1971).

EOCENE HYDER PLUTONIC SUITE (55-51 Ma)

The Cretaceous and early Tertiary was a time of extensive syntectonic and post-tectonic plutonism and uplift in the Coast Plutonic Complex. In the Ketchikan area, the Coast Belt can be divided into three suites on the basis of age: western tonalite (55-57 Ma); central orthogneiss (ca. 127 Ma); and eastern granite (52-53 Ma; Arth *et al.*, 1986). The eastern suite, equivalent to the Hyder Plutonic Suite of Woodsworth *et al.* (1991), is the most extensive of the plutonic suites in the study area (Figure 3-9). The plutons passively intruded strata along the eastern edge of the Coast Belt at shallow crustal levels; they are coeval with volcanic rocks of the Sloko Group, which are exposed in a discontinuous belt to the east.

CHRISTINA PLUTON

The Christina pluton underlies an area of about 75 square kilometres in the southwestern corner of the study area near Christina Creek. It is compositionally similar to Middle Jurassic granodiorites, but yielded concordant K-Ar dates of 56.1 ± 2.0 Ma (hornblende) and 54.2 ± 1.7 Ma (biotite; Appendix 12). A younger biotite K-Ar date of 45.1 ± 2 Ma was reported by White *et al.* (1968), but is considered to be partially reset.

SAWBACK PLUTON

The Sawback pluton, which underlies an area of 450 square kilometres, is the largest pluton exposed in the west-central part of the map area. It consists of equigranular, dull grey to pink, biotite granite, characterized by its medium to coarse grain size, well developed but widely spaced joints (Photo 3-3) and relatively unaltered nature. Quartz is commonly coarse grained, in contrast with that in the Middle

Jurassic granites, and forms up to 50% of the rock. Potassium feldspar ranges up to 30% and is locally megacrystic; plagioclase averages 20% and biotite less than 4%. Hornblende is absent, helping to distinguish the Eocene plutons from the Middle Jurassic Yehiniko and Saffron plutons.

Limestone and rare argillite pendants within the granite are altered to skarn, foliated, and at Mount Jonquette, exhibit "chocolate tablet" boundinage. Exoskarn and less common endoskarn assemblages consist of garnet, diopside and wollastonite. Mafic dikes intrude the pendants, are deformed with the limestone, and are cut by the granite. Fine to medium-grained diorite also intrudes the limestone pendants. Garnet (almandine)-bearing aplite dikes, less than 1 metre wide, crosscut both the diorite pendants and the granite. Along the Stikine River in Klootchman Canyon, the pluton is strongly fractured. Farther north, near Missusjay Creek, pendants of recrystallized limestone, several hundreds of metres across, crop out along the margin of the pluton, and fine-grained granite and aplite dikes extend into the country rock. Three kilometres south of Mount Jonquette, the southern margin of the pluton is marked by a heterogeneous, xenolith-rich zone over 100 metres wide, which contains angular to rounded inclusions of folded phyllitic to schistose metavolcanic(?) rocks and diorite (Photo 3-4). The variation in degree of deformation of xenoliths suggests they were derived from different crustal levels or they had different residence times within the magma chamber. The more de-

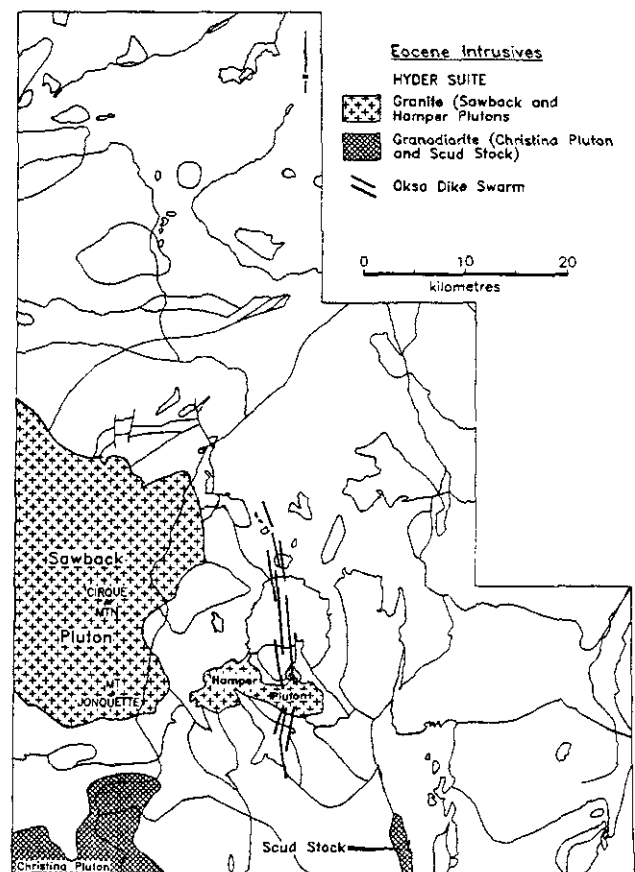


Figure 3-9. Distribution of Eocene Hyder Plutonic Suite.



Photo 3-3. Well jointed exposures, a characteristic of the Eocene Sawback granite pluton, in the Sawback Range, Coast Mountains, 3 kilometres north of Cirque Mountain.

formed blocks were either heated to higher temperatures, allowing them to deform ductily, or they originated at deeper crustal levels where higher stresses may have been prevalent.

A middle Eocene K-Ar biotite date of 48.0 ± 1.7 Ma (Appendix 12) is a minimum age for intrusion of the Sawback pluton. Two small plugs south of Galore Creek included in the suite, yielded K-Ar biotite dates of 48.9 ± 4 and 53.5 ± 4 Ma (Panteleyev, 1975, 1976).

HAMPER PLUTON

The Hamper pluton, about 35 square kilometres in area, is included in the Hyder suite. It intrudes the late Early Jurassic Strata Glacier pluton and Oksa Creek pluton and is similar in composition (biotite granite) and texture to the Sawback pluton. Mirolitic cavities lined with quartz, epidote and pyrite occur in the intrusion near Oksa Creek. Like the Sawback pluton, it is also associated with skarns. Near the headwaters of Oksa Creek, the Hamper pluton intrudes Permian limestone and a garnet (two phases), diopside, epidote and wollastonite skarn is developed for up to 10 metres from the irregular contact. Boudinaged calcisilicate layers and pods in grey marble contain quartz cores surrounded by radiating wollastonite needles and an outer rim of diopside. Malachite-stained fractures occur near the contact, in both the limestone and intrusions.

The Hamper pluton intrudes diorite and granodiorite plutons 5 kilometres southeast of Oksa Mountain (Photo 3-5). This area of multiphase intrusion and brecciation resembles that described for the Sawback pluton south of Mount Jonquette, except no metamorphic xenoliths were identified. Inclusions vary from subrounded, ductily deformed mafic schlieren to angular fragments of diorite. The xenoliths increase in size and abundance toward the contact of the Davo diorite. Irregular patches of hornblende-potassium feldspar-quartz pegmatite with acicular hornblende occur in this area. At one locality, a granodiorite breccia xenolith is itself a block in the granite. The intrusive relationships indicate that diorite and granodiorite were intruded prior to the granite. A single granite xenolith observed within granodiorite is an exception to this sequence.

OKSA CREEK DIKE SWARM

A steeply dipping, north-striking bimodal dike swarm extends north for more than 35 kilometres from the headwaters of Navo Creek to the confluence of Dokdaon and Strata creeks. The swarm, up to 3 kilometres wide, is dominated by prominent buff to white-weathering, quartz-phyric felsite and rhyolite dikes 1 to 10 metres wide. Some are flow banded and others are stained with manganese oxide on joint surfaces. The felsite dikes intrude Permian limestone and crosscut a swarm of vesicular basalt dikes that trend north to northeast near the headwaters of Oksa Creek. The mafic



dikes are narrower, up to 2 metres wide, closer spaced and more uniform in width.

A biotite-rich felsite body exposed within the Oksa dike swarm at the head of Dokdaon Creek yielded a K-Ar biotite date of 49.7 ± 1.7 Ma (Appendix 12). Therefore, the felsite dikes and coeval Sawback pluton may be intrusive equivalents of Sloko Group volcanic rocks.

TERTIARY(?) GRANODIORITE

Limonitic weathering plagioclase-porphyratic granodiorite in the headwaters of the Scud River forms an elongate, north-trending body, covering an area of 7.5 square kilometres, subparallel to the Scud Glacier fault. The granodiorite intrudes Permian limestone, contains prominent white plagioclase laths in a fine-grained green groundmass, and is pervasively fractured and altered (chlorite, sericite, pyrite). The pluton is tentatively included in the Tertiary suite because of its porphyritic, high-level nature. Alternatively, it may correlate with a dated Early Jurassic pluton (Scud River pluton) exposed northeast of Galore Creek (*cf. White et al., 1968; Logan et al., 1993a,b*).

LATE MIOCENE (?) OR YOUNGER DIKES

East-trending, metre-scale olivine(?) and pyroxene-porphyratic basalt dikes form two swarms several kilometres wide, one within the Hickman pluton and the other near the contacts of the Yehiniko and Nightout plutons (Kuys dike swarm; Figure 4-2). The mafic dikes are probably Late Miocene or younger, and related to Mount Edziza Complex magmatism.

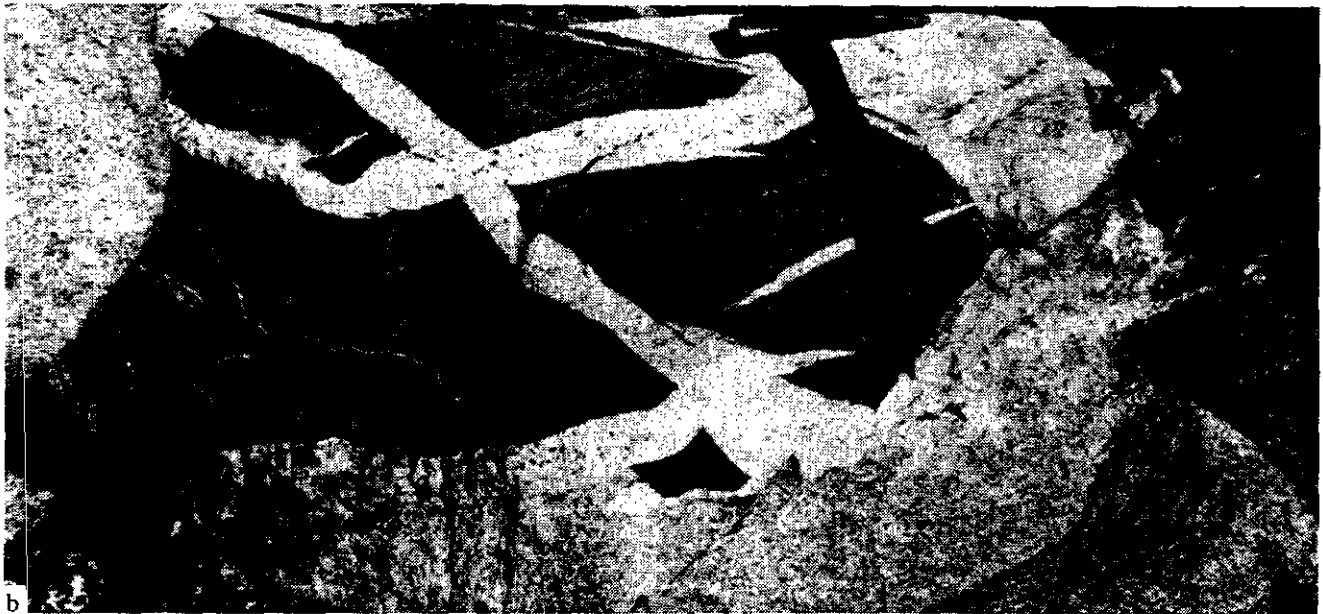


Photo 3-4. (a) Tightly folded, amphibolite-grade phyllite xenolith within the Geology Ridge diorite, along the migmatic northern contact zone with the Sawback pluton (DBR-90-18). Lithology and style of deformation of the xenolith suggest a probable Stikine assemblage protolith. (b) Brecciated diorite xenolith and multiphase intrusion of granite along the southern contact of the Sawback pluton, 3 kilometres south of Mount Jonquette and 500 metres north of (a) (DBR-90-19). Diorite blocks are angular to wispy, defining different degrees of deformation and foliation in both brittle and ductile regimes.



Photo 3-5. Complex transition breccia zone with Jurassic diorite and granodiorite inclusions hosted by Eocene granite of the Hamper pluton, 2.6 kilometres southeast of Hamper Mountain (Photograph by M. McDonough).

GEOCHEMISTRY AND TECTONIC DISCRIMINATION OF INTRUSIVE ROCKS

Classification schemes for plutonic rocks attempt to achieve two goals: they distinguish rock types and help to interpret tectonic settings. Determination of modal mineral proportions of quartz, alkali feldspar, plagioclase and feldspathoids remains the preferred method of subdividing plutonic rocks because of its simplicity and ease of application (Le Bas and Streckeisen, 1991). Classification schemes based solely on chemistry have inherent limitations because rock chemistry can be significantly modified by processes which include fractional crystallization, crustal contamination, migration of volatile phases, crystallization of minerals rich in trace or rare earth elements (*e.g.* monazite), and post-crystallization alteration (Pearce *et al.*, 1984). Despite these variations, general trends are recognized that form the basis for discrimination of igneous suites and corroborate field divisions.

Alkali-silica and AFM diagrams distinguish plutonic rock suites and help subdivide the ultramafic cumulate bodies. Whole-rock samples that plot along the FeO-MgO tie line on the AFM diagram are interpreted to reflect cumulate mineral phases, not the bulk composition of the parent magma. However, samples that plot off the tie line may reflect magmatic compositions. These factors are important when interpreting a suite of samples distributed on the diagrams.

Whole-rock chemical analyses of 65 samples of intrusive rocks from the Stikine project area corroborate the field

observations and petrographic examinations that distinguish plutonic suites. Voluminous calcalkaline, subalkaline plutons comprise the Triassic Stikine suite (Hickman, Nightout, Tahltan Lake, Little Tahltan Lake, Tahltan River plutons), the Early Jurassic Texas Creek suite (Limpoke pluton), the late Early Jurassic Cone Mountain suite (Cone Mountain, Navo, Niko, Strata Glacier, Dokdaon plutons), the Middle Jurassic Three Sisters suite (Yehiniko, Saffron, Conover plutons) and the Eocene Hyder suite (Sawback pluton). Two ultramafic suites display distinct chemistry relative to each other and to the calcalkaline suites; they are Middle to Late Triassic Alaskan-type intrusions (Mount Hickman, Middle Scud and Yehiniko ultramafites) along the flanks of the Hickman batholith, and Late Triassic to Early Jurassic ultramafites (Rugged Mountain, Latimer Lake and Damnation), associated with alkaline plutons. The following discussion summarizes the chemical characteristics of each plutonic suite in the project area and reviews their tectonic implications.

MIDDLE TO LATE TRIASSIC

ALASKAN-TYPE ULTRAMAFIC PLUTONS

Samples from the Mount Hickman, Middle Scud and Yehiniko ultramafites form a cluster on the alkali-silica diagram, and scatter along the FeO-MgO tie line of the AFM diagram (Figure 3-10a and b). Cumulate diopsidic pyroxene, olivine and magnetite observed in thin section determine where samples plot. The positions of each sample on the AFM diagram reflect different cumulate mineral proportions and mineral compositions; the Yehiniko and Middle Scud bodies tend to have a restricted compositional range and less magnetite compared to Mount Hickman.

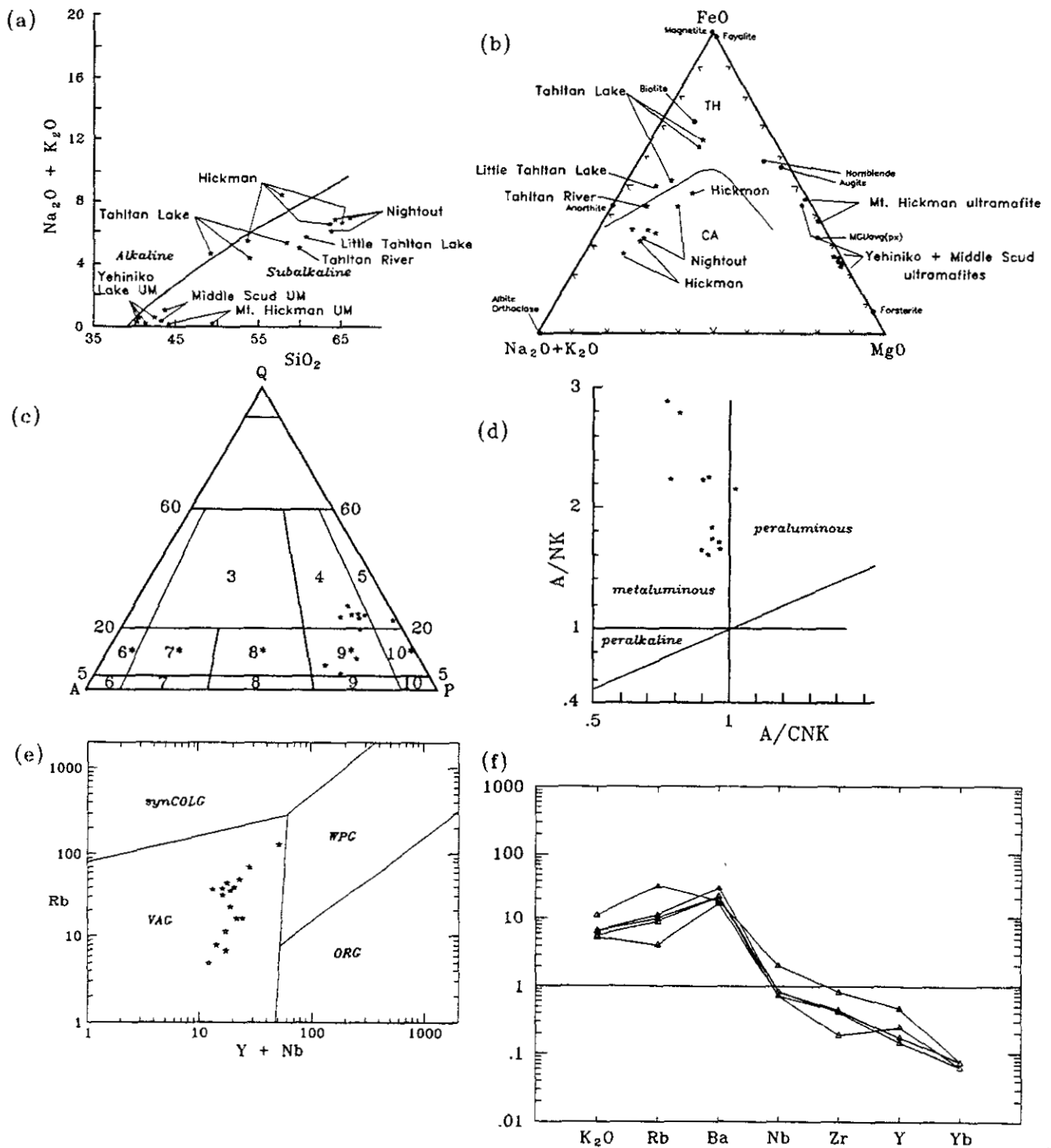


Figure 3-10. Chemical characteristics of the Stikine suite compared with the Alaskan-type ultramafites: (a) Alkali-silica diagram. (b) AFM diagram. (c) Quartz - alkali feldspar - plagioclase diagram of Streckeisen (1976); Q=quartz, A=alkali feldspar, P=plagioclase, 3=granite, 4=granodiorite, 5=tonalite, 6=alkali feldspar syenite, 6*=quartz alkali-feldspar syenite, 7=syenite, 7*=quartz syenite, 8=monzonite, 8*=quartz monzonite, 9=monzodiorite, 9*=quartz monzodiorite, 10=diorite, 10*=quartz diorite. (d) Shand index values. (e) Tectonic discrimination diagram after Pearce *et al.* (1984); VAG = volcanic-arc granites, ORG = ocean-ridge granites, WPG = within-plate granites, synCOLG = syncollision granites. (f) Ocean-ridge granite (ORG) normalized geochemical patterns; ORG normalizing values are listed in Table 3 of Pearce *et al.* (1984).

The MgO/MnO ratios distinguish the Middle to Late Triassic Alaskan-type and the Late Triassic to Early Jurassic alkaline ultramafites; ratios greater than 90 are characteristic of the Mount Hickman, Middle Scud and Yehiniko plutons, whereas ratios less than 90 characterize the Rugged Mountain, Latimer Lake and Damnation intrusions. The ratios are a function of pyroxene compositions; Alaskan-type plutons have diopsidic pyroxene and alkaline plutons contain aegirine-augite (Neill and Russell, 1993). The Alaskan-type ultramafites differ from the alkaline suite in their lack of syenite phases, pyroxene compositions and absence of garnet.

STIKINE SUITE

Some of the largest plutons in the project area belong to the Stikine suite. They range in composition from monzodiorite to granodiorite and tonalite with subalkaline, calc-alkaline to tholeiitic affinities (Figure 3-10a, b and c). The Tahltan Lake and Little Tahltan Lake plutons plot in the tholeiitic field on an AFM diagram, presumably due to higher magnetite and biotite contents than the other plutons (Figure 3-10b). Stikine suite samples display I-type characteristics, a term defined by Chappell and White (1974) to signify pluton derivation from partial melting of igneous protoliths, followed by normal igneous differentiation. The Stikine suite has relatively high sodium ($\text{Na}_2\text{O} > 3.2\%$ in felsic varieties), Shand's index less than 1.1 (metaluminous; Shand, 1951; Figure 3-10d), CIPW normative diopside or normative corundum less than 1%, a wide compositional spectrum, hornblende, biotite, accessory titanite and no muscovite. Shand's index reflects the degree of alumina saturation; as alumina increases, the source crust is interpreted to be more evolved. Rock classification of the Stikine suite using normative chemistry on the QAP ternary diagram (Figure 3-10c) agrees closely with modal classification of stained slabs performed in the field (compare "rock code" with "QAP" in Appendix 11).

LATE TRIASSIC TO EARLY JURASSIC ALKALINE & ULTRAMAFIC PLUTONS

The Rugged Mountain suite varies in composition from syenite to clinopyroxenite and has clear alkaline characteristics, in contrast to other plutons in the study area (Figure 3-11a). Monzonite dike, syenite and hybrid (mafic syenite) samples fall along a line on the AFM diagram that can be extended from the distinct cluster of clinopyroxenites to the alkali-rich dikes (Figure 3-11b). The pattern illustrates an alkali-enrichment trend, which is compatible with extraction of cumulate aegirine-augite from an assumed parent melt (clinopyroxenite cluster). Evolution to more potassium rich residual melts ultimately produced the potassium-feldspar megacrystic dikes. Cumulate aegirine-augite, magnetite and melanite garnet in the ultramafite samples (Neill and Russell, 1993) determine where samples plot on the AFM diagram (Figure 3-11b). In the study area, these phases are unique to the alkaline suite and explain the distinct distribution on the AFM diagram relative to the Alaskan-type ultramafites discussed previously. Although the syenites are nepheline normative and plot in the foid-bearing syenite field, no modal nepheline or other feldspathoids have been

recognized, possibly because they have been altered (Neill and Russell, 1993; Figure 3-11c). Normative values were determined with all iron assigned to Fe_2O_3 ; despite this, no normative silica was calculated. Neill and Russell (1993) documented that the phases are comagmatic and that the Rugged Mountain samples show an iron-depletion trend, toward the potassium feldspar apex from hybrid to dike phases (Figure 3-11). All the noncumulate samples are metaluminous (Figure 3-11d).

Stuhini Group rocks in the area of the Rugged Mountain pluton were not sampled in detail, however, shoshonitic lavas may occur in the area. For example, shoshonitic extrusive equivalents of the alkaline plutons are recognized around Galore Creek (Logan and Koyanagi, 1994) and in the Nicola Group of the southern Intermontane Belt (Mortimer, 1987).

TEXAS CREEK SUITE

The Early Jurassic Texas Creek suite is represented by a sample of quartz monzodiorite from the Limpoke pluton and two samples from the Pereleshin pluton (Figure 3-12a, b, c and d). They plot in overlapping fields with the Stikine suite samples (Figures 3-10, 3-15) and display I-type affinity.

CONE MOUNTAIN SUITE

Late Early Jurassic Cone Mountain suite samples are subalkaline. They have lower alkali contents at comparable silica values relative to samples of the Stikine and Three Sisters suites (Figures 3-12a; 3-15). However, the three suites overlap on the AFM diagram [Figure 3-15(b)]. Samples collected from the Cone Mountain, Navo, Dokdaon and Strata Glacier plutons were identified as granodiorite in the field but range from tonalite to granite on Figure 3-12c. They display I-type affinities with metaluminous to mildly peraluminous character (Figure 3-12d).

THREE SISTERS SUITE

Plutons of the Middle Jurassic Three Sisters suite are subalkaline, calcalkaline, I-type granites, except for one dike sample that falls in the alkaline field (Figure 3-13a, b and c). The intrusions are dominantly peraluminous (Figure 3-13c), with normative corundum greater than 1%. Samples from two phases of the Saffron pluton are represented: the main granite and the border quartz monzodiorite. They are widely separated on the plots. A monzodiorite from the Saffron pluton, a monzonite from the Conover pluton, and a granodiorite dike plot in the metaluminous field (Figure 3-13d).

HYDER SUITE

Chemical characteristics of the Eocene Hyder suite plutons are similar to those of the Three Sisters suite; they are dominated by subalkaline, calcalkaline granite of I-type affinity (Figure 3-14a, b and c). They range in composition from tonalite to granite (Figure 3-14c). The intrusions are peraluminous and metaluminous (Figure 3-14d), with normative corundum greater than 1%.

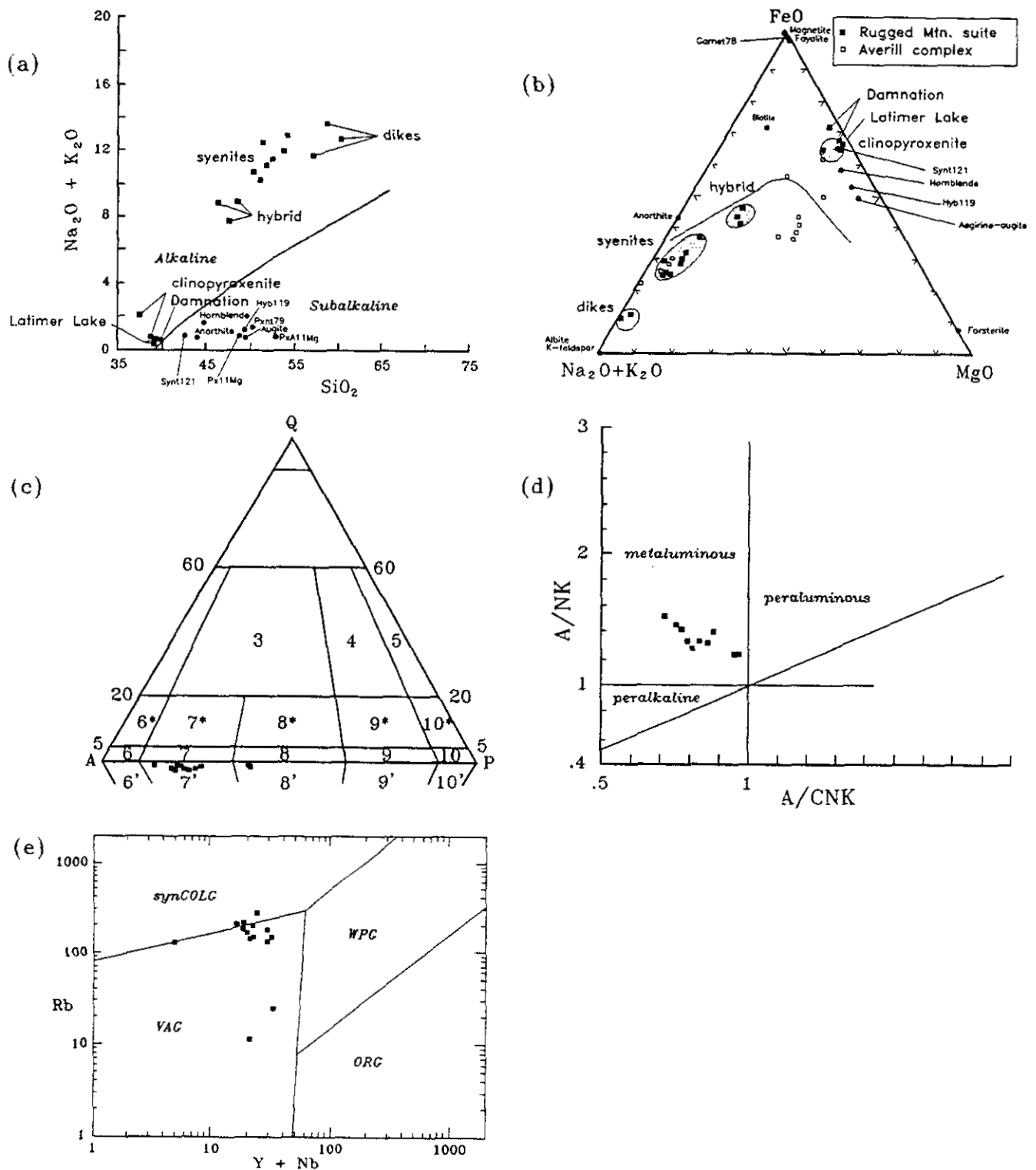


Figure 3-11. Chemical characteristics of the Rugged Mountain complex: (a) Alkali-silica diagram. (b) AFM diagram with mineral compositions obtained from microprobe studies by Neill (1992), Gunning (1993a), and Deer *et al.* (1977). Comparison of Rugged Mountain intrusions and Averill Plutonic Complex (from Neill, 1992). Solid squares = Rugged Mountain intrusions, open squares = Averill Complex. (c) Quartz - alkali feldspar - plagioclase diagram; 7' = foid-bearing syenite, 8' = foid-bearing monzonite. (d) Shand index values. (e) Tectonic discrimination diagram after Pearce *et al.* (1984); abbreviations as in Figure 3-10(e).

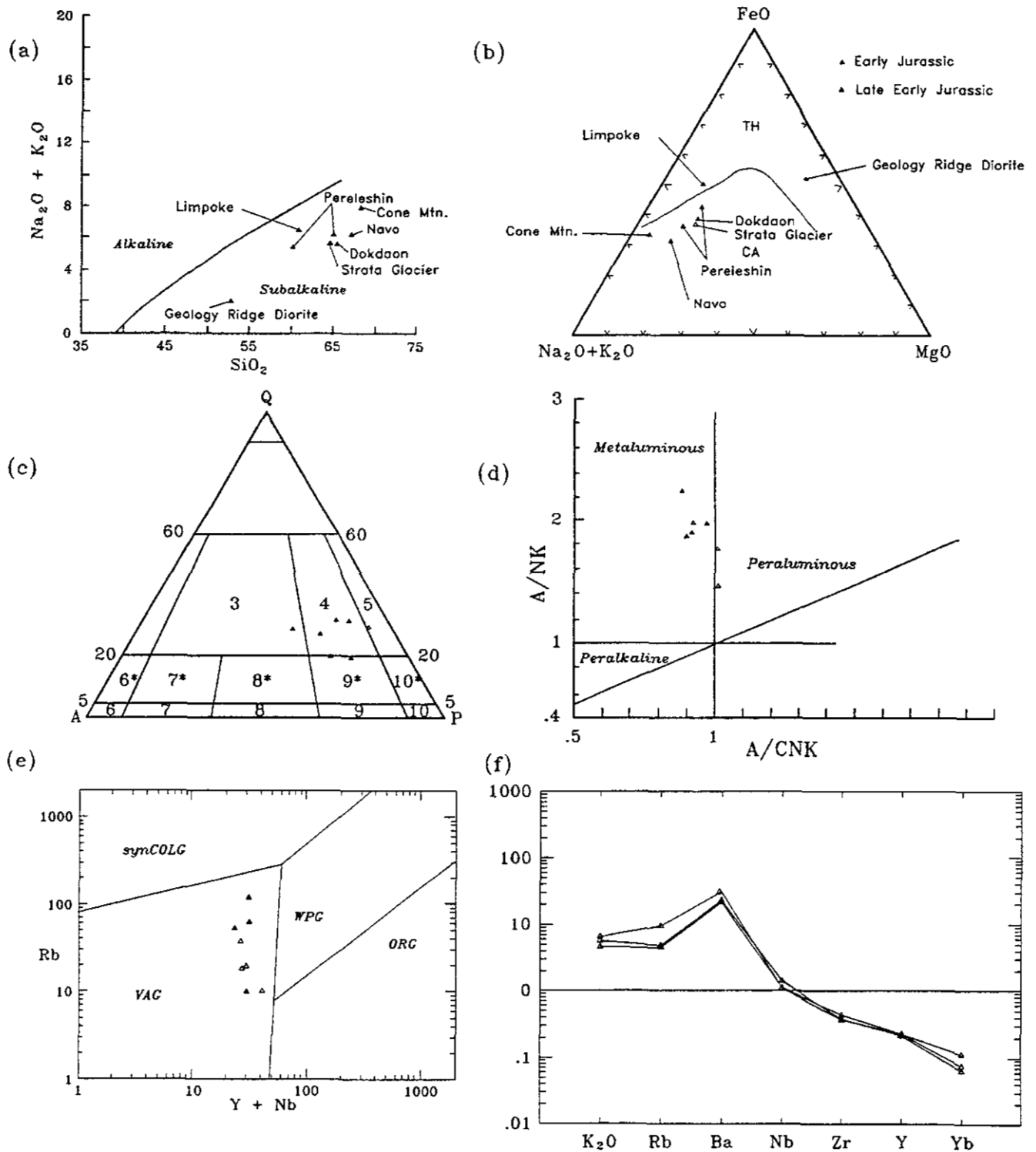


Figure 3-12. Chemical characteristics of the Early Jurassic Texas Creek and late Early Jurassic Cone Mountain suites: (a) Alkali-silica diagram. (b) AFM diagram. (c) Quartz - alkali feldspar - plagioclase diagram with fields and abbreviations as shown in Figure 3-10(c). (d) Shand index values. (e) Tectonic discrimination diagram after Pearce *et al.* (1984). (f) Ocean-ridge granite (ORG) normalized geochemical patterns; ORG normalizing values are listed in Table 3 of Pearce *et al.* (1984).

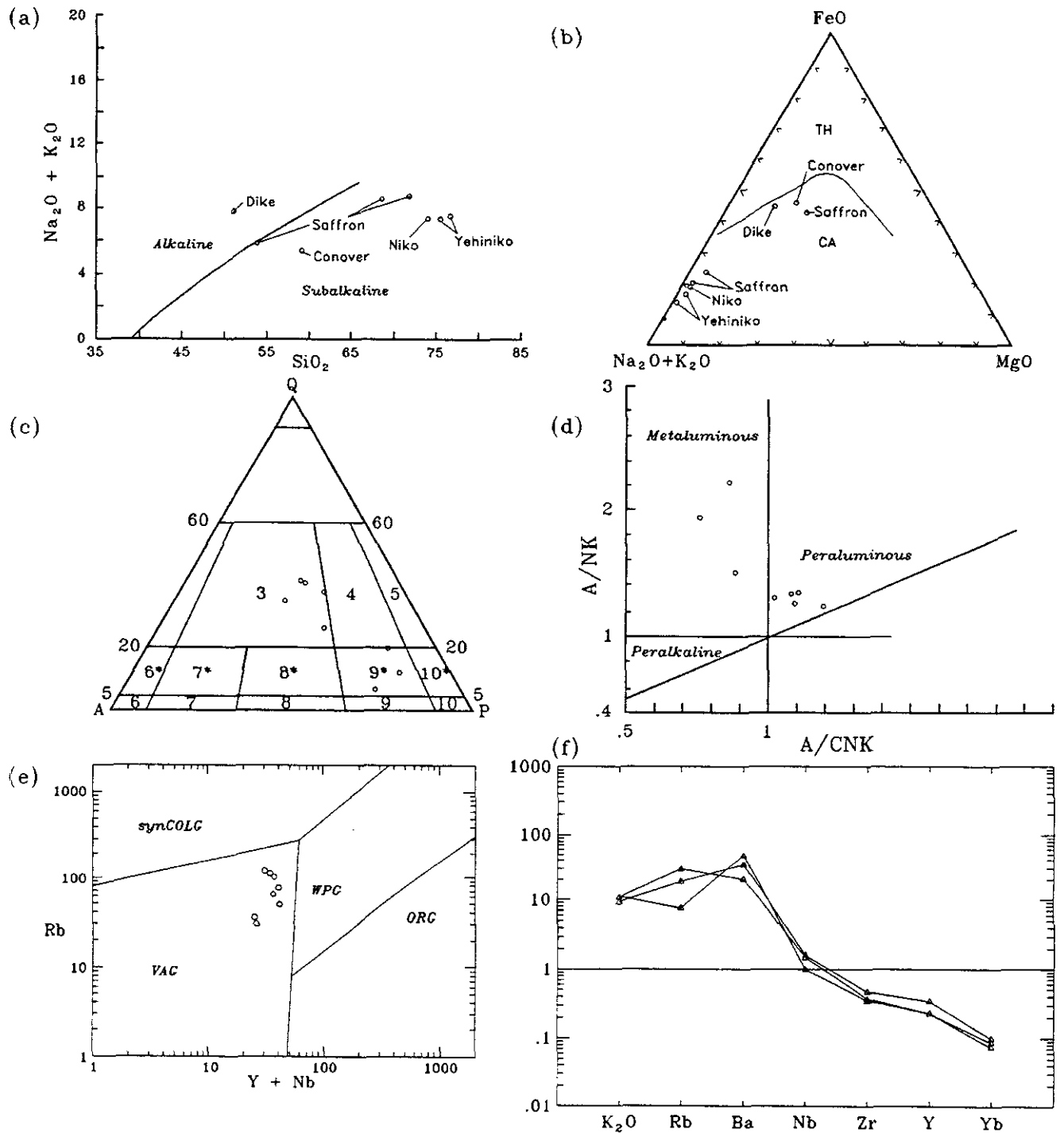


Figure 3-13. Chemical characteristics of the Middle Jurassic Three Sisters suite: (a) Alkali-silica diagram. (b) AFM diagram. (c) Quartz - alkali feldspar - plagioclase diagram with fields and abbreviations as shown in Figure 3-10(c). (d) Shand index values. (e) Tectonic discrimination diagram after Pearce *et al.* (1984). (f) Ocean-ridge granite (ORG) normalized geochemical patterns; ORG normalizing values are listed in Table 3 of Pearce *et al.* (1984).

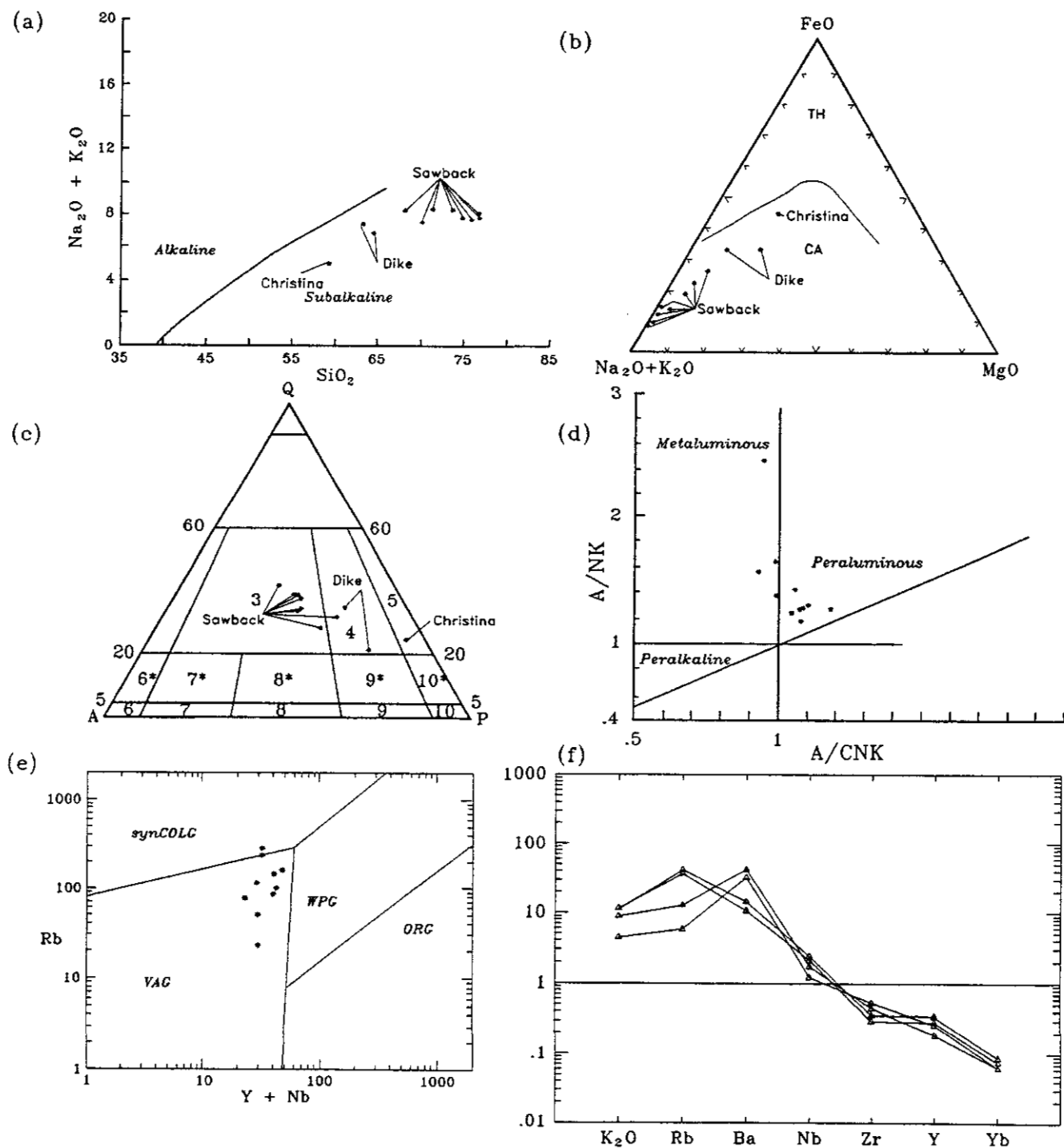


Figure 3-14. Chemical characteristics of the Eocene Hyder suite: (a) Alkali-silica diagram. (b) AFM diagram. (c) Quartz - alkali feldspar - plagioclase diagram with fields and abbreviations as shown in Figure 3-10(c). (d) Shand index values. (e) Tectonic discrimination diagram after Pearce *et al.* (1984). (f) Ocean-ridge granite (ORG) normalized geochemical patterns; ORG normalizing values are listed in Table 3 of Pearce *et al.* (1984).

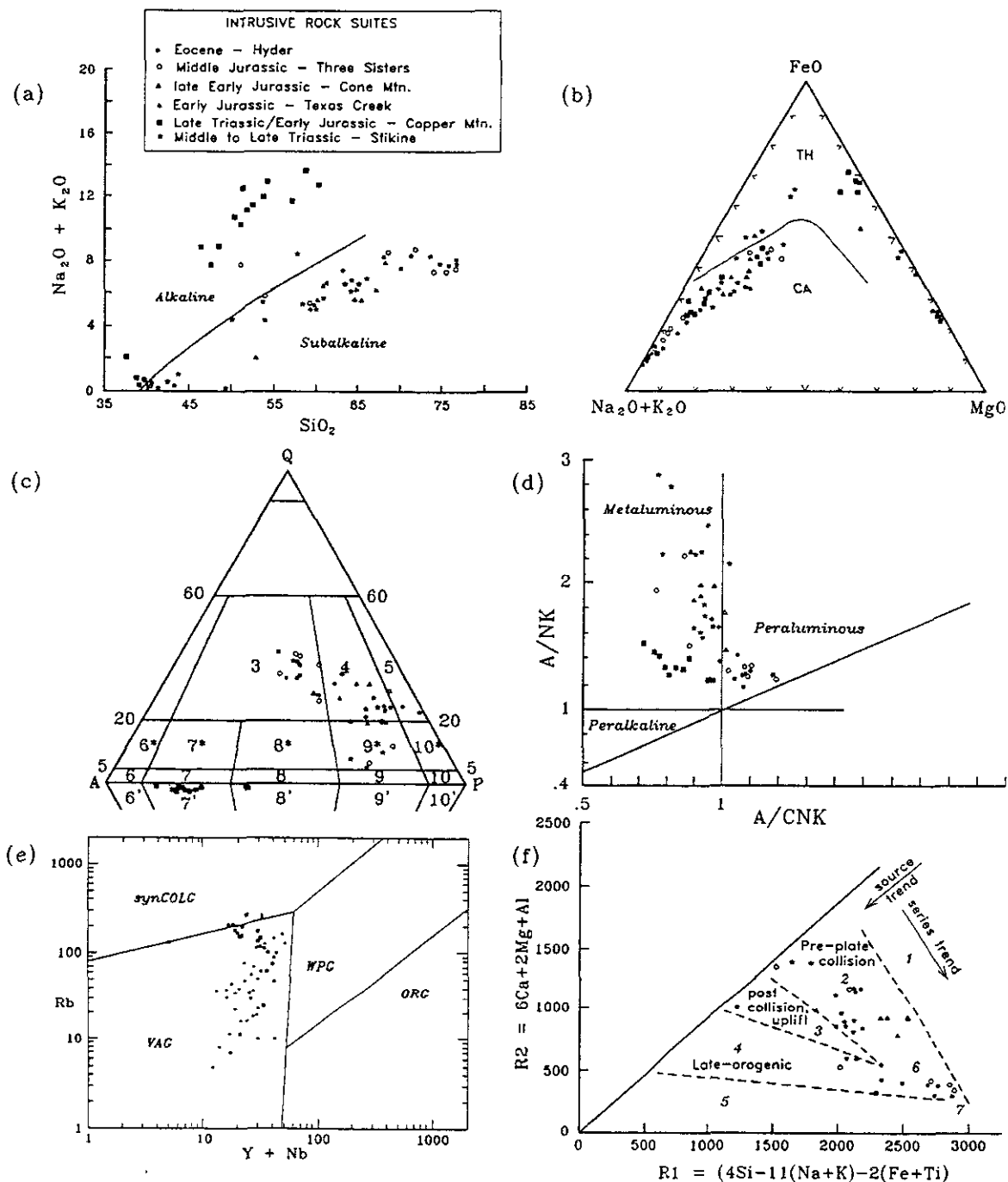


Figure 3-15. (a) Total alkali-silica variation diagram displaying the distinctly alkaline character of the Rugged Mountain pluton compared to all the other suites (alkaline - subalkaline division after Irvine and Baragar, 1971). The Yehiniko and Sawback plutons are clearly the most silicic. Mafic border phases of the plutons have not been included in this plot. Mineral compositions are from microprobe studies by Neill (1992), Gunning (1993a), and Deer *et al.* (1977). (b) AFM diagram (calcalkaline-tholeiitic division after Irvine and Baragar, 1971) for plutonic rocks from the project area; note that ultramafic rocks plot within the tholeiitic field. Eocene Hyder suite samples are from the Sawback pluton, except one from Christina pluton. (c) Quartz - alkali feldspar - plagioclase - feldspathoid diagram for plutonic rocks using the classification scheme of Streckeisen (1976), based on modal mineralogy for rocks with less than 90% mafic minerals. (d) Shand's index diagram showing relative alumina saturation (Shand, 1951); most plutons are metaluminous, only the granites are peraluminous. $A/NK = \text{Al}_2\text{O}_3/(\text{Na}_2\text{O} + \text{K}_2\text{O})$, $A/CNK = \text{Al}_2\text{O}_3/(\text{CaO} + \text{Na}_2\text{O} + \text{K}_2\text{O})$. (e) Tectonic discrimination diagram for plutonic rocks; (Y+Nb) versus Rb (after Pearce *et al.*, 1984). (f) Granitoid samples plotted on the R1 - R2 multicatication diagram with superimposed tectonic environment boundaries (Batchelor and Bowden, 1985).

TECTONIC DISCRIMINATION

Since Chappell and White (1974) first proposed the I and S-type subdivision, I-type granites have been further subdivided into M and A-type granites with respective derivation from oceanic and continental crust (Pitcher, 1982). Empirical and theoretical studies combined with higher precision analytical data continue to refine chemical classification schemes and discrimination of granitoid tectonic regimes, most notably for A-type granites (*cf.* Whalen *et al.*, 1987; Eby, 1992). As well, rare earth element (REE) patterns can be employed to discriminate among tectonic settings (eg. Pearce *et al.*, 1984). Ocean ridge granite (ORG) normalized geochemical patterns for the subalkaline Triassic, Early and Middle Jurassic and Eocene plutons all display a similar pattern of strong enrichments in large-ion lithophile elements (Sr, K, Rb and Ba) and depleted Nb, Zr, Ti, Y and Yb relative to the norm (Figure 3-10(f) to 14(f)); such features are typical of volcanic arc granitoids (Pearce *et al.*, 1984). Extrusive rocks of the Stuhini Group mimic plutonic chemistry, with REE patterns typical of subduction-generated calcalkaline arcs (Pearce, 1983; *cf.* Chapter 2). Mesozoic plutons of Stikinia have chemical characteristics similar to those of Pacific and Andean-type magmas (Pitcher, 1982). Our geochemical data suggest that the Stikine Terrane crust evolved from a primitive island arc in the Late Triassic to a mature continental arc by the Middle Jurassic. This corroborates tectonic models proposed for northern Stikinia. The general enrichment in silica and alkalis from Triassic through to Middle Jurassic and Eocene is illustrated in Figure 3-15(a); the same feature is reflected by the progression from metaluminous to peraluminous compositions. Trace element data for the subalkaline plutons show similar trends from primitive to more evolved volcanic-arc signatures through time (Figure 3-15(f)). The following discussion considers four plutonic periods and their tectonic implications: Late Triassic, Early Jurassic, Middle Jurassic and Eocene.

LATE TRIASSIC

Stuhini Group intravolcanic conglomerate contains granitoid clasts that are indistinguishable from Hickman pluton granodiorite. Conglomerate occurs predominantly along the western flank of the pluton. Anderson (1983a), documents similar polymictic conglomerate within the Stuhini Group adjacent to the Hotailuh batholith. The sub-rounded clasts provide evidence of rapid unroofing of Triassic plutons during Late Triassic volcanism.

Samples from the Rugged Mountain pluton straddle the field boundary between the volcanic arc and syncollisional granite fields of Pearce *et al.* (1984; Figure 3-11(e)). The alkaline chemistry and mineralogy is unique among the plutonic suites but the tectonic setting is ambiguous.

EARLY JURASSIC

The monzodiorite sample for the Limpoke pluton falls within the volcanic-arc granite field on the (Nb+Y) *versus* Rb plot of Pearce *et al.* (1984; Figure 3-12e). This is compatible with the interpreted arc setting for Hazelton volcanism farther south in the Iskut-Stewart area (*e.g.*, Anderson, 1993).

MIDDLE JURASSIC

Analyses from most Middle Jurassic Three Sisters suite plutons plot in the corner of the volcanic-arc granitoid field, close to the syncollisional field (Figure 3-13e). They mark the first episode of evolved granitic plutonism in the study area and presumably signify a maturing (thickening) of the crust. Their extrusive equivalents may be the less extensive, younger part of the Hazelton Group.

EOCENE

The voluminous Eocene Sawback pluton of the Hyder suite displays volcanic-arc granitoid chemical characteristics much like the Middle Jurassic Three Sisters suite (Figure 3-14e). The extensive plutonism is attributed to subduction of Pacific oceanic plates beneath the North American plate.

TEMPORAL EVOLUTION OF PLUTONS: THE OROGENIC CYCLE

In general, a temporal progression from metaluminous, low-silica quartz diorite to granodiorite plutons in the Triassic to more evolved peraluminous granite plutons by the Middle Jurassic and Eocene is evident (Figure 3-15). Batchelor and Bowden (1985) modelled the progression of compositions through an orogenic cycle on a multicationic diagram (Figure 3-15(f)). The majority of calcalkaline intrusions fall within the pre-plate collision (destructive plate margin) field, except for Middle Jurassic and Eocene granites that lie in the late-orogenic field. The diagram illustrates that Triassic, pre-plate collision granitoids evolved compositionally toward Middle Jurassic granite, as predicted for typical orogenic cycles (*cf.* Batchelor and Bowden, 1985).

CHAPTER 4 STRUCTURE AND METAMORPHISM

The study area lies between three regionally extensive fault systems: King Salmon fault (Souther, 1971; about 100 km north), Sumdum-Fanshaw fault (McClelland *et al.*,

1991; about 75 km southwest), and Skeena fold belt (Evenchick, 1991b, c; 125 km east; Figure 4-1). They control the structural grain of much of northern Stikinia. The

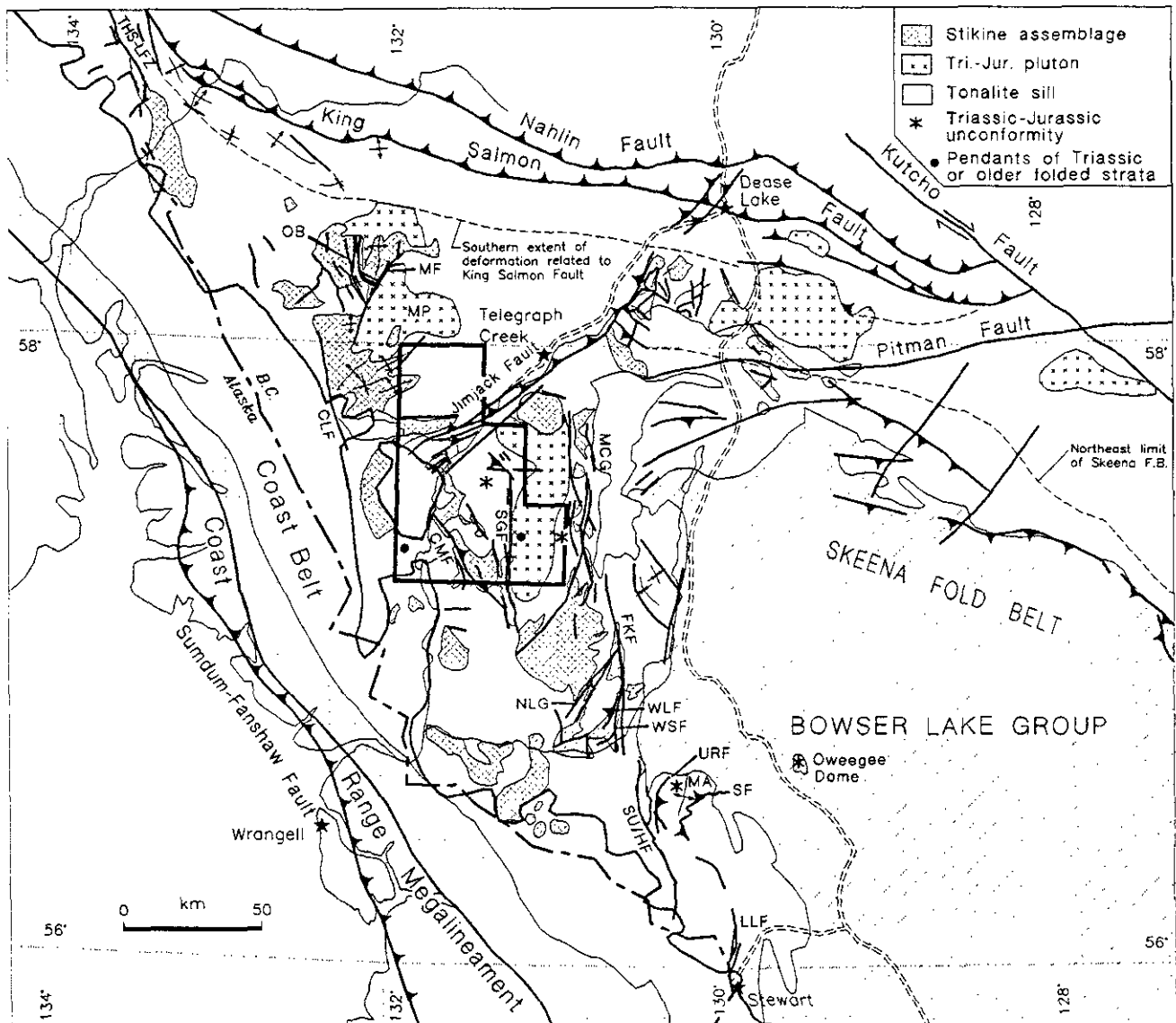


Figure 4-1. Distribution of major faults in northwestern British Columbia, modified after Bradford and Brown, 1993a; Evenchick, 1991b,c; Lewis, 1992; Logan *et al.*, 1992b; Mihalynuk *et al.*, 1994; Read, 1983, 1984; Souther, 1959, 1971, 1972; and Wheeler and McFeeley, 1991. CLF = Chutine Lake fault, CMF = Cone Mountain fault, FKF = Forrest Kerr fault, LLF Long Lake fault, MA = McTagg anticlinorium, MCG = Mess Creek graben, MF = Moosehorn fault, MP = Moosehorn pluton, NLG = Newmont Lake graben, OB = Ophir Break, SF = Sulphurets fault, SGF = Scud Glacier fault, SU/HF = South Unuk/Harremel fault, THS-LFZ = Tally Ho shear-Llewellyn fault zone, URF = Unuk River fault, WLF = West Lake fault, WSF = West Slope fault.

King Salmon fault system comprises west to northwest-trending, southwest-verging folds and faults which involve rocks as young as the Lower Jurassic Laberge Group, that developed during Middle Jurassic contractional deformation (Thorstad and Gabrielse, 1986). This is interpreted to mark the final accretion and obduction of Cache Creek Terrane onto Stikinia. The Skeena fold belt comprises north-east-verging folds and faults that developed in the Bowser Lake and lower Sustut groups in latest Jurassic to Early Cretaceous and latest Cretaceous to early Tertiary time, during accretion of the Intermontane Superterrane to ancestral North America (Evenchick, 1991b, c). The Sumdum-Fan-shaw deformation occurred in mid-Cretaceous to Paleocene time and may represent the underthrusting of Alexander Terrane beneath Yukon-Tanana and Taku terranes (McClelland *et al.*, 1991). Brittle deformation postdating the Skeena fold belt is characterized by north-trending transcurrent and extensional faults, which formed in Miocene and later time (Souther, 1970), following a change from pure convergence to oblique convergence of Pacific plates relative to the western ancestral North America margin (Engerbretson *et al.*, 1985).

In this chapter we describe structures related to four episodes of deformation, review several fault systems and conclude with a brief discussion of metamorphism. The goal is to document numerous structural elements that may ultimately be used to develop a more detailed structural evolution for the region. Our challenge was to group diverse and disparate features and determine age constraints. The timing of many structural features is poorly constrained due to lack of marker horizons, and because different fold styles develop where competency contrast between lithologic units is high. In addition, the paucity of Jurassic or younger strata in most areas prevents unequivocal assignment of many features to specific deformational episodes.

Four episodes of deformation in the study area are (Ta-

ble 4-1): pre-Late Triassic contraction (D₁), and structural culmination development (D₂); post-Late Triassic to pre-Toarcian contraction (D₃); and Middle Jurassic to Cretaceous contraction (D₄). The earliest episode was synmetamorphic and produced widespread chlorite-sericite foliation (S₁) and rare isoclinal folds (F₁) in Carboniferous rocks. S₁ was folded during D₂ into open to tight chevron folds (F₂). Evidence for the timing of D₂ remains equivocal. Open folds, overturned bedding and reverse faults, possibly northeast-verging, developed during D₃, and the younger age limit is an angular unconformity at the base of the Lower Jurassic Hazelton Group. D₄ produced crenulations in phyllitic Carboniferous strata and tight folds in Permian limestone and mylonitic foliations in a late Early Jurassic pluton.

A notable feature in the project area is the contrast in structural trends of Paleozoic and Triassic strata. North of the Stikine River, folds and faults trend northeast and east, but to the south, they trend north and northwest (Figure 4-2). The orientation of Permian limestone massifs delineates these trends most clearly. This change in orientation is also illustrated in Carboniferous strata between Devils Elbow and Missusjay Creek; however, the closure itself is under the Stikine valley alluvial fill. West of the map area, a similar flexure from west to northwest-trends has been documented by Souther (1959). These changes are probably due to a combination of folding and faulting. However, delineating exact contact relationships remains elusive due to poor exposures in critical areas.

PRE-LATE TRIASSIC DEFORMATION (D₁ and D₂)

Four southwest-widening structural culminations (Little Tahltan Lake, Barrington River, Chutine River and Missusjay Creek culminations), and one trending south southeast near the Scud River, are underlain by variably foliated and folded Permian and older rocks (Figure 4-2). They

TABLE 4-1
SUMMARY OF STRUCTURAL FEATURES IN THE PROJECT AREA

Timing	Fold style	Planar structure	Linear structure	Metamorphic minerals	Orientation of fold planes	Area
pre-Late Triassic	Isoclinal (none observed in map area)	Axial planar foliation (S ₁)	F ₁ fold axes (none recognized in map area)	Chlorite, sericite	Variable due to later folding	Little Tahltan Lake, Barrington River, Chutine River, Scud River, Butterfly Lake
post-Middle Triassic pre-Late Triassic?	Tight, chevron, similar folds + structural culminations	Spaced axial planar cleavage (S ₂)	F ₂ fold axes, S ₀ -S ₁ lineations	Rare	Consistent within domains	Little Tahltan Lake, Barrington River, Chutine River
post-Norian - pre-Toarcian	Faulted open folds	none	none	None	Northwest	Crocus Mountain
Middle Jurassic to Cretaceous	SW-vergent + upright, chevron	Axial planar cleavage	Chevron fold axes	None	Northwest to north	Cone Mountain

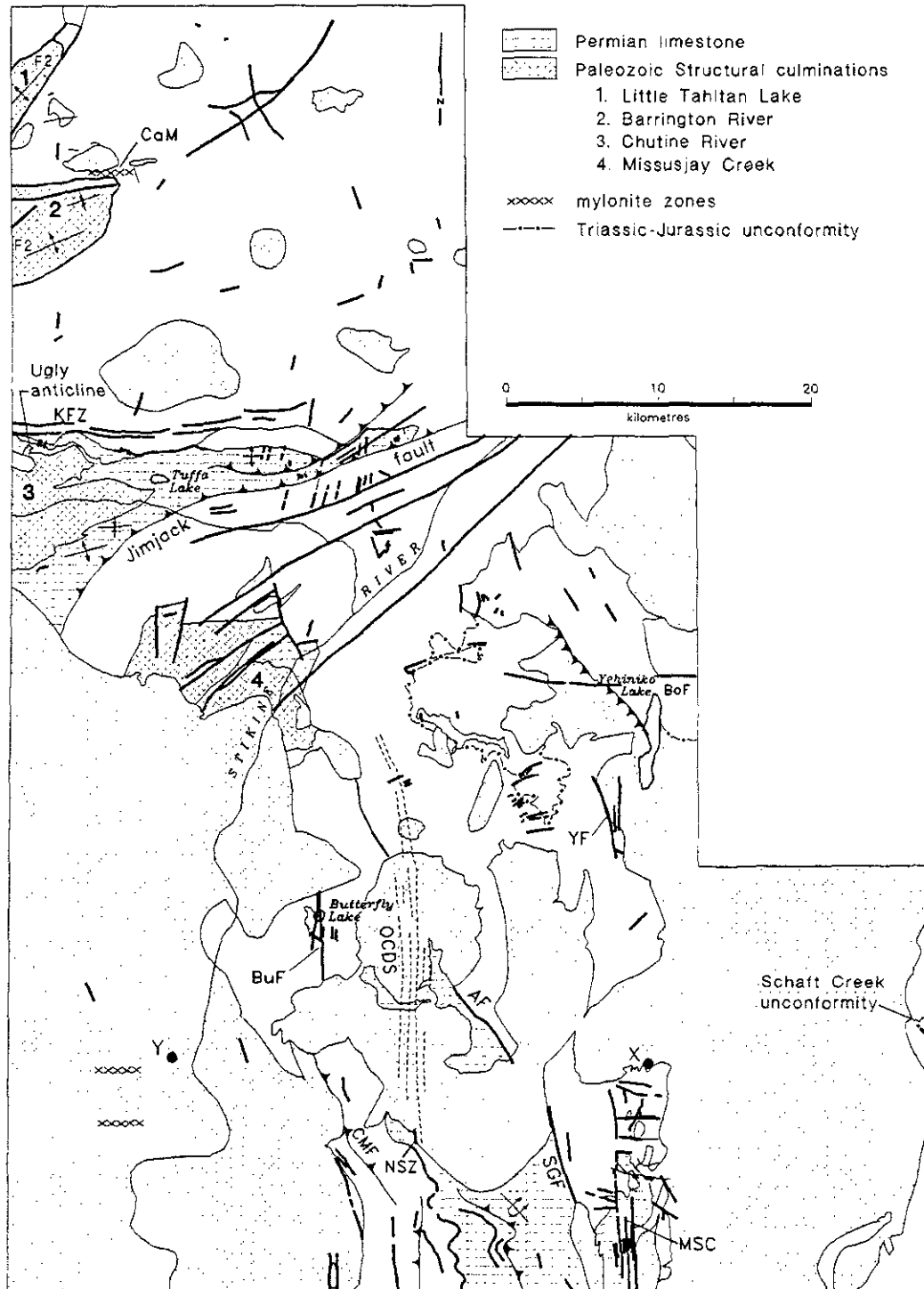


Figure 4-2. Major structural elements in the project area. AF = Ambition fault, BoF = Boomerang fault, BuF = Butterfly fault, CaM = Castor mylonite, CMF = Cone Mountain fault, KFZ = Kitchener fault zone, KDS = Kuys dike swarm, MSC = Middle Scud Creek faults, NSZ = Navo shear zone, OCDS = Oksa Creek dike swarm, SGF = Scud Glacier fault, X = pendant of folded metavolcanic rocks, Y = pendant of folded schist within Geology Ridge diorite, and YF = Yehiniko fault.

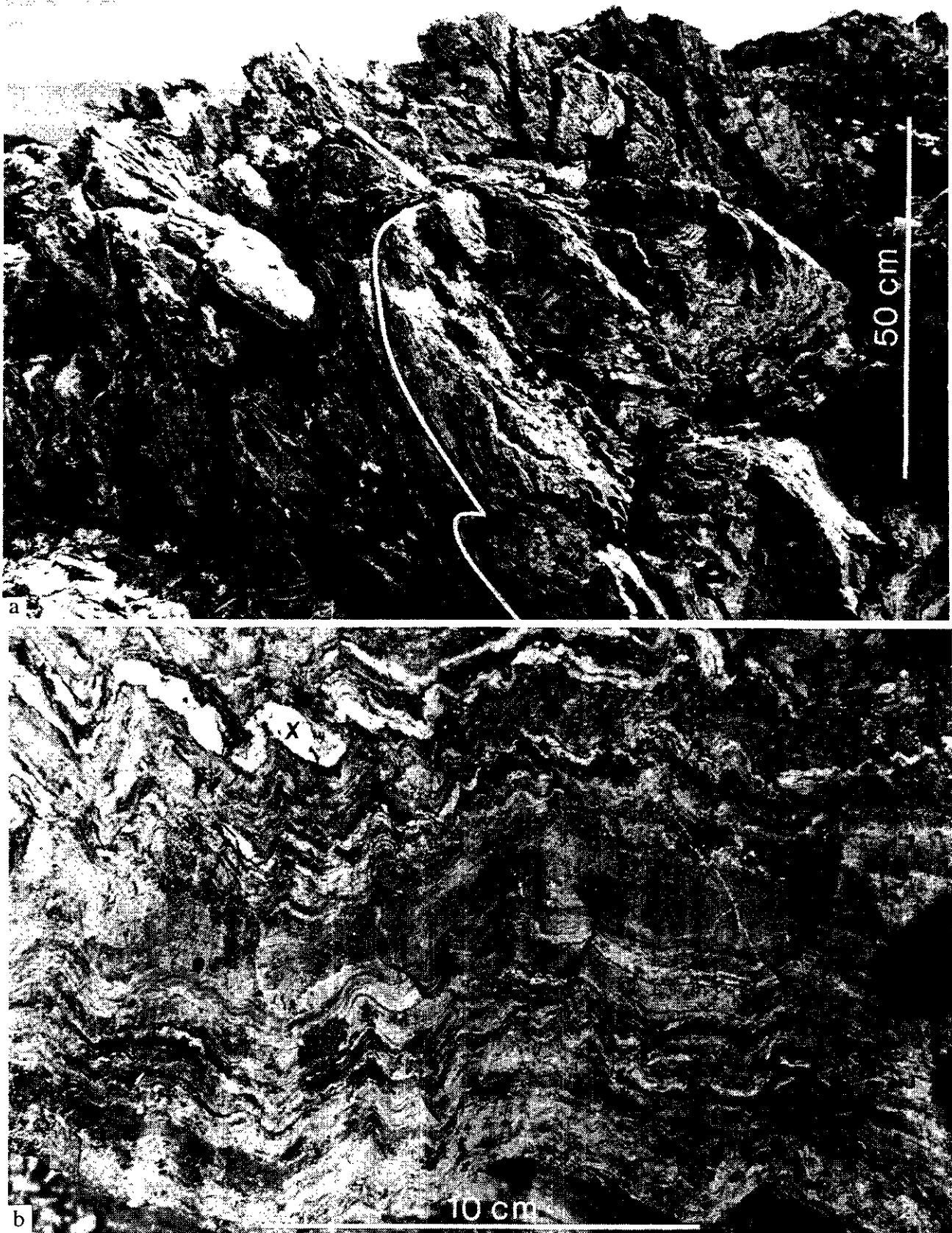


Photo 4-1. Characteristic deformation in Stikine assemblage phyllitic tuff in the Tahltan Lake structural culmination: (a) Northwest-verging, tight, angular polyharmonic folds of green and grey phyllite with axial planar cleavage; (b) Centimetre-scale, north-verging, rounded to chevron-style folds. The chlorite-sericite foliation (S_1) is coplanar to bedding (S_0) and both are folded, therefore, at least two phases of deformation are evident. Deformed quartz vein is shown by the "x".

record at least two phases of pre-Late Triassic deformation and contrast sharply with surrounding more massive Mesozoic strata. The northern two culminations expose poorly dated, tightly folded (D_2), penetratively foliated (D_1) rocks, correlated with dated Carboniferous or older units to the north (Bradford and Brown, 1993b) and south (Holbek, 1988; Logan and Drobe, 1993b) on the basis of lithology, metamorphic grade and fabric. The lack of penetrative fabrics in surrounding massive Mesozoic strata, and more intense and tighter folding and metamorphism of Paleozoic strata within the culminations are used to conclude that these are structural culminations.

PHYLLOSILICATE FOLIATION (D_1)

Penetrative phyllosilicate foliations, variably developed in pre-Triassic strata of the culminations, are interpreted to be products of the oldest deformation and metamorphic episode (D_1). The chlorite and sericite mineral growth suggests that deformation was synchronous with greenschist-grade metamorphism. Synmetamorphic quartz veins formed at this time and were deformed by later folding (D_2 ; see Photo 3a in Gunning, 1993a). Rare, rootless isoclinal folds are products of this earliest phase of deformation, they are more common in correlative strata to the northwest (Bradford and Brown, 1993a).

The foliation observed in Carboniferous strata may correlate with a pre-Permian deformation. Kerr (1948a) described a subtle structural discordance between pre-Permian and Permian strata and a chert-bearing conglomerate at the base of the Permian limestone at Missusjaj Mountain. Farther south in the Sphaler Creek and Forrest Kerr map areas, Logan and Koyanagi (1994) and Logan, Drobe and McClelland (in preparation) provide evidence of pre-Permian deformation where isoclinal folds of mid-Carboniferous limestone are overlain by Late Carboniferous to Permian polymictic volcanic conglomerate containing mid-Carboniferous limestone clasts.

DEVELOPMENT OF STRUCTURAL CULMINATIONS (D_2)

Tight to close D_2 chevron-style folding of compositional layering and S_1 , and the development of culminations are interpreted to be pre-Late Triassic. Late Triassic and younger rocks do not exhibit tight folding adjacent to the northern culminations, and in general, bedding attitudes in Upper Triassic strata do not conform to the margins of the culminations. Locally, such as at Missusjaj Creek, Upper Triassic rocks appear to lie unconformably on foliated Carboniferous strata. Folded northeast-trending Permian limestone lies within a massive Late Triassic pluton (Moosehorn pluton, Figure 4-1), immediately northwest of the study area (Bradford and Brown, 1993a, b). However, the data are somewhat equivocal and competency contrast during post-Triassic deformation may account for the differences in structural style between pre- and Late Triassic units. For the remainder of this discussion it is assumed that these culminations formed before the Late Triassic. If they are younger, they may represent the deeper crustal level, northwestern extension of the Skeena fold belt.

LITTLE TAHLTAN LAKE CULMINATION

The Little Tahltan Lake culmination is characterized by tight chevron folds (F_2) and strata with a penetrative chlorite-sericite foliation (S_1) developed in greenschist-grade metavolcanic rocks and rare limestone. Northwest of Little Tahltan Lake, thinly layered, green and maroon phyllitic rocks are intensely folded into moderately to steeply southeast-inclined folds with subhorizontal, northeast-trending fold axes (F_2 ; Photo 4-1). The centimetre to metre-scale, open to tight chevron folds verge northwest. Locally, this second phase of folding has generated spaced axial planar cleavage and crenulated S_1 foliations. No new mineral growth is evident on the axial planar surfaces of F_2 folds. White quartz veins and pods, presumably synmetamorphic (D_1), are deformed, which suggests that D_2 deformation occurred after the peak of metamorphism (Photo 4-1). Locally, mullions parallel the S_0 - S_1 intersections and macroscopic fold axes and are developed where competency contrast is great, such as in interlayered limy tuff and siliceous tuff.

Tightly folded phyllite and limestone of the Stikine assemblage contrast with massive limestone and unfoliated tuffaceous sedimentary rocks of the Stuhini Group across the faulted southeast contact of the Little Tahltan Lake culmination. The northern contact was not mapped.

BARRINGTON RIVER CULMINATION

In contrast to the Little Tahltan Lake culmination, few macroscopic tight folds were observed in the Barrington River culmination. Rocks within it display a penetrative, moderate to steep south to southeast-dipping phyllitic fabric (S_1) that intersects bedding (S_0) at low angles, suggesting that tight folds are present, although closures are rare. Bedding-cleavage intersections suggest that there is a major antiformal closure that plunges gently to the east in the Barrington River valley, with secondary closures on the northern limb. As in the Little Tahltan Lake culmination, quartz tension veins are common but appear less deformed. Local kinked (D_2) phyllosilicate foliation has a moderate south-dipping axial plane and plunges gently east or west. Strong ductile to brittle deformation of Carboniferous tuff in the culmination (Photo 4-2) contrasts with massive Stuhini tuff exposed to the east. Contacts between constituent lithologies were not observed.

CHUTINE RIVER CULMINATION

Permian limestone delineates the east-trending Chutine River culmination. The thickness of limestone changes from less than 200 metres near Wimpson Creek to over 2800 metres east of Tuffa Lake, probably due to D_2 folding and faulting. A northward-inclined open fold on the northwest limb of the culmination, the Ugly anticline, has an amplitude of more than 150 metres and is outlined by Early Permian limestone with a core of variably foliated, rusty weathering, siliceous siltstone, tuff and minor, discontinuous, recrystallized limestone (Photo 4-3). Lapilli tuff contains a pervasive phyllitic foliation but pillow basalt is massive to faintly foliated, illustrating that strain is partially controlled by lithology. East-trending beds and foliation planes dip steeply to the south or north.

West of the Ugly anticline and south of the Chutine River, Permian limestone is complexly folded into open folds with rounded closures, and tight chevron folds. Chevron-folded Middle Triassic black mudstone and chert crop out immediately north of the Permian limestone and within the Kitchener fault zone (Photo 4-4). Locally, folds are disharmonic with thickened hinge zones and thinned limbs, and some are rootless. Faint sericite-chlorite phyllitic foliation parallel to bedding is common. North of Ugly Creek and the Kitchener fault zone Upper Triassic strata are gently dipping.

Farther east within the Chutine River culmination, east of the Barrington placer mining camp, folds in the limestone are tight to isoclinal and are associated with bedding-parallel faults. Small-scale fault duplex structures are common. An east-trending, upright isoclinal fold contrasts with a recumbent fold of darker weathering, well bedded limestone exposed on a cliff face north of Jimjack Lake and illustrates the complexity of the deformation.

The contact between Permian and Triassic rocks which outlines the culmination is well exposed immediately north of the Ugly anticline, where Lower Permian limestone beds dip steeply north and are overlain paraconformably by buff-weathering Middle Triassic chert beds (unit mTc). This area lies within the southern limit of the Kitchener fault zone, where numerous faults are subparallel to steeply dipping

bedding. However, at this locality there is no gouge or shearing to suggest significant faulting. Elsewhere within the Kitchener fault zone, both units are folded and faulted. Farther east, near Tuffa Lake, the chert unit is absent, probably due to faulting, and Stuhini Group tuffaceous wacke structurally overlies Lower Permian limestone (unit IPSc). Northwest of Tuffa Lake, Middle Triassic chert and Stuhini Group tuffaceous wacke are structurally interleaved within the Kitchener fault zone. On the northeast wall of the Barrington River canyon, upstream from the placer operation, competent middle Triassic chert is folded into chevrons directly above folded Permian limestone.

AGE CONSTRAINTS AND TAHLTANIAN OROGENY

Folding of Paleozoic strata in these culminations occurred before the Late Triassic and Early Jurassic. Massive augite-phyric basalt dikes, interpreted to be feeders to Stuhini Group volcanic rocks, intrude folded, phyllitic rocks in the Barrington River culmination. In the Chutine River culmination, folded Paleozoic rocks are cut by massive felsic dikes related to the Early Jurassic Limpoke pluton. Farther south, near the Scud River, angular blocks of tightly folded (D_2 folds) mafic schist occur within massive Geology Ridge diorite, correlated with the Early Jurassic diorite suite (Photo 4-5; locality Y on Figure 4-2). Assuming the schist

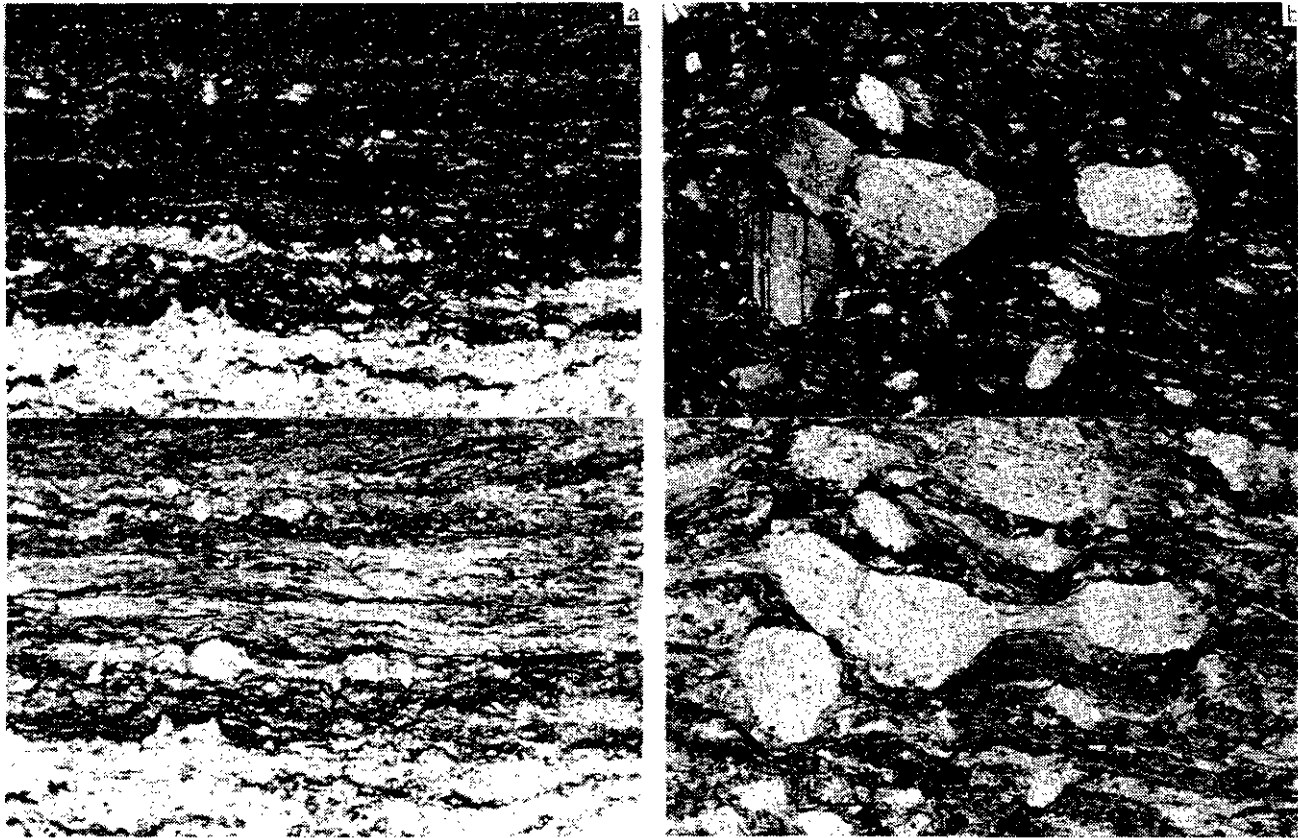


Photo 4-2. Characteristic microfabrics of rocks in the Barrington River culmination: (a) Chlorite-sericite-rich ash tuff interlayered with recrystallized limestone (INE91-360); (b) Well foliated crystal tuff with prominent pressure shadows between plagioclase crystals (JTI91-182).

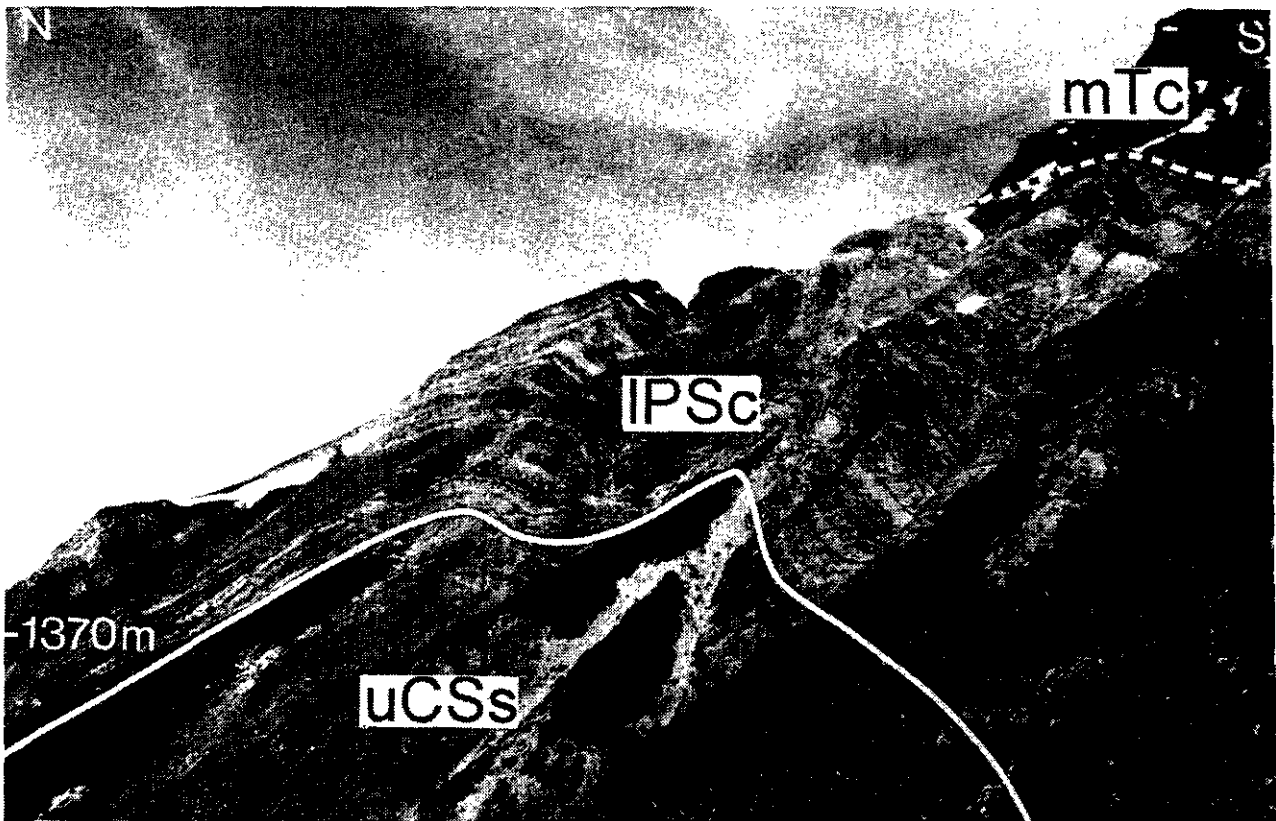


Photo 4-3. View northwest to the Ugly anticline, an inclined, open fold of rusty weathering siltstone (uCSs) and well bedded Lower Permian limestone (IPSc) which are overlain unconformably by Middle Triassic chert (mTc; see Figure 2-8). The nature of the contact is equivocal; beds are parallel across the contact and the chert appears to rest paraconformably on the limestone. Alternatively, there may be a bedding-parallel fault between the two units.



Photo 4-4. Chevron folded Middle Triassic chert on northern edge of the Chutine River culmination, illustrating the marked competency contrast between the chert and calcareous layers. Chert deforms by brittle failure and calcareous layers flow into the fold closures.



Photo 4-5. Tight folds with subangular closures developed in mafic schist that occurs in angular pendants within massive Early Jurassic Geology Ridge diorite (note: pluton is outside field of view; DBR90-18).

is correlative with the Stikine assemblage, this provides another pre-Early Jurassic age constraint.

It is suggested that the culminations formed during the Tahltanian orogeny, a Permo-Triassic episode of uplift, folding, regional metamorphism and plutonism recognized in the Tulsequah and Telegraph Creek areas (Souther, 1971). This interval corresponds to an Early to Middle Triassic depositional hiatus noted throughout much of Stikinia (Souther, 1971; Read and Okulitch, 1977). Coeval events to the northeast and south are the Cassiar orogeny (White, 1959) and Sonoman orogeny of the southwestern United States (Wyld, 1991). Read (1983, 1984) and Read *et al.* (1983) suggest a slightly older, Late Permian to Early Triassic age for this event.

POST-NORIAN AND PRE-TOARCIAN CONTRACTION OF STUHINI GROUP (D3)

A spectacular exposure of an angular unconformity establishes an important deformational event that has not been much discussed in the literature. It correlates with a regional angular unconformity east of Schaft Creek (*cf.* Logan and Drobe, 1993b), near Unuk River fault (Henderson *et al.*, 1992; Lewis *et al.*, 1993) and at Oweege Dome (Figure 4-2) as documented by Greig and Gehrels (1992).

Steeply dipping, folded and faulted Norian Stuhini Group clastic rocks are unconformably overlain by gently to moderately dipping Toarcian Hazelton Group volcanic rocks along the ridge between Strata and Quattrin creeks

(Figure 4-3; Photo 2-15). Norian beds are locally overturned to the northeast immediately below the angular unconformity. Elsewhere, more massive and competent Stuhini Group volcanic strata underlie the well bedded clastic rocks and have steeper bedding attitudes than the Hazelton strata.

The angular unconformity is a sharp contact with no evidence of faulting; the surface is essentially flat, and a basal conglomerate or regolith is notably absent along this ridge (Photo 4-6). A basal polymictic conglomerate is exposed to the north. The unconformity surface displays significant relief farther north-northwest in Helveker Creek (*cf.* Chapter 2; Photo 2-14). East of Mount Kirk, it is marked by a basal Hazelton Group volcanic conglomerate lying on massive Stuhini flows.

Elsewhere in the study area, bedding attitudes of the Stuhini Group vary greatly. Folds are rare and recognized only in thinly bedded sequences; axial planar cleavages are absent, in contrast with Paleozoic rocks. More massive volcanic rocks and local limestone horizons are unfolded and lack penetrative foliations, except north of the Scud River where mafic crystal tuff displays a chlorite foliation (Gunning, 1993a). An isolated recumbent fold of tuffaceous wacke within massive volcanic rocks is exposed on a cliff face north of Rugged Mountain. Upright, northwest-trending open folds with subhorizontal axes are developed in thinly bedded siltstone and Carnian limestone near the west shore of Tahltan Lake. These folds may be correlative with the northeast-directed contractional event defined between Strata and Quattrin creeks.

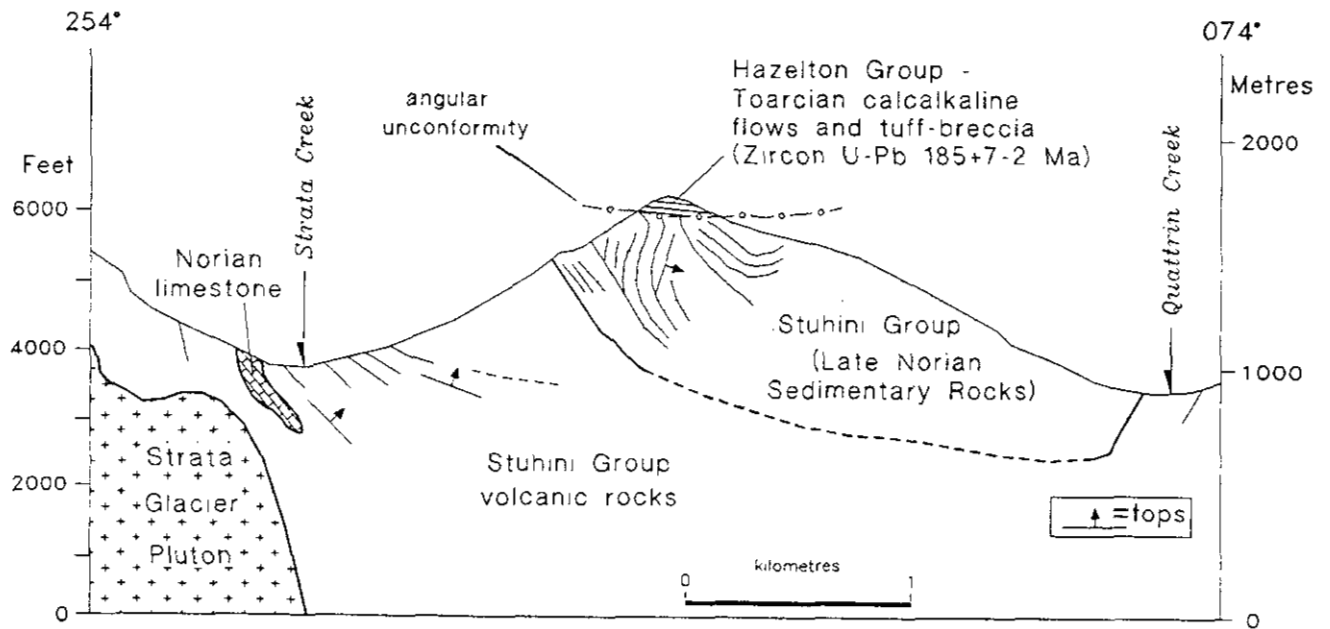


Figure 4-3. Schematic cross-section illustrating deformed upper Norian clastic rocks of the Stuhini Group unconformably overlain by Toarcian flows and tuffs, between Strata and Quattrin creeks.



Photo 4-6. Structural discordance between thinly bedded Norian sedimentary rocks and overlying Lower Jurassic volcanic rocks. This close-up of the contact that is also shown in Photo 2-15 illustrates the angular discordance and lack of basal conglomerate or regolith.

AGE CONSTRAINTS

A period of post-Norian and pre-Toarcian contraction is well constrained by dated strata above and below the angular unconformity between Strata and Quattrin creeks. The vergence of the contractional event is difficult to determine, but may have been northeast-directed if the attitudes of overturned bedding represent fold vergence. Truncation of steeply dipping Stuhini Group beds by the massive late Early Jurassic Dokdaon and Strata Glacier plutons may also indicate folding prior to their intrusion. Farther south, in the Sulphurets area, a possibly correlative post-Late Triassic and pre-Hettangian angular unconformity is marked by a basal conglomerate (Jack formation; Henderson *et al.*, 1992; Lewis *et al.*, 1993).

STRUCTURES NEAR SCUD GLACIER

More intensely deformed and metamorphosed, undated upper greenschist to amphibolite facies metavolcanic rocks (Photo 4-7) resemble strata of the Stuhini Group and crop out around Middle Scud Creek, east of the Scud Glacier and west of the Hickman Ultramafic Complex. Alternatively, they may correlate with Carboniferous volcanic rocks of the Stikine assemblage. They are characterized by metre-scale, locally rootless, tight, upright, gently northeast to north-plunging folds developed in biotite schist and mafic metatuff adjacent to foliated pyroxene gabbro sills. Rare biotite lineations plunge gently to the south on moderate west-dipping foliation surfaces. Foliated and infolded recrystallized limestone and chloritic tuff are exposed east of the Scud Glacier. Here, an open, gently northeast plunging anticline is cored by Upper Permian limestone. Three kilometres farther south, limestone is folded into open, gently southeast-plunging, southwest-vergent synform-antiform pairs disrupted by faults and at one locality intruded by the border phase of the Hickman pluton. Well foliated to massive diorite related to the Hickman pluton locally cuts compositional layering. A similar style of minor folding was observed in correlative rocks on the northeast margin of the Strata Glacier pluton.

A pendant of these folded metavolcanic rocks within the southwest margin of the Yehiniko pluton constrains folding as pre-Middle Jurassic (Photo 4-7). The lower age limit is either Late Triassic or Carboniferous, depending on the lithologic correlation used (Stuhini Group or Carboniferous part of the Stikine assemblage). If the foliated gabbro sills are related to the Hickman pluton, then the deformation is younger than Late Triassic. This local deformation and metamorphism may be related to the intrusion of the Hickman pluton or the more regional Late Triassic to Early Jurassic event. Why the eastern border of the pluton is not equally deformed remains unknown.

MIDDLE JURASSIC OR CRETACEOUS CONTRACTION (D₄)

Two styles of macroscopic folds, and northeast-dipping contractional faults north of the Scud River (Figure 4-4) are discussed below. They are believed to be related to a Middle Jurassic or Cretaceous contractional event.

FOLDS

In the area of Navo and Rugose creeks, felsic tuffs of the Navo formation are folded into upright to inclined, open to tight, gently southeast-plunging chevron folds (Figure 4-4). Where fold closures are absent, bedding-cleavage relationships suggest that the strata are tightly folded (Photo 4-9). Farther east, toward the Scud Glacier, decimetre-scale, upright, open to tight, north-trending folds and smaller scale, parasitic minor folds occur in Lower Permian limestone. In contrast, a steep to vertical, northwest-striking bedding and chlorite-sericite foliation characterize argillite and siltstone of Carboniferous or Late Triassic age (Photo 4-8), in the Scud River valley. No fold closures were observed.

In addition to the upright chevron folds, southwest-verging asymmetric minor folds are common in Navo Creek area (Photos 4-10, 4-11). A gently inclined major synform, with an amplitude of 3 kilometres, contains secondary S, Z and M-type macroscopic folds exposed along a cliff face on the north side of Rugose Glacier (area 2 in Figure 4-4). The upper limb is truncated by a moderately to steeply east dipping reverse fault. Discrete zones of isoclinally folded cylindrical corals, asymmetrically folded microscopic



Photo 4-7. A pendant of chevron folded metavolcanic rocks (Stuhini Group?) within massive granite of the Middle Jurassic Yehiniko pluton (DBR88-206).

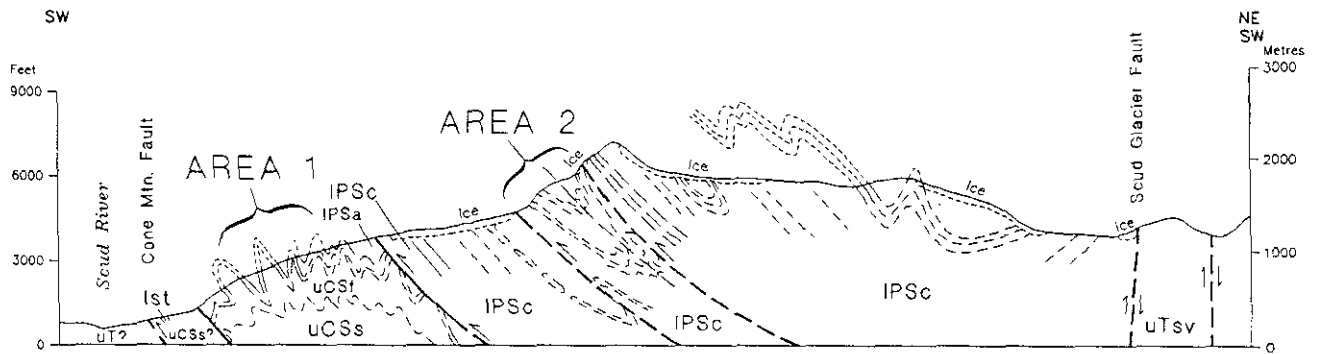


Figure 4-4. Schematic cross-section illustrating the contrast in deformation between felsic tuff (Navo formation, uCSf) and overlying Permian limestone succession (Ambition formation; IPSc), and the series of northwest-trending reverse faults, including the Cone Mountain fault. Other abbreviations: uCSs? = possible Carboniferous strata (or Upper Triassic?); IPSa = argillite; uTsv = Upper Triassic Stuhini Group. The two styles of folding are illustrated here as area 1 and 2; the tighter, upright folds in area 1 could be in the closure of a larger anticline. In fact, it may be the hangingwall anticline to the Cone Mountain fault.



Photo 4-8. Typical steeply dipping to vertical foliation developed in Carboniferous (or Upper Triassic?) metasedimentary rocks in the Scud River valley (unit uCS?).



Photo 4-9. View to the south of bedding-cleavage intersections in felsic tuff (Navo formation), on the southwest limb of a shallow southwest-plunging, upright synform (DBR88-135). Pencil at top of photo for scale, refracted cleavage is prominent.

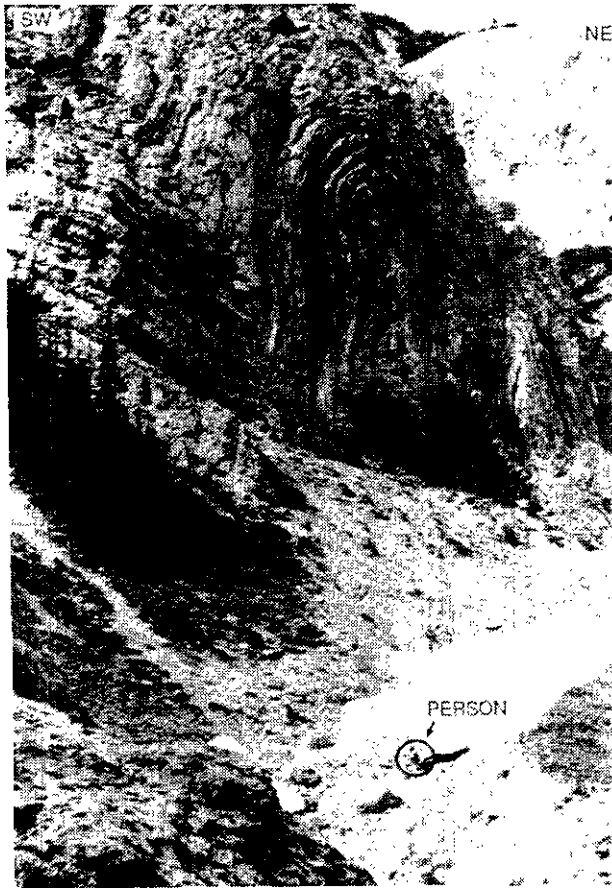


Photo 4-10. View northwest to asymmetric, southwest-vergent fold in Lower Permian limestone (unit IPSc; DBR88-19).

bioclasts, dissolution fabrics and local pervasive cleavage are characteristic of some of the reverse faults. The folding and faulting imbricate and greatly thicken the limestone succession. Our previous interpretation invoked separate phases of deformation, producing upright folds and then asymmetric folds (Brown and Gunning, 1989a), however, we now suggest they are products of the same contractional event.

CONTRACTIONAL FAULTS

A series of northwest-striking, subvertical to moderately northeast-dipping faults, including the Cone Mountain fault, trend northwest from the Scud River north to the Hamper pluton, and may extend as far north as the Butterfly Lake fault (Figures 4-2, 4-4, 4-5). Contractional faults produced older-over-younger relationships in the Ambition Formation limestone in the Rugose Glacier area, defined by fusulinid biostratigraphy, and by local overturned beds and asymmetric folds south of Rugose Creek (Figure 4-4; Photo 4-10; Appendix 2). The reverse faults can be traced 20 kilometres to the south to Copper Canyon, where Permian limestone is structurally interleaved with Lower and Middle Triassic shale and siltstone (Souther, 1972; Logan and Koyanagi, 1994).

CONE MOUNTAIN FAULT

The Cone Mountain fault is a zone of mylonitic granodiorite and foliated Stikine assemblage metavolcanic rocks 500 metres wide (Figure 4-5). Massive granodiorite in the footwall (Cone Mountain pluton) becomes increasingly strained over about 100 metres, and contains foliated granitoid with discrete layers of ultramylonite in the zone of highest strain (Photo 4-12). Northeast-dipping biotite and chlorite foliation rarely display east-plunging lineations.

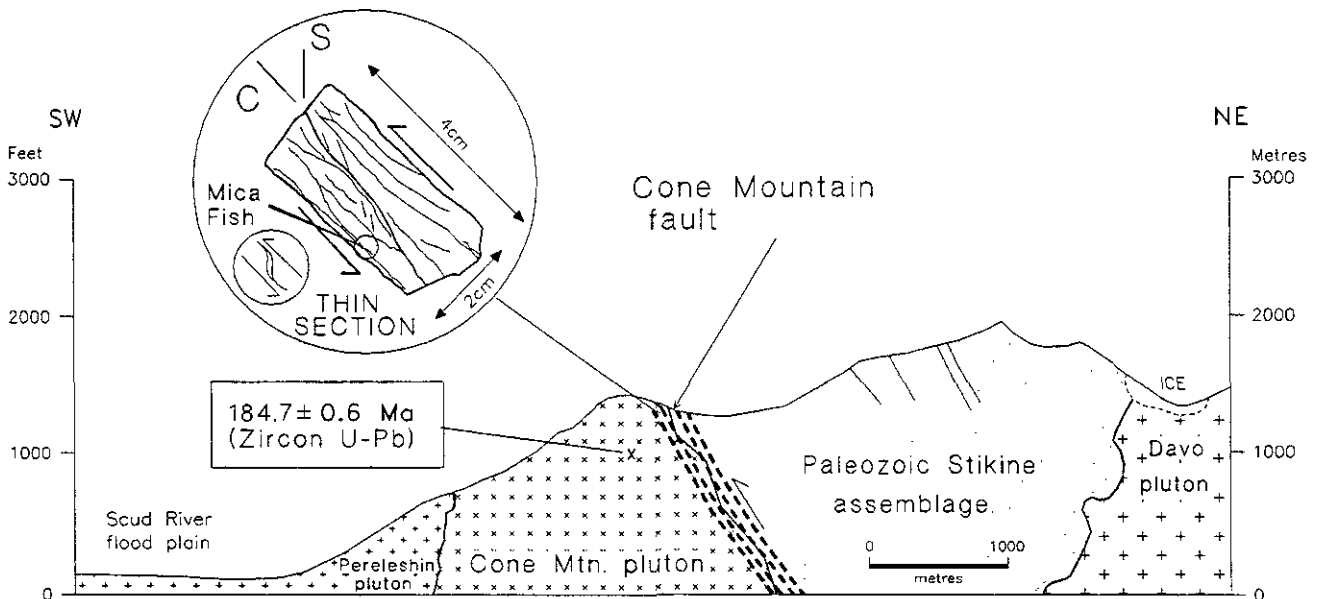


Figure 4-5. Relationship of the Cone Mountain fault to the Cone Mountain pluton and hanging wall Stikine assemblage rocks. Southwest vergence is based on S-C fabrics, mica fish in the deformed pluton. Similar vergence for related reverse faults in the Ambition Formation limestone is based on asymmetric folds and older-on-younger relationships defined by fusulinid species which indicate stratigraphic repetition.

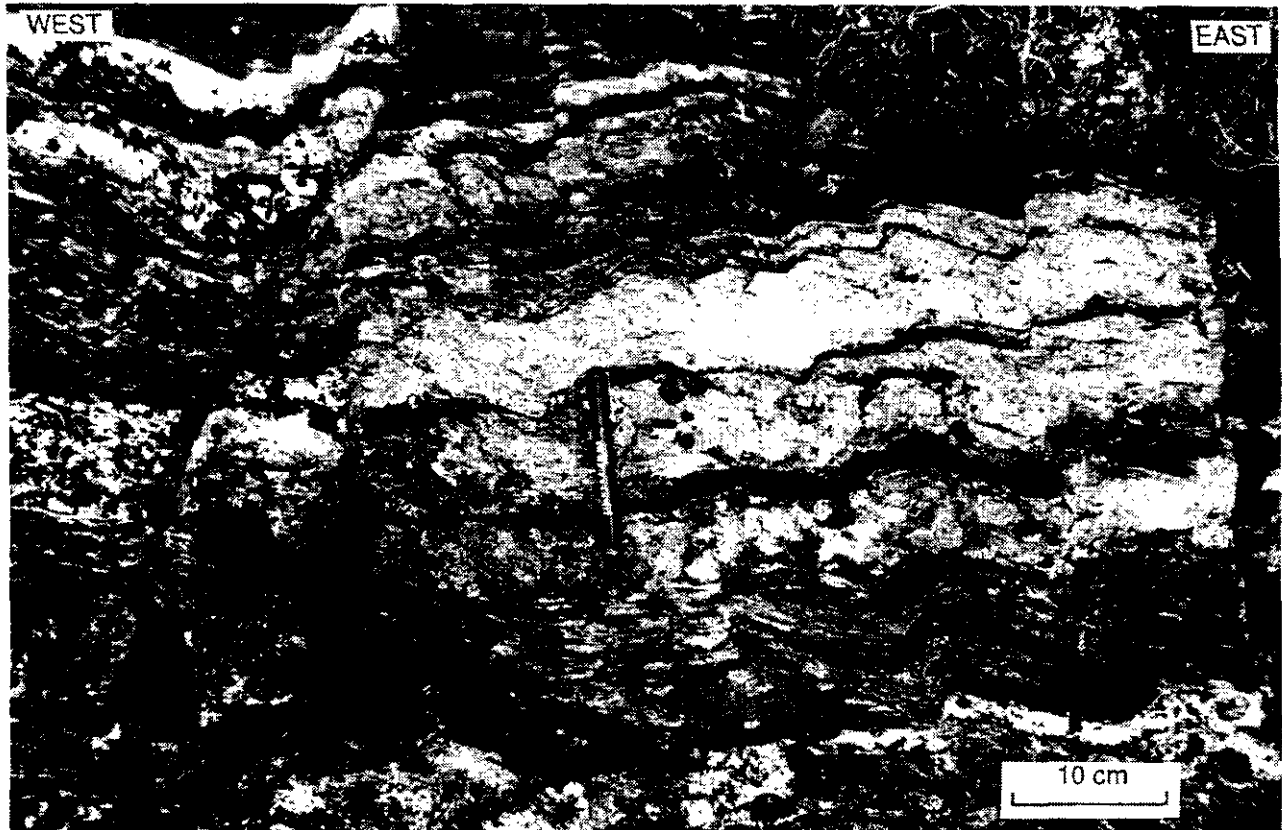


Photo 4-11. West-verging minor folds in foliated metamorphosed tuffaceous rocks (Butterfly member; DBR88-52).

The hangingwall is foliated chlorite phyllite of the Stikine assemblage (Figure 4-5).

The deformed granitoid rocks display well-developed S-C fabrics (Simpson and Schmid, 1983) and rare mica fish (Lister and Snoke, 1984) which indicate a southwest-directed sense of shear (Photo 4-12; Figure 4-5). Polygonized quartz grains reflect ductile processes but plagioclase crystals have discrete microfaults implying brittle failure. The down-dip, biotite and chlorite stretching lineations reflect the southwest-directed transport direction. This shear sense is compatible with locally overturned, west to southwest-verging minor folds in the hangingwall Permian limestone stratigraphy (Photo 4-10).

BUTTERFLY LAKE AND RELATED FAULTS

Discrete mylonite and cataclasite zones east of the margin of the Butterfly Lake syenite may be a northern extension of the Cone Mountain fault system. The most prominent, the Butterfly Lake fault (Figure 4-2), is a steep, north-trending brittle fault zone containing sheared and fractured mafic dikes and Carboniferous volcanic rocks. Polished fault surfaces along the mafic dike margins are serpentized and talcose. If related to the Cone Mountain fault, the Butterfly Lake structure should be a dextral transcurrent fault. Oblique to the Butterfly Lake fault is a zone of northeast-trending mylonitic syenite, 30 centimetres wide, that contains a chlorite foliation and en echelon quartz tension

gashes. The attitude of the mylonitic foliation relative to the quartz veins suggests a reverse, southeast-directed sense of motion along the northeast-trending mylonite (Photo 4-13).

NAVO SHEAR ZONE

The Navo Shear zone may be the northern extension of the Rugose fault in a similar way that the Cone Mountain fault and Butterfly Lake faults are related. A 50 metre wide ductile and brittle shear zone, at the western contact of the Davo pluton with adjacent Lower Permian limestone is well exposed in the headwaters of Navo Creek (Photo 4-14a, b). It comprises recrystallized limestone with a subvertical foliation and foliated diorite of the Davo pluton. Elliptical amphibolite and diorite xenoliths are boudinaged and flattened, and black basalt dikes are brecciated and stretched within the diorite (Photo 4-14a).

AGE CONSTRAINTS

Most of the southwest-directed deformation is interpreted to be late Early Jurassic to Paleocene. It must be post-Triassic because Upper Triassic strata are folded into southwest-verging folds and faulted north of the Scud River. Farther south, near Copper Canyon, Middle Triassic strata are folded and faulted within correlative structures (Souther, 1972; Logan and Koyanagi, 1994). However, some pre-Early Jurassic movement is indicated along a north-trending, gently west dipping, west-side-down fault and shear

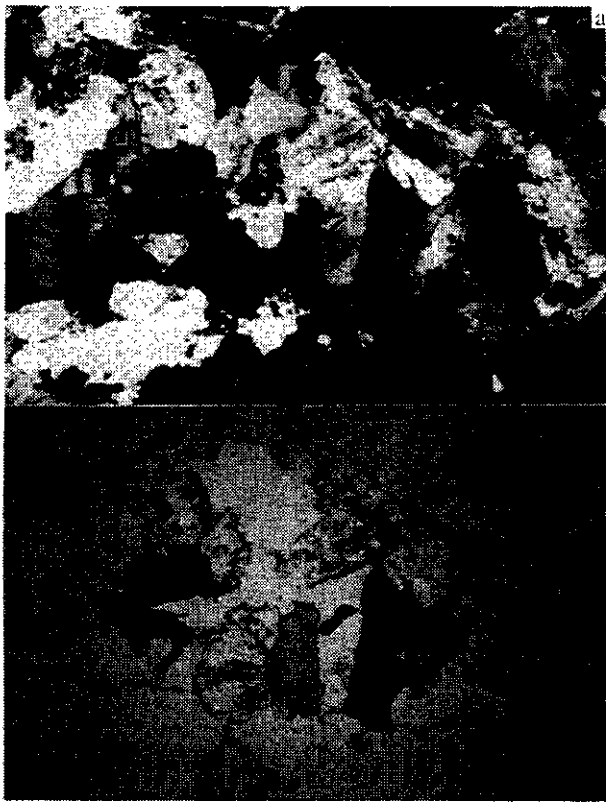


Photo 4-12. Photomicrographs comparing undeformed to mylonitic Cone Mountain pluton; (a) Massive biotite hornblende granodiorite (DBR90-40); (b and c) Mylonitic granodiorite containing polygonized quartz grains and micro-faulted plagioclase grains. Crossed polarized light photographs above plane light images for each.



Photo 4-13. View northeast to the mylonitic Butterfly Lake syenite - Carboniferous volcanic rock contact (Butterfly formation; DBR90-33), showing quartz tension gashes which indicate a reverse sense of movement.



Photo 4-14. (a) View northwest to brecciated basalt dikes and diorite within mylonitic diorite adjacent to the contact with Permian limestone, on the west side of the headwaters of Navo Creek (DBR88-1). Flattened and aligned diorite/amphibolite schlieren foliation is moderately to steeply southwest dipping. Discrete minor faults dip moderately to the north and display reverse sense of motion where they displace the foliation and schlieren. (b) View southeast to subvertical, southwest-striking layered marble immediately east of Navo Creek headwaters (DBR88-2).

zone at Galore Creek where Early Jurassic metasomatic biotite overprints ductile fabrics (Tom Heah, personal communication, 1994). A younger, late Early Jurassic constraint is provided by ductile deformation of the 185 Ma Cone Mountain pluton. The upper age limit is provided by undeformed Eocene granite with blocks of folded limestone west of the Stikine River.

REGIONAL CORRELATION

The relationship of the Cone Mountain fault system to the regional strain pattern is unknown but our age constraints for displacement overlap deformation associated with the Middle Jurassic King Salmon fault (Thorstad and Gabrielse, 1986) and the Late Jurassic to Tertiary Skeena fold belt (Evenchick, 1991b, c; Figure 4-1). The King Salmon fault (*sensu stricto*) is mapped at the base of the Sinwa Formation (Souther, 1971), however, Takwahoni Group strata farther south are folded and faulted by the same deformational event. Therefore, the southernmost extent of strain related to this deformation is indicated by the dotted line on Figure 4-1. Southwest-vergence is dominant in the King Salmon fault and common in the Cone Mountain structure. Components of the Skeena fold belt, however, also have southwest vergence, for example the Unuk River thrust fault, which is interpreted to be linked, via back-thrusting, to the Sulphurets fault (Lewis, 1992). This last example illustrates that vergence does not differentiate specific structural events.

FAULTS

High-angle faults trend north, east, northwest and northeast and locally control map unit distribution (Figure 4-2). Relative timing of movement on these fault sets is unclear. A series of north-dipping reverse faults is orthogonal to the north-trending strike-slip faults.

NORTH-TRENDING FAULTS

North-trending faults with poorly defined displacements are abundant in the Scud Glacier area, southwest of Yehiniko lake, near Butterfly Lake and north of the Stikine and Chutine rivers. They include the Scud Glacier, Middle Scud Creek and Butterfly faults, Navo shear zone and coplanar Oksa Creek dike swarm (Figure 4-2). Some are reactivated faults with complicated reverse, normal and transcurrent movements, and locally mineralized.

SCUD GLACIER FAULT

The most prominent north-trending fault, the vertical Scud Glacier fault (previously interpreted as the southern extension of the Ambition fault by Brown and Gunning, 1989b), juxtaposes Permian limestone with Stuhini Group west of Scud Glacier (Figure 4-2), implying over 1200 metres of east-side-down displacement. The fault zone comprises a series of polished fault planes and a splay, containing 3 metres of clay gouge and en echelon pods of rusty, sheared and polished mafic volcanic rocks (Figure 4-6), 3 kilometres northwest of the toe of the Scud Glacier. The polished fault planes are curvilinear, with horizontal to gently south plunging slickensides, which suggest dextral transcurrent motion. A Miocene(?) basalt dike, 1 to 5 metres thick, within and parallel to the fault has slickensided contacts, but is not dismembered or truncated and was probably intruded late in the development of the zone.

Fault motion is post-Late Triassic. A small, altered, feldspar-porphyrific intrusion (possibly Eocene) cuts faulted, cleaved and altered Stuhini Group rocks 3 kilometres northwest of the toe of the Scud Glacier. The fault projects southward toward the Scud River valley, where it may be plugged by another poorly exposed feldspar porphyry intrusion. The fault extends southward beyond this body into the South Scud River valley and beyond (Logan *et al.*, 1993b). To the north, the fault trace is covered by glaciers and icefields, but it may link with north-trending faults ex-

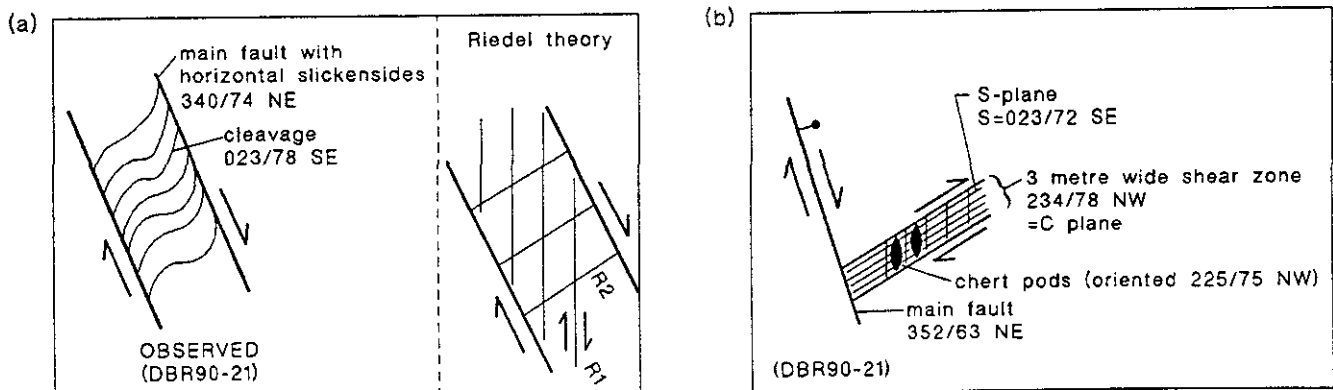


Figure 4-6. Fabrics associated with the Scud Glacier fault; (a) Plan view of the main fault with deflected spaced cleavage indicating a right-lateral sense of displacement. Riedel model from McClay (1987); (b) 3 metre wide shear zone splay off main fault.

posed along the west margin of the Yehiniko ultramafite, the Yehiniko fault zone.

The Scud Glacier fault is interpreted to be a dextral oblique-slip fault. The sense of motion is based on the orientation of the main fault zone relative to a spaced cleavage (Figure 4-6a) and the acute angle between the main fault and a conjugate gouge zone, 3 metres wide. The coplanar Mess Creek fault zone, 30 kilometres to the east, was active from Early Jurassic to Recent time (Souther and Symons, 1974). However, earlier sinistral motion is possible, as shown for the Tally Ho shear - Llewellyn fault to the northwest by Hart and Mihalynuk (1992). They describe a complex, long-lived transcurrent structure with ductile sinistral motion between 220 and about 180 Ma and dextral brittle displacement in middle to Late Cretaceous. The Harrymel - South Unuk fault system may be analogous with early ductile sinistral motion (P.D. Lewis, personal communication, 1994). It is difficult to assess the extent of reactivation on faults in the study area.

MIDDLE SCUD CREEK FAULTS

A series of north-trending vertical faults parallel the Scud Glacier fault and interleave Permian limestone, maroon tuff, chert and gabbro in Middle Scud Creek canyon. Limestone and tuff are steep to vertical. Local fault breccia northeast of Middle Scud Creek, 1 to 2 metres wide, contains angular fragments of country rock. The faults extend southward where they are named "south Scud River fault zone" by Logan and Koyanagi (1994).

Farther north, on the flanks of Mount Helveker, north and northeast-striking, high-angle normal faults displace the basal contact of the Sloko Group by about 50 metres. Coplanar faults cut Sustut strata on Strata Mountain. Minor vertical displacements are also common on the series of small north-trending faults cutting Permian limestone in the eastern half of the Chutine culmination (Brown *et al.*, 1993).

OKSA CREEK DIKE SWARM

The Oksa Creek dike swarm is a series of prominent, steeply dipping, north-trending, light grey weathering felsite dikes, up to 10 metres wide, that cut narrower, northeast-striking, black basalt dikes in the vicinity of Oksa and Navo creeks (Figure 4-2). The dikes underlie as much as 20% of a zone 2 kilometres wide, but they do not extend farther north than Strata Creek or south of the Scud River. The dikes represent local but significant east-west extension, probably in the Tertiary perhaps related to back-arc (*i.e.* Coast Belt) extension.

EAST-TRENDING FAULTS

KITCHENER FAULT ZONE

The Kitchener fault zone is an east-trending zone of subvertical faults within middle Triassic chert and the Stuhini Group, and forms the northern boundary of the Chutine River culmination. The zone is about a kilometre wide between the headwaters of Cave and Ugly creeks. The eastern extent of the zone and its relationship with the south-directed Jimjack fault remains unclear due to poor exposure. Middle Triassic chert beds are folded into tight chevron folds with amplitudes up to about 5 metres (Photo 4-4). In contrast, folds are not evident in massive Stuhini Group tuf-

faceous wacke, but bedding is rotated into the fault zone. Movement on the Kitchener fault, presumably north side down, is post-Triassic.

BOOMERANG AND RELATED FAULTS

The east-trending, south-dipping Boomerang fault, located north of Boomerang Creek, has Sustut Group sedimentary rocks in its hangingwall and Hazelton Group volcanic rocks in its footwall (Figure 4-2). The fault is not exposed, but steep, south-dipping and vertical beds of Sustut Group are truncated against altered granitic dikes and Hazelton Group volcanic rocks. The probable western extension of the fault, on the west side of the Yehiniko Creek valley, is a shear zone 10 centimetres wide, which offsets the contact of the Sustut Group and the Saffron pluton. The fault contains zones of limonitic, brecciated granite and several 15-centimetre sections of clay gouge. It offsets the contact approximately 500 metres in a left-lateral sense and may represent a south-dipping, oblique-slip shear zone. The Tertiary or younger Boomerang fault may be a reactivated Jurassic structure, because the Jurassic granitic dikes have a similar orientation to the fault.

Narrow west-striking, subvertical and gently north dipping extensional faults east of the Scud Glacier and between Quattrin and Strata creeks may be part of the Boomerang system. The faults cut Stuhini Group and most show north-side-down displacement. A prominent, rusty weathering, west-striking fault that juxtaposes Permian limestone with quartz monzonite near the headwaters of Middle Scud Creek has horizontal slickensides, indicating that latest motion was strike-slip.

DUCTILE FABRICS

A series of discrete, east-trending ductile and brittle shear zones, each less than a metre wide, deform Early Jurassic diorite along Geology Ridge. Their sense of shear and relationships to other structures is unclear, although similar zones occur south of the Anuk River, 25 kilometres southeast of Geology Ridge (Logan and Koyanagi, 1994). Farther north, several discrete, east-striking mylonite zones of foliated hornblende quartz diorite and chlorite schist are exposed along the southern margin of the Castor pluton. Adjacent Stuhini limestone and andesitic volcanics are also foliated.

JIMJACK FAULT SYSTEM

North-dipping Stuhini Group volcanic rocks are structurally overlain by concordant Permian limestone along the northeast-striking, moderately northwest dipping Jimjack reverse fault. It does not crop out. Triassic strata in the footwall dip to the north as imbricated, homoclinal fault panels. Permian limestone in the hangingwall farther north is complexly folded and upright, east-striking, tight to isoclinal symmetrical folds are most common.

Movement on the Jimjack fault is post-Triassic (Stuhini Group) and pre-Eocene as the Sawback pluton is not faulted. The faults may be correlative with northeast-striking contractional faults in the Tanzilla River area, 75 kilometres to the northeast (Figure 4-1), where Read (1983) has described post-Eocene, normal displacement.

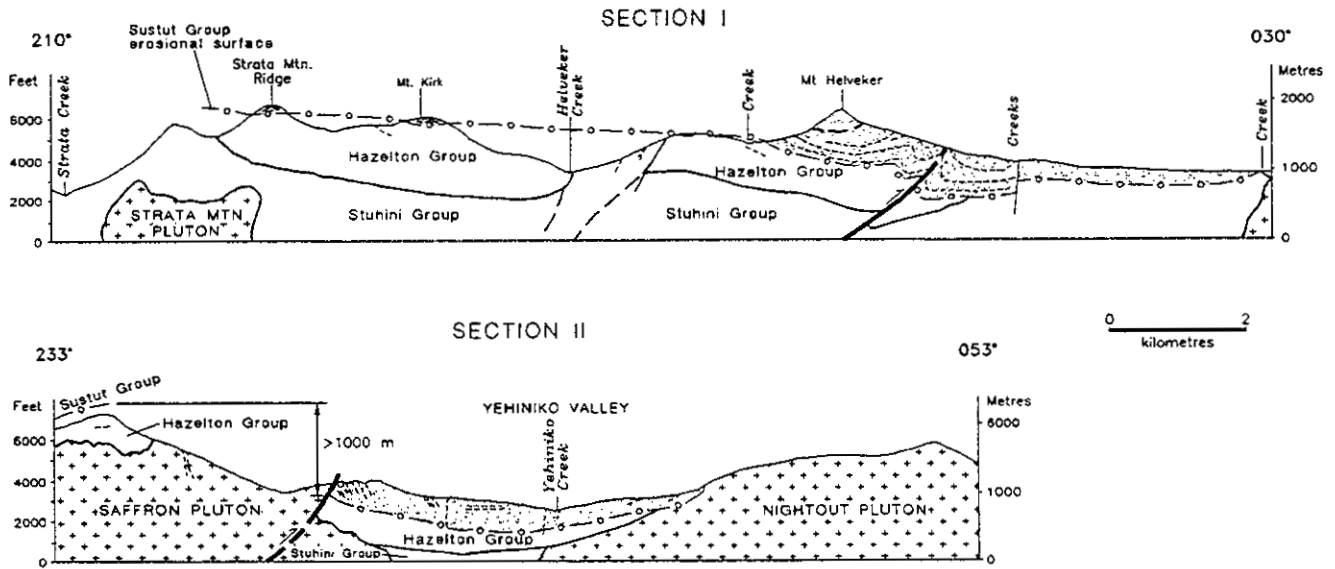


Figure 4-7. Schematic cross-sections of the Sustut Group between Strata Mountain and Yehiniko valley, locations shown on Figure 4-8. Section I illustrates the gentle north-northeast gradient of the sub-Sustut unconformity, and the structural complexity northeast of Mount Helveker. Section II shows the Saffron pluton reverse-faulted against the Sustut Group and the pronounced difference in elevation (1000 m) of the basal contact across the fault.

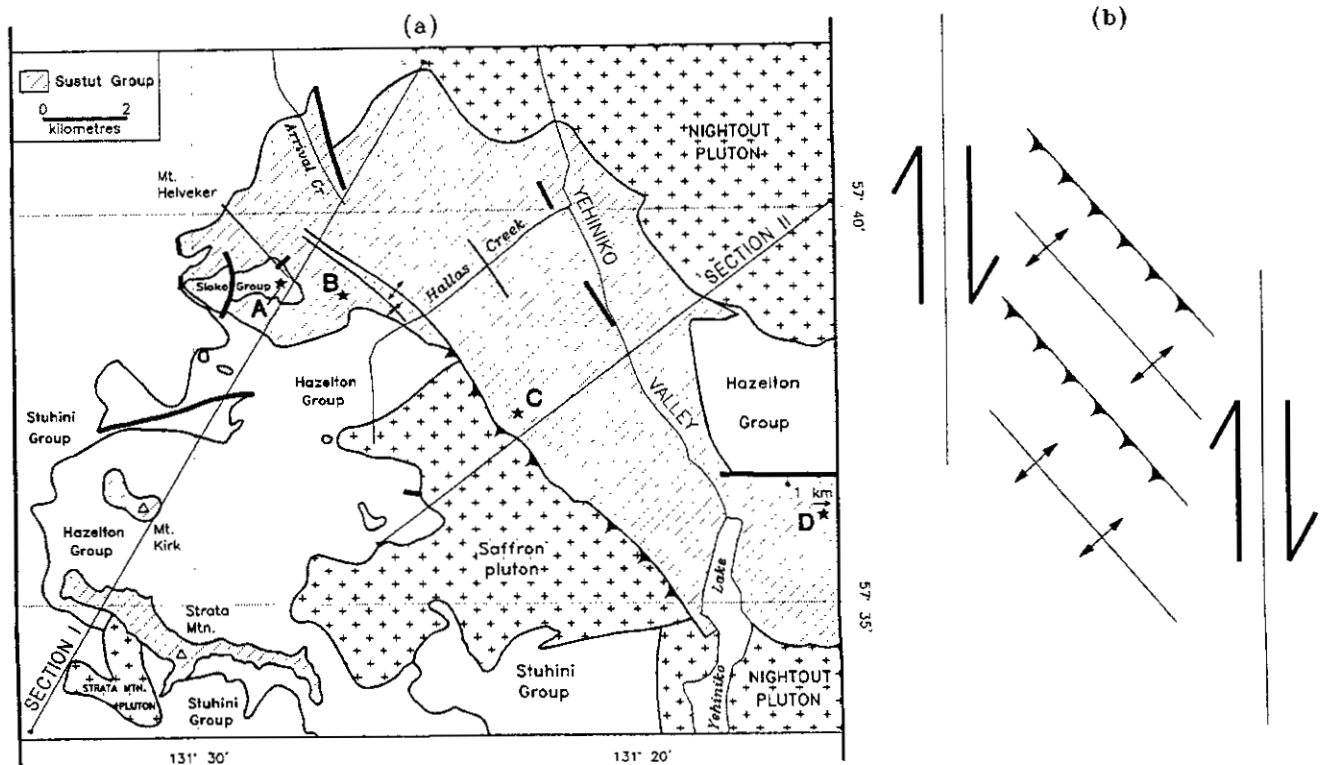


Figure 4-8. (a) Distribution of Sustut Group in the Yehiniko valley and (b) interpreted en echelon left-stepping, dextral wrench fault system that may have produced the abrupt dip changes and reverse fault.

NORTHWEST-TRENDING FAULTS

Bedding of Sustut Group on Strata Mountain, Mount Kirk and Mount Helveker is gently dipping to horizontal; however, northeast of Mount Helveker and in the Yehiniko Creek valley, beds strike to the northwest, dip steeply, and display abrupt reversals in dip direction. No fold closures have been observed, except for a possible drag fold on the eastern flank of Mount Helveker (R.T. Bell, written communication, 1989). A contractional fault that dies out into an anticline along strike to the northwest has been inferred to explain three features of the conglomerate: the abrupt dip reversals, beds dip underneath the older Saffron pluton; and the incipient cataclastic deformation of greywacke northwest of Yehiniko Lake (Figure 4-7).

A left-stepping, dextral wrench fault may have produced the contractional faults and folds in the Sustut Group in this area (Figure 4-8). The distribution of preserved Sustut Group has a similar geometry to the Mess Creek graben (Souther, 1972) and a larger area south of the Grand Canyon of the Stikine River (Read, 1983; Wheeler and McFeely, 1991). The basins and structures may be related to a latest Cretaceous to early Tertiary right-lateral wrench fault system, perhaps linked to the terminal stages of deformation in the Skeena fold belt.

METAMORPHISM

Most rocks in the study area have undergone subgreenschist or greenschist grade metamorphism. Primary textures are preserved in Mesozoic strata, but most Paleozoic rocks display some penetrative fabric which has obliterated original textures. Pluton emplacement has partially controlled metamorphic mineral assemblages in several areas and amphibolite grade (hornblende hornfels) is attained locally (Figures 4-9, 4-10). The project area is divided into areas of similar metamorphic facies based on conodont colour alteration indices (CAI; Appendix 3), on petrographic identifications of metamorphic mineral assemblages and on some x-ray diffraction analyses (Appendix 10). Areas of greenschist facies correspond to CAIs greater than 5 and less than 7, and occur across the northern third of the Tahltan Lake map area, north of the Jimjack fault, and south of the Hazelton outlier (Figure 4-10). Zeolite to lower greenschist facies rocks with CAIs less than 5 and greater than 1 underlie an area between Yehiniko Lake and the confluence of the Chutine and Stikine rivers (Figure 4-10). Local thermal anomalies related to intrusions are evident throughout the area; for example, Tahltan Lake and Scud Glacier areas. Zeolite grade Stuhini volcanic rocks are common north of Mount Helveker and in the northeast-trending belt of rocks in the Stikine valley. Farther north, laumontite occurs in amygdules and veinlets in Stuhini basalts near the Damnation pluton.

CONODONT COLOUR ALTERATION INDICES

The study of conodonts in Triassic and older rocks provides an index of thermal maturation in the region. Carboniferous and Permian limestone CAI values are similar, averaging about 5, and indicating probable greenschist grade metamorphic conditions. Permian limestone is typi-

cally more recrystallized than Late Triassic limestone, even when CAI values are equal. Carnian conodonts in the Tahltan Lake and Tahltan River areas have values of about 5, equal to those obtained from Lower Permian limestone along the Chutine River (Figures 4-9, 4-10). These CAI values of 5 to 5.5 are indicative of lower greenschist grade metamorphism (chlorite zone), with temperatures between 300° and 440°C (Rejebian *et al.*, 1987). There is a significant thermal contrast in Carnian rocks across the Jimjack fault, with an abrupt drop to CAI values of 3.5 or less, which indicate zeolite facies metamorphism. This supports the interpretation of the fault as a north-side-up reverse fault.

Some of the highest colour alteration indices are found adjacent to intrusions. For example, Upper Permian limestones have CAI values between 7 and 8, implying amphibolite grade, where intruded by a Late Triassic diorite plug east of the toe of the Scud Glacier. Elevated CAI values also occur west of the Tahltan Lake pluton and north of the Rugged Mountain and Half Moon plutons (Figure 4-10).

In contrast to Paleozoic strata in the project area, Carboniferous and some Lower Permian strata farther to the southeast near Newmont Lake show anomalously low CAIs (Brown *et al.*, 1991). Late Triassic signatures are varied; Carnian limestone values indicate an abrupt change from zeolite to greenschist grade across the Jimjack thrust fault. Norian values are uniformly within the zeolite facies, but are restricted in their distribution adjacent to the Hazelton outlier. Near Galore Creek, Middle to Late Triassic conodonts have comparable values of about 5 (Logan and Koyanagi, 1994). The fact that older rocks do not necessarily have higher CAIs demonstrates that the area has a varied thermal history. This may be related to a combination of plutonism and regional faulting (Figures 4-9 and 4-10).

LATE PERMIAN TO EARLY TRIASSIC(?) METAMORPHISM

The oldest metamorphic fabrics are pervasive to faintly developed penetrative phyllosilicate foliations in Paleozoic strata. Sericite and chlorite foliations are best developed in the Little Tahltan Lake and Barrington River culminations. Foliation is less pervasive in the Chutine River and Scud River culminations where Gunning (1993a) defines the greenschist assemblage as calcite, quartz, epidote (zoisite), white mica and magnesium-rich chlorite (corundophilite). Amphibolite and greenschist grade Carboniferous volcanic and sedimentary rocks in the Butterfly Lake area display moderately developed foliations.

Age constraints for metamorphism are poorly established. We interpret the event to be pre-Middle Triassic in age, based on the presence of intensely deformed greenschist grade rocks of probable Permian and older age, which are juxtaposed with less deformed and lower grade Late Triassic strata, such as in the Little Tahltan Lake culmination. The same contrasts are noted, but are less well expressed in the other culminations. The foliations formed before or during D₁ recumbent fold development, as recognized farther north in the Tulsequah map area (Bradford and Brown, 1993a). The postulated pre-Middle Triassic metamorphic event correlates with a post-Early Permian, pre-Middle Tri-

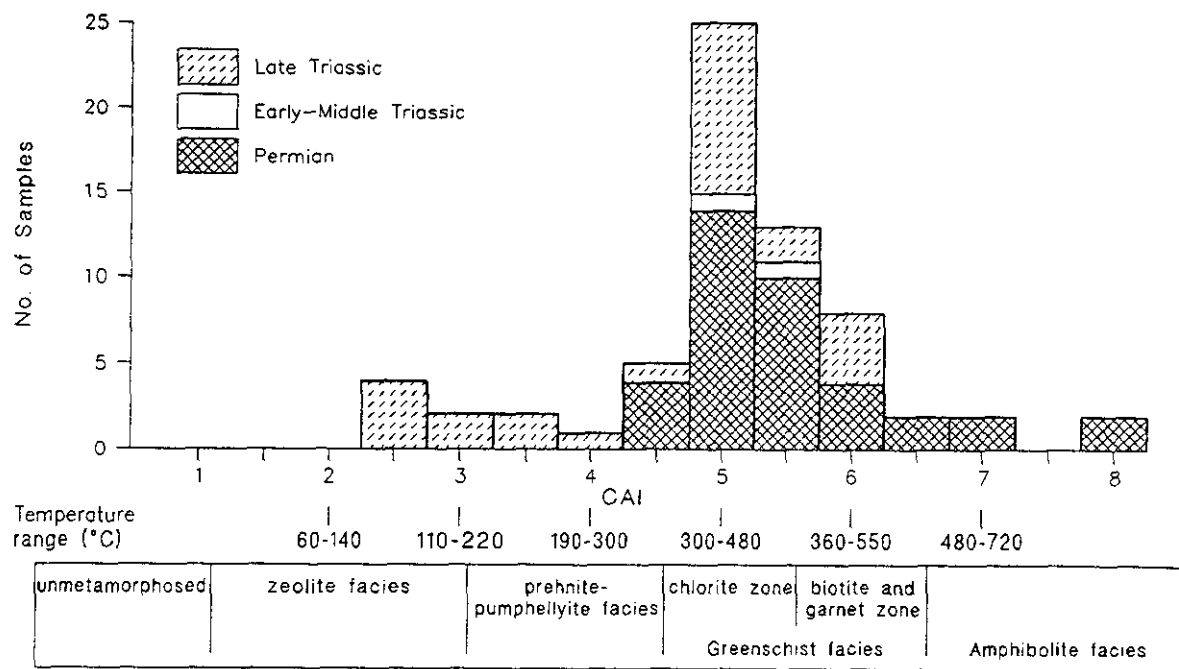


Figure 4-10. Histograms illustrating the distribution of CAI values relative to age. Temperature ranges are from Epstein *et al.* (1977) and Rejebian *et al.* (1987).

assic low-grade metamorphic and deformation event noted by Read (1984) and Read *et al.* (1989) to the east and south-east, and more widely by Monger (1977b).

JURASSIC TO PRE-LATE CRETACEOUS METAMORPHISM

Stuhini and Hazelton group rocks are characterized by zeolite to lowermost greenschist grade mineral assemblages (Appendix 10). There is no evidence of a regional pre-Hazelton (pre-Jurassic) metamorphic event affecting the Stuhini Group that would correlate with the post-Norian/pre-Toarcian deformation discussed above. Variations in metamorphic grade of Mesozoic strata tend to reflect proximity to plutons and localized heat flow. Laumontite identified in the Stuhini Group near the Damnation pluton limits the depth of burial to less than 11 or 12 kilometres (Lion, 1971), assuming a normal geothermal gradient of about 30°C per kilometre.

The timing of the metamorphic event that affected Stuhini and Hazelton strata is poorly constrained. Metamorphic amphibole from the Moscovian volcanic unit (Butterfly member) yielded a 155 Ma date by conventional K-Ar techniques (Appendix 12), however, it is unclear whether this reflects the thermal peak or represents partial resetting during the Eocene plutonic episode. Similarly, 166 and 148 Ma dates obtained from Aalenian and Toarcian volcanic rocks are equivocal estimates for the metamorphic event. The thermal event was probably coeval with emplacement of the Middle Jurassic Three Sisters plutonic suite. An upper age limit is provided by overlying Sustut Group strata, which are less metamorphosed. Similar relationships are evident in north-central British Columbia where Sustut Group strata

truncate isograds within the Takla Group (Greenwood *et al.*, 1991).

EOCENE BURIAL METAMORPHISM

Petrography and limited x-ray diffraction analyses of rhyolite tuff and porphyritic basaltic andesite from the Sustut and Sloko groups identified zeolites in fracture fillings and matrix (Appendix 10). Zeolites are probably the product of burial metamorphism. Similar conditions are evident from vitrinite reflectance data for a sample of coalified wood from the Sustut Group (Figure 4-9) which falls in the high-volatile bituminous coal series, with random reflectance (R_m) of 0.72 and mean maximum reflectance (R_{max}) of 0.75. Similar rank Eocene coal occurs near Tuya River (104J/2,7: Ryan, 1991). A white crystal-vitric rhyolite ash tuff from the Sustut Group produced a 51.6 ± 1.8 Ma whole-rock K-Ar date. This may represent the age of zeolite burial metamorphism during Sloko volcanism. Uranium-lead dates of the Sloko Group 250 kilometres farther north are slightly older, at about 53 Ma (M. Mihalynuk, unpublished data).

CONTACT METAMORPHISM

Contact aureoles adjacent to plutons extend up to 500 metres from intrusive contacts. Secondary garnet-wollastonite skarns and biotite hornfels are common, and andalusite was identified at Devils Elbow Mountain. The strongest thermal effects occur adjacent to ultramafite bodies where secondary amphibole is common and biotite hornfels is well developed. This presumably reflects the higher temperatures of emplacement of the ultramafic rock. Plutonic rocks underlie more than 50% of some parts of the map area and the elevated metamorphic mineral assemblages reflect this plutonism.

SUMMARY OF METAMORPHISM

Late Permian to Middle Triassic and Middle Jurassic metamorphic events are documented. A Permo-Triassic greenschist grade event may have been synchronous with regional deformation which produced chlorite and biotite phyllite characterizing Stikine assemblage rocks in the culminations. The postulated Jurassic event affected Mesozoic

strata but did not generate penetrative fabrics. Zeolites present in the Stuhini Group in the Stikine valley and in the Hazelton Group outlier indicate that Late Triassic and younger rocks were never deeply buried. This may corroborate stratigraphic evidence that the Stikine Arch remained a topographic high for much of the Mesozoic.

CHAPTER 5

ECONOMIC GEOLOGY

The map area lies within an important metallogenic province along the eastern margin of the Coast Belt, from Alice Arm north to the Taku River, that hosts numerous precious and base metal mineral deposits (Figure 5-1). Past mineral production in the project area has been limited to placer gold mined along the Barrington River. The mineral potential of the region is highlighted by the Schaft Creek and Galore Creek porphyry copper deposits, immediately east and south of the project area, where large, unexploited copper resources have been defined. In this chapter, mineral occurrences within the study area are classified according to deposit type, and age constraints on mineralizing episodes are summarized. Finally, recent exploration activity and viable exploration targets are reviewed.

No mineral occurrences in the study area have published reserve estimates, but exploration has been limited because the area is remote and rugged. Known showings are primarily concentrated in eight main areas: the Scud River, Schaft Creek, the Yehiniko fault zone, Dokdaon-Strata-Helveker creeks, Devils Elbow, Mount Conover, Limpoke pluton and Tahltan Lake pluton (Figure 5-2).

The most economically significant deposit types in northern Stikine Terrane are: alkaline and calcalkaline porphyries; transitional and mesothermal veins; epithermal veins; volcanogenic massive sulphide (VMS) deposits, and skarns. Classification of some of the showings in the project area is speculative due to lack of data. This is most common

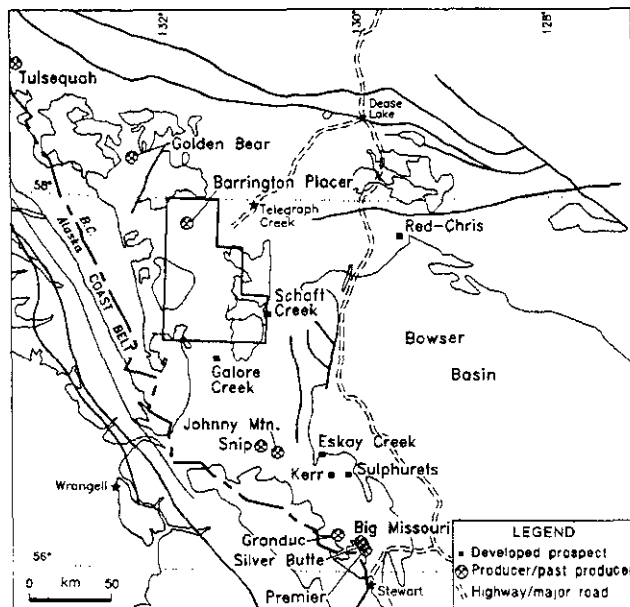


Figure 5-1. Major mineral deposits, mines and past producers between Stewart and Tulsequah.

in the case of transitional veins, some of which may represent distal parts of porphyry systems. Given the relatively undeveloped nature of most of the mineral prospects, any classification of deposit types must be viewed as provisional.

Certain deposit types are associated with particular stratigraphic intervals or intrusive suites, while others represent widely separated mineralizing episodes. For example, in the Stikine Terrane, submarine volcanic arc settings favourable for massive sulphide deposits developed in Devonian, Carboniferous and Middle Jurassic sequences. Alkaline and calcalkaline porphyry copper deposits and transitional veins developed where plutons intruded oceanic arcs during the Late Triassic and Early to Middle Jurassic. More evolved silicic porphyry deposits and epithermal veins are associated with Eocene continental volcanism and plutonism.

PORPHYRY DEPOSITS

Northern Stikine Terrane contains examples of three types of porphyry deposits. The Schaft Creek and Galore Creek deposits (Figure 5-1) exemplify calcalkaline and alkaline porphyries, respectively. The Ben showing is hosted by Eocene plutonic rocks and has affinities with porphyry molybdenum deposits. Although significant metal resources have been defined at both Galore Creek and Schaft Creek, neither has been developed.

Fifteen of the fifty seven mineral occurrences recorded in the MINFILE database for the project area are classed as porphyry showings (Table 5-1). All showings, with the exception of the Ben showing, are hosted by Stuhini Group volcanics and Late Triassic to Middle Jurassic intrusions.

CALCALKALINE PORPHYRY COPPER DEPOSITS

Calcalkaline porphyry copper deposits are associated with high-level to deep-seated felsic intrusive bodies, generally occurring along convergent margins in oceanic or continental arc settings. Gold and molybdenum contents may be significant. The association with calcalkaline intrusive suites is a fundamental characteristic. Typical features include annular or shell-like alteration zones with potassic (potassium-feldspar and/or biotite) cores and sericitic to propylitic outer zones (McMillan and Panteleyev, 1988; McMillan, 1992). Schaft Creek is the outstanding example in the northern Stikine Terrane.

SCHAFT CREEK (LIARD COPPER)

Schaft Creek is a high-level, calcalkaline porphyry copper-molybdenum deposit (Sutherland Brown, 1971; Fox *et al.*, 1976; Seraphim *et al.*, 1976) located near the intrusive contact between the Middle Jurassic Yehiniko pluton and

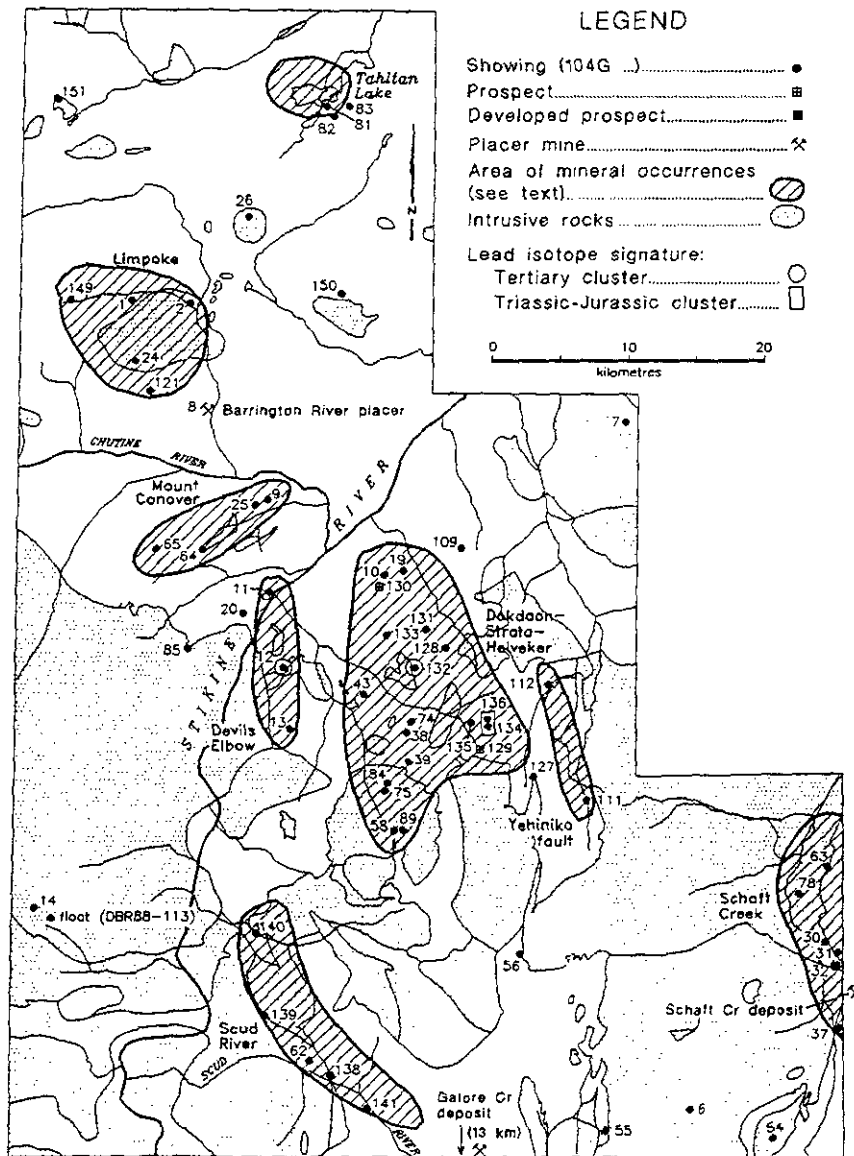


Figure 5-2. Mineral occurrences in the project area and the eight main areas discussed in the text. Numbers identify MINFILE number (104G-...) and correspond to those in Table 5-1.

the Late Triassic Hickman pluton, immediately east of the project area. It was staked in 1957 and Liard Copper Mines Ltd. was formed to hold the property. Subsequently it was explored by Silver Standard Mines Ltd., American Smelting and Refining Company, Hecla Mining Company and Teck Corporation. Chalcopyrite-bornite-molybdenite mineralization occurs in two north-trending zones, one of which is an intrusive tourmaline breccia pipe (Main or Saddle and Tourmaline Breccia zones: Fox *et al.*, 1976). Both potassic and propylitic alteration suites are present. The deposit is hosted by mafic flows, subvolcanic intrusions and epiclastics of the Stuhini Group, with only 10% of mineralization in felsic dikes and quartz feldspar porphyry (Linder, 1975). These were originally believed to be comagmatic with the Yehiniko pluton. However, altered monzonite from drill

core has yielded a Late Triassic (220 ± 5 Ma) U-Pb date (J.M. Logan, personal communication, 1993). It is possible that both Late Triassic and Middle Jurassic hydrothermal events contributed to the Schaft Creek deposit. A whole-rock K-Ar date of 185 ± 10 Ma (recalculated with decay constants of Steiger and Jäger, 1977; from Panteleyev and Dudas, 1973) was obtained on hydrothermal biotite. Up to 1975, about 34 500 metres of surface diamond drilling had been completed in 115 holes (Fox *et al.*, 1976). Drill-indicated and inferred resources are 910 million tonnes with an average grade of 0.3% copper, 0.03% molybdenum and 0.113 gram per tonne gold (Linder, 1975). The size of the deposit makes Schaft Creek one of the largest copper, molybdenum and gold deposits in British Columbia.

TABLE 5-1
SUMMARY OF MINERAL OCCURRENCES

MINFILE NO. (104G)	NAME	NTS MAP	UTM EAST	(Zone 09) NORTH	HOST MAP UNIT	ECONOMIC MINERALS	DESCRIPTION	REFERENCES
Calcalkaline porphyry copper showings:								
030, 031, 032	Nabs 21, Nabs 13, Nabs 30 FR (part of Schaft Creek deposit)	104G/06	378600	6362500	Yehiniko pluton	cpy, bn	Finely disseminated chalcopyrite and lesser bornite are hosted by silicified and chloritized quartz monzonite of the Yehiniko pluton near its contact with the Stuhini Group.	Jeffery (1967), Lammle (1966), Betmanis (1978), Sutherland Brown (1971), Dudas (1972), Panteleyev and Dudas (1973)
037	Hicks	104G/06	379400	6356200	Stuhini Group	bn, cpy, mo, py	Blebs, stringers, and disseminations of pyrite, chalcopyrite, bornite and lesser molybdenite occur mainly in Stuhini Group volcanics near the eastern margin of the Hickman pluton.	GEM 1971-72, Mark (1970)
063	Late	104G/06	378850	6368000	Stuhini Group/ Yehiniko pluton	cpy, bn, py	Pyrite, chalcopyrite and bornite occur as stringers and disseminations along a sheared contact between the Yehiniko pluton and flows and pyroclastics of the Stuhini Group.	Holbek (1981)
078	Arc, Post	104G/06	376800	6366000	Stuhini Group/ Yehiniko pluton	cpy, bn, cc, py	Chalcopyrite, bornite, chalcocite and pyrite stringers and blebs occur within purple pyroclastics of the Stuhini Group and along shears within the Yehiniko pluton.	GEM 1972, Phelps and Guttrath (1972), Mullian and Bell (1972)
038, 039	LLK, Dok 35	104G/12	348600	6378900	Stuhini Group	maf, az, cpy, mo, py	Oxidized disseminated and fracture-filling chalcopyrite-molybdenite-pyrite is accompanied by propylitic alteration.	Veitch (1970), Marud (1990b)
043	Dok	104G/12	345650	6381700	Stuhini Group	cpy, py	Disseminated and fracture-filling pyrite-chalcopyrite is accompanied by propylitic and local potassic alteration.	Veitch (1970), Ulrich (1971), Folk (1981b), Marud (1990b)
074	PR	104G/12	349000	6379700	Stuhini Group	cpy, py	cm-scale chalcopyrite and pyrite-rich veins are associated with felsic dikes	Veitch (1970), Scheilly (1972), Marud (1990b)
Alkaline porphyry copper showings:								
150	Rugged Mtn.	104G/13	344400	6311540	Stuhini Group	cpy	Rare disseminated chalcopyrite occurs in the clinopyroxenite phase of the Rugged Mountain pluton.	Marud (1990b), Brown <i>et al.</i> (1992a), Neill (1992), Neill and Russell (1993)
001	Poke	104G/13	329920	6410757	Stuhini Group	cpy	Disseminated chalcopyrite occurs along fracture zones in altered Stuhini Group volcanics adjacent to the marginal phase of the Limpoke pluton.	Hallof (1963), Folk (1981a), Kerr (1948a), Souther (1972)
002	Gordon	104G/13	334119	6410365	Stuhini Group	cpy	Disseminated chalcopyrite is associated with alkali feldspar syenitic dike swarms which outcrop northeast of the Limpoke pluton.	Hallof (1966), Marud (1990c), Kerr (1948a), Souther (1972)
024	New Limpoke	104G/13	330116	6406383	Stuhini Group	cpy, py, mo, po	Disseminated chalcopyrite occurs within altered quartz monzonite to monzodiorite of the Limpoke pluton. Pyrite, pyrrhotite and molybdenite are also present.	Kerr (1948a), Souther (1972)
Porphyry molybdenum showings:								
014	Ben	104G/05	320674	6366176	Tertiary stock	mo, cpy, py, tet, sch	Zones of intense brecciation, pervasive silica, manganese and sericite alteration is associated with molybdenite, chalcopyrite, pyrite and tetrahedrite-bearing stockworks in a large Eocene biotite granite stock.	Bapty (1964), Anonymous (1972), Brown and Gunning (1989a)

MINFILE NO. (104G)	NAME	NTS MAP	UTM EAST	(Zone 09) NORTH	HOST MAP UNIT	ECONOMIC MINERALS	DESCRIPTION	REFERENCES
Early to Middle Jurassic mesothermal and transitional vein showings:								
140	Oksa Gold	104G/05	337500	6364500	Stikine assemblage	py, cpy, sph, gln, po	Quartz veins up to 1.5 m wide strike 015 ^U and dip 60-65 ^U easterly within porphyritic volcanics.	Kushner (1990a, 1991); Chung (1990a)
138	Jameson	104G/05	342500	6354000	Stikine assemblage	py, cpy, sph	Mineralized quartz-calcite vein in pyritic argillites returned values of 50 ppb Au, 1.4 ppm Ag, 691 ppm Cu, 6830 ppm Zn.	Kasper (1990a)
139	Snow	104G/05	338000	6358500	Stikine assemblage	py, po, sph	Quartz veins in limestone are mineralized with pyrite, pyrrhotite, chalcopyrite and sphalerite.	Chung (1990c)
056	North Scud, Alicia, Otis, Moped	104G/06	356387	6362368	Stuhini Group	cpy, bn	Small lenses of massive chalcopyrite, bornite, and magnetite up to 25 cm long occur within Stuhini Group andesite tuff and breccia near the western margin of the Yehiniko pluton.	Gale (1964), Johnson and Jones (1990a, b, c)
111	Yehiniko East	104G/06	361523	6373332	Stuhini Group/ Yehiniko pluton	Unknown	Unspecified copper mineralization is reported within large, possibly fault-controlled alteration zones along the contact of Stuhini Group volcanics and the Yehiniko pluton.	Souther (1972)
112	Yehiniko West	104G/11	359000	6382000	Stuhini Group	cpy?	Possible chalcopyrite mineralization occurs in a N-trending alteration zone.	Souther (1972)
129	Chuckster	104G/11	353660	6377330	Stuhini Group	cpy, gln, sph, py	NNE-trending, steeply dipping carbonate-quartz veinlets 1-4 cm wide in a 5 m- wide zone contain chalcopyrite, galena, sphalerite and pyrite.	new occurrence (CGR89-307; Appendix 14)
134	Plum	104G/11	354563	6379169	Stuhini Group	cpy, gln, py	A quartz-carbonate vein <2 cm thick, trending 042/78SE, contains chalcopyrite, galena and pyrite.	new occurrence (DBR89-298; Appendix 14)
135	Muffle	104G/11	353336	6379465	Stuhini Group	cpy, gln, py, mal	A discontinuous quartz-carbonate vein up to 20 cm thick contains chalcopyrite, galena, pyrite and malachite.	new occurrence (DBR89-266; Appendix 14)
136	Player	104G/11	354555	6379720	Stuhini Group	co, hem, mal	A 077/84SE trending, discontinuous quartz vein, up to 7 cm thick, contains chalcocite, specular hematite and malachite.	new occurrence (DBR89-302; Appendix 14)
010	August	104G/12	347400	6390250	Stuhini Group	cpy, bn, py	cm-scale quartz veins in NE-trending, steeply dipping fracture zones contain chalcopyrite, bornite and pyrite.	Kerr (1948a), Graf (1985b)
019	Mtn. Goat, Kirk Cu	104G/12	348744	6390502	Stuhini or Hazelton	cpy, bn	Quartz veins or lenses up to 1 m thick along dike contacts contain chalcopyrite and bornite.	Kerr (1948a), Graf (1985b)
130	Steep Creek	104G/12	346971	6389455	Stuhini Group	py, cpy?	Pyrite and possibly chalcopyrite occur in a NE-trending, steeply dipping cm-scale siliceous pyritic vein or layer(?).	new occurrence (CGR89-460; Appendix 14)
009	Jackson, BIK, Conover Ck.	104G/12	339250	6396000	Stuhini Group	cpy, gln, sph, py	NE to NW-trending quartz and carbonate breccia zones contain chalcopyrite, galena, sphalerite and pyrite.	Lammie (1964) Kerr (1948a), Dirom (1964), Graf (1985a)
025	Lady Jane	104G/12	338350	6395650	Stuhini Group	cpy, gln, sph, py	A quartz-carbonate breccia zone trending north and dipping 60°W contains chalcopyrite, galena, sphalerite and pyrite.	Kerr (1948a), Dirom (1964), Graf (1985a)

MINFILE NO. (104G)	NAME	NTS MAP	UTM EAST	(Zone 09) NORTH	HOST MAP UNIT	ECONOMIC MINERALS	DESCRIPTION	REFERENCES
064	Conover Mt.	104G/13	334512	6392515	Stuhini Group	cpy	Quartz, calcite and chalcopyrite veins occur at the contact between the Conover intrusions and surrounding volcanic rocks.	Kerr (1948a), Davis (1988)
065	Mist	104G/13	331200	6392700	Stuhini Group	py, po, cpy	Quartz veins with minor pyrite, pyrrhotite, chalcopyrite and gold are associated with felsic and dioritic dikes intruding Stuhini Group volcanics and sediments.	Kerr (1948a), Eccles (1981), Korenic (1982b)
006	Alberta	104G/06	368378	6350607	Stuhini Group	cpy, mag	Chalcopyrite and magnetite occur as fracture fillings with minor malachite in a small pendant of Stuhini Group mafic flows and pyroclastics within the Hickman pluton.	
007	Callbreath	104G/11	365200	6400750	Nightout pluton	cpy, bn	NE-trending, steeply dipping quartz veins with chalcopyrite and bornite are associated with epidote-chlorite alteration.	Morgan (1973)
020 085	Lucky Strike	104G/12	337300	6387800	Stikine assemblage	gln, cpy, sph, po, py	Native Au is reported from a NW-trending, gently-dipping fracture zone with quartz veining. (Possibly equivalent to 104G085).	Davis (1988)
127	Brownie	104G/12	357650	6375300	Stuhini Group	py, sph, gln, cpy	Disseminated to semimassive pyrite, sphalerite, galena and minor chalcopyrite hosted within a 15 cm wide quartz - iron carbonate vein.	new occurrence (DBR88-302-2; Appendix 14)
149	Poker	104G/13	325064	6411133	Stuhini Group	po, py, cpy, sph, gln	Quartz-sulphide boulder train has been traced to the Limpoke Glacier area where drilling has attempted to locate the source.	Westcott (1989b), Aspinall <i>et al.</i> (1990), Aspinall (1991)
Eocene mesothermal and transitional vein showings:								
075, 084	Gu, Gu North	104G/05	347000	6374500	Strata Glacier pluton	cpy, gln, sph, mo, sch	Chalcopyrite, galena, sphalerite, molybdenite and rare scheelite in narrow quartz veinlets occur in a volcanic pendant within a large body of Middle Jurassic granodiorite. The veinlets are associated with a prominent NW joint set. Narrow quartz veinlets peripheral to a 1.5 m ankerite vein contain traces of chalcopyrite in a volcanic pendant.	Chung (1990b), Kushner (1990b)
058	Marg West	104G/05	347500	6371600	Stuhini Group	cpy, mo, sch, gln	Quartz veinlets <10 cm wide contain chalcopyrite, molybdenite, pyrite, scheelite and minor galena. They occur over a width of 100 m in a 300 by 600 m pendant of Stuhini Group volcanic breccia within Middle Jurassic granodiorite.	Folk (1981b), Brown and Gunning (1989a)
089	Marg East	104G/05	348150	6371600	Stuhini Group	cpy, py	Chalcopyrite and pyrite occur in zones of pervasive silica and epidote alteration at the sheared margin of a Stuhini Group volcanic pendant within a Middle Jurassic granodiorite body.	(Folk (1981b), Brown and Gunning (1989a)
128	Fossil Vein	104G/11	351657	6384893	Stuhini Group	cpy, mal	An ENE-trending, steeply dipping quartz vein up to 5 cm wide contains minor chalcopyrite.	new occurrence (CGR89-166; Appendix 14)
131	Dikes	104G/12	350289	6386230	Hazelton Group	Fe-carbonate, gln, sph	A N-trending, vertical, 5-15 cm wide carbonate vein-breccia zone contains galena and sphalerite.	new occurrence (CGR89-247; Appendix 14)

MINFILE NO. (104G)	NAME	NTS MAP	UTM EAST	(Zone 09) NORTH	HOST MAP UNIT	ECONOMIC MINERALS	DESCRIPTION	REFERENCES
132	Forgotten	104G/12	349343	6383521	Stuhini Group	py, gln	Discontinuous pyrite-galena-carbonate-quartz veins, up to 4 cm wide, are hosted by Stuhini volcanics. Clay-alteration extends about 15 cm into wallrock from the veins.	new occurrence (DBR89-382, 384; Appendix 14)
133	Captain	104G/12	347412	6385901	Hazelton Group	py, cpy	Pyrite-chalcocopyrite occurs in cm-scale quartz veins.	new occurrence (DBR89-273, 277-1, 277-2; Appendix 14)
Massive sulphide vein showings (or volcanogenic massive sulphide):								
121	Tuff, Goat	104G/13	331080	6404200	Stuhini Group	py, pyr, aspy, cpy	Massive sulphide pods less than 10 cm wide and 1 to 20 m long occur in Stuhini volcanics over an area of about 1200 x 1200 m.	Kerr (1948a), Strain (1981), Korenic (1982a), Lehtinen (1989), Van Angeren (1991)
Skarn showings:								
081, 082, 083,	VB 20, VB 5, VB 12	104G/13	342250	6425670	Stuhini Group	mgt, po, cpy, py, hem	Magnetite, pyrrhotite and chalcocopyrite are associated with garnet, epidote, actinolite and diopside-bearing skarns within Stuhini Group limestone and volcanoclastic rocks intruded by a Triassic-Jurassic (?) hornblende diorite pluton. Pyrite and specular hematite are also present.	Hodgson and LeBel (1974), Marud (1990a), Southam (1991), Brown <i>et al.</i> (1992a)
011	Drapich	104G/12	339200	6389300	Stikine assemblage	cpy, sph, gln, mag, py, po, cpy, bn	Irregular chalcocopyrite lenses, <1 m thick, occur in skarn developed along a granodiorite contact.	Kerr (1948a), Davis (1988)
012	Devil's Elbow	104G/12	339998	6383847	Stikine assemblage	mag, py, gln, cpy, sph, sch, po	Irregular sulphide lenses occur in skarn developed at a granodiorite contact.	Mandy (1930), Kerr (1948a), Keep (1983), Lloyd (1989), Dunn (1990), Webster and Ray (1991)
013	Apex	104G/12	340340	6379464	Stikine assemblage	gln, sph, mag, cpy,	Mineralization not described.	Kerr (1948a)
062	Cos	104G/05	341042	6355104	Stikine assemblage/ Pereleshin pluton	cpy, bn	Chalcocopyrite and bornite stringers occur within a large skarn zone at the contact of pre-Permian limestone with Early Jurassic orthoclase megacrystic quartz monzonite.	Kasper (1990a)
141	JD1, Seud River, CB1, CB2	104G/05	348559	6351591	Stikine assemblage	po, py, cpy, aspy, mgt	Boulders with up to 80% sulphides in a garnet - actinolite gangue from the toe of <i>Rugose Glacier</i> returned assay values of 14.0 g/t Au; the source of the boulders was traced to a gossanous limestone cliff. Blebs of chalcocopyrite and pyrite with minor galena occur in a 4 cm - wide quartz vein in the centre of a shear zone 1.0 m wide by 30 m long following a contact between greywacke and argillite. Quartz veins 25 cm wide along a sheared contact between pre-Permian limestone and volcanics contain 3-15% pyrite and pyrrhotite; grab samples returned values 1.58 g/t Au, 6.5 g/t Ag, 878 ppm Cu.	Awmack (1989), Ross (1989), Brown and Gunning (1989a)
151	Mag	104G/13	324558	6425807	Stuhini Group	mag	Massive magnetite pod (over 6m wide by 30 m long) occurs within Stuhini Group limestone where it is intruded by an altered granodiorite pluton.	Brown <i>et al.</i> (1992a)

MINFILE NO. (104G)	NAME	NTS MAP	UTM EAST	(Zone 09) NORTH	HOST MAP UNIT	ECONOMIC MINERALS	DESCRIPTION	REFERENCES
Placer gold deposit:								
008	Barrington River	104G/12	335200	6402600	Qal	Au	Placer gold deposits occur within unconsolidated gravel of the lower section of the Barrington River. The source of gold may be the intrusive rocks which outcrop upstream along the Barrington River and Limpoke Creek.	EMPR AR 1925, '29, '31-33, '35, Kerr (1948a)
Stratabound U showing:								
109	Hcl	104G/11	353000	6392000	Sustut Group	salecite, torbernite	A cm-scale zone of stratabound secondary uranium mineralization in conglomerate and coaly fragments in sandstone.	Salat and Noakes (1979), Bell (1981), Graf (1985b)
Ultramafic-hosted showings:								
026	MH, Shakes Creek	104G/13	338500	6416500	Stuhini Group	mag, py, cpy	Tuffaceous siltstone and andesite are intruded by magnetite-rich clinopyroxenite of the Latimer Lake pluton. Up to 20% magnetite occurs interstitially as grains and blebs. Pyrite veins, 30-40 cm wide, cut the occurrence and carry minor chalcocopyrite.	Hedley (1966b), McIntyre (1966), Souther (1972)
054	Mount Hickman	104G/06	374341	6348316	Hickman ultramafite	asb	Narrow seams of antigorite occur in pyroxene gabbro and olivine pyroxenite, near the southeast margin of the Hickman Ultramafic Complex.	Souther (1972)
055	Middle Scud	104G/06	362200	6349300	Middle Scud Creek ultramafite	tet, agt, cpy	A 75 cm long pod of massive tetrahedrite and chalcocopyrite occurs in pyroxenite within the Middle Scud Creek ultramafic body along its eastern contact with Permian limestone and argillite.	Bapty (1965), Lammle (1964)

ABBREVIATIONS:

Alt = alteration; agt = argentite; asb = asbestos; Au = native gold; az = azurite; bn = bornite; cc = chalcocite; cm = centimetres; cnt = contact; cpy = chalcocopyrite; diss = disseminated; ep = epidote; Fe-carb = iron carbonate; fr = fracture; GEM = Geology, Exploration and Mining; gin = galena; gd granodiorite; irreg = irregular; L-MJr = Lower to Middle Jurassic Hazelton Group rocks; m = metres; mal = malachite; mgt = magnetite; minlzn = mineralization; mo = molybdenite; occ = occurrence; py = pyrite; po = pyrrhotite; qz = quartz; rpl = replacement; sch = scheelite; sil = silicification; sph = sphalerite; stck = stockwork; tet = tetrahedrite; vn = vein; vng = veining; wo = wollastonite.

SHOWINGS NEAR SCHAFT CREEK

The most significant concentration of calcalkaline porphyry copper showings in the project area extends north from the Schaft Creek deposit along the eastern margin of the Yehiniko pluton. These include the Late and Arc/Post (MINFILE 104G 063 and 078) and Nabs prospects (104G 030, 031 and 032). The Hicks showing (104G 037), just south of Schaft Creek, along the eastern contact of the Hickman pluton, may also be related to this suite. Mineralogy consists of pyrite, chalcocopyrite, magnetite, bornite and rare molybdenite as disseminations along fracture zones and sheared intrusive contacts. Silicification and propylitic alteration are present. Mineralization was probably controlled by north-trending structures near the margins of the Hickman and Yehiniko plutons.

DOKDAON - STRATA CREEK AREA

Strongly oxidized pyritic alteration zones between Dokdaon and Strata creeks contain several showings with disseminated and fracture-filling chalcocopyrite and molybde-

nite (Table 5-1: LLK, Dok 35, Dok and PR; MINFILE 104G 038, 039, 043, 074). Mineralized veins occur in propylitic and potassic alteration zones associated with north-north-east and northeast-striking, pink granite to syenite dikes intruding Stuhini volcanic rocks. These dikes may be comagmatic with the Middle Jurassic Saffron pluton. This area has good potential for discovery of additional copper and gold mineralization.

ALKALIC PORPHYRY COPPER DEPOSITS

Alkalic porphyry copper deposits occur in Late Triassic to Early Jurassic rocks of Quesnellia and the northern Stikine Terrane, where high-level monzonitic to syenitic stocks and plugs intrude comagmatic volcanics which commonly have shoshonitic affinities. Magnetite-rich breccias, potassic and albite-epidote alteration and a molybdenum-poor, copper-gold metallic suite are typical features of alkalic systems, as exemplified by Galore Creek, just south of the project area.

GALORE CREEK

Mineralization at Galore Creek is associated with several phases of potassium feldspar megacrystic syenite dikes and sills of the Copper Mountain suite, which intrude Stuhini Group volcanics and pyroxene and orthoclase-phyric flows and breccias (Allen *et al.*, 1976; Logan and Koyanagi, 1994). Potassic and propylitic alteration suites are present, and andradite to grossularite garnet is widespread. Mineralized zones contain abundant pyrite, chalcopyrite, magnetite and bornite, with local secondary cuprite and covellite. Published drill-indicated and inferred reserves of 113 million tonnes grading 1.06% copper, 0.45 g/t gold and 8.6 g/t silver make Galore Creek one of the largest deposits of its type (Allen *et al.*, 1976).

RUGGED MOUNTAIN PLUTON

The Rugged Mountain pluton is classed with the Copper Mountain suite of Late Triassic to Early Jurassic alkalic intrusions. Anomalous but relatively low copper and gold values are reported from the clinopyroxenite border phase and from isolated rusty weathering pyrite-malachite alteration zones (up to 2.32% Cu and 1.57 g/t Au; Marud, 1990b). The presence of alkalic intrusions at Rugged Mountain suggests an analogous setting to Galore Creek; however, prospecting to date has found only low copper and gold values and weak alteration.

LIMPOKE PLUTON

Several copper showings peripheral to the Limpoke pluton may represent alkalic porphyry mineralization (Table 5-1: Gordon, Poke, New Limpoke; MINFILE 104G 001, 002, 024). Disseminated pyrite and chalcopyrite occur within fracture zones in altered Stuhini Group volcanics, in altered quartz monzonite to monzodiorite, and in altered zones associated with potassium feldspar porphyritic syenite dikes. Potassic alteration (biotite and potassium feldspar) affects both intrusive and adjacent volcanic rocks. Potassium feldspar porphyritic syenite is mineralized at the Gordon showing. Minor molybdenite is present at the New Limpoke showing, while bornite occurs at the Gordon showing. Recent sampling on these zones returned low precious metal values (Marud, 1990c).

PORPHYRY MOLYBDENUM DEPOSITS

Porphyry molybdenum deposits are distinct from calcalkaline copper porphyries in ore mineralogy, tectonic setting, intrusion composition and alteration suites. They are generally related to granitic hypabyssal intrusions in extensional settings in cratons or highly evolved arcs, and are copper and gold poor. Mineralization is associated with intense silicification and phyllic alteration.

BEN - DEEKER CREEK AREA

The Ben porphyry molybdenum occurrence (Table 5-1: Ben; MINFILE 104G 014) is within a zone of argillic and silicic alteration and manganese staining, up to 1000 metres wide. Quartz stringers with disseminations of molybdenite and lesser chalcopyrite, pyrite and tetrahedrite, are hosted by a fine-grained felsic intrusion of probable Tertiary age and biotite granite of the Eocene Sawback pluton. The large oxidized alteration zone is a prominent feature (Photo 5-1).

The Ben showing has similarities to better known deposits in the Alice Arm area, south of Stewart (e.g. Kitsault).

Two types of mineralized boulders were found south of the Ben prospect, along Deeker Creek, in the course of this project. The first consists of rusty weathering, semimassive to massive pyrite layers in fine-grained, white vuggy quartz (Photo 5-2). The second is a manganese-stained, vuggy quartz-carbonate vein and breccia with disseminated chalcopyrite, galena and pyrite. The latter vein type forms a boulder train that Ashworth Exploration Ltd. traced (in 1990) southwest to an area covered by an unnamed glacier. The source of the mineralized boulders is not known.

MESOTHERMAL AND TRANSITIONAL VEIN DEPOSITS

Mesothermal vein systems occur in both ductile and brittle shear zones commonly associated with regional fault systems. Most vein systems probably developed at a depth where the transition from ductile shear to seismogenic brittle failure occurs (Sibson *et al.*, 1988). This level is a function of temperature and fluid pressure and is strongly affected by intrusive and regional deformational events. Vein systems at higher crustal levels, above the brittle-ductile transition zone, may be produced by high fluid pressures associated with devolatilizing magmatic bodies or associated wallrock reactions. These veins are of economic interest where they contain high gold values, although significant base metals may be present.

The northern Stikine Terrane contains numerous examples of such "transitional" veins, many of which are associated with Early Jurassic intrusions. To the south, in the Stewart-Iskut belt, the Premier and Sulphurets deposits are hosted by Early Jurassic Hazelton volcanic rocks associated with coeval calcalkaline potassium feldspar megacrystic sills and dikes of the Texas Creek suite. Mineralization occurred during the Early Jurassic (about 190 Ma), based on U-Pb dates from genetically associated intrusions (Alldrick *et al.*, 1986, 1987; Brown, 1987; Alldrick, 1993). The Snip deposit in the Iskut area is a gold and base metal rich vein within a brittle-ductile shear zone. It is hosted by Upper Triassic Stuhini(?) greywacke that is intruded by the Red Bluff porphyry, an Early Jurassic altered potassium feldspar megacrystic body that is elongated subparallel to the shear zone (Macdonald *et al.*, 1992; Rhys and Godwin, 1992). The Golden Bear deposit, northwest of the project area, consists of gold-bearing silicified Permian carbonate lenses and pyritic gouge in contact with Triassic or older mafic volcanic rocks along a north-trending strike-slip fault. Although no Early Jurassic intrusions are exposed, an Early Jurassic age of mineralization is inferred from several K-Ar dates on alteration zones (Schroeter, 1987).

At least 22 of the 57 mineral occurrences recorded in MINFILE for the project area can be classified as transitional or mesothermal veins (Table 5-1). Porphyry occurrences are preferentially hosted in Upper Triassic Stuhini volcanic rocks and intrusive rocks of various ages. Structural features, in particular high-angle fault systems, and proximity to Jurassic and Tertiary intrusions, are more significant controls than stratigraphy. The orientation of veins varies

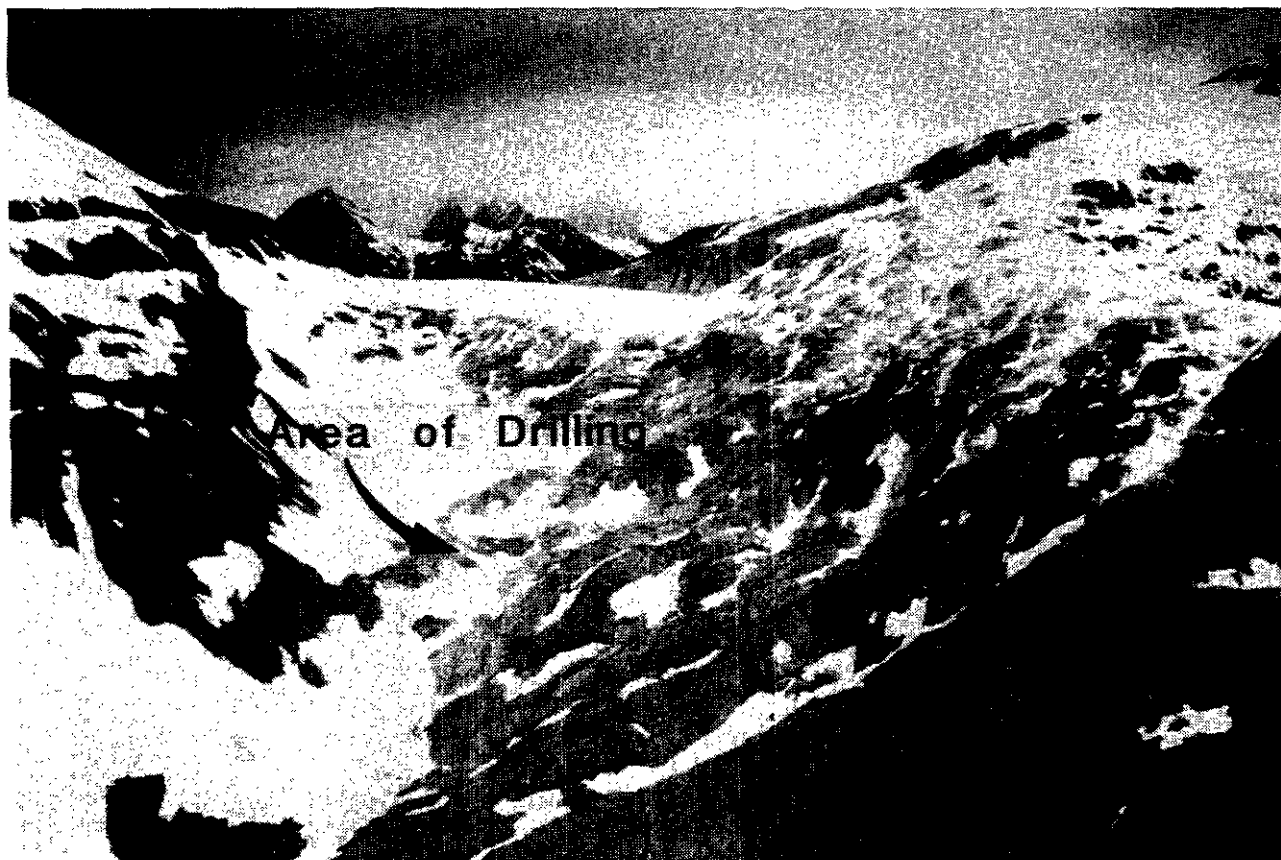


Photo 5-1. Aerial view of propylitic alteration zone at Ben Mo-Cu-W prospect (MINFILE 104G/014), drilled in 1971 but little work has been done since. Quartz-sericite alteration and stockworks with disseminated molybdenite, chalcopyrite and pyrite occur along the northwest-trending faulted intrusive contact of an Eocene granite/felsite intruded into the Middle Jurassic Geology Ridge diorite that contains pendants of Permian(?) limestone.

widely from area to area, with north, northeast and northwest-trending fault systems being most prominent.

Seven mineralized districts contain most of the vein showings: Scud River, Yehiniko fault zone, north of the Strata Glacier pluton, pendants in the Strata Glacier pluton, north of the Strata Mountain pluton, Helveker Creek and Conover Creek. Two of these districts are tentatively classed as Eocene (pendants in the Strata Glacier pluton and north of the Strata Mountain pluton); the rest probably result from Early to Middle Jurassic events.

EARLY TO MIDDLE JURASSIC

YEHINIKO FAULT ZONE

Copper occurrences reported by Souther (1972) in the upper part of both forks of Yehiniko Creek (Table 5-1: Yehiniko East and West; MINFILE 104G 111, 112) are probably related to north-trending faults marginal to the Yehiniko pluton. Little else is known about these occurrences.

NORTH OF THE STRATA GLACIER PLUTON

Four polymetallic quartz-carbonate vein showings are hosted by Stuhini Group volcanics north of the Early Jurassic Strata Glacier pluton (Table 5-1: Chuckster, Plum, Mist, Player; MINFILE 104G 129, 134, 135, 136). Veins generally trend northeasterly in this area. High gold assays have

been obtained from the Chuckster vein, where a grab sample ran 136 g/t (Photo 5-3a, b). Thin quartz-carbonate veins carrying chalcopyrite and galena at the Plum occurrence are illustrated in Photo 5-4.

HELVEKER CREEK

Several auriferous quartz-chalcopyrite vein showings are hosted by Stuhini Group volcanics south of the Stikine River in the Helveker Creek area (Table 5-1: August, Mountain Goat/Kirk, Steep Creek; MINFILE 104G 010, 019, 130). These northeast-trending veins parallel northeast-trending faults in the Stikine River valley. Exploration of one of these veins in the 1920s included driving an adit (Mandy, 1931).

CONOVER CREEK

In the Conover Creek area, polymetallic quartz-carbonate veins and breccia zones occur north and west of the Middle Jurassic(?) Conover pluton (Table 5-1: Lady Jane, Jackson, Conover Mountain and Mist; MINFILE 104G 009, 025, 064 and 065). The Lady Jane vein, traced over 350 metres, strikes north and dips about 60° west (Dirom, 1964). In contrast, the smaller and less extensive Jackson veins, strike northwest to north (*ibid.*). Veins are associated with silicification and iron carbonate alteration. The two vein systems were described by Mandy (1930) and Kerr (1948a). The northeasterly elongation of the pluton may indicate co-



Photo 5.2. Vuggy, coarsely crystalline quartz vein with disseminated pyrite, chalcopyrite and galena, near headwaters of Decker Creek (MINFILE 104G-014; DBR88-113-1). Wallrock fragments are argillically altered intrusive rock



Photo 5-3. (a) Gold-rich (136 g/t Au) Chuckster vein of intergrown prismatic quartz needles with disseminated chalcopyrite, pyrite and trace galena, cutting Stuhini Group epiclastic rocks, headwaters of Strata Creek (MINFILE 104G-129; CGR89-307-2).



Photo 5-3. (b) Silicified and potassically altered Middle Jurassic(?) plutonic rock with chaledonic quartz-carbonate vein containing pyrite and galena that assayed 5 g/t gold, between Strata and Dokdaon creeks (CGR89-411).



Photo 5-4. Multiphase veins - sheared quartz, disseminated chalcopyrite-pyrite, and carbonate-galena, 1 kilometre east of headwaters of Strata Creek (MINFILE 104G-134; DBR89-298).

eval intrusion and activation of northeasterly trending faults with allied hydrothermal activity. The vein systems are controlled by brittle shear zones conjugate to the regional structural trends.

SCUD GLACIER AREA

The Otis and Moped showings are gold-bearing arsenopyrite-quartz stockworks and veins along a west-striking, north-dipping fault zone (Johnson and Jones, 1990a, b, c). In addition to the veins, two modes of possible porphyry-style mineralization have been identified; lenses and fracture fillings of massive chalcopyrite, bornite and pyrite, and disseminated chalcopyrite in mafic tuff (*ibid.*). The Alicia occurrence (previously known as the "North Scud"; Gale, 1964) lies on the west side of the Scud Glacier; it appears to be an extension of the Otis and Moped mineralized zone (Johnson and Jones, 1990a, b, c). On the east side of the glacier and around Middle Scud Creek, narrow and discontinuous quartz - iron carbonate veins carrying chalcopyrite, tetrahedrite and pyrite cut metavolcanic rocks (Photo 5-5).

LIMPOKE GLACIER AREA

A quartz-sulphide boulder train was traced by Cominco Ltd. from the Limpoke Creek valley to the southern edge of the Limpoke Glacier where three types of mineralized boulders were identified: quartz-sulphide, massive pyrrhotite-pyrite-chalcopyrite-sphalerite-galena, and zinc-bearing quartz-carbonate (MINFILE 104G 149; Westcott, 1989b). Geochemical and geophysical surveys, geological mapping programs and four diamond-drill holes have been completed along the south side of the glacier (Aspinall *et al.*, 1990, Aspinall, 1991).

EOCENE

PENDANTS IN THE STRATA GLACIER PLUTON

Stuhini Group roof pendants in the Early Jurassic Strata Glacier pluton host several polymetallic quartz-carbonate vein showings (Table 5-1: Gu, Gu North, Marg West and Marg East; MINFILE 104G 075, 084, 058 and 089). The occurrences are located just east of a major north-trending felsic dike swarm of probable Eocene age, that extends from the headwaters of Navo Creek to Strata Creek. Felsic dikes crop out near the Marg showings. Mineralization consists of pyrite, chalcopyrite, molybdenite, sphalerite, galena and scheelite in sheared and silicified zones. The proximity of the felsic dike swarm and the presence of tungsten mineralization suggest that these showings are Eocene in age.

NORTH OF THE STRATA MOUNTAIN PLUTON

Scattered vein mineralization occurs in Hazelton Group and Stuhini Group volcanics north and east of the Middle Jurassic Strata Mountain pluton (Table 5-1: Fossil Vein, Dikes, Captain, Forgotten; MINFILE 104G 128, 131, 132, 133; Photo 5-6a, b). Felsic dikes of probable Tertiary age have been mapped near the Captain and Fossil Vein showings. Further, lead isotopes from the Forgotten vein plot in the Tertiary cluster of Godwin *et al.* (1991), suggesting a possible Eocene age for mineralization in this district.

A larger north-trending belt of Tertiary mineral showings can be defined parallel to the Navo Creek - Strata Creek dike swarm, and extending as far north as Mount Helveker, which is capped by Sloko Group volcanics. The dike swarm suggests the possibility that Sloko Group rocks were deposited along the entire length of this belt, and subsequently eroded south of Mount Helveker. Mineralization in the sub-Sloko basement consists of transitional veins, with higher level epithermal mineralization having been removed by erosion.

EPITHERMAL VEIN DEPOSITS

Given their high-level setting, epithermal deposits tend to be associated with specific stratigraphic intervals and volcanic facies rather than with particular intrusive episodes.



Photo 5-5. Narrow (10 cm), north-trending quartz - iron carbonate breccia zone containing minor chalcopyrite, malachite and green mica hosted by Stuhini mafic volcanic rocks. Listwanite alteration is common in Stuhini Group mafic volcanic rocks (DBR88-187).

Although no epithermal systems have been described in the map area, regional considerations suggest the potential for epithermal gold associated with Jurassic and Eocene rocks. The Skukum deposit, south of Whitehorse, is hosted by Eocene intermediate to felsic volcanic rocks correlative with the Sloko Group. Numerous small deposits occur in dominantly subaerial andesitic to dacitic volcanics of the Early Jurassic Hazelton Group in the Toadoggonne district, east of the Bowser Basin. In the Iskut River district, epithermal systems are found in Hazelton Group volcanics in the Treaty Glacier area, and the Eskay Creek deposit (Figure 5-1) has affinities with both volcanogenic massive sulphide and epithermal systems.

Although none of the vein systems in the project area can be classified as epithermal, prospective Jurassic and Eocene stratigraphy covers a limited area north of Strata Creek. Structural levels south of Strata Creek and north of the Stikine River are probably too deep for Jurassic and younger epithermal mineralization.

VOLCANOGENIC MASSIVE SULPHIDE DEPOSITS

In northern Stikine Terrane, Kuroko deposits are known to occur in Devonian-Mississippian and Jurassic arc sequences. The Tulsequah Chief deposit, in the Taku River area (Figure 5-1), is associated with Early Mississippian rhyolite of the Stikine assemblage (J. Mortensen, written communication, 1992). At Eskay Creek, Early to Middle Jurassic volcanics of the Hazelton Group host gold-rich massive sulphides near the stratigraphic transition from an active volcanic arc to a starved basin setting (Anderson and Thorkelson, 1990).

No volcanogenic massive sulphide occurrences are known to occur in Stikine assemblage or Hazelton Group in the project area. However, gold-bearing massive sulphide pods occur in the Stuhini Group on the Goat claims, north of Tuffa Lake in the headwaters of Cave Creek (MINFILE 104G121). They contain pyrrhotite with minor chalcopyrite and gold assays up to 40 g/t (Strain, 1981; Korenic, 1982a). Other styles of mineralization on the claims include quartz-carbonate veins with pyrite, arsenopyrite and chalcopyrite and pluton-hosted massive magnetite pods (Lehtinen, 1989; Van Angeren, 1991).

SKARN DEPOSITS

Widespread carbonate-rich volcanic-sedimentary sequences intruded by dioritic to granitic plutons suggest the potential for significant skarn mineralization in northern Stikine Terrane. The best known example is the McLymont northwest zone, south of the project area, an oxidized (retrograde) gold-bearing skarn in Carboniferous Stikine assemblage tuffs and sediments (Ray *et al.*, 1991).

Several copper-iron and polymetallic skarn showings occur in Paleozoic and Upper Triassic volcanic and carbonate sequences in the project area. The main clusters of skarn mineralization are copper skarns related to the Tahltan Lake pluton and polymetallic skarns in the Devils Elbow area.

TAHLTAN LAKE

The Tahltan Lake copper skarns (MINFILE 104G 081, 082) and the newly discovered Mag skarn are hosted by Stuhini Group tuffaceous sedimentary rocks intruded by diorite to granodiorite plutons of probable Late Triassic age. At Tahltan Lake, skarn occurs over an area 400 metres wide by 800 metres long (Marud, 1990a). Sulphide-bearing zones are 1 to 2 metres wide and up to 5 metres long. The northern part of the skarn contains specular hematite and the southern part is principally magnetite with minor pyrite (D. Marud, personal communication, 1991). This change from reduced conditions close to the intrusion to more oxidized conditions farther from the contact is analogous to the Craigmont deposit (Rennie, 1962; Morrison, 1974).

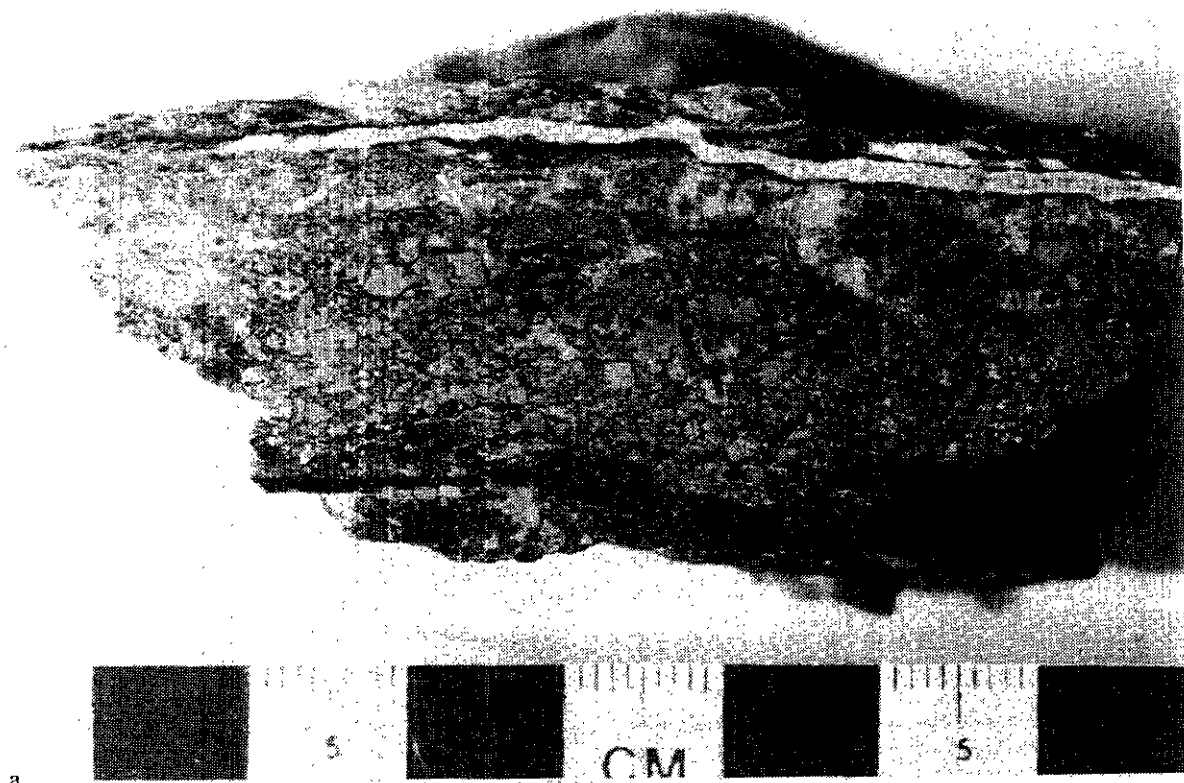
DEVILS ELBOW

Polymetallic skarns at the Devils Elbow, Apex and Drapich showings (Table 5-1: MINFILE 104G 12, 13, 11) occur in Paleozoic volcanic and sedimentary rocks just east of the Eocene Sawback pluton. The Lucky Strike, located southwest of the Drapich showing near the Sawback pluton, is a polymetallic transitional quartz-vein showing. The Devils Elbow showing contains scheelite in discontinuous lenses of disseminated sphalerite, galena, chalcopyrite, pyrite and pyrrhotite that are up to 15 metres long and 1.5 metres wide. It is hosted by Upper Carboniferous Stikine assemblage limy siltstone, argillite and limestone intruded by Middle Jurassic(?) hornblende granodiorite (Dunn, 1990; Keep, 1983; Webster and Ray, 1991). The showings have been intermittently explored from about 1910 to the present. In 1915 numerous trenches and three adits were driven (90 m long at 603 m elevation, 18 m at 648 m, and 6 m at 672 m; Kerr, 1948a). In 1952, tungsten ore was mined but never shipped, and additional prospecting was conducted in 1970, 1982 and 1989 (Lloyd, 1989). In 1990 the Northair Group prospected and mapped the area; Dunn (1990) concluded that the skarns were small and contained little gold. Lead from the Devils Elbow showing plots within the Tertiary cluster of Godwin *et al.* (1991), suggesting a genetic link to the Sawback pluton, and confirming the link between Tertiary systems and tungsten mineralization, as inferred above in the discussion of Eocene transitional vein deposits.

At the Drapich showing, sheared massive sulphide and garnetite skarn is developed in Permian(?) Stikine assemblage limestone intruded by Middle Jurassic(?) hornblende granodiorite. Two adits (20 m and 8 m long) were driven along the mineralized contact in the 1930s. Sulphides include pyrite, pyrrhotite, chalcopyrite, sphalerite and minor galena. The showing was resampled in 1988 (Davis, 1988).

SCUD RIVER

A number of vein and skarn showings have been discovered in a northwest-trending belt northeast of the Perekleshin pluton, in the Scud River area (Table 5-1: Oksa Gold, Snow, Cos, Jameson, JD-1, JD-3 and CB-1, CB-2; MINFILE 104G140, 139, 062, 138, 141). Most of these are recently discovered occurrences, consisting of gold and silver-bearing quartz veins in Stikine assemblage sedimentary and volcanic rocks, with pyrite, pyrrhotite, chalcopyrite, sphalerite and galena. The Split zone, in skarn-altered



a



b

Photo 5-6. (a) Pyrite euhedra within iron carbonate quartz vein, immediately west of Strata Mountain (MINFILE 104G-132; DBR89-382), note undeformed nature in contrast to (b). (b) Ductile and brittle deformation in quartz-pyrite-chalcopyrite vein, west-northwest of Strata Mountain (MINFILE 104G-133; DBR89-277-2).

argillite along the contact with a granodiorite intrusion, comprises massive to weakly banded pyrite, pyrrhotite, sphalerite, chalcopyrite and minor galena (Kushner, 1991). Outwash boulders of garnet-actinolite skarn found at the headwaters of Rugose Creek contain disseminated to massive pyrite, magnetite, pyrrhotite and minor chalcopyrite. The Rugose Glacier covers the contact where granodiorite cuts Early Permian limestone, the probable source area for the float. Geochemical analyses of samples from these boulders are included in Appendix 14 and Ross (1989). These showings may be related to the Early Jurassic Pereleshin pluton or the Cone Mountain pluton. The Cos showing is a copper skarn developed at the contact of the Pereleshin pluton with Stikine assemblage limestone. A genetic link between the pluton and proximal skarn and distal vein showings is likely.

OTHER DEPOSIT TYPES

PLACER GOLD

Placer gold accumulations in gravels immediately south of the Barrington River canyon (MINFILE 104G008) have been worked intermittently since the late 1920s. Reported gold recovery in 1933 was 3.1 kilograms, and 6.8 kilograms in 1935 (B.C. Minister of Mines Annual Reports 1933, 1935). More recently, Barrington Gold Ltd. purchased the placer claims from Integrated Resources Ltd. and now mines the deposit on a seasonal basis. Test mining in 1990 produced 12.4 kilograms of gold from about 36 000 cubic metres of gravel (Integrated Resources Ltd., News Release, October 21, 1991). The gold occurs as flakes that are 5 millimetres in diameter and smaller. The lode source of the gold is thought to lie within the Barrington River or Limpoke Creek watersheds, probably associated with marginal phases of the Limpoke pluton.

STRATABOUND URANIUM

Uranium occurrences on the Hel claims (MINFILE 104G109) are hosted by Sustut Group conglomerate and sandstone near Mount Heleveker. They occur as secondary minerals in conglomerate, as radioactive coaly fragments in sandstone, and as radioactive Sloko Group trachyte talus (Bell, 1981). The source of the uranium is thought to be Sloko Group volcanic rocks which lie 20 to 30 metres above the main showing. Uranium may have been leached from the Sloko Group by migrating groundwater and precipitated on organic-rich material as secondary uranium minerals (Bell, 1981; Salat and Noakes, 1979).

CUMULATE MAGNETITE

The Shakes Creek cumulate iron occurrence (MINFILE 104G026) consists of a magnetite-rich clinopyroxenite (Latimer Lake pluton) that intrudes Stuhini Group tuffaceous siltstone and andesite. Intercumulate and cumulate magnetite averages 13 to 19% of the clinopyroxenite (McIntyre, 1966). The property was trenched and drilled in the late 1960s. At this time a bulldozer trail was established from Glenora on the Stikine River to the iron deposit, however, it has since been overgrown.

TIMING OF REGIONAL METALLOGENIC EVENTS

Regional metallogenic analysis supports links between a number of metallogenic events and specific stratigraphic intervals and intrusive episodes. By far the most significant metallogenic period spans the Late Triassic to Middle Jurassic (about 203-175 Ma).

PALEOZOIC: VOLCANOGENIC MASSIVE SULPHIDE DEPOSITS

Paleozoic arc rocks containing felsic volcanic sequences and associated Kuroko-type volcanogenic massive sulphide deposits are widely distributed in "McCloud belt" terranes (Miller, 1987; Brown *et al.*, 1991). In northern Stikine Terrane, the Tulsequah Chief and Big Bull deposits are the most significant examples. Tulsequah is probably of Devonian-Mississippian age; rhyolite in the footwall yielded a zircon U-Pb date of 350.6 ± 14.7 -6.2 Ma (J.K. Mortensen, in Sherlock *et al.*, 1994). Felsic arc volcanics are also regionally prominent in Upper Carboniferous to Lower Permian sequences, although no VMS showings of this age have been found. Elsewhere in the McCloud belt, Lower to Middle Devonian bimodal volcanics in the eastern Klamath Terrane of northern California (Copley greenstone and the Balaklala rhyolite) formed in an extensional arc setting and host several deposits (Lapierre *et al.*, 1985).

LATE TRIASSIC TO JURASSIC PORPHYRY DEPOSITS AND TRANSITIONAL TO EPITHERMAL VEINS

Upper Triassic Stuhini Group volcanics and Late Triassic to Early Jurassic Copper Mountain suite alkalic intrusive complexes host significant porphyry copper-gold deposits like Galore Creek. At Galore Creek, K-Ar dates for hydrothermal biotite associated with mineralization range from 177 to 201 Ma (White *et al.*, 1968). Lack of zircons has thwarted attempts to date the Galore trachytes by U-Pb techniques. It is probable that the age of emplacement of the Galore intrusions is closer to the older biotite alteration dates. This is supported by a 204 ± 10 Ma K-Ar date from the Pereleshin pluton, believed to be coeval with the Galore intrusions. The Rugged Mountain pluton has geochemical similarities and may be coeval, although no dating has been done. Possible alkalic porphyry systems peripheral to the Limpoke pluton may be younger, if they are related to syenitic intrusions that cut the pluton, which has an emplacement age of 194 ± 2 Ma (Brown *et al.*, 1992c; Appendix 13).

Early Jurassic Texas Creek suite alkaline to calcalkaline magmatism is associated with a broad spectrum of deposits in the Stewart-Iskut belt, including porphyry copper-gold (Kerr), transitional veins (Premier, Sulphurets, Snip, Stonehouse) and high-sulphidation epithermal systems (Treaty Glacier). The association of precious metal mineralization with more alkaline intrusions is well documented (Barr *et al.*, 1976). A well dated example is the Premier mine, where Premier Porphyry dikes have been dated at 194.8 ± 2 Ma by U-Pb on zircon (Alldrick *et al.*, 1986). In the project area, vein and skarn mineralization related to the Early Jurassic magmatic event is found primarily in older rocks, suggest-

ing a lower structural level at the time of mineralization. Examples include the Scud River area, where veins in Paleozoic sequences may be genetically related to the Early Jurassic Pereleshin pluton. Younger, Early Jurassic mineralization related to plutons of the Cone Mountain suite (187-180 Ma) is suggested by the proximity of polymetallic vein systems to the Strata Glacier pluton.

EARLY TO MIDDLE JURASSIC: VOLCANOGENIC MASSIVE SULPHIDE DEPOSITS

Early to Middle Jurassic metallogeny of the Iskut camp also includes volcanogenic massive sulphide deposits, with Eskay Creek being the outstanding example. Farther south, in the Hazelton Group of the Alice Arm area, silver-rich lead-zinc-barite deposits of the Dolly Varden camp have also been interpreted as Early Jurassic volcanogenic exhalites (Devlin and Godwin, 1986). Analogous mineralization has not been discovered in the Stikine project area, reflecting the relatively limited exposure of the Hazelton Group.

MIDDLE JURASSIC: CALCALKALINE PORPHYRY DEPOSITS AND TRANSITIONAL VEINS

Secondary biotite from Schaft Creek yielded a 185 ± 5 Ma K-Ar age (Panteleyev and Dudas, 1973), which overlaps the range of K-Ar dates for Galore Creek; in addition, the error is in the range of dates for the Middle Jurassic Yehiniko pluton. The significance of this date is therefore unclear. Although the Middle Jurassic Three Sisters suite is not regionally known for significant associated mineral deposits, synmineral felsic dikes at Schaft Creek may be related to the Yehiniko pluton. Other possible Middle Jurassic examples in the project area include prospects along the Yehiniko fault zone, and vein systems close to the Conover pluton.

EOCENE: EPITHERMAL TO TRANSITIONAL VEINS, PORPHYRY MOLYBDENUM-COPPER DEPOSITS

Epithermal gold mineralization is known in the Eocene Skukum Group volcanics in the southern Yukon; correlative Sloko Group volcanics extend as far south as Mount Helveker in the project area. Extensive Eocene dike swarms, intruding Jurassic and older rocks south of Strata Creek, suggest that the higher level manifestations of Eocene mineralization have been eroded in the project area. Within this north-trending belt, tungsten-bearing polymetallic transitional vein mineralization has been interpreted to be related to Eocene magmatism. The style of mineralization reflects a deeper, subvolcanic structural level. Porphyry-style molybdenum-copper-silver showings at the Ben prospect are further evidence of Eocene mineralization.

GALENA-LEAD ISOTOPE RESULTS

Galena-lead isotope data from the Stewart-Iskut area define two main clusters which loosely fingerprint Jurassic and Tertiary ages of mineralization (Godwin *et al.*, 1991). Interpretation of Pb-Pb cluster ages is based on comparison

with deposits for which K-Ar, U-Pb or biostratigraphic dates are available. Resolution of the Pb-Pb data does not discriminate between Early and Middle Jurassic, or Jurassic and Late Triassic events, but does provide good discrimination between Triassic-Jurassic and Tertiary events. Galena from five showings in the project area can be compared with the Pb-Pb fingerprints developed for the Stewart-Iskut belt (Figure 5-3; Appendix 15).

Lead from the Plum and Player transitional veins falls within the Jurassic cluster, consistent with a genetic link to the nearby Strata Glacier pluton, which is part of the Early Jurassic Cone Mountain suite. Vuggy quartz-sulphide (epithermal?) vein float sampled in Deeker Creek (sample 113) within the Eocene Sawback pluton, falls within the Tertiary cluster, consistent with its geologic setting. Lead signatures from two other showings are more problematic. The Forgotten showing, another transitional vein, is immediately east of the Strata Mountain pluton but plots in the Tertiary cluster, suggesting that an unmapped Tertiary intrusion may be the heat source for this system. The Devils Elbow skarn showing is spatially associated with the Devils Elbow plu-

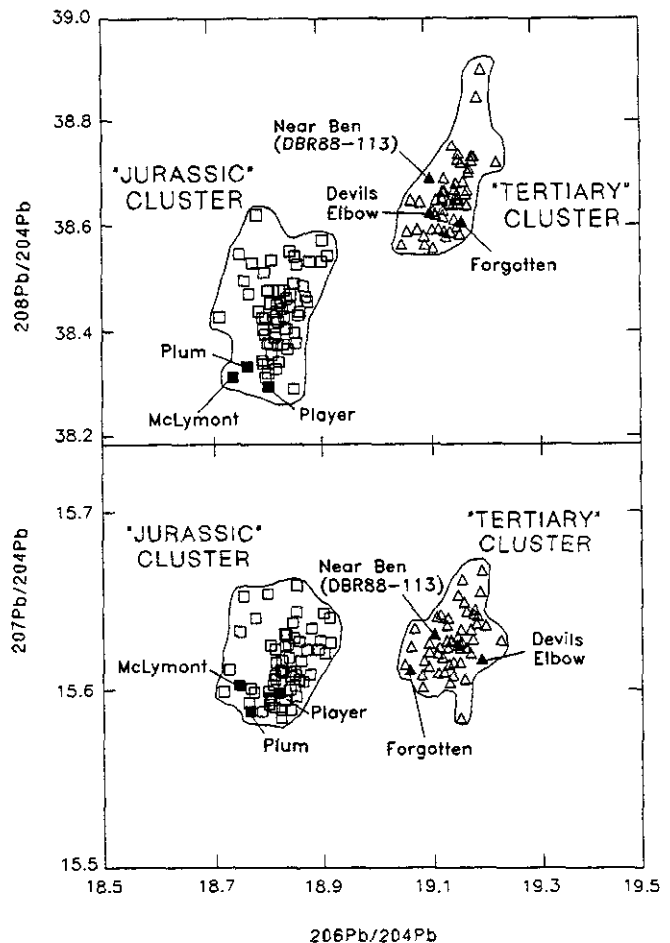


Figure 5-3. Five new galena lead isotope signatures for mineral showings in the project area (solid black symbols) relative to the two clusters of Godwin *et al.* (1991) that were derived for deposits in the Stewart - Iskut area. Includes date for Devils Elbow from I.C.L. Webster (personal communication, 1990) and McLymont Creek data from A.D. Ettlinger (personal communication, 1991).

ton, believed to be Middle Jurassic in age. Its lead signature also plots in the Tertiary cluster, suggesting either that mineralization is genetically related to the Eocene Sawback Pluton, which crops out a kilometre to the west, or that the Devils Elbow pluton is younger than presently interpreted.

EXPLORATION ACTIVITY

Exploration focused on porphyry deposits in the 1960s and 1970s. This resulted in widespread activity centred on the Galore Creek and Schaft Creek discoveries. Following a lull from the late 1970s until the mid-1980s, gold-related exploration activity increased dramatically. Spurred by the July 1987 release of Regional Geochemical Survey data and exploration successes in the Stewart-Iskut and Toadoggone camps, companies returned to the Telegraph Creek map area. The amount of unstaked ground in the region compared with almost complete claim coverage in the "Golden Triangle" to the south also provided opportunities.

Preliminary property work and regional prospecting were completed by Cominco Exploration Limited, Homestake Mineral Development Company, Equity Engineering Limited, Coast Mountain Geological Services Limited, Hi-Tec Ltd. and Teck Corporation. Integrated

Resources' Barrington River placer operation had intermittent production during this time (no production statistics are available).

MINERAL POTENTIAL

During the mapping project 133 grab samples were collected to characterize mineral occurrences. They were analysed for precious and base metals and pathfinder elements (Appendix 14). Mineral potential is varied but remains incompletely tested because the area is remote and rugged (Table 5-2). Several areas of regional geochemical anomalies and newly discovered small showings warrant further exploration and evaluation. Contact zones around Limpoke pluton remain exploration targets with silicified and pyritized float and placer gold known nearby. The syenite dike swarm and associated limonitic alteration zones hold potential for porphyry mineralization. Prominent rusty, pyritic alteration zones north of Devils Elbow Mountain could host copper-gold skarns. Local areas of Stuhini Group submarine felsic volcanic rocks are a favourable setting for massive sulphide deposits. Early Jurassic alkaline plutons and sub-volcanic intrusions remain prime targets for gold exploration.

TABLE 5-2
SUMMARY OF DEPOSIT TYPES AND MINERAL
POTENTIAL SETTINGS IN THE PROJECT AREA

Model	Northern B.C. Examples	Area With Potential
Calcalkaline porphyry copper-molybdenum	Schaft Creek, Red Chris	Early-Middle Jurassic calcalkaline intrusions and peripheral volcanic sequences
Alkaline porphyry copper-gold	Galore Creek Kerr	Early Jurassic K-feldspar megacrystic porphyry intrusions
Porphyry molybdenum-silver	Alice Arm, Adanac	Eocene intrusions
Transitional/mesothermal veins (Au ± Ag, Cu, Zn, Pb)	Snip, Premier, Johnny Mountain, Golden Bear	Early Jurassic K-feldspar megacrystic intrusions, shear zones
Epithermal veins (Au, Ag)	Mount Skukum, Toadoggone, Premier(?), Treaty Glacier	Sloko Group, Hazelton Group
Volcanogenic massive sulphide: Kuroko-type (Cu, Zn, Pb, Au, Ag)	Tulsequah Chief Eskay Creek	Devonian-Permian Stikine assemblage Hazelton Group (Mount Dilworth and Salmon River formations)
Skarns (Au, Cu, Zn-Pb, W)	McLymont Creek	Widespread (mixed carbonate-volcanic sequences intruded by plutons)
Stratabound uranium		Sustut Group
Coal	Tuya River coalfield	Sustut Group
Placer gold	Barrington River, Dease Lake, Cassiar	Barrington River

CHAPTER 6

SUMMARY AND CONCLUSIONS

The following conclusions stem from the four field seasons of mapping in the western Telegraph Creek map area. The general stratigraphic sequence, intrusive episodes and deformational events are illustrated on Figure 6-1. The map area is underlain by Carboniferous to Permian Stikine assemblage strata unconformably overlain by unnamed Lower and Middle Triassic sedimentary rocks in isolated localities and by extensive Upper Triassic volcanic rocks of the Stuhini Group. Lower Jurassic volcanic rocks correlated with the Hazelton Group lie unconformably on the Stuhini Group in one area. They, in turn, are overlain unconformably by Upper Cretaceous to Paleocene polymictic conglomerate tentatively included in the Sustut Group. Eocene pyroclastic volcanic rocks and associated sills/flows cap the succession. Five new U-Pb and six new K-Ar dates, together with numerous macro and microfossil age determinations, help refine the stratigraphic successions.

Paleozoic rocks of the Stikine assemblage span about 65 Ma in the study area, older Devonian strata, as found in the Forrest Kerr Creek area, are unrecognized here. The as-

semblage, with no exposed base, is divided into Upper Carboniferous tholeiitic volcanic rocks and sedimentary rocks both containing discontinuous limestone intervals (Devils Elbow and Butterfly units), Upper Carboniferous to Lower Permian felsic tuff (Navo formation), thick Permian limestone (Ambition Formation) and tuff, wacke and chert (Scud Glacier formation). The deposition of Early Permian limestone worldwide has no strictly valid modern analogues because many Paleozoic reef builders are now extinct (Kennett, 1982). These shallow-water carbonate accumulations, like the Ambition Formation, were very important in the global carbonate budget before 100 Ma, before deep-sea carbonate-secreting organisms (planktonic foraminifera and calcareous nannoplankton) developed (ibid). The thick accumulation of open-marine limestone suggests a relatively stable tectonic setting for at least 30 Ma. The low-diversity fauna was dominated by benthic organisms. By the Upper Permian, interbedded tuff, representing local calalkaline pyroclastic volcanism, and chert and argillite were deposited.

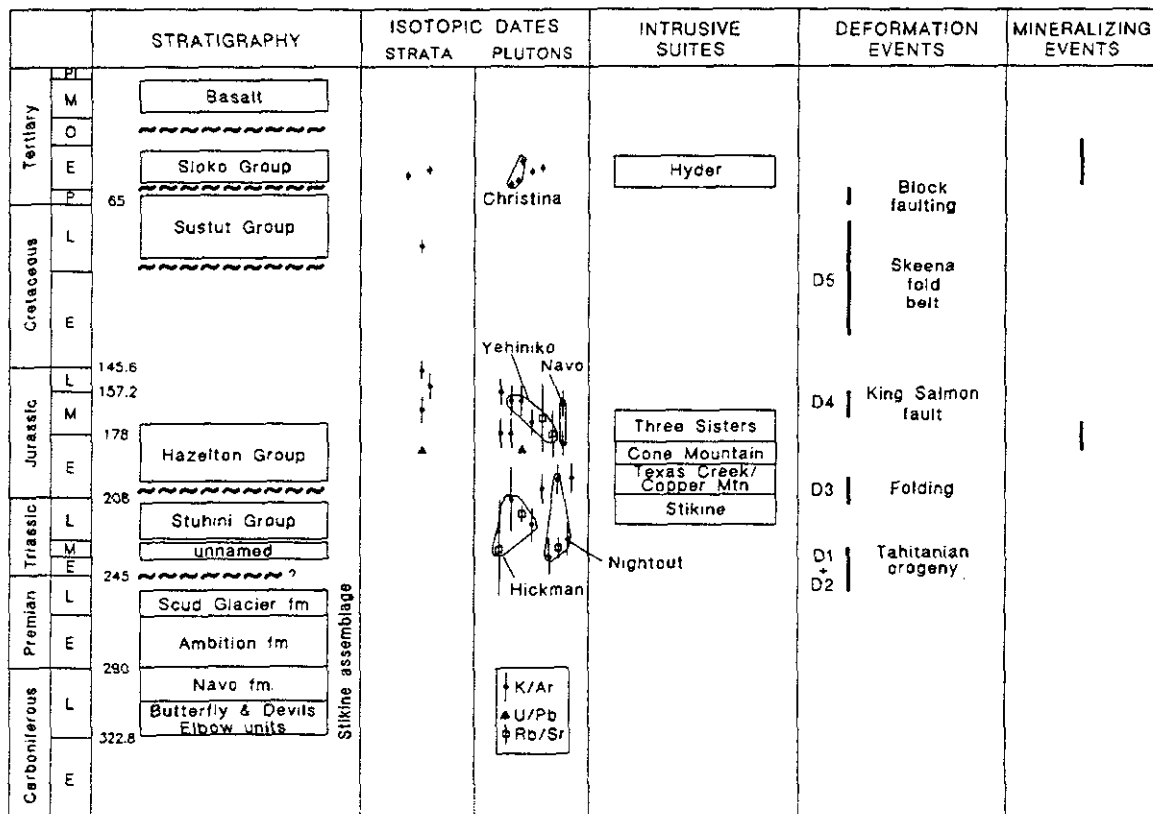


Figure 6-1. Summary of stratigraphic, intrusive, structural and mineralizing events for western Telegraph Creek map area. Isotopic data from Holbek (1988) and White et al. (1968) is included.

Lower and Middle Triassic siltstone, argillite and impure limestone occur as isolated and rare exposures between the Stikine assemblage and Upper Triassic Stuhini Group.

The Upper Triassic (Stuhini Group) records the establishment of extensive submarine arc volcanism with local subaerial conditions and reworking of material by fluvial processes. Coarse breccias indicate significant relief and the diverse clast compositions suggest unroofing of the plutons (e.g. Hickman pluton) synchronous with erosion of the Triassic volcanic pile and some of the Paleozoic strata. The composition of the flows varies from tholeiitic to calcalkaline. Some of the volcanic rocks have shoshonitic affinity and they commonly contain large augite phenocrysts. The group is divided into several sedimentary and volcanic-dominated facies with Carnian and Norian fossil ages. By the late Norian there was a lull in volcanism and a marine transgression.

An angular unconformity between Upper Triassic strata and Lower to Middle Jurassic Hazelton Group rocks is locally apparent. Folded Norian siltstone and argillite are overlain by subhorizontal Toarcian or older flows in an exposure west of Yehiniko Lake. Interfingering marine and subaerial volcanic rocks comprise this Hazelton Group outlier. Buff-weathering limy wackes with ammonites, belemnites and *Weyla* fragments illustrate shallow-marine conditions for part of the succession. Nearby, subaerial maroon-weathering hornblende-plagioclase-phyric flow-banded dacite and andesite are Toarcian or older. These strata are overlain by submarine amygdaloidal basalt (possibly Bajocian) with interpillow carbonate.

Middle to Upper Jurassic Bowser Lake Group and Cretaceous Skeena Group and lower Sustut Group characterize the northeastern Skeena fold belt, but are absent in the study area, either due to nondeposition or erosion. Upper Cretaceous to Paleocene alluvial fan deposits of the Brothers Peak Formation (Sustut Group) lie unconformably on the Hazelton and Stuhini Groups. The polymictic fanglomerates mark a major erosional event, probably related to uplift of the Coast Belt. The braided alluvial fans also had local boggy sections where coal seams developed. In addition, episodic pyroclastic volcanism blanketed the area with felsic ash tuff. Eocene magmatism is represented by an isolated outlier of Sloko Group continental arc volcanic rocks, and large coeval batholiths that form much of the Coast Belt at this latitude. Flat-lying basalt flows near Latimer Lake are correlated with Neogene volcanic rocks from either the Mount Edziza Complex to the east or Level Mountain shield volcano to the north.

PLUTONISM

Seven new U-Pb and fourteen new K-Ar age determinations help define eight plutonic suites emplaced during six episodes: Middle to Late Triassic, Late Triassic to Early Jurassic, Early Jurassic, a new late Early Jurassic, Middle Jurassic and Eocene plutonic suites. Two groups of Middle to Late Triassic plutons are defined: small, isolated Alaskan-type ultramafic bodies (Mount Hickman Ultramafic Complex and two smaller bodies) and much larger Stikine suite calcalkaline plutons (e.g. Hickman batholith), both of

which are coeval and probably comagmatic with Stuhini Group volcanism. Late Triassic to Early Jurassic alkaline plutons (Copper Mountain suite) have ultramafic and syenite phases and include the Rugged Mountain pluton and Butterfly pluton in the study area and the Galore Creek intrusions with associated Cu-Au mineralization immediately to the south. The Early Jurassic event, genetically related to vein deposits in the Stewart-Iskut area, comprises the Texas Creek suite with large, calcalkaline heterogeneous plutons (e.g. Limpoke pluton). A new, late Early Jurassic intrusive suite has been proposed based on data for the Cone Mountain pluton; these plutons are coeval with part of the Hazelton Group volcanism. Middle Jurassic plutons (Three Sisters suite) includes the Yehiniko pluton that is bordered on the north and south by Late Triassic plutons. The lack of Cretaceous plutons and volcanic rocks in the area reflects a prominent magmatic hiatus. Much of the western part of the map area is underlain by Eocene plutons of the Hyder suite, with extrusive equivalents represented by the Sloko Group. The chemistry of the plutons shows a temporal progression from metaluminous, low-silica quartz diorite to granodiorite in the Late Triassic to more evolved peraluminous granite by the Middle Jurassic and Eocene.

STRUCTURE

The study area lies between three regionally extensive fault systems: King Salmon fault (100 km north), Sumdum-Fanshaw fault (75 km southwest), and Skeena fold belt (125 km east). In this area, four episodes of deformation are defined: pre-Late Triassic contraction (D₁), and structural culmination development (D₂, Tahltanian orogeny); post-Late Triassic to pre-Toarcian contraction (D₃); and Middle Jurassic to Cretaceous contraction (D₄). The earliest episode was synmetamorphic and produced chlorite-sericite foliation (S₁) and rare isoclinal folds (F₁) in Carboniferous rocks. S₁ was folded during D₂ into open to tight chevron style folds (F₂). Evidence for the timing of D₂ remains equivocal. Open folds, overturned bedding and reverse faults, possibly northeast directed, developed during D₃, and the younger age limit is an angular unconformity at the base of the Lower Jurassic Hazelton Group. D₄ produced crenulations in phyllitic Carboniferous strata, tight folds in Permian limestone and mylonitic foliations of a late Early Jurassic Cone Mountain pluton. The paucity of Jurassic or younger strata prevents unequivocal assignment of features to specific deformational episodes.

The contrast in structural trends of Paleozoic and Triassic strata is noteworthy. North of the Stikine River, folds and faults trend northeast and east, but to the south, they trend north and northwest. The orientations of Permian limestone massifs delineate these trends most clearly. They are partially controlled by contraction faults (e.g. Cone Mountain and Jimjack faults). The bend from northwest to east-trending southwest of the Chutine River remains enigmatic, partly because the closure is intruded by an Eocene pluton. Four structural culminations (Little Tahltan Lake, Barrington River, Chutine River and Missisjajay Creek) cored by Paleozoic strata display more penetrative fabrics than surrounding Mesozoic rocks.

In addition, several fault systems are described, including the Cone Mountain and Scud Glacier faults. The Cone Mountain fault and related structures are part of a major southwest-verging compressional event post-late Early Jurassic. North, northeast, northwest and east-trending faults are also common.

METAMORPHISM

Most rocks in the map area display greenschist grade mineral assemblages, including quartz, albite, carbonate, chlorite, epidote, clay minerals and pyrite. Primary textures are commonly preserved in most Mesozoic rocks, it is only in the Paleozoic strata that penetrative deformation has obscured original features. These penetrative fabrics developed during the first of two thermal events, a Permo-Triassic metamorphic event ("Tahltanian orogeny"). The second, a Middle Jurassic event, is postulated from partially reset K-Ar dates and coincides with emplacement of the Three Sisters Plutonic Suite.

ECONOMIC GEOLOGY

The map area lies within an important metallogenic belt encompassing active mines and past producers between Stewart and Tulsequah, British Columbia. The potential for undiscovered mineral occurrences remains very high but potential for economic deposits is probably moderate; exploration targets include: porphyry deposits in Mesozoic and Cenozoic rocks (e.g. Galore Creek, Schaft Creek and Ben showing); volcanogenic massive sulphides in the Devonian and Carboniferous part of the Stikine assemblage (e.g. Tulsequah Chief) and Jurassic Hazelton Group (e.g. Eskay Creek); shear-hosted gold (e.g. Snip mine along the Iskut River); fault-controlled mesothermal gold (e.g. Golden Bear mine); precious metal veins (e.g. Premier, Sulphurets, Skukum mine).

Alkaline and calkalkaline porphyry copper deposits and veins developed where plutons intruded active oceanic arcs during the Late Triassic (Stuhini Group) and Early to Middle Jurassic (Hazelton Group). Stuhini Group volcanic rocks and coeval subvolcanic intrusive rocks host the Galore Creek copper-gold and Schaft Creek copper-molybdenum porphyry deposits, and remain unexploited resources; improved infrastructure would facilitate their development. Eocene calkalkaline porphyry molybdenum systems are also known, for example, the Ben occurrence lies along the eastern flank of the Coast Plutonic Complex. These hydrothermal systems have potential for hosting high-grade silver veins as exploited south of Stewart.

Vein deposits are common in the Lower Jurassic Hazelton Group in the Stewart-Iskut area. The Hazelton outlier near Yehiniko Lake therefore holds potential for additional occurrences. Shear-hosted veins like the Snip deposit are small targets but the spatial (and perhaps genetic?) link to the Red Bluff potassium feldspar megacrystic porphyry provides a guide to exploration. The Rugged Mountain and Limpoke pluton areas have similar porphyries and volcano-sedimentary hostrocks and these areas remain prospective for gold-bearing veins.

Environments favourable for Kuroko-type massive sulphide deposition existed during the Devonian, Carboniferous and Middle Jurassic, when submarine arc volcanism was prevalent. Parts of the Stikine and Hazelton Group have massive sulphide potential, especially where rhyolitic volcanic rocks are deposited on more mafic flows and tuffs.

More evolved, precious metal bearing, silicic porphyry deposits and epithermal veins are associated with Eocene continental volcanism (Sloko Group) and plutonism (Hyder suite).

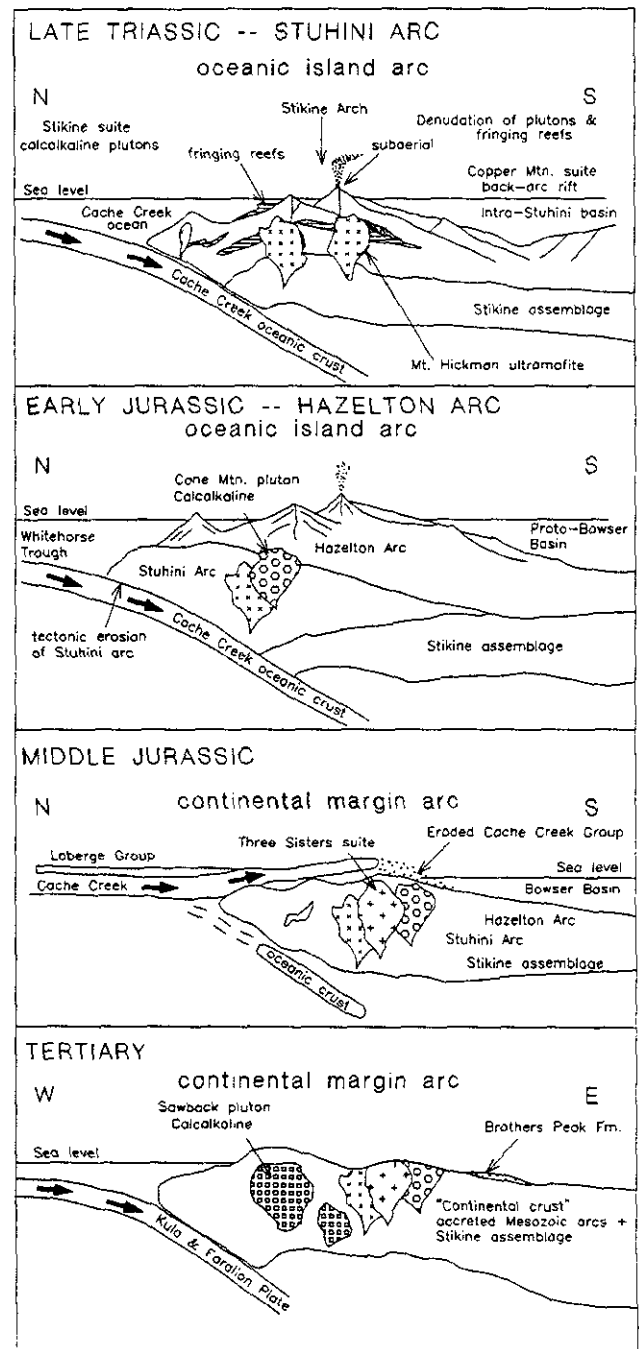


Figure 6-2. Schematic Mesozoic tectonic evolution of the project area.

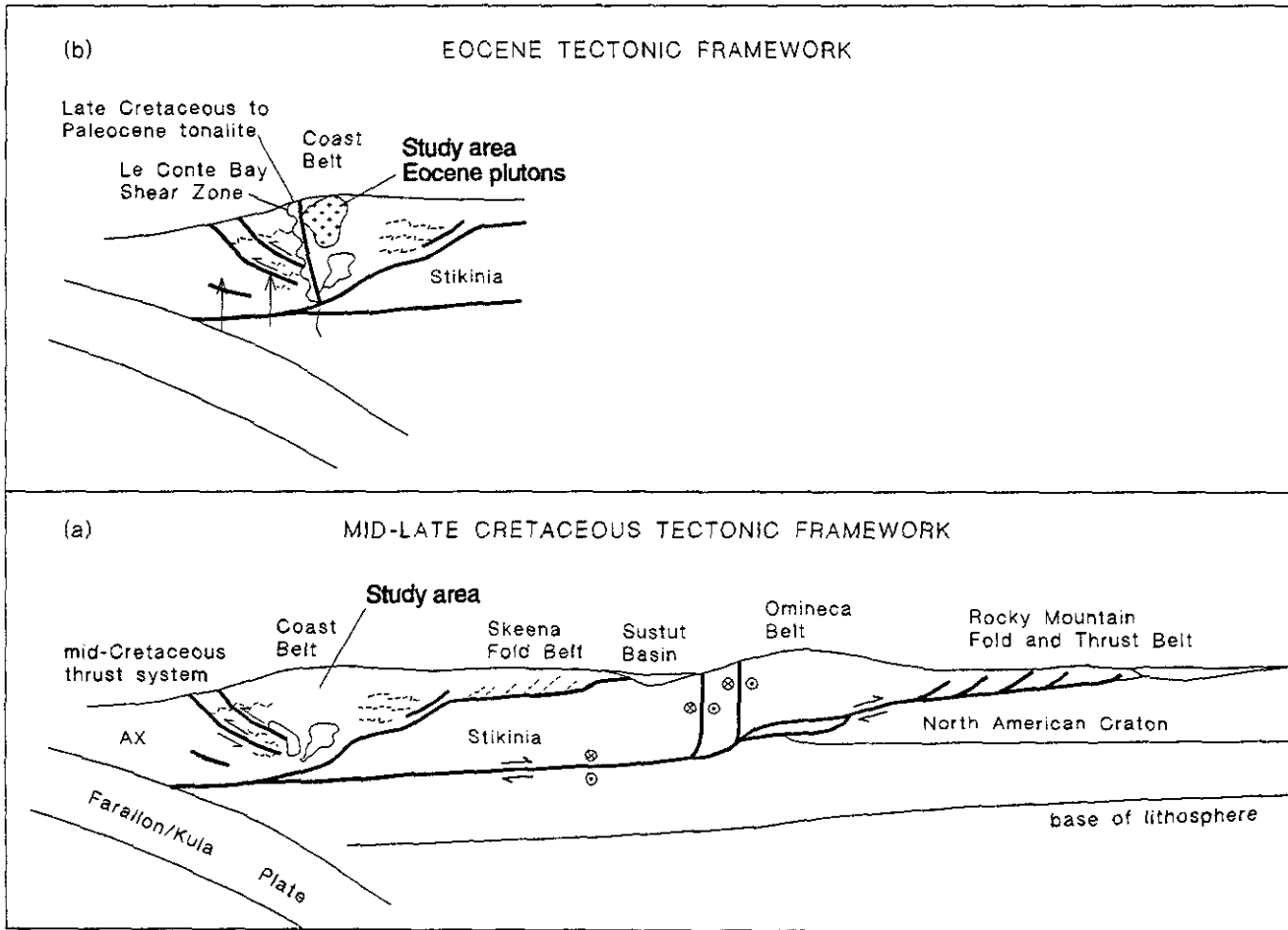


Figure 6-3. Schematic (a) Cretaceous and (b) Eocene tectonic framework for northern Cordillera with the general position of the study area illustrated (Modified from Evenchick, 1991c; McClelland *et al.*, 1991; Hollister, 1992).

TECTONIC MODEL

The Mesozoic tectonic evolution of the region is summarized in Figure 6-2. The *Stuhini* arc accumulated on a "basement" of Carboniferous and Permian strata of the *Stikine* assemblage, during subduction of the Cache Creek oceanic crust. The Early Jurassic Hazelton arc formed in a similar manner and overlapped the Triassic arc. By the Middle Jurassic the crust had thickened sufficiently to generate granite plutons (Three Sisters suite) and finally the Cache Creek ocean closed and obducted onto Stikinia. The Cretaceous record is poorly represented in the map area but is shown diagrammatically in Figure 6-3. Amalgamation of the Alexander Terrane and Wrangellia to the North American margin in the Cretaceous may link through basal décolle-

ments to the Skeena fold belt (Evenchick, 1991b, c). Ductile deformation along the Sumdum and Fanshaw fault systems may represent the underthrusting of Alexander Terrane beneath Yukon-Tanana and Taku terranes (McClelland *et al.*, 1991). At this time, the study area lay in the less deformed hinterland, between two thrust systems of opposite vergence, the Sumdum-Fanshaw and Skeena fold belt (Figure 6-3a). By the Late Cretaceous to Paleocene the Coast Range megaclineament (Le Conte shear zone) developed west of the study area; it can be traced over 800 kilometres along the west margin of the Coast Belt. The Tertiary saw renewed subduction to produce an extensive magmatic episode, the Hyder plutonic suite and extrusive equivalents, the Sloko Group (Figures 6-2 and 6-3).

REFERENCES

- Alaska Geographic Society (1979): The Stikine River; *Alaska Geographic*, Volume 6, No. 4, 94 pages.
- Alldrick, D.J., Brown, D.A., Harakal, J.E. Mortensen, J.K. and Armstrong, R.L. (1987): Geochronology of the Stewart Mining Camp; in *Geological Fieldwork 1986*, B.C. Ministry of Energy, Mines and Petroleum Resources, Paper 1987-1, pages 81-92.
- Alldrick, D.J., Mortensen, J.K. and Armstrong, R.L. (1986): Uranium-Lead Age Determinations in the Stewart Area (104B/1); in *Geological Fieldwork 1985*, B.C. Ministry of Energy, Mines and Petroleum Resources, Paper 1986-1, pages 217-218.
- Alldrick, D.J. (1993): Geology and Metallogeny of the Stewart Mining Camp, Northwestern B.C.; *B.C. Ministry of Energy, Mines and Petroleum Resources*, Bulletin 85.
- Allen, D.G., Panteleyev, A. and Armstrong, A.T. (1976): Galore Creek; in *Porphyry Deposits of the Canadian Cordillera*, Sutherland Brown, A., Editor, *Canadian Institute of Mining and Metallurgy*, Special Volume 15, pages 402-414.
- Anderson, R.G. (1983a): Geology of the Hotailuh Batholith and Surrounding Volcanic and Sedimentary Rocks, North-central British Columbia; unpublished Ph. D. thesis, *Carleton University*, 669 pages.
- Anderson, R.G. (1983b): Jurassic Magmatism in NW Stikinia and North-central Wrangellia, British Columbia; *Geological Society of America*, Abstracts with Programs, San Diego, California, page A190.
- Anderson, R.G. (1989): A Stratigraphic, Plutonic, and Structural Framework for the Iskut River Map Area, Northwestern British Columbia; in *Current Research, Part E*, *Geological Survey of Canada*, Paper 89-1E, pages 145-154.
- Anderson (1993): A Mesozoic Stratigraphic and Plutonic Framework for Northwestern Stikinia (Iskut River Area), Northwestern British Columbia, Canada; in Dunne, G. and McDougall, K., Editors, *Mesozoic Paleogeography Symposium Volume*, *Society of Economic Paleontologists and Mineralogists*, Pacific Section.
- Anderson, R.G. and Thorkelson, D.J. (1990): Mesozoic Stratigraphy and Setting for some Mineral Deposits in Iskut River Map Area, Northwestern British Columbia; in *Current Research, Part E*, *Geological Survey of Canada*, Paper 90-1E, pages 131-139.
- Anonymous (1972): Ben; in *Geology, Exploration and Mining in British Columbia 1971*, B.C. Ministry of Energy, Mines and Petroleum Resources, page 38.
- Arth, J.G., Barker, F., Stern, T.W. and Zmuda, C. (1986): The Coast Batholith, Southeast Alaska: Geochronology and Geochemistry; *Geological Society of America*, Programs with Abstracts, page 529.
- Aspinall, N.C. (1991): Assessment Report on the Drilling Program on the Poker Property; *B.C. Ministry of Energy, Mines and Petroleum Resources*, Assessment Report 21,532.
- Aspinall, N.C., Strain, D.M. and Blain, A. (1990): Assessment Report on Geological Mapping, Geochemical Sampling, Geophysical Surveying and Prospecting on the Poker Property; *B.C. Ministry of Energy, Mines and Petroleum Resources*, Assessment Report 20,724.
- Awmack, H.J. (1989): 1988 Summary Report on the JD I and II Claims; *B.C. Ministry of Energy, Mines and Petroleum Resources*, Assessment Report 18,264.
- Bamber, W.E. (1988): Report on 30 Collections of Fossils from the Scud River Area; *Geological Survey of Canada, Paleontology Subdivision*, Calgary, Report number C2-EWB-1988.
- Bamber, W.E. (1988): Report on 17 Collections of Fossils from the Telegraph Creek Area; *Geological Survey of Canada, Paleontology Subdivision*, Calgary, Report number C3-EWB-1988.
- Bamber, W.E. (1990): Report on 8 Collections of Fossils from the Scud River Area; *Geological Survey of Canada, Paleontology Subdivision*, Calgary, Report number C1-EWB-1990.
- Bapty, H. (1964): Decker Creek; in *Annual Report 1963*, B.C. Ministry of Energy, Mines and Petroleum Resources, page 8.
- Bapty, H. (1965): BIK, BUD; in *Annual Report 1964*, B.C. Ministry of Energy, Mines and Petroleum Resources, page 13.
- Barr, D.A., Fox, P.E., Northcote, K.E. and Preto, V.A. (1976): The Alkaline Suite Porphyry Deposits: A Summary; in *Porphyry Deposits of the Canadian Cordillera*, Sutherland Brown, A., Editor, *Canadian Institute of Mining and Metallurgy*, Special Volume 15, pages 359-36.
- Batchelor, R.A. and Bowden, P. (1985): Petrogenetic Interpretation of Granitoid Rock Series Using Multicationic Parameters; *Chemical Geology*, Volume 48, pages 43-55.
- Bell, R.T. (1981): Preliminary Evaluation of Uranium in Sustut and Bowser Successor Basins, British Columbia; in *Current Research, Part A*, *Geological Survey of Canada*, Paper 81-1A, pages 241-246.
- Berger, W.H. (1974): Deep-sea Sedimentation; in *The Geology of Continental Margins*, Burke, C.A., and Drake, C.L., Editors, *Springer Verlag*, New York, Heidelberg, Berlin, pages 213-241.
- Betmanis, A.I. (1978): Report on the Geology (including Prospector's Report) of the Lacasse and Schaft Claims; *B.C. Ministry of Energy, Mines and Petroleum Resources*, Assessment Report
- Bevier, M.L. and Anderson, R.G. (1991): Jurassic Geochronometry in NW Stikinia (56-57_N), British Columbia; *Geological Society of America*, Abstracts with Programs, San Diego, California, page A191.
- Bloomer, S.H., Stern, R.J., Fisk, E. and Geschwind, C.H. (1989): Shoshonitic Volcanism in the Northern Mariana Arc. I. Mineralogic and Major and Trace Element Characteristics; *Journal of Geophysical Research*, Volume 94, pages 4469-4496.
- Bradford, J.A. and Brown, D.A. (1993a): Geology of the Bearskin and Tatsamenie Lakes Area, Northwestern British Columbia (104K/1 and 8S); in *Geological Fieldwork 1992*, Grant, B. and Newell, J.M., Editors, *B.C. Ministry of Energy, Mines and Petroleum Resources*, Paper 1993-1, pages 159-176.
- Bradford, J.A. and Brown, D.A. (1993b): Geology, Mineral Occurrences and Geochemistry of the Bearskin and Tatsamenie Lakes Areas, Northwestern British Columbia (NTS 104K/1

- and 8S); *B.C. Ministry of Energy, Mines and Petroleum Resources*, Open File 1993-1, 3 sheets.
- Brew, D.A. (1988): Latest Mesozoic and Cenozoic Igneous Rocks of Southeast Alaska - A Synopsis; *U.S. Geological Survey*, Open-File Report 88-845.
- Brew, D.A., Ovenshine, A.T., Karl, S.M. and Hunt, S.J. (1984): Preliminary Reconnaissance Geologic Map of the Petersburg and parts of the Port Alexander and Sumdum 1:250,000 Quadrangles, Southeastern Alaska; *U.S. Geological Survey*, Open-File Report 84-405, 43 pages.
- Bridge, D.A., Marr, J.A., Hashimoto, K., Obara, M. and Suzuki, R. (1986): Geology of the Kutcho Creek Volcanogenic Massive Sulphide Deposit, Northern British Columbia; *Canadian Institute of Mining and Metallurgy*, Special Volume 37, pages 115-128.
- Brown, D.A. (1987): Geological Setting of the Volcanic-hosted Silbak Premier Mine, Northwestern British Columbia; unpublished M.Sc. thesis, *The University of British Columbia*, 216 pages.
- Brown, D.A. (1993): Geology of the Tahltan Lake Area, Northwestern British Columbia (104G/13); *B.C. Ministry of Energy, Mines and Petroleum Resources*, Geoscience Map 1993-6.
- Brown, D.A. and Greig, C.J. (1990): Geology of the Stikine River - Yehiniko Lake Area, Northwestern British Columbia (104G/11W, 12E); in *Geological Fieldwork 1989*, *B.C. Ministry of Energy, Mines and Petroleum Resources*, Paper 1990-1, pages 141-151.
- Brown, D.A. and Gunning, M.H. (1989a): Geology of the Scud River Area, Northwestern British Columbia (104G/5,6); in *Geological Fieldwork 1988*, *B.C. Ministry of Energy, Mines and Petroleum Resources*, Paper 1989-1, pages 251-267.
- Brown, D.A. and Gunning, M.H. (1989b): Geology and Geochemistry of the Scud River Area, Northwestern British Columbia (104G/5,6); *B.C. Ministry of Energy, Mines and Petroleum Resources*, Open File 1989-7.
- Brown, D.A. and Gunning, M.H. (1993a): Geology of the Scud River Area, Northwestern British Columbia (104G/5); *B.C. Ministry of Energy, Mines and Petroleum Resources*, Geoscience Map 1993-3.
- Brown, D.A. and Gunning, M.H. (1993b): Geology of the Scud Glacier Area, Northwestern British Columbia (104G/6); *B.C. Ministry of Energy, Mines and Petroleum Resources*, Geoscience Map 1993-4.
- Brown, D.A., Greig, C.J. and Gunning, M.H. (1990): Geology and Geochemistry of the Stikine River - Yehiniko Lake Area, Northwestern British Columbia (104G/11W, 12E); *B.C. Ministry of Energy, Mines and Petroleum Resources*, Open File 1990-1.
- Brown, D.A., Greig, C.J. and Gunning, M.H. (1993): Geology of the Yehiniko Lake and Chutine River Area, Northwestern British Columbia (104G/11W, 12); *B.C. Ministry of Energy, Mines and Petroleum Resources*, Geoscience Map 1993-5.
- Brown, D.A., Logan, J.M., Gunning, M.H., Orchard, M.J. and Bamber, W.E. (1991): Stratigraphic Evolution of the Paleozoic Stikine Assemblage in the Stikine and Iskut Rivers Area, Northwestern British Columbia; *Canadian Journal of Earth Sciences*, Volume 28, pages 958-972.
- Brown, D.A., Harvey-Kelly, F.E.L., Neill, I. and Timmerman, J. (1992a): Geology of the Chutine River - Tahltan Lake Area (104G/12W, 13); in *Geological Fieldwork 1991*, Grant, B. and Newell, J.M., Editors, *B.C. Ministry of Energy, Mines and Petroleum Resources*, Paper 1992-1, pages 179-195.
- Brown, D.A., Neill, I., Timmerman, J., Harvey-Kelly, F., Gunning, M.G. and Greig, C.J. (1992b): Geology, Mineral Occurrences and Geochemistry of the Tahltan Lake - Chutine River Area, Northwestern British Columbia (104G/12W, 13); *B.C. Ministry of Energy, Mines and Petroleum Resources*, Open File 1992-2.
- Brown, D.A., Greig, C.J., Bevier, M.L. and McClelland, W.C. (1992c): U-Pb Zircon Ages for the Hazelton Group and Cone Mountain and Limpoke Plutons, Telegraph Creek Map Area, Northwestern British Columbia: Age Constraints on Volcanism and Deformation; in *Radiogenic Age and Isotopic Studies: Report 6*; *Geological Survey of Canada*, Paper 92-2, pages 153-162.
- Brown, G.C., Thorpe, R.S. and Webb, P.C. (1984): The Geochemical Characteristics of Granitoids in Contrasting Arcs and Comments on Magma Sources; *Journal of the Geological Society of London*, Volume 141, pages 413-426.
- Buddington, A.F. (1929): Geology of Hyder and Vicinity, Southeastern Alaska; *U.S. Geological Survey*, Bulletin 807, 124 pages.
- Carmichael, R.G. and Holbek, P.M. (1989): 1989 Prospecting Report on the Rugged Mountain Property Canyon 25 Claim; *B.C. Ministry of Energy, Mines and Petroleum Resources*, Assessment Report 19,072.
- Carter, E.S., Orchard, M.J., Ross, C.A., Ross, J.R.P., Smith, P.L. and Tipper, H.W. (1991): Part B, Paleontological Signatures of Terranes; in Chapter 2 of *Geology of the Cordilleran Orogen in Canada*, Gabrielse, H., and Yorath, C.J., Editors, *Geological Survey of Canada*, Geology of Canada, No. 4, pages 28-38.
- Chappell, B.W. and White, A.J.R. (1974): Two Contrasting Granite Types; *Pacific Geology*, Volume 8, pages 173-174.
- Chung, P.L. (1990a): Geochemical Report on the Oksa Creek Property; *B.C. Ministry of Energy, Mines and Petroleum Resources*, Assessment Report 19,876.
- Chung, P.L. (1990b): Geochemical Report on the DOK Property; *B.C. Ministry of Energy, Mines and Petroleum Resources*, Assessment Report 19,892.
- Chung, P.L. (1990c): Prospecting Report on the Snow Property; *B.C. Ministry of Energy, Mines and Petroleum Resources*, Assessment Report 20,002.
- Cordey, F. (1992): Report on Radiolarians and other Microfossils; *Geological Survey of Canada*, Report number FC-1992-2
- Cox, D.P. and Singer, D.A., Editors (1986): Mineral Deposit Models; *United States Geological Survey*, Bulletin 1693, 379 pages.
- Currie, L.D. (1992): Metamorphic Rocks in the Tagish Lake Area, Northern Coast Mountains, British Columbia: A Possible Link between Stikinia and parts of the Yukon-Tanana Terrane, in *Current Research, Part A*, *Geological Survey of Canada*, Paper 92-1A, pages 199-208.
- Davis, J.W. (1988): Geological and Geochemical Report on the MJ 1 to 16 Claims, Stikine River Area; *B.C. Ministry of Energy, Mines and Petroleum Resources*, Assessment Report 18,134.
- Dawson, G.M. (1889): Report on an Exploration in the Yukon District, N.W.T. and adjacent northern portion of British Columbia; *Geological and Natural History Survey of Canada*, Annual Report 1887-88, Volume III, Part B, 7B.

- Dawson, K.M., Panteleyev, A., Sutherland Brown, A. and Woodsworth, G.J. (1991): Regional Metallogeny; Chapter 19, in *Geology of the Canadian Orogen in Canada*, Gabrielse, H. and Yorath, C.J., Editors, *Geological Survey of Canada*, Geology of Canada, No. 4, pages 707-768.
- Deer, W.A., Howie, R.A. and Zussman, J. (1977): *An Introduction to the Rock-forming Minerals*; Longman, 528 pages.
- de Rosen Spence, A. (1985): Shoshonites and Associated Rocks of Central British Columbia; in *Geological Fieldwork 1984*, B.C. Ministry of Energy, Mines and Petroleum Resources, Paper 1985-1, pages 426-442.
- Devlin, B.D. and Godwin, C.I. (1986): Geology of the Dolly Varden Camp, Alice Arm Area (103P/11, 12); in *Geological Fieldwork 1985*, B.C. Ministry of Energy, Mines and Petroleum Resources, Paper 1986-1, pages 327-330.
- Dirom, G.A. (1964): Preliminary Geological Report on Conover Creek Group; B.C. Ministry of Energy, Mines and Petroleum Resources, Assessment Report 591.
- Drobe, J.R., Logan, J.M. and McClelland, W.C. (1992): Early Carboniferous Plutonism in Stikinia, Stikine and Iskut Rivers Area, Northwestern British Columbia; in *Abstract Volume, Cordilleran Tectonics Workshop*, University of Edmonton, Report No. 24.
- Dudas, B.M. (1972): Sno, Bird (Liard Copper); in *Geology, Exploration and Mining in British Columbia*, B.C. Ministry of Energy, Mines and Petroleum Resources, pages 39-40.
- Dunn, (1990): Latimer Lake Project, Report on Geological, Geochemical and Geophysical Programs on the Dole 1-4, Lake 1-4, Bake 1-4 and EN Claims; B.C. Ministry of Energy, Mines and Petroleum Resources, Assessment Report 20,523.
- Eby, G.N. (1992): Chemical Subdivision of the A-type Granitoids: Petrogenetic and Tectonic Implications; *Geology*, Volume 20, pages 641-644.
- Eccles, L. (1981): Geological and Geochemical Report on the Mist 1 and 2 Claims; B.C. Ministry of Energy, Mines and Petroleum Resources, Assessment Report 9218.
- Eisbacher, G.H. (1974): Sedimentary History and Tectonic Evolution of the Sustut and Sifton Basins, North-central British Columbia; *Geological Survey of Canada*, Paper 73-31, 57 pages.
- Engerbretson, D.C., Cox, A. and Gorden, P.C. (1985): Relative Plate Motions Between Oceanic and Continental Plates in the Pacific; *Geological Association of America*, Special Paper 206, 59 pages.
- Epstein, A.G., Eptsein, J.B. and Harris, L.D. (1977): Conodont Color Alteration - an Index to Organic Metamorphism; *U.S. Geological Survey Professional Paper* 995, 27 pages.
- Evenchick, C. (1986): Structural Style of the Northeast Margin of the Bowser Basin, Spatsizi Map Area, North-central British Columbia; in *Current Research, Part B*, *Geological Survey of Canada*, Paper 86-1B, pages 733-739.
- Evenchick, C.A. (1991a): Jurassic Stratigraphy of East Telegraph Creek and West Spatsizi Map Areas, British Columbia; in *Current Research, Part E*, *Geological Survey of Canada*, Paper 91-1E, pages 155-162.
- Evenchick, C.A. (1991b): Structural Relationships of the Skeena Fold Belt West of the Bowser Basin, Northwest British Columbia; *Canadian Journal of Earth Sciences*, Volume 28, pages 973-983.
- Evenchick, C.A. (1991c): Geometry, Evolution, and Tectonic Framework of the Skeena Fold Belt, North Central British Columbia; *Tectonics*, Volume 10, pages 527-546.
- Fladmark, K.R. (1985): Glass and Ice, The Archaeology of Mt. Edziza; *Department of Archaeology, Simon Fraser University*, Publication 14, 217 pages.
- Folk, P. (1981a): Geochemical Report on the Limp #2 Claim; B.C. Ministry of Energy, Mines and Petroleum Resources, Assessment Report 9092.
- Folk, P.G. (1981b): Report on the Geology, Trenching and Sampling of the Marg and Dok Claims; in *Assessment Report* 9617.
- Fox, P.E., Grove, E.W., Seraphim, R.H., Sutherland Brown, A. (1976): Schaft Creek; in *Porphyry Deposits of the Canadian Cordillera*, Sutherland Brown, A., Editor, *Canadian Institute of Mining and Metallurgy*, Special Volume 15, pages 219-226.
- Frith, R.A. and Fryer, B.J. (1985): Geochemistry and Origin of the Regan Intrusive Suite and other Granitoids in the North-eastern Slave Province, Northwest Canadian Shield; *Canadian Journal of Earth Sciences*, Volume 22, pages 1048-1065.
- Gabrielse, H. (1980): Dease Lake Map Area; *Geological Survey of Canada*, Open File 707.
- Gabrielse, H. (1985): Major Dextral Transcurrent Displacements along the Northern Rocky Mountain Trench and Related Lineaments in North-central British Columbia; *Geological Society of America*, Bulletin, Volume 96, pages 1-14.
- Gabrielse, H. (1991): Late Paleozoic and Mesozoic Terrane Interactions in North-central British Columbia; *Canadian Journal of Earth Sciences*, Volume 28, No. 6, pages 947-957.
- Gabrielse, H. and Yorath, C.J. (1991): Tectonic Synthesis, Chapter 18; in *Geology of the Cordilleran Orogen in Canada*, Gabrielse, H. and Yorath, C.J., Editors, *Geological Survey of Canada*, Geology of Canada, No. 4, pages 677-705.
- Gabrielse, H., Monger, J.W.H., Templeman-Kluit, D.J., and Woodsworth, G.J. (1991a): Structural styles, Part C. Intermontane Belt; in Chapter 17 of *Geology of the Cordilleran Orogen in Canada*, Gabrielse, H. and Yorath, C.J., Editors, *Geological Survey of Canada*, Geology of Canada, No. 4, pages 591-603.
- Gabrielse, H., Souther, J.G., Woodsworth, G.J., Tipper, H.W. and Monger, J.W.H. (1991c): The Intermontane Belt in Chapter 9, *Geology of the Cordilleran Orogen in Canada*, Gabrielse, H. and Yorath, C.J., Editors, *Geological Survey of Canada*, Geology of Canada, No. 4, pages 345-351.
- Gabrielse, H., Monger, J.W.H., Wheeler, J.O. and Yorath, C.J. (1991b): Morphogeological Belts, Tectonic Assemblages and Terranes, in Chapter 2 of *Geology of the Cordilleran Orogen in Canada*, Gabrielse, H. and Yorath, C.J., Editors, *Geological Survey of Canada*, Geology of Canada, No. 4, pages 15-28.
- Gale, R.E. (1964): Geological Report of Mineral Claims BIK 137 to BIK 160; B.C. Ministry of Energy, Mines and Petroleum Resources, Assessment Report 592.
- Geological Survey of Canada (1957): Operation Stikine, Map 9-1957.
- Gill, J. and Whelan, P. (1989): Early Rifting of an Oceanic Island Arc (Fiji) Produced Shoshonitic to Tholeiitic Basalts; *Journal of Geophysical Research*, Volume 94, pages 4561-4578.

- Godwin, C.I., Pickering, A.D.R. and Gabites, J.E. (1991): Interpretation of Galena Lead Isotopes from the Stewart Area (103O, P; 104A,B,G), in *Geological Fieldwork 1990*, B.C. Ministry of Energy, Mines and Petroleum Resources, Paper 1991-1, pages 235-243.
- Graf, C. (1985a): Chutine 1,2,3 Mineral Claims (Conover Creek); B.C. Ministry of Energy, Mines and Petroleum Resources, Assessment Report 14,216.
- Graf, C. (1985b): Kirk Mineral Claim; B.C. Ministry of Energy, Mines and Petroleum Resources, Assessment Report 13,662.
- Greenwood, H.J., Woodsworth, G.J., Read, P.B., Ghent, E.D. and Evenchick, C.A. (1991): Metamorphism, Chapter 16; in *Geology of the Cordilleran Orogen in Canada*, Gabrielse, H. and Yorath, C.J., Editors, *Geological Survey of Canada*, Geology of Canada, No. 4, pages 533-570.
- Greig, C.J. and Gehrels, G.E. (1992): Latest Triassic - Earliest Jurassic Orogenesis, Stikine Terrane, Northwestern British Columbia, *Geological Society of America*, Abstracts with Programs, Volume 24, No. 5, page 28.
- Grybeck, D.J., Berg, H.C. and Karl, S.M. (1984): Map and Description of the Mineral Deposits in the Petersburg and Eastern Port Alexander Quadrangles, Southeastern Alaska; U.S. Geological Survey Open-File Report 84-837, scale 1:250,000, 87 pages.
- Gunning, M.H. (1990): Stratigraphy of the Stikine Assemblage, Scud River Area, Northwest British Columbia; in *Geological Fieldwork 1989*, B.C. Ministry of Energy, Mines and Petroleum Resources, Paper 1990-1, pages 153-161.
- Gunning, M.H. (1993a): Character and Evolution of an Upper Carboniferous to Upper Permian Succession in an Extensional, Oceanic Tectonic Setting; Stikine Assemblage, Northwest Stikinia, Scud River Area (NTS 104G), British Columbia, Unpublished M.Sc. thesis, *University of Western Ontario*, 305 pages.
- Gunning, M.H. (1993b): Character of Upper Paleozoic Strata and Plutons, Lower Forrest Kerr Creek Area, Northwestern British Columbia; in *Current Research, Part A, Geological Survey of Canada*, Paper 93-1A, pages 27-36.
- Gunning, M.H., Bamber, E.W., Brown, D.A., Rui, L., Mamet, B.L. and Orchard, M.J. (1994): The Permian Ambition Formation of Northwestern Stikinia, British Columbia; in *Pangea: Global Environments and Resources*, Embry, A.F., Beauchamp, B. and Glass, D.J., Editors, *Canadian Society of Petroleum Geologists*, Memoir 17, pages 589-619.
- Hallof, P.G. (1963): Geophysical Survey of the Poke Claim Group; B.C. Ministry of Energy, Mines and Petroleum Resources, Assessment Report 535.
- Hallof, P.G. (1966): Report on the Induced Polarization and Resistivity Survey on the Gordon Claim Group; B.C. Ministry of Energy, Mines and Petroleum Resources, Assessment Report 847.
- Hamilton, T.S. (1981): Late Cenozoic Alkaline Volcanics of the Level Mountain Range, Northwestern British Columbia: Geology, Petrology and Paleomagnetism; unpublished Ph.D. thesis, *University of Alberta*, 490 pages.
- Harayama, S. (1992): Youngest Exposed Granitoid Pluton on Earth: Cooling and Rapid Uplift of the Pliocene-Quaternary Takidani Granodiorite in the Japan Alps, Central Japan, *Geology*, Volume 20, No. 7, pages 657-660.
- Harland, W.B., Armstrong, R.L., Cox, A.V., Craig, L.E., Smith, A.G. and Smith, D.G. (1990): *A Geological Time Scale 1989*; Cambridge University Press, Cambridge, 263 pages.
- Hart, G. and Mihalynuk, M. (1992): The Tally-Ho Shear - Lewellyn Fault Zone: Controls on Timing and Types of Interactions between Nisling and Stikine Terranes in Northern British Columbia and Southern Yukon Territory; Cordilleran Tectonics Workshop, *University of Alberta*, Report No. 24, page 87.
- Hedley, M.S. (1966a): Limpoke; in *Lode Metals in British Columbia*, B.C. Ministry of Energy, Mines and Petroleum Resources, page 18.
- Hedley, M.S. (1966b) MH; in *Lode Metals in British Columbia*, B.C. Ministry of Energy, Mines and Petroleum Resources, page 18.
- Henderson, J.R., Kirkham, R.V., Hendrson, M.N., Payne, J.G., Wright, T.O. and Wright, R.L. (1992): Stratigraphy and Structure of the Sulphurets Area, British Columbia; in *Current Research, Part A, Geological Survey of Canada*, Paper 92-1A, pages 323-332.
- Hodgson, C.J. and LeBel, J.L. (1974): South Tahltan Lake Property (# 656 A) Magnetometer Survey; B.C. Ministry of Energy, Mines and Petroleum Resources, Assessment Report 5097.
- Holland, S.S. (1950): Placer Gold Production of British Columbia; B.C. Ministry of Energy, Mines and Petroleum Resources, Bulletin 28, 89 pages.
- Holland, S.S. (1976): Landforms of British Columbia, A Physiographic Outline; B.C. Ministry of Energy, Mines and Petroleum Resources, Bulletin 48, 138 pages.
- Holbek, P.M. (1981): Geological Report on the Late Claim; B.C. Ministry of Energy, Mines and Petroleum Resources, Assessment Report 9660.
- Holbek, P.M. (1988): Geology and Mineralization of the Stikine Assemblage, Mess Creek Area, Northwestern British Columbia; unpublished M.Sc. thesis, *The University of British Columbia*, 174 pages.
- Hunt, P.A. and Roddick, J.C. (1994): A Compilation of K-Ar and ⁴⁰Ar-³⁹Ar Ages: Report 2; in *Radiogenic Age and Isotopic Studies*; Report 8, *Current Research 1994-F, Geological Survey of Canada*, pages 139-140.
- Irving, E. and Monger, J.W.H. (1987): Preliminary Paleomagnetic Results from the Asitka Group, British Columbia; *Canadian Journal of Earth Sciences*, Volume 24, pages 1490-1497.
- Irvine, T.N. and Baragar, W.R.A. (1971): A Guide to the Chemical Classification of Common Volcanic Rocks; *Canadian Journal of Earth Sciences*, Volume 8, pages 523-548.
- Jeffery, W.G. (1967) Nabs, Paramount Mining Ltd.; in *Annual Report 1966*, B.C. Ministry of Energy, Mines and Petroleum Resources, pages 29-30.
- Johnson, D. and Jones, P.W. (1990a): Scud Property - 1045, Scud 10, 11, 12, 13, 14 Claims; B.C. Ministry of Energy, Mines and Petroleum Resources, Assessment Report 20,184.
- Johnson, D. and Jones, P.W. (1990b): Scud Property - 1045, Scud 4, 5, 6, 7 and 8 Claims; B.C. Ministry of Energy, Mines and Petroleum Resources, Assessment Report 20,185.
- Johnson, D. and Jones, P.W. (1990c): Scud Property - 1045, Scud #1, 2, 3, Alicia, Robyn Claims; B.C. Ministry of Energy, Mines and Petroleum Resources, Assessment Report 20,186.

- Kasper, B. (1990a): Geological and Geochemical Report on the Jameson 1-41 Claims; *B.C. Ministry of Energy, Mines and Petroleum Resources*, Assessment Report 19,791.
- Kasper, B. (1990b): Geological and Geochemical Report on the Rattle and Roll Claims; *B.C. Ministry of Energy, Mines and Petroleum Resources*, Assessment Report 19870.
- Keep, G. (1983): Prospecting Report on the Lode Mineral Claims 1-9 (inclusive) 11-12; *B.C. Ministry of Energy, Mines and Petroleum Resources*, Assessment Report 11,262.
- Keep, M and Russell, J.K. (1989): The Geology of the Averill Plutonic Complex, Grand Forks, British Columbia; in *Geological Fieldwork 1988*, *B.C. Ministry of Energy, Mines and Petroleum Resources*, Paper 1989-1, pages 27-32.
- Kennet (1982): *Marine Geology*; Prentice-Hall, Inc., 813 pages.
- Kerr, F.A. (1927): Preliminary Report on Stikine River Area, British Columbia; *Geological Survey of Canada*, Summary Report 1926, Part A, pages 14A-34A.
- Kerr, F.A. (1929): Second Preliminary Report on Stikine River Area, British Columbia; *Geological Survey of Canada*, Summary Report 1928, Part A, pages 11A-26A.
- Kerr, F.A. (1930): Preliminary Report on Iskut River Area, British Columbia; *Geological Survey of Canada*, Summary Report 1929, Part A, pages 30A-61A.
- Kerr, F.A. (1931): Explorations between Stikine and Taku Rivers, British Columbia; *Geological Survey of Canada*, Summary Report 1930, Part A, pages 41A-55A.
- Kerr, F.A. (1935): Stikine River Area, Cassiar District, British Columbia; *Geological Survey of Canada*, Map 310A.
- Kerr, F.A. (1948a): Lower Stikine and Iskut River Areas, British Columbia; *Geological Survey of Canada*, Memoir 246, 94 pages.
- Kerr, F.A. (1948b): Taku River Map-area, British Columbia; *Geological Survey of Canada*, Memoir 248, 84 pages.
- Kerr, P.F. (1959): *Optical Mineralogy*, Third Edition; McGraw-Hill Book Company, Inc., 442 pages.
- Korenic, J.A. (1982a): 1981 Assessment Report of Geological, Geochemical and Geophysical Work Performed on the Tuff 1 Claim; *B.C. Ministry of Energy, Mines and Petroleum Resources*, Assessment Report 10,475.
- Korenic, J.A. (1982b): 1981 Assessment Report of Geological, Geochemical and Geophysical Work Performed on the Mist 1 and 2 Claims; *B.C. Ministry of Energy, Mines and Petroleum Resources*, Assessment Report 10,476.
- Kushner, W.R. (1990a): 1989 Summary Report on the Oksa Gold Property, *B.C. Ministry of Energy, Mines and Petroleum Resources*, Assessment Report 19,576.
- Kushner, W.R. (1990b): 1989 Summary Report on the Dokdaon Property; *B.C. Ministry of Energy, Mines and Petroleum Resources*, Assessment Report 19,908.
- Kushner, W.R. (1991): 1990 Summary Report on the Oksa Gold Property; *B.C. Ministry of Energy, Mines and Petroleum Resources*, Assessment Report 20,840.
- Lambert, M.B. (1974): The Bennett Lake Cauldron Subsidence Complex, British Columbia and Yukon Territory; *Geological Survey of Canada*, Bulletin 227, 213 pages.
- Lammle, C.A.R. (1964): Geological Report on Mineral Claims BIK 117-136 Inclusive; *B.C. Ministry of Energy, Mines and Petroleum Resources*, Assessment Report 589.
- Lammle, C.A.R. (1966): Geological and Geophysical Report on Nabs 1-34 Mineral Claims; *B.C. Ministry of Energy, Mines and Petroleum Resources*, Assessment Report 900.
- Lapierre, H., Albarede, F., Albers, J., Cabanis, B and Coulon, C. (1985): Early Devonian Volcanism in the Eastern Klamath Mountains, California: Evidence for an Immature Island Arc; *Canadian Journal of Earth Sciences*, Volume 22, pages 214-227.
- Lehtinen, J. (1989): 1989 Geological and Geochemical Report of the Goat 1 to 11 Claims; *B.C. Ministry of Energy, Mines and Petroleum Resources*, Assessment Report 19439.
- Lehtinen, J. (1990): 1989 Geological and Geochemical Report on the Bar 1 to 11 Claims; *B.C. Ministry of Energy, Mines and Petroleum Resources*, Assessment Report 19836.
- Le Bas, M.J. and Streckeisen, A.L. (1991): The IUGS Systematics of Igneous Rocks; *Journal of the Geological Society*, London, Volume 148, pages 825-833.
- Le Maitre, R.W., Editor (1989): A Classification of Igneous Rocks and Glossary of Terms; *Blackwell Scientific Publications*, 193 pages.
- Lewis, P.D. (1992): Structural Evolution of the Iskut River Area: Preliminary Results; Mineral Deposit Research Unit, *The University of British Columbia*, Annual Technical Report - Year 2, pages 2.1-2.21.
- Lewis, P.D., Thompson, J.F.H., Nadaraju, G., Anderson, R.G. and Johansson, G. (1993): Lower and Middle Jurassic Stratigraphy in the Treaty Glacier Area and Geological Setting of the Treaty Glacier Alteration System, Northwestern British Columbia; in *Current Research, Part A*, *Geological Survey of Canada*, Paper 93-1A, pages 75-86.
- Lin Rui (1990): Report on 23 Collections of Fossils from the Scud River Area; *Geological Survey of Canada, Paleontology Subdivision*, Calgary, report No. 1-RUI-1990.
- Lin Rui (1991): Report on 1 Collection of Fossils from the Scud River Area, Southwestern Telegraph Creek Map Area; unpublished report No. 1-RUI-1992.
- Lin Rui (1992): Report on 2 Collections of Fossils from the Telegraph Creek Area; unpublished report No. 1-RUI-1992.
- Linder, H. (1975): Geology of the Schaft Creek Porphyry Copper Molybdenum Deposit, Northwestern B.C.; *Canadian Institute of Mining and Metallurgy*, Volume 68, No. 758, pages 49-63.
- Lion, J.G. (1971): P-T Stabilities of Laumontite, Wairakite, Lawsonite, and Related Minerals in the System, $\text{CaAl}_2\text{Si}_3\text{O}_8\text{-SiO}_2\text{-H}_2\text{O}$; *Journal of Petrology*, Volume 12, pages 379-411.
- Lister, G.S. and Snoke, A.W. (1984): S-C Mylonites; *Journal of Structural Geology*, Volume 6, No. 6, pages 617-638.
- Lloyd, C. (1989): Summary Report of the 1989 Exploration Program on the Rapid Property; *B.C. Ministry of Energy, Mines and Petroleum Resources*, Assessment Report 19713.
- Logan, J.M. and Drobe, J.R. (1993a): Geology and Mineral Occurrences of the Mess Lake Area (104G/7W); in *Geological Fieldwork 1992*, Grant, B. and Newell, J.M., Editors, *B.C. Ministry of Energy, Mines and Petroleum Resources*, Paper 1993-1, pages 135-148.
- Logan, J.M. and Drobe, J.R. (1993b): Geology of the Mess Lake Area, Northwestern British Columbia (104G/7W); *B.C. Ministry of Energy, Mines and Petroleum Resources*, Open File 1993-6.

- Logan, J.M., Drobe, J.R. and McClelland, W.C. (In Preparation): Geology along the Forrest Kerr and Mess Lake Faults, Iskut River Area, Northwestern British Columbia (104B/15, 104G/2 & 7); *B.C. Ministry of Energy, Mines and Petroleum Resources, Bulletin*.
- Logan, J.M. and Koyanagi, V.M. (1989): Geology and Mineral Deposits of the Galore Creek Area, Northwestern B.C. (104G/3&4); in *Geological Fieldwork 1988, B.C. Ministry of Energy, Mines and Petroleum Resources, Paper 1989-1*, pages 269-284.
- Logan, J.M. and Koyanagi, V.M. (1994): Geology and mineral deposits of the Galore Creek area; *B.C. Ministry of Energy, Mines and Petroleum Resources, Bulletin 92*.
- Logan, J.M., Drobe, J.R. and Elsby, D. (1992a): Geology of the More Creek Area, Northwestern British Columbia (104G/2); in *Geological Fieldwork 1991*, Grant, B. and Newell, J.M., Editors, *B.C. Ministry of Energy, Mines and Petroleum Resources, Paper 1992-1*, pages 161-178.
- Logan, J.M. and Drobe, J.R. and Elsby, D.C. (1992b): Geology, Geochemistry and Mineral Occurrences of the More Creek Area, Northwestern British Columbia (104G/2); *B.C. Ministry of Energy, Mines and Petroleum Resources, Open File 1992-5*.
- Logan, J.M., Koyanagi, V.M. and Drobe, J.R. (1990a): Geology of the Forrest Kerr Creek Area, Northwestern British Columbia (104B/15); in *Geological Fieldwork 1989, B.C. Ministry of Energy, Mines and Petroleum Resources, Paper 1990-1*, pages 127-139.
- Logan, J.M., Koyanagi, V.M. and Drobe, J.R. (1990b): Geology, Geochemistry and Mineral Occurrences of the Forrest Kerr - Iskut River Area, Northwestern B. C. (104B/10, 15); *B.C. Ministry of Energy, Mines and Petroleum Resources, Open File 1990-2*.
- Logan, J.M., Koyanagi, V.M. and Rhys, D. (1989): Preliminary Geology and Mineral Occurrences of the Sphaler Creek and Flood Glacier (104G/3&4); *B.C. Ministry of Energy, Mines and Petroleum Resources, Open File 1989-8*.
- Logan, J.M., Koyanagi, V.M. and Rhys, D. (1993a): Geology and Mineral Occurrences of the Galore Creek Area (NTS 104G/03); *B.C. Ministry of Energy, Mines and Petroleum Resources, Geoscience Map 1993-1*.
- Logan, J.M., Koyanagi, V.M. and Rhys, D. (1993b): Geology and Mineral Occurrences of the Galore Creek Area (NTS 104G/04); *B.C. Ministry of Energy, Mines and Petroleum Resources, Geoscience Map 1993-2*.
- Logan, J.M., Drobe, J.R., McClelland, W.C. and Anderson, R.G. (1993c): Devonian Intraoceanic Arc Magmatism in Northwestern Stikinia; *Geological Association of Canada, Program with Abstracts*.
- Long, D.G.F. (1981): Dextral Strike Slip Faults in the Canadian Cordillera and Depositional Environments of Related Freshwater Intermontane Coal Basins; in *Sedimentation and Tectonics in Alluvial Basins*, Miall, A.D., Editor, *Geological Association of Canada, Special Paper 23*, pages 153-186.
- Lueck, B.A. and Russell, J.K. (1994): Geology and Origins of the Zippa Mountain Igneous Complex with Emphasis on the Zippa Mountain Pluton, Northern British Columbia; in *Current Research Part A, Geological Survey of Canada, Paper 94-1A*, pages 77-85.
- McClay, K. (1987): *The Mapping of Geological Structures; Halsted Press, John Wiley & Sons*, 161 pages.
- McClelland, W.C. (1992): Permian and Older Rocks of the Southwestern Iskut River Map Area, Northwestern British Columbia; in *Current Research, Part A, Geological Survey of Canada, Paper 92-1A*, pages 303-307.
- McClelland, W.C., Anovitz, L.M. and Gehrels, G.E. (1991): Thermobarometric Constraints on the Structural Evolution of the Coast Mountains Batholith, Central Southeastern Alaska; *Canadian Journal of Earth Sciences*, Volume 28, pages 912-928.
- McIntyre, J.F. (1966): Engineering, Geophysical and Geological Report, Shakes East and Shakes West Groups; *B.C. Ministry of Energy, Mines and Petroleum Resources, Assessment Report 773*.
- McKenzie, K.J. (1985): Sedimentology and Stratigraphy of the Southern Sustut Basin, North-central British Columbia; unpublished M.Sc. thesis, *The University of British Columbia*, 120 pages.
- McMillan, W.J. (1978): Geology of the Guichon Creek Batholith and Highland Valley Porphyry Copper District, British Columbia; *B.C. Ministry of Energy, Mines and Petroleum Resources, Preliminary Map 30*.
- McMillan, W.J. (1992): Porphyry Deposits in the Canadian Cordillera; in *Ore Deposits, Tectonics and Metallogeny in the Canadian Cordillera, B.C. Ministry of Energy, Mines and Petroleum Resources, Paper 1991-4*, pages 253-276.
- McMillan, W.J. and Panteleyev, A. (1988): Porphyry Copper Deposits; in *Ore Deposit Models*, Roberts, R.G. and Sheahan, P.A., Editors, *Geoscience Canada, Reprint Series 3*, pages 45-58.
- Macdonald, J.A., van der Hayden, P., Lefebvre, D.V. and Alldrick, D.J. (1992): Geochronometry of the Iskut River Area - An Update (104A and B); in *Geological Fieldwork 1991*, Grant, B. and Newell, J.M., Editors, *B.C. Ministry of Energy, Mines and Petroleum Resources, Paper 1992-1*, pages 495-501.
- Mamet, B.L. (1991): Report on Stikine Assemblage Samples; Report Misc-02-BLM-1991, *University of Montreal*.
- Mandy, J.D. (1930): Stikine and Liard Mining Divisions; in *Report of the Minister of Mines 1929; B.C. Ministry of Energy, Mines and Petroleum Resources, page C115*.
- Mandy, J.D. (1931): Stikine and Liard Mining Divisions; in *Report of the Minister of Mines 1930; B.C. Ministry of Energy, Mines and Petroleum Resources, pages A117-119*.
- Mark, D.G. (1970): Geochemical - Geophysical Report on Magnetic and Soil Sampling Survey, Northern Valley Mines Ltd.; *B.C. Ministry of Energy, Mines and Petroleum Resources, Assessment Report 2954*.
- Marsden, H. and Thorkelson, D.J. (1992) Geology of the Hazelton Volcanic Belt in British Columbia: Implications for the Early to Middle Jurassic Evolution of Stikinia; *Tectonics*, Volume 11, pages 1266-1287.
- Marud, D. (1990a): Report of Activities on the Tahltan Lake Property; *B.C. Ministry of Energy, Mines and Petroleum Resources, Assessment Report 20,149*.
- Marud, D. (1990b): Report of Activities on the Dokdaon Creek Property; *B.C. Ministry of Energy, Mines and Petroleum Resources, Assessment Report 20,153*.
- Marud, D. (1990c): Report of Activities on the Rugged Mountain Property; *B.C. Ministry of Energy, Mines and Petroleum Resources, Assessment Report 20,154*.

- Marud, D. (1990d): 1990 Assessment Report on the Gran 16 Claim; B.C. Ministry of Energy, Mines and Petroleum Resources, Assessment Report 20,302.
- Miall, A.D. (1978): Tectonic Setting and Syndepositional Deformation of Molasse and other Nonmarine-paralic Sedimentary Basins; *Canadian Journal of Earth Sciences*, Volume 15, pages 1613-1632.
- Miall, A.D. (1981): Alluvial Basins: Tectonic Setting and Basin Architecture; in Sedimentation and Tectonics in Alluvial Basins, Miall, A.D., Editor, *Geological Association of Canada*, Special Paper 23, pages 1-33.
- Mihalynuk, M.G., Smith, M.T. Hancock, K.D. and Dudka, S. (1994): Regional and Economic Geology of the Tulsequah River and Glacier Areas (104K/12 & 13); in Geological Fieldwork 1993, Grant, B. and Newell, J.M., Editors, *B.C. Ministry of Energy, Mines and Petroleum Resources*, Paper 1994-1, pages 171-197.
- Miller, M.M. (1987): Displaced Remnants of a Northeast Pacific Fringing Arc: Upper Paleozoic Terranes of the Permian McCloud Faunal Affinity, Western U.S.; *Tectonics*, Volume 6, pages 807-830.
- Monger, J.W.H. (1970): Upper Paleozoic Rocks of Stikine Arch, British Columbia; *Geological Survey of Canada*, Paper 70-1, Part A, pages 41-43.
- Monger, J.W.H. (1977a): Upper Paleozoic Rocks of Northwestern British Columbia; Part A, *Geological Survey of Canada*, Paper 77-1A, pages 255-262.
- Monger, J.W.H. (1977b): Upper Paleozoic Rocks of the Western Canadian Cordillera and their Bearing on Cordillera Evolution; *Canadian Journal of Earth Sciences* Volume 14, pages 1832-1859.
- Monger, J.W.H. (1977c): The Triassic Takla Group in McConnell Creek Map Area, North-central British Columbia; *Geological Survey of Canada*, Paper 76-29, 45 pages.
- Monger, J.W.H. and Irving, E. (1980): Northward Displacement of North-central British Columbia; *Nature*, Volume 285, pages 289-293.
- Monger, J.W.H., Wheeler, J.O., Tipper, H.W., Gabrielse, H., Harms, T., Struik, L.C., Campbell, R.B., Dodds, C.J., Gehrels, G.E. and O'Brien, J. (1991): Cordilleran Terranes; in Chapter 8 of Geology of The Cordilleran Orogen in Canada, Gabrielse, H and Yorath, C.J., Editors, *Geological Survey of Canada*, Geology of Canada, No. 4, pages 281-327.
- Morgan, D.R. (1973): Geological Report on the B #1-10 and the BM #13-16, 25-28, 37-40 and 49-53 Claims of Bart Mines, Ltd.; *B.C. Ministry of Energy, Mines and Petroleum Resources*, Assessment Report 4717.
- Morgan, J.T. (1976): Geology of the Ten Mile Creek Syenite - Pyroxenite Pluton, Telegraph Creek, B.C.; unpublished B.Sc. thesis, *The University of British Columbia*, 42 pages.
- Morrison, G.W. (1974): Stratigraphic Control of Cu-Fe Skarn Ore Distribution and Genesis at Craigmont, British Columbia; *Canadian Institute of Mining and Metallurgy*, Bulletin, Volume 73, pages 109-123.
- Morrison, G.W. (1980): Characteristics and Tectonic Setting of the Shoshonitic Rock Association; *Lithos*, Volume 13, pages 97-108.
- Mortimer, N. (1987): The Nicola Group: Late Triassic and Early Jurassic Subduction-related Volcanism in British Columbia; *Canadian Journal of Earth Sciences*, Volume 24, pages 2521-2536.
- Mullan, A.W. and Bell, R.A. (1972): Report on Induced Polarization and Resistivity Survey, Project 124, Columbia River Grid (Arc and Rose Claim); *B.C. Ministry of Energy, Mines and Petroleum Resources*, Assessment Report 3986.
- Mullen, E.D. (1983): MnO₂/TiO₂/P₂O₅: A Minor Element Discriminant for Basaltic Rocks of Oceanic Environments and its Implications for Petrogenesis; *Earth and Planetary Science Letters*, Volume 36, pages 121-132.
- Neill, I. (1992): Geology, Petrography, and Chemistry of the Rugged Mountain Alkaline Pluton, Northwestern British Columbia (104G/13); unpublished B.Sc. thesis, *The University of British Columbia*, 75 pages.
- Neill, I. and Russell, J.K. (1993): Mineralogy and Chemistry of the Rugged Mountain Pluton: A Melanite-bearing Alkaline Intrusion (104G/13); in Geological Fieldwork 1992, Grant, B. and Newell, J.M., Editors, *B.C. Ministry of Energy, Mines and Petroleum Resources*, Paper 1993-1, pages 149-157.
- Nelson, J. and Payne, J. G. (1984): Paleozoic Volcanic Assemblages and Volcanogenic Massive Sulphide Deposits near Tulsequah, British Columbia; *Canadian Journal of Earth Sciences*, Volume 21, pages 379-181.
- Nixon, G.T. and Rublee, V.J. (1988): Alaskan-type Ultramafic Rocks in British Columbia: New Concepts of the Structure of the Tulemeen Complex; in Geological Fieldwork 1987, *B.C. Ministry of Energy, Mines and Petroleum Resources*, Paper 1988-1, pages 281-294.
- Nixon, G.T., Archibald, D.A. and Heaman, L.M. (1993): ⁴⁰Ar-³⁹Ar and U-Pb Geochronometry of the Polaris Alaskan-type Complex, British Columbia: Precise Timing of Quesnellia - North America Interaction; *Geological Association of Canada*, Program and Abstracts, May, Edmonton, page A-76.
- Nixon, G.T., Ash, C., Connelly, J.N. and Case, G. (1989): Alaskan-type Ultramafic Rocks in British Columbia: 2. The Hickman, Gnat Lakes, and Menard Mafic-Ultramafic Complexes; in Geological Fieldwork 1988, *B.C. Ministry of Energy, Mines and Petroleum Resources*, Paper 1989-1, pages 429-442.
- Oliver, J. and Gabites, J. (1993): Geochronology of Rocks and Polyphase Deformation, Bearskin (Muddy) and Tatsamenie Lakes District, Northwestern British Columbia; in Geological Fieldwork 1992, Grant, B. and Newell, J.M., Editors, *B.C. Ministry of Energy, Mines and Petroleum Resources*, Paper 1993-1, pages 177-183.
- Orchard, M.J. (1990): Report on Conodonts and other Microfossils Collected by the B.C. Geological Survey; *Geological Survey of Canada*, Report No. MJO/Nov 90.
- Orchard, M.J. (1992): Report on Conodonts and other Microfossils Collected by the B.C. Geological Survey; *Geological Survey of Canada*, Report Number OF-1992-26..
- Panteleyev, A. (1975): Galore Creek Map-area; in Geological Fieldwork 1974, *B.C. Ministry of Energy, Mines and Petroleum Resources*, Paper 1975-2, pages 59-62.
- Panteleyev, A. (1976): Galore Creek Map-area, Geological Fieldwork, 1975, *B.C. Ministry of Energy, Mines and Petroleum Resources*, Paper 1976-1, pages 79-82.
- Panteleyev, A. and Dudas, B.M. (1973): Sno, Bird (Liard Copper); Nabs (Paramount); in *Geology, Exploration and Mining in British Columbia* 1972, pages 527-528.
- Pearce, J.A. (1983): Role of the Sub-continental Lithosphere in Magma Genesis at Active Continental Margins; in Hawkesworth, C.J. and Norry, M.J., Editors, *Continental Basalts and Mantle Xenoliths*; *Shiva Publications Ltd.*, pages 230-249.

- Pearce, J.A. and Cann, J.R. (1973): Tectonic Setting of Basic Volcanic Rocks Using Trace Element Analyses; *Earth and Planetary Science Letters*, Volume 19, pages 290-300.
- Pearce, J.A. and Norry, M.J. (1979): Petrogenetic Implications of Ti, Zr, Y and Nb Variations in Volcanic Rocks; *Contributions to Mineralogy and Petrology*, Volume 69, pages 33-47.
- Pearce, J.A., Harris, N.B.W. and Tindle, A.G. (1984): Trace Element Discrimination Diagrams for the Tectonic Interpretation of Granitic Rocks; *Journal of Petrology*, Volume 25, Part 4, pages 956-983.
- Perchanok, M.S. (1980): Reconnaissance of Glacier-dammed Lakes in the Stikine and Iskut River Basins; *National Hydrology Research Institute, Inland Water Directorate, Environment Canada*, 32 pages.
- Phelps, G.B. and Gutath, G.C. (1972): Report on a Geological, Geochemical and Magnetometer Survey of the Arc, Port and Rose Claim Groups; *B.C. Ministry of Energy, Mines and Petroleum Resources*, Assessment Report 3985.
- Pitcher, M.G. (1960): Fusulinids of the Cache Creek Group, Stikine River Area, Cassiar District, British Columbia, Canada; unpublished M.Sc. thesis, *Brigham Young University*, 64 pages.
- Pitcher, W.S. (1982): Granite Type and Tectonic Environment; in Mountain Building Processes, Hsu, K.J., Editor, *Academic Press*, pages 19-40.
- Preto, V.A. (1977): The Nicola Group: Mesozoic Volcanism Related to Rifting in Southern British Columbia; in *Volcanic Regimes in Canada*, Barager, W.R.A., Coleman, L.C. and Hall, J.M., Editors, *Geological Association of Canada*, Special Paper 16, p. 39-57.
- Ray, G.E., Jaramillo, V.A. and Ettlinger, A.D. (1991): The McLymont Northwest Zone, Northwest British Columbia: A Gold-rich Retrograde Skarn? (104B); in *Geological Fieldwork 1990*, B.C. Ministry of Energy Mines and Petroleum Resources, Paper 1991-1, pages 255-262.
- Ray, G.E., Webster, I.C.L., Dawson, G.L. and Ettlinger, A.D. (1993): A Geological Overview of the Hedley Gold Skarn District, Southern British Columbia (92H); in *Geological Fieldwork 1992*, Grant, B. and Newell, J., Editors, B.C. Ministry of Energy Mines and Petroleum Resources, Paper 1993-1, pages 269-279.
- Read P.B. (1983): Geology, Classy Creek (104J/2E and Stikine Canyon (104J/2W), British Columbia; *Geological Survey of Canada*, Open File 940.
- Read P.B. (1984): Klastline River (104G/16E), Ealue Lake (104H/13W), Cake Hill (104I/4W), and Stikine Canyon (104J/1E); *Geological Survey of Canada*, Open File 1080.
- Read, P.B. and Okulitch, A.V. (1977): The Triassic Unconformity of South-central British Columbia; *Canadian Journal of Earth Sciences*; Volume 14, pages 606-638.
- Read P.B., Brown, R.L., Psutka, J.F., Moore, J.M., Journeay, M., Lane, L.S. and Orchard, M.J. (1989): Geology, More and Forrest Kerr Creeks (parts of 104B/10, 15, 16 & 104G/1, 2), Northwestern British Columbia; *Geological Survey of Canada*, Open File 2094.
- Read P.B., Psutka, J.F., Brown, R.L. and Orchard, M.J. (1983): "Tahltanian" Orogeny and Younger Deformations, Grand Canyon of the Stikine British Columbia; *Geological Association of Canada*, Programs with Abstracts, May 11-13, Victoria, Volume 8, page A57.
- Rejebian, V.A., Harris, A.G. and Huebner, J.S. (1987): Conodont Color and Textural Alteration: An Index to Regional Metamorphism, Contact Metamorphism and Hydrothermal Alteration; *Geological Society of America*, Bulletin, Volume 99, pages 471-479.
- Rennie, C.C. (1962): Copper Deposits in the Nicola Rocks, Craigmont Mine; *Western Miner & Oil Review*, February, pages 50-52.
- Rhys, D.A. and Godwin, C.I. (1992): Preliminary Structural Interpretation of the Snip Mine (104B/11); in *Geological Fieldwork 1991*, Grant, B. and Newell, J.M., Editors, B.C. Ministry of Energy, Mines and Petroleum Resources, Paper 1992-1, pages 549-554.
- Ross, T.V. (1989): Geological and Geochemical Report on the Scud River Project; B.C. Ministry of Energy, Mines and Petroleum Resources, Assessment Report 19516.
- Rust, B.R. (1980a): Facies Model 2. Coarse Alluvial Deposits; in *Facies Models*, Walker, R.G. Editor, *Geoscience Canada*, Reprint Series 1, Second Printing, pages 9-21.
- Rust, B.R. (1980b): Alluvial Deposits and Tectonic Style: Devonian and Carboniferous Successions in Eastern Gaspé; in *Sedimentation and Tectonics in Alluvial Basins*, Miall, A.D., Editor, *Geological Association of Canada*, Special Paper 23, pages 49-76.
- Ryan, B. (1991): Geology and Potential Coal and Coalbed Methane Resource of the Tuya River Coal Basin (104J/2.7); in *Geological Fieldwork 1990*, B.C. Ministry of Energy Mines and Petroleum Resources, pages 419-429.
- Ryder, J.M. (1984): Terrain Inventory for the Stikine-Iskut River Area (NTS 104F, 104G and parts of 104B and 104H); B.C. Ministry of Environment, Lands and Parks, Technical Report 11, 85 pages.
- Salat, M.H. and Noakes, D.J. (1979): Geological, Geochemical Report on Hel Claims; B.C. Ministry of Energy, Mines and Petroleum Resources, Assessment Report 7708.
- Schielly, H. (1972): Report on a Geological Survey done on the PR Group; B.C. Ministry of Energy, Mines and Petroleum Resources, Assessment Report 3846.
- Schroeter, T.G. (1987): Golden Bear Project; in *Geological Fieldwork 1986*, B.C. Ministry of Energy, Mines and Petroleum Resources, Paper 1987-1, pages 103-109.
- Seraphim, R.H., Sutherland Brown, A. and Grove, E.W. (1976): Discussion of "Geology of the Schaft Creek Porphyry Copper and Molybdenum Deposit, North-western B.C."; in Linder, H., *Canadian Institute of Mining and Metallurgy*, Bulletin, Volume 69, pages 96-99.
- Shand, S.J. (1951): *Eruptive Rocks*; J. Wiley, New York.
- Sherlock, R.L., Childe, F., Barrett, T.J., Mortensen, J.K., Lewis, P.D., Chandler, T., McGuigan, P., Dawson, G.L. and Allen, R. (1994): Geological Investigations of the Tulsequah Chief Massive Sulphide Deposit, Northwestern British Columbia (104K/12); in *Geological Fieldwork 1993*, B.C. Ministry of Energy, Mines and Petroleum Resources, Paper 1994-1, pages 371-377.
- Shervais, J. (1982): Ti-V Plots and the Petrogenesis of Modern and Ophiolitic Lavas; *Earth and Planetary Science Letters*, Volume 59, pages 101-118.
- Sibson, R.H., Robert, F. and Poulsen, K.H. (1988): High-angle Reverse Faults, Fluid-pressure Cycling, and Mesothermal Gold-Quartz Deposits; *Geology*, Volume 16, pages 551-555.
- Simpson, C. and Schmid, S.M. (1983): An Evaluation of Criteria to Deduce the Sense of Movement in Sheared Rocks; *Geo-*

- logical Society of America*, Bulletin, Volume 94, pages 1281-1288.
- Smith, J.G. (1977): Geology of the Ketchikan D-1 and Bradfield Canal A-1 Quadrangles, Southeastern Alaska; *U.S. Geological Survey*, Bulletin 1425, 49 pages.
- Smith, P.L., Thomson, R.C. and Tipper, H.W. (1984): Lower and Middle Jurassic Sediments and Volcanics in the Spatsizi Map Area, British Columbia; in *Current Research, Part A, Geological Survey of Canada*, Paper 84-1A, pages 117-120.
- Southam, P. (1991): 1990 Exploration Report on the Tahltan Lake Property (Canyon 1-20, TL-1, TL-2 and TL-3 claims); *B.C. Ministry of Energy, Mines and Petroleum Resources*, Assessment Report 21,320.
- Souther, J.G. (1959): Chutine; *Geological Survey of Canada*, Map 7-1959.
- Souther, J.G. (1970): Volcanism and its Relationship to Recent Crustal Movements in the Canadian Cordillera; *Canadian Journal of Earth Sciences*, Volume 7, pages 553-568.
- Souther, J.G. (1971): Geology and Mineral Deposits of Tulsequah Map Area; *Geological Survey of Canada*, Memoir 362, 76 pages.
- Souther, J.G. (1972): Telegraph Creek Map Area; British Columbia, *Geological Survey of Canada*, Paper 71-44, 38 pages.
- Souther, J.G. (1977): Volcanism and Tectonic Environments in the Canadian Cordillera - A Second Look; in *Volcanic Regimes of Canada*, Baragar, W.R.A., Coleman, L.C. and Hall, J.M., Editors, *Geological Association of Canada*, Special Paper 16, pages 3-24.
- Souther, J.G. (1988): Mount Edziza Volcanic Complex, British Columbia; *Geological Survey of Canada*, Map 1623A.
- Souther, J.G. (1992): The Late Cenozoic Mount Edziza Volcanic Complex, British Columbia; *Geological Survey of Canada*, Memoir 420, 320 pages.
- Souther, J.G. and Symons, D.T.A. (1974): Stratigraphy and Paleomagnetism of Mount Edziza Volcanic Complex, Northwestern British Columbia; *Geological Survey of Canada*, Paper 73-32, 48 pages.
- Souther, J.G. and Yorath, C.J. (1991): Neogene Assemblages, Chapter 10 in *Geology of the Cordilleran Orogen in Canada*, Gabrielse, H. and Yorath, C.J., Editors, *Geological Survey of Canada*, Geology of Canada, No. 4, pages 373-401.
- Souther, J.G., Armstrong, R. L. and Harakal, J. (1984): Chronology of the Peralkaline, Late Cenozoic Mount Edziza Volcanic Complex, Northern British Columbia, Canada; *Geological Society of America*, Bulletin, Volume 95, pages 337-349.
- Spooner, I.S. (1994): Quaternary Climate Change in the Stikine Plateau Region, Northwestern British Columbia; *unpublished Ph.D. thesis, University of Calgary*.
- Steiger, R.H. and Jäger, E. (1977): Subcommission on Geochronology: Convention on the Use of Decay Constants in Geochronology and Cosmochronology; *Earth and Planetary Science Letters*, Volume 36, pages 359-362.
- Stevens, R.D., Delabio, R.N. and Lachance, G.R. (1982): Age Determinations and Geological Studies, K-Ar Isotopic Ages; *Geological Survey of Canada*, Report 16, page 4.
- Strain, D.M. (1981): Geological and Geochemical Report on the Tuff Claims; *B.C. Ministry of Energy, Mines and Petroleum Resources*, Assessment Report 9200.
- Streckeisen, A. (1976): To Each Plutonic Rock Its Proper Name; *Earth Science Reviews*, Volume 12, pages 1-33.
- Sutherland Brown, A. (1971): Sno, Bird (Liard Copper); in *Geology, Exploration and Mining in British Columbia 1970*, B.C. Ministry of Energy, Mines and Petroleum Resources, pages 49-57.
- Sweet, A.R. (1989): Report on 5 Samples from the Sustut Group; *Geological Survey of Canada, Paleontology Subdivision*, Calgary, Report AS-1989-6.
- Sweet, A.R. (1990): Report on 5 Samples from the Sustut Group; *Geological Survey of Canada, Paleontology Subdivision*, Calgary, Report AS-90-08.
- Thomson, R.C., Smith, P.L. and Tipper, H.W. (1986): Lower to Middle Jurassic (Pliensbachian to Bajocian) Stratigraphy of the Northern Spatsizi Area, North-central British Columbia; *Canadian Journal of Earth Sciences*, Volume 23, pages 1963-1973.
- Thorstad, L.E. and Gabrielse, H. (1986): The Upper Triassic Kutcho Formation, Cassiar Mountains, North-central British Columbia; *Geological Survey of Canada*, Paper 86-16, 53 pages.
- Tipper, H.W. (1989): Unpublished report on Jurassic fossils; *Geological Survey of Canada*, Report J4-89-HWT.
- Tipper, H.W. and Richards, T.A. (1976): Jurassic Stratigraphy and History of North-central British Columbia; *Geological Survey of Canada*, Bulletin 270, 73 pages.
- Tuttle, O.F. and Bowen, N.L. (1958): Origin of Granite in the Light of Experimental Studies in the System NaAlSi₃O₈-KAlSi₃O₈-SiO₂-H₂O; *Geological Society of America*, Memoir 74, 153 pages.
- Tozer, E.T (1989): Report on Fossils from the Telegraph Creek Area; *Geological Survey of Canada*, Report Ir 9 ETT 1989.
- Ulrich, G.D. (1971): Report on Geological, Geochemical and Geophysical Surveys and Physical Work Done on the Empire Metals Corporation Ltd. (N.P.L.) Property, Dokdaon Creek, B.C.; *B.C. Ministry of Energy, Mines and Petroleum Resources*, Assessment Report 3238.
- Ulrich, G.D. (1971): Report on Geological, Geochemical and Geophysical Surveys and Physical Work on Dokdaon Creek Area; *B.C. Ministry of Energy, Mines and Petroleum Resources*, Assessment Report 3238.
- Vandall, T.A., Brown, D.A. and Wheaton, P.M. (1992): Paleomagnetism of Toarcian Hazelton Group Volcanic Rocks in the Yehiniko Lake Area (104G/11,12): A Preliminary Report; in *Geological Fieldwork 1991*, Grant, B. and Newell, J.M., Editors, *B.C. Ministry of Energy, Mines and Petroleum Resources*, Paper 1992-1, pages 213-220.
- Van Angeren, P. (1991): Assessment Report on the 1990 Exploration Results (Geology, Geochemistry and Drilling) of the Goat 4 to Goat 7 Claims; *B.C. Ministry of Energy, Mines and Petroleum Resources*, Assessment Report 20,988.
- Veitch, J. (1970): Geological Report for Canadex Mining Corporation, Ltd. on the EWK 1-4, LLK 1-4, DOK 1-36 Claims; *B.C. Ministry of Energy, Mines and Petroleum Resources*, Assessment Report 3029.
- Webster, I.C.L. and Ray, G.E. (1991): Skarns in the Iskut River - Scud River Region, Northwest British Columbia (104B, G); in *Geological Fieldwork 1990*; *B.C. Ministry of Energy, Mines and Petroleum Resources*, Paper 1991-1, pages 245-253.
- Westcott, M.G. (1989a): Geological and Geochemical Work on the TRI 5-7, 9 and RUSH 5-8, 23-24 Claims; *B.C. Ministry of Energy, Mines and Petroleum Resources*, Assessment Report 19,143.

- Westcott, M.G. (1989b): Geological and Geochemical Work on the Poker 1-7 Claims; *B.C. Ministry of Energy, Mines and Petroleum Resources*, Assessment Report 19,247.
- Whalen, J.B., Currie, K.L. and Chappell, B.W. (1987): A-type Granites: Geochemical Characteristics, Discrimination and Petrogenesis; *Contributions to Mineralogy and Petrology*, Volume 95, pages 407-419.
- Wheeler, J.O. (1961): Whitehorse Map-area, Yukon Territory (105D); *Geological Survey of Canada*, Memoir 312, 156 pages.
- Wheeler, J.O. and McFeely, P. (1991): Tectonic Assemblage Map of the Canadian Cordillera and Adjacent Parts of the United States, *Geological Survey of Canada*, Map 1721A.
- White, W.M.H. (1959): Cordilleran Tectonics in British Columbia; *American Association of Petroleum Geologists Bulletin*, Volume 43, pages 60-100.
- White, W.M., Harakal, J.E. and Carter, N.C. (1968): Potassium-Argon Ages of Some Ore Deposits in British Columbia; *Canadian Institute of Mining and Metallurgy*, Bulletin, Volume 61, pages 1326-1334.
- Woodsworth, G.J., Anderson, R.G., Armstrong, R.L. Struik, L.C. and van der Heyden, P. (1991): Plutonic Regimes; in Chapter 15 of *Geology of the Cordilleran Orogen in Canada*, Gabrielse, H. and Yorath, C.J., Editors, *Geological Survey of Canada*, Geology of Canada, No. 4, pages 491-531.
- Wyld, S.J. (1991): Permo-Triassic Tectonism in Volcanic Arc Sequences of the Western U.S. Cordillera and Implications for the Sonoma Orogeny; *Tectonics*, Volume 5, pages 1007-1017.
- Yorath, C.J. (1991): Upper Jurassic to Paleogene Assemblages, in Chapter 9 of *Geology of the Cordilleran Orogen in Canada*, Gabrielse, H. and Yorath, C.J., Editors, *Geological Survey of Canada*, Geology of Canada, No. 4, pages 331-371.

APPENDICES

APPENDIX 1
MACROFOSSIL IDENTIFICATIONS

MAP CODE	FIELD NO.	GSC NO.	NTS MAP	UTM Zone 09		DESCRIPTION OF FAUNA	AGE	REF.
				EAST	NORTH			
HAZELTON GROUP								
IJHs	CGR89-250	C168017	104G12	349990	6385659	belemnites, ammonite (<i>Haugia</i> sp. or <i>Pleydellia</i> ?), <i>Ostrea</i> sp.	Early Jurassic, m. - I. Toarcian	3A
IJHs	DBR89-327	C158943	104G11	354706	6381236	frags. of <i>Weyla</i> , true belemnites(?), brachiopods, coleoids	Early Jurassic, poss. Toarcian	3A
IJHs	DBR89-423-1	C168048	104G11	354726	6381282	<i>Terebratulid</i> brachiopods (<i>lobothyris punctata subpunctata</i>)	L. Jurassic, I. Pleins.-Toarcian	4
IJHs	DBR89-423-2	C168048	104G11	354726	6381282	bivalves: <i>Meleagrinea</i> sp. (?) and <i>Pecten</i> sp.	Late Triassic-Jurassic	3A
IJHs	DBR89-423-3	C168049	104G11	354726	6381282	belemnites, bivalves, gastropod	Toarcian to late Early Cretaceous	3A
IJHs	DBR89-424	C168050	104G11	354787	6381410	ammonite: flattened <i>Hammatocheras</i> sp.?, bivalves	late(?) Toarcian	3A
IJHs	DBR90-155	C168072	104G11	354584	6381575		late(?) Toarcian	3
STUHNH GROUP								
uTSs1	DBR91-1-3	C189817	104G13	344443	6411542	<i>Halobia</i>	Carnian	1B
uTSs1	DBR91-151	C189816	104G13	344240	6411681	<i>Halobia</i> , <i>Perihalobia</i> ?	early Norian	1B
uTSs1	DBR91-274	C189815	104G13	339527	6406037	<i>Halobia</i>	Carnian	1B
uTSs1	DBR91-281	C189818	104G13	340481	6405709	<i>Halobia</i>	Carnian	1B
uTSs1	DBR91-281-2	C189812	104G13	340481	6405709	<i>Halobia</i>	Carnian	1B
uTSs2	CGR89-168	C168014	104G12	351657	6389893	poorly preserved bivalves(?)	indeterminate	1A
uTSs2	CGR89-170	C168015	104G12	351657	6389893	corals(?)	indeterminate	1A
uTSs2	CGR89-178	C168016	104G12	351614	6389732	bivalve	indeterminate	3A
uTSv	CGR89-260	C168018	104G11	345571	6400983	corals	indeterminate	3A
uTSs1	CGR89-302	C168020	104G12	340607	6399452	terebratulid(?), bivalve, crinoid fragments	possibly Triassic	3A
uTSv	CGR89-454	C168023	104G11	347500	6389101	nothing determined	indeterminate	1A
uTSs1	DBR89-48	C168026	104G12	348353	6400672	" <i>Pecten</i> " sp., spiriferid brachiopod probably	Late Triassic	1A
uTSs2	DBR89-157	C158938	104G11	349589	6389142	<i>Monotis subcircularis</i> Gabb	late Norian	1A
uTSs2	DBR89-158	C158939	104G11	349440	6389208	<i>Myophorignia</i> sp.	Late Triassic, prob. late Norian	1A
uTSs2	DBR89-159	C158940	104G11	349468	6389147	<i>Monotis</i> sp.	late Norian	1A
uTSs1	DBR89-215	C158941	104G12	349962	6403101	<i>Perihalobia</i> sp., <i>Stikinoceras</i> sp.	early Norian	1A
fmJHv	DBR89-267-3	C168046	104G11	353320	6379515	<i>Monotis alaskana</i> Smith	late Norian	1A
lmJHv	DBR89-291	C168045	104G11	355092	6378763	fragmentary spiriferid brachiopod, coral fragments	probably Late Triassic	1A
uTSv	DBR89-353	C158944	104G12	336853	6395239	poorly preserved pectinids	indeterminate	1A
uTSv	DBR89-510	C167907	104G12	345979	6399421	crushed serpenticone ammonite with simple ribs	Triassic or Jurassic	1A
uTSv	DBR89-527-2	C167908	104G12	344216	6400424	ragments of spiriferid brachiopods	prob. Triassic	1A
uTSv	DBR89-528	C167909	104G12	344201	6400372	fragments of ammonoid: <i>Griesbachites</i> (?); indeter. bivalves prob.	Late Triassic	1A
uTSv	DBR89-528-2	C167910	104G12	344201	6400372	ammonites: <i>Griesbachites</i> 2 sp.; <i>Stikinoceras</i> sp.	prob. early Norian	1A
uTSsz	DBR88-305	C175920	104G11	356920	6375670	<i>Monotis subcircularis</i> Gaff	Late Triassic, late Norian, Cordilleranus zone	1B
STIKINE ASSEMBLAGE								
1PSc	CGR89-398	C168021	104G12	335482	6402326	nothing determined	indeterminate	1A
1PSc	DBR88-010-1	C159118	104G05	348602	6351685	Bothrophyllid coral, fusulinacean foraminifers	Late Carboniferous or Permian	2A
1PSc	DBR88-010-3	C158910	104G05	348608	6351665	Tabulate coral, possibly <i>Multithecopora</i> sp.	Late Carboniferous or Permian	2A
1PSc	DBR88-117-1	C159141	104G05	350625	6350300	<i>Heritschioides</i> sp (coral), fenestrate bryozoans, bothrophyllid corals, fusulinaceans foraminifers	Permian, probably Early Permian	2A
1PSc	DBR88-118-1	C159142	104G05	350901	6350357	Clisiophyllid coral, schwagerinid, fusulinacean foraminifers	Early Permian	2A
1PSc	DBR88-123-1	C158913	104G05	349794	6349995	Fusulinacean foraminifers	Late Carb. or Perm., probably not older than Moscovian	2A
IPSa	DBR88-131-2	C159121	104G05	348130	6351100	Indeterminate syringipora coral probably	Carboniferous or Permian	2A
1PSc	DBR88-164-2	C159144	104G06	351414	6350401	Indeterminate bryozoans, schwagerinid, fusulinacean foraminifers	Early Permian	2A
1PSc	DBR88-166-2	C159145	104G06	351268	6350405	Indeterminate tabulate corals, fusulinacean foraminifers	Late Carb. or Perm., probably not older than Moscovian	2A
1PSc	DBR88-169-1	C159146	104G06	351030	6350365	Fusulinacean foraminifers	Probably Permian, could be as old as Moscovian	2A
1PSc	DBR88-250-1	C159148	104G06	358474	6353463	Indeterminate solitary coral, fusulinacean foraminifers.	Permian, probably Artinskian or younger	2A
1PSc	DBR88-251-1	C159149	104G06	358400	6353471	Indeterminate lophophyllid coral, schwagerinid, fusulinacean foraminifers	Permian, probably Artinskian or younger	2A
1PSc	DBR88-332-1	C159147	104G05	350514	6350320	<i>Bothrophyllum</i> sp (coral), indeterminate fenestrate and ranching bryozoans, rhynchonellid brachiopods, gastropod, schwagerinid fusulinacean foraminifers	Permian	2A

1PSc	MMC88-039-1	C154262	104G06	352470	6347570	Solitary rugose coral, fusulinacean foraminifers	Late Carboniferous or Permian, probably Early Permian	2A
uCS?	MGU88-067-1	C158903	104G05	340618	6357169	Echinoderm columnals	Indeterminate	2A
1PSc	MGU88-198-1	C158904	104G06	350472	6350814	Indeterminate fenestellid bryozoans, echinoderm columnal	Ordovician to Permian	2A
1PSc	MGU88-199-1	C158905	104G06	350453	6350693	Echinoderm columnals	Indeterminate	2A
1PSc	MGU88-200-1	C158906	104G06	350280	6350361	? <i>Hertschioides</i> sp., schwagerinid fusulinacean foraminifers	Permian, probably Early Permian	2A
1PSc	MGU88-202-1	C158908	104G06	350351	6350343	Bothrophyllid coral, echinoderm columnals, schwagerinid fusulinacean foraminifers	Permian	2A
1PSc	MGU88-203-1	C158909	104G06	350442	6350345	? <i>Bothrophyllum</i> sp., schwagerinid fusulinacean foraminifers	Permian	2A
uCSs	MGU89-64	C158922	104G12	339087	6402542	Bothrophyllid corals, schwagerinid(?), fusulinacean foraminifers	probably early Permian	2B
uCSs	MGU89-140	C158927	104G12	340524	6381697	corals, <i>Fomichavella</i> sp. and <i>Arachnolasma</i> (?) sp.	Carboniferous	2B
uCSs	MGU89-142	C168065	104G12	340555	6380961	Bothrophyllid corals, tabulate coral	Carboniferous	2B
1PSc	MGU89-349	C168029	104G/05	348651	6350874	Bothrophyllid corals, bryozoans, brachiopods, schwagerinid fusulinacean foraminifers	Permian, Artinskian or younger	2B
1PSc	MGU89-353	C168033	104G/05	348370	6351229	Bothrophyllid corals, syringoporoid coral, gastropods, nodosarid foraminifers, schwagerinid fusulinacean foraminifers	Early Permian	2B
1PSc	MGU89-358	C168066	104G/05	349636	6351263	<i>Schizophoria</i> sp., nodosarid foraminifers	Permian	2B
1PSc	MGU89-378	C168054	104G/06	355381	6350040	Gastropods	probably Permian	2B
1PSc	MGU89-383	C168068	104G/06	358499	6353502	Solitary coral, schwagerinid fusulinacean foraminifers	Permian, Artinskian or younger	2B

REFERENCES:

1. E. T. Tozer, Geological Survey of Canada; A = Report TR-9-ETT-1989; B = Report ETT-1995-2.
2. E. W. Bamber, Institute of Sedimentary and Petroleum Geology, Paleontology Subdivision, Calgary, Alberta; A = Report C2-EWB-1988; B = Report C1-EWB-1990.
3. H. W. Tipper, Geological Survey of Canada, Vancouver; A = Report J4-89-HWT.
4. D. Ager, written communication, 1989.

APPENDIX 2
FUSULINACEAN AGE DETERMINATIONS

FIELD NO.	GSC NO.	NTS MAP	UTM EAST	Zone 09 NORTH	AGE	REF.
DBR88-132-2	C159123	104G05	348010	6351148	early Leonardian (Artinskian)	1
DBR88-117	C159141	104G06	350625	6350300	middle to late Wolfcampian (Asselian-Sakmarian)	1
DBR88-123	C158913	104G06	349794	6349995	middle to late Wolfcampian (Asselian-Sakmarian)	1
DBR88-125	C158914	104G06	349358	6350114	early Guadalupian (Wordian)	1
DBR88-126-1	C158915	104G05	349154	6350206	early Guadalupian (Wordian)	1
MGU88-203-1	C158909	104G06	350442	6350345	middle to late Wolfcampian (Asselian-Sakmarian)	1
MMC88-039-1	C154262	104G06	352470	6347570	middle to late Wolfcampian (Asselian-Sakmarian)	1
DBR88-332-1	C159147	104G05	350514	6350320	middle to late Wolfcampian (Asselian-Sakmarian)	1
DBR88-164-1	C159143	104G06	351416	6350418	middle to late Wolfcampian (Asselian-Sakmarian)	1
DBR88-164-2	C159144	104G06	351414	6350401	middle to late Wolfcampian (Asselian-Sakmarian)	1
DBR88-166-2	C159145	104G06	351268	6350411	Wolfcampian (?) (Asselian-Sakmarian)	1
DBR88-169-1	C159146	104G06	351030	6350365	middle to late Wolfcampian (Asselian-Sakmarian)	1
DBR88-118-1	C159142	104G05	350901	6350357	middle to late Wolfcampian (Asselian-Sakmarian)	1
MGU88-201-1	C158907	104G06	350280	6350361	middle to late Wolfcampian (Asselian-Sakmarian)	1
MGU88-202-1	C158908	104G06	350351	6350343	middle to late Wolfcampian (Asselian-Sakmarian)	1
MGU89-349	C168029	104G05	348651	6350874	early Guadalupian (Wordian)	1
MGU89-353	C168033	104G05	348370	6351229	Leonardian (Artinskian-Roadian)	1
MGU89-383	C168068	104G06	358499	6353502	early Guadalupian (Wordian)	1
DBR88-131-1	C159120	104G05	348112	6351112	Leonardian(?) (Artinskian-Roadian)	1
DBR88-010-1	C159118	104G05	348602	6351685	Leonardian (Artinskian-Roadian)	1
DBR88-010-2	C159119	104G05	348602	6351685	early Leonardian (Artinskian)	1
DBR88-250-1	C159148	104G06	358474	6353463	early Guadalupian (Wordian)	1
DBR88-251-1	C159149	104G06	358400	6353471	early Guadalupian (Wordian)	1
DBR88-252-1	C159150	104G06	358372	6353514	early Guadalupian (Wordian)	1
MMC88-046-1	C154263	104G06	354315	6347603	Wolfcampian (?) (Asselian-Sakmarian)	1
DBR91-340	C189813	104G12	325715	6396977	early Wolfcampian (Asselian)	3
INE91-144	C189814	104G12	327344	6402893	middle Leonardian (Artinskian)	3
MGU89-64	C158922	104G12	339087	6402542	late Wolfcampian (Sakmarian)	2

REFERENCES:

1. = Lin Rui, Report Number 1-RUI-1990, ISPG Calgary, Alberta.
2. = Lin Rui, Report Number 5-RUI-1991, ISPG Calgary, Alberta.
3. = Lin Rui, Report Number 1-RUI-1992, ISPG Calgary, Alberta.

** faunal lists are available upon request.

*** Time chart from Carter *et al.* (1991); those in brackets are from Harland *et al.* (1989).

APPENDIX 3
CONODONT IDENTIFICATIONS

MAP CODE	FIELD NO.	GSC No./ Map No.	NTS MAP	UTM EASTING	ZONE 09 NORTHING	DESCRIPTION OF FAUNA	AGE	CAI	REF.
STUHINI									
uTSs1	CGR89-171	C-168004	104G/12	351657	6389893	<i>Epigondolella ex gr. bidentata</i> (Mosher)	Late Triassic, late Norian	2.0-3.0	1
uTSs2	CGR89-232	C-168007	104G/12	357021	6381053	blade fragment ?	Ordovician - Triassic	-	1
L1	CGR89-260-1	C-168009	104G/12	345571	6400983	<i>Metapolygnathus primitus</i> (Mosher)	Late Triassic, late Carnian-early Norian	~3.0	1
L1	CGR89-260-2	C-168009	104G/12	345571	6400983	<i>Metapolygnathus?</i> sp.	Late Triassic	2.0-3.0	1
L1	CGR89-261	C-168010	104G/11	346037	6401176	<i>Metapolygnathus?</i> sp.	Late Triassic	2.0-3.0	1
uTSs2	CGR89-451	C-168022	104G/11	347639	6388801	<i>Epigondolella</i> sp.	Late Triassic, middle-late Norian	2.0-3.0	1
L2	DBR89-267-2	C-167912	104G/11	353320	6379515	<i>Epigondolella ex gr. bidentata</i> (Mosher)	Late Triassic, late Norian	~4.0	1
uTSs1	DBR89-49	C-158919	104G/12	348274	6400792	<i>Epigondolella n. sp.</i> C Orchard	Late Triassic, Middle Norian	~3.0	1
L1	DBR89-527	C-167915	104G/12	344216	6400424	<i>Metapolygnathus primitus</i> (Mosher)	Late Triassic, late Carnian-early Norian	3.0-4.0	1
uTSs1	DBR89-528-3	C-167916	104G/12	344201	6400372	<i>Metapolygnathus primitus</i> (Mosher)	Late Triassic, late Carnian-early Norian	3.0-4.0	1
uTSs1	DBR91-5	C-168096	104G/13	344430	6412093	<i>Neogondolella?</i> sp.	Triassic	6?	2
L1	DBR91-128	C-168097	104G/13	344859	6424406	<i>Metapolygnathus</i> sp., ramiform elements	Late Triassic, late Carnian	5.5-6.0	2
L1	DBR91-242	C-189803	104G/13	338687	6406402	<i>Metapolygnathus nodosus</i> (Hayashi 1968)	Late Triassic, late Carnian	5.0	2
uTSs1	DBR91-271	C-168073	104G/13	339475	6406661	<i>Metapolygnathus</i> sp. cf. <i>M. nodosus</i> (Hayashi 1968)	Late Triassic, late Carnian	4.5-5.5	2
uTSs1	DBR91-280	C-189802	104G/13	340451	6405804	<i>Metapolygnathus</i> sp., ramiform elements	Late Triassic, Carnian	5.0	2
L1	DBR91-298	C-168075	104G/13	340789	6426290	<i>Metapolygnathus</i> spp., ' <i>Neospathodus</i> ' sp.	Late Triassic, late? Carnian	5.5-7.0	2
L1	DBR91-322	C-189801	104G/13	331687	6404574	<i>Metapolygnathus</i> sp. cf. <i>M. nodosus</i> (Hayashi 1968)	Late Triassic, late Carnian	5.0	2
L1	DBR91-403	C-189808	104G/13	343012	6423956	<i>Metapolygnathus ex gr. nodosus</i> (Hayashi 1968), ramiform element	Late Triassic, late Carnian	5.0	2
L1	DBR91-449	C-168088	104G/13	328794	6421791	<i>Metapolygnathus</i> sp.	Late Triassic, Carnian	5.0	2
L0	INE91-130	C-168095	104G/13	336148	6425028	<i>Metapolygnathus ex gr. polygnathiformis</i> (Budurov and Stefanov 1965)	Late Triassic, early Carnian	4.5-5.5	2
L0	INE91-130	C-168095	104G/13	336148	6425028	<i>Metapolygnathus tadpole</i> (Hayashi 1968)			
L0	INE91-130	C-168095	104G/13	336148	6425028	<i>Neogondolella</i> sp. cf. <i>N. inclinata</i> (Kovacs 1983), ramiform elements			
L0	INE91-131	C-168094	104G/13	335841	6424799	<i>Metapolygnathus?</i> sp.	Middle-Late Triassic, late Ladinian-Carnian	6?	2
L0	INE91-131-2	C-168093	104G/13	335841	6424799	<i>Metapolygnathus</i> sp.	Late Triassic, Carnian	4.5	2
L1	INE91-231	C-189832	104G/13	333511	6430543	<i>Metapolygnathus</i> sp.	Late Triassic, Carnian	5.0-6.0	2
L1	INE91-235	C-168090	104G/13	333309	6431727	<i>Metapolygnathus nodosus</i> (Hayashi 1968), <i>Neogondolella inclinata</i> (Kovacs 1983)	Late Triassic, late Carnian	4.5-5.5	2
L1	INE91-235	C-168090	104G/13	333309	6431727	<i>Metapolygnathus</i> sp., <i>Neocaviteilla?</i> sp., <i>Neospathodus?</i> sp., ramiform elements			2
L1	JT191-59	C-189827	104G/13	331469	6431230	<i>Neogondolella?</i> sp.	probably Triassic	6.0	2
L1	JT191-61	C-189828	104G/13	344895	6427843	<i>Metapolygnathus</i> sp., ramiform elements	Late Triassic, Carnian	5.0-5.5	2
uTSs1	JT191-141	C-189830	104G/13	322323	6405003	<i>Metapolygnathus nodosus</i> (Hayashi 1968), ramiform elements	Late Triassic, late Carnian	5.0	2
TRIASSIC									
mTc	MGU89-396	C-168063	104G/06	357916	6353867	<i>Neogondolella</i> sp., ramiform elements	Triassic?	—	1
mTc	DBR91-139-2	C-167945	104G/12	323237	6403975	<i>Neostreptognathodus?</i> sp., <i>Hindeodus</i> sp., ramiform elements	Carboniferous? - Early Permian	5.0	2
mTc	DBR91-632	C-189824	104G/13	329002	6404711	<i>Neogondolella nepalensis</i> (Kozur and Mostler 1976), <i>Ellisonia</i> sp.	Early Triassic, Smithian	5.5	1
mTc	DBR91-632	C-189824	104G/13	329002	6404711	<i>Neospathodus</i> sp. cf. <i>N. pakistanensis</i> (Sweet 1970), ramiform element			1
mTc	DBR91-671	C-189825	104G/12	338266	6404658	<i>Neogondolella ex gr. foliata</i> (Budurov 1975), ramiform element	Middle Triassic, Ladinian	5.0	1
STIKINE									
IPSc	DBR88-124-1	C-154278	104G/05	349625	6349989	<i>Neogondolella</i> sp., <i>Neostreptognathodus</i> cf. <i>N. pequopensis</i> (Behnken 1975)	Early Permian, Artinskian	5.5-6.0	1
IPSc	DBR88-126-1	C-154280	104G/05	349154	6350206	<i>Neostreptognathodus</i> cf. <i>N. pequopensis</i> (Behnken 1975)	Early Permian, Artinskian	5.0-6.0	1
IPSc	DBR88-164-1	C-154288	104G/06	351416	6350418	<i>Neostreptognathodus</i> sp.	Early Permian, Artinskian	4.5-5.0	1
IPSc	DBR88-164-2	C-154289	104G/06	351414	6350401	<i>Neostreptognathodus?</i> sp.	Early Permian	5.0	1
IPSc	DBR88-166-2	C-154292	104G/06	351268	6350405	<i>Hindeodus</i> sp., ramiform elements	Carboniferous-Early Triassic	5.0-6.0	1
IPSc	DBR88-167-1	C-154293	104G/06	351199	6350390	<i>Neogondolella</i> sp.; <i>Neostreptognathodus</i> sp., ramiform elements	Early Permian, Artinskian	5.0-7.0	1
IPSc	DBR88-168-1	C-154294	104G/06	351149	6350384	<i>Neogondolella</i> sp.; <i>Neostreptognathodus?</i> sp.	Early Permian	5.0-6.0	1
IPSc	DBR88-169-3	C-154295	104G/06	351030	6350365	<i>Neostreptognathodus</i> sp., ramiform elements	Probably Early Permian	5.0-6.0	1

APPENDIX 3. Continued

uPs	DBR88-246-1	C-159127	104G/06	357894	6353908	<i>Neogondolella</i> sp., ramiform elements	Pemian	4.0-6.0	1
uPs	DBR88-250-1	C-159129	104G/06	358474	6353463	<i>Neogondolella</i> cf. <i>phosphoriensis</i> (Youngquist, Hawley & Miller).	Late Permian	8.0	1
uPs	DBR88-251-1	C-159130	104G/06	358400	6353471	<i>Hindeodus</i> sp.; <i>Neogondolella</i> sp., ramiform elements	Pemian	8.0	1
uPs	DBR88-252-1	C-159131	104G/06	358372	6353514	<i>Hindeodus</i> sp.; <i>Neogondolella</i> sp., ramiform elements	Late? Permian	6.5-7.0	1
uPs	DBR88-252-2	C-159132	104G/06	358379	6353513	<i>Hindeodus</i> sp.; <i>Neogondolella</i> sp., ramiform elements	Late? Permian	6.5-7.0	1
IPSc	DBR89-239	C-158936	104G/12	339524	6401229	Ramiform elements	Ordovician - Triassic	5.5	1
1PSc	MGU88-198-1	C-159134	104G/06	350472	6350814	<i>Ellisonia</i> sp., <i>Hindeodus</i> sp., <i>Neogondolella</i> sp., <i>Neostreptognathodus</i> sp.	Early Permian, Artinskian	4.5-5.5	1
1PSc	MGU88-199-1	C-159135	104G/06	350453	6350693	<i>Ellisonia</i> sp., <i>Hindeodus</i> sp., <i>Neogondolella</i> sp., <i>Neostreptognathodus</i> sp.	Early Permian, Artinskian	5.5-7.0	1
1PSc	MGU88-200-1	C-158906	104G/06	350409	6350560	Indeterminate productoid brachiopods, echinoderm columnal.	Carboniferous or Permian	5.0-5.5	1
1PSc	MGU88-200-1	C-159136	104G/06	350409	6350560	<i>Hindeodus</i> sp., ramiform elements	Carboniferous-Early Triassic	5.0-5.5	1
1PSc	MGU88-202-1	C-159138	104G/06	350351	6350343	Ramiform elements	Indeterminate	5.0+	1
1PSc	MGU88-203-1	C-159139	104G/06	350442	6350345	<i>Neogondolella</i> sp., <i>Neostreptognathodus</i> sp., ramiform elements	Early Permian	5.0-6.0	1
mTc	MGU89-29	C-158920	104G/12	338434	6403213	<i>Neogondolella</i> sp., <i>Neostreptognathodus?</i> sp., ramiform elements	Early Permian, ?Artinskian	5.0	1
uCSv	MGU89-300-2	C-158947	104G/12	343960	6376764	Ramiform elements	Ordovician-Triassic	5.0	1
1PSc	MGU89-327	C-168024	104G/05	349204	6350695	<i>Hindeodus</i> sp.	Early Carboniferous - Permian	5.5	1
1PSc	MGU89-337	C-168027	104G/06	350188	6350474	<i>Neogondolella</i> sp., <i>Ellisonia</i> sp., <i>Neostreptognathodus</i> sp.	Early Permian, Artinskian	5.5	1
uCSc	MGU89-359-2	C-168037	104G/05	343828	6357848	Ramiform elements	Pemian - Triassic	5.0	1
uCSc	MGU89-362-2	C-168040	104G/05	343537	6357594	<i>Neogondolella</i> sp., <i>Diplognathodus?</i> sp.	Late Carboniferous - Permian	5.0	1
IPSc	MGU89-376	C-168051	104G/06	354914	6350057	<i>Neogondolella</i> sp., <i>Sweetognathus</i> sp., <i>Ellisonia</i> sp., ramiform elements	Pemian	4.0-6.0	1
IPSc	MGU89-377	C-168052	104G/06	355094	6350052	<i>Neogondolella</i> sp., <i>Sweetognathus?</i> sp., ramiform elements	Pemian	5.0-7.0	1
IPSc	MGU89-378	C-168053	104G/06	355381	6350040	<i>Neostreptognathodus</i> sp.	Early Permian, Artinskian	4.5-5.0	1
IPSc	MGU89-383	C-168055	104G/06	358499	6353502	<i>Ellisonia</i> sp., <i>Hindeodus</i> sp., <i>Neogondolella</i> sp., ramiform elements	Late? Permian	7.0+	1
IPSc	MGU89-63	C-158921	104G/12	339186	6402477	<i>Adetognathus</i> sp., ramiform elements	Late Carboniferous - Early Permian (Sakmarian)	4.5	1
IPSc	MGU89-64	C-158923	104G/12	339087	6402542	<i>Adetognathus</i> sp., ' <i>Neostreptognathodus</i> ' sp., ramiform elements	Artinskian-Sakmarian, ? Artinskian	4.5	1
IPSc	MMC88-185-1	C-159113	104G/06	346956	6354862	Ramiform elements	Indeterminate	5.0-5.5	1
IPSc	DBR91-227	C-167949	104G/12	345997	6403031	<i>Neostreptognathodus?</i> sp. aff. <i>N. pequopensis</i> (Behnken 1975)	Early Permian, Artinskian	5.0-5.5	2
IPSc	DBR91-227	C-167949	104G/12	345997	6403031	<i>Neogondolella</i> sp. cf. <i>N. idahoensis</i> , ramiform elements			2
uCSv	DBR91-493	C-189810	104G/13	324733	6428028	<i>Neogondolella</i> sp. indet.	Probably Permian	6.0	2
IPSc	DBR91-688	C-189822	104G/12	335416	6403201	platform fragment	?Carboniferous-Triassic	5.5-6.0	2

Reference:

1. Orchard, M.J., 1990, Geological Survey of Canada, Report number MJO/Nov. 90.
2. Orchard, M.J., 1992, Geological Survey of Canada, Report number OF-1992-26

APPENDIX 4
BARREN CONODONT COLLECTIONS

MAP CODE	FIELD NO.	GSC NO.	NTS MAP	UTM EASTING	Zone 09 NORTHING
STUHINI GROUP					
uTSmv	DBR88-103-1	C-154271	104G/06	360103	6357504
L1	CGR89-260-2	C-168008	104G/11	345571	6400983
L1	CGR89-303	C-158949	104G/12	340341	6399465
L2	CGR89-308	C-168042	104G/12	353543	6377410
L1	DBR89-51	C-158925	104G/12	348323	6400898
L2	DBR89-156	C-158934	104G/11	349338	6389208
L2	DBR89-291	C-167911	104G/11	355092	6378763
uTSmv	MMC88-163-1	C-159109	104G/06	360688	6359191
uTSmv	MMC88-163-2	C-159110	104G/06	360689	6359183
uTSmv	MMC88-164-1	C-159111	104G/06	360595	6359040
uTpm	DBR88-043-1	C-154270	104G/06	358583	6354676
uTp	MMC88-160-1	C-159108	104G/06	360873	6359576
uTSs1	CGR89-302	C-158950	104G/12	340607	6399452
uTSs1	DBR89-498-3	C-168041	104G/12	352240	6402171
uTSs1	CGR89-169	C-168003	104G/12	351657	6389893
uTSs1	CGR89-172	C-168005	104G/12	351657	6389893
uTSs2	DBR89-160	C-167913	104G/11	349517	6389094
uTSv	CGR89-391	C-168043	104G/11	335917	6391964
uTSs2	CGR89-230	C-168006	104G/12	356984	6381096
uTSv	DBR89-495-5	C-167914	104G/12	349820	6400261
uTSs1	DBR89-497-1	C-167917	104G/12	351176	6401499
uTs	MMC88-146-3	C-159106	104G/06	356073	6357142
mTc	CGR89-278	C-168012	104G/12	343101	6402251
uTSs1	CGR89-288	C-168013	104G/12	344401	6402644
uTSs1	DBR89-247-1	C-158937	104G/12	342741	6401677
uTSs1	DBR91-604	C-189826	104G/13	322954	6411474
mTc	DBR91-139-2	C-167945	104G/13	323237	6403975
uTSv	JTI91-31	C-189809	104G/13	324428	6422678
IPSc	DBR91-340	C-189804	104G/13	325715	6396977
uTSs	DMU91-93	C-168077	104G/13	326575	6413930
uTSv	INE91-92	C-168098	104G/13	330641	6414764
uTSs1	INE91-229	C-189831	104G/13	333856	6430863
uTSv	DBR91-400	C-168089	104G/13	335449	6415727
uTSs1	DBR91-185	C-167947	104G/13	342895	6413535
IPSc	JTI91-80	C-189829	104G/13	342904	6424881
IPSc	INE91-182-3	C-168091	104G/13	343055	6428199
uTSv	INE91-3	C-168100	104G/13	348970	6416453
STIKINE ASSEMBLAGE					
IPSc	CGR89-275	C-168071	104G/11	343164	6402043
uCs	CGR89-398-2	C-167919	104G/11	335482	6402326
uCs	CGR89-398-3	C-167920	104G/11	335482	6402326
IPSc	DBR88-010-2	C-154266	104G/05	348608	6351666
IPs	DBR88-024-1	C-154267	104G/06	357507	6351702
IPSc	DBR88-117-3	C-154274	104G/05	350625	6350300
IPSc	DBR88-118-3	C-154275	104G/05	350901	6350357
IPSc	DBR88-125-1	C-154279	104G/05	349358	6350114
IPSc	DBR88-127-1	C-154281	104G/05	348928	6350248
IPSc	DBR88-128-1	C-154282	104G/05	348671	6350220
IPSa	DBR88-129-1	C-159133	104G/05	347956	6351246
IPSc	DBR88-131-3	C-154283	104G/05	348112	6351112
IPSa	DBR88-132-1	C-154284	104G/05	348010	6351148
IPSa	DBR88-132-4	C-154285	104G/05	348032	6351146
IPSc	DBR88-165-1	C-154290	104G/06	351348	6350409
IPSc	DBR88-166-1	C-154291	104G/06	351268	6350411
Ist	DBR88-178-1	C-159102	104G/05	345672	6352353
uCs?	DBR88-179-1	C-159103	104G/05	345570	6352397
IPSc	DBR88-332-5	C-159140	104G/05	350514	6350320
IPSc	DBR89-228	C-158935	104G/12	336721	6400940
uCSs	MGU88-001-1	C-154272	104G/05	343659	6357535
Ist	MGU88-060-1	C-154296	104G/05	340602	6357836
Ist	MGU88-061-1	C-154297	104G/05	340639	6357660
Ist	MGU88-062-1	C-154298	104G/05	340639	6357586
Ist	MGU88-063-1	C-154299	104G/05	340613	6357470
Ist	MGU88-067-1	C-154300	104G/05	340618	6357169
Ist	MGU88-068-1	C-158901	104G/05	340618	6357083
Ist	MGU88-130-1	C-159105	104G/05	341285	6356625
IPSc	MGU88-201-1	C-159137	104G/06	350280	6350361
uCSs	MGU89-140	C-158928	104G/12	340524	6381697
uCSs	MGU89-142	C-158930	104G/12	340555	6380961
uCSs	MGU89-201	C-158931	104G/12	336440	6388157
IPSc	MGU89-207-1	C-158932	104G/12	336698	6389294
IPSc	MGU89-207-2	C-158933	104G/12	336698	6389294

IPSc	MGU89-286		104G/05	342352	6373628
uCSv	MGU89-300-2	C-158947	104G/12	344000	6376764
uCSv	MGU89-300-3	C-158948	104G/12	344000	6376764
IPSc	MGU89-329	C-168025	104G/05	349099	6350812
IPSc	MGU89-330	C-168026	104G/05	349000	6350990
IPSc	MGU89-349	C-168028	104G/06	348651	6350874
IPSc	MGU89-350	C-168030	104G/06	348621	6350930
IPSc	MGU89-352	C-168031	104G/05	348468	6351134
IPSc	MGU89-353	C-168032	104G/05	348370	6351229
IPSc	MGU89-354	C-168034	104G/05	348290	6351320
IPSc	MGU89-357-1	C-168035	104G/05	348559	6351559
IPSc	MGU89-357-2	C-168036	104G/05	348511	6351558
uCSs	MGU89-360		104G/05	343778	6357807
uCSs	MGU89-361		104G/05	343574	6357618
uCSs	MGU89-79-2	C-158924	104G/12	338431	6385488
uCSv	MMC88-030-1	C-154258	104G/05	340820	6361353
uCSv	MMC88-031-1	C-154259	104G/05	340908	6361445
uCSv	MMC88-033-1	C-154260	104G/05	341115	6361418
IPSc	MMC88-040-1	C-154261	104G/06	352653	6347550
IPSc	MMC88-046-3	C-158916	104G/06	354315	6347603
sls	MMC88-060-1	C-154264	104G/05	340624	6357735
uCS?	MMC88-089-1	C-154265	104G/05	346375	6349322
uCSs	MMC88-181-1	C-159112	104G/06	346185	6354849
st	MMC88-188-1	C-159114	104G/06	347072	6354478
IPSc	MMC88-189-1	C-159115	104G/06	347083	6354350
uCSv	MMC88-194-2	C-159116	104G/05	341883	6361269
uCSs	MMC88-200-1	C-159117	104G/05	343031	6361417
IPSc	DBR90-006	C-167928	104G/05	346868	6348115
IPSc	DBR90-009	C-167939	104G/05	347026	6347869
uTSmv	DBR90-090	C-167930	104G/06	360766	6358728
uTSmv	DBR90-091	C-167931	104G/06	360767	6358728
uTSs1	DBR90-116	C-167936	104G/12	329496	6403156
uTSs1	DBR90-117	C-167938	104G/12	329381	6403081
uTSs1	DBR90-124	C-167932	104G/12	328549	6403285
uTSs1	DBR90-125	C-167933	104G/12	328587	6403262
uTSv	DBR90-144	C-167934	104G/06	359271	6355660
IPSc	DBR91-129	C-167942	104G/13	322211	6403938
uCSc	INE91-341-2	C-189833	104G/13	322331	6395934
uTSs	DBR91-643-2	C-189823	104G/13	322620	6413673
IPSc	INE91-49	C-168080	104G/13	322837	6403554
IPSc	INE91-50	C-168081	104G/13	322846	6403450
IPSc	DBR91-137	C-167943	104G/13	323175	6403844
IPSc	INE91-159	C-168092	104G/13	323629	6402593
uCS	DBR91-359	C-189807	104G/13	324350	6402940
uTSs	DBR91-487	C-189806	104G/13	324745	6427267
IPSc	DBR91-150	C-167946	104G/13	324852	6403611
ICSv	DBR91-505	C-189805	104G/13	324932	6429347
st	DBR91-567	C-189821	104G/13	326919	6420317
mTc	INE91-144	C-168099	104G/13	327344	6402893
uTSs1	DBR91-628	C-189820	104G/13	328397	6404309

References:

- Orchard, M.J. (1990): Geological Survey of Canada, Report number MJO/Nov. 90.
Orchard, M.J. (1992): Geological Survey of Canada, Report number OF-1992-1.

APPENDIX 5
RADIOLARIAN AGE DETERMINATIONS

FIELD NO.	GSC NO.	NTS MAP	UTM ZONE 09		AGE	REF.
			EAST	NORTH		
STUHINI GROUP						
DBR88-043-1	C154270	104G06	358583	6354676	indeterminate	1
DBR91-604	C189826	104G13	322958	6411698	Phanerozoic	2
Unit mTc						
DBR90-117	C167938	104G12	329381	6403081	Middle Triassic - Ladinian	3
DBR90-139	C167944	104G12	323257	6404186	Phanerozoic	2
DBR91-222	C167948	104G12	346614	6403173	Phanerozoic	2
DBR91-628	C189820	104G12	328390	6404519	late Early Permian - Artinskian to Kungurian	2
STIKINE ASSEMBLAGE						
MGU88-001-1	C154272	104G05	343659	6357535	indeterminate	1

Fauna descriptions are available upon request.

REFERENCES:

1. Orchard, M.J., 1990, Geological Survey of Canada, Report number MJO/Nov. 90.
2. Cordey, F., 1992, Geological Survey of Canada, Report number FC-1992-2.
3. Cordey, F., personal communication, July 13, 1992.

APPENDIX 6
SAMPLES BARREN OF RADIOLARIA

FIELD NO.	GSC NO.	NTS MAP	UTM Zone 09		REF.
			EAST	NORTH	
STUHINI GROUP					
MMC88-158-3	C159107	104G06	360977	6359852	1
DBR89-247	C158937	104G12	342741	6401677	2
STIKINE ASSEMBLAGE					
DBR88-171-1	C159101	104G05	346401	6351266	1
DBR88-075-1	C158917	104G05	340333	6372881	1
CGR89-278	C168012	104G11	343101	6402251	2
CGR89-288	C168013	104G11	344401	6402644	2
DBR88-133-2	C154287	104G05	347811	6351332	1
MGU88-004-1	C154273	104G05	343752	6357140	1
DBR88-024-2	C154268	104G06	357512	6351717	1
DBR88-025-1	C154269	104G06	357883	6353807	1
DBR88-242-1	C158918	104G06	359308	6350367	1
DBR88-245-1	C159126	104G06	358029	6353881	1
DBR88-246-1	C159127	104G06	357894	6353908	1
DBR88-247-1	C159128	104G06	357836	6353958	1

REFERENCES:

1. Orchard, M.J., 1990. Geological Survey of Canada, Report number MJO/Nov. 90.
2. Cordey, F., 1992, personal communication.

APPENDIX 7
PALYNOMORPH COLLECTIONS

MAP NO.	MAP CODE	FIELD NO.	GSC NO.	NTS MAP	UTM Zone 09 EAST	NORTH	AGE	REF.
SUSTUT								
C4	KTS	DBR89-414	C167903	104G11	369925	6384925	early Paleocene	1
C1	KTS	CGR89-68	C167905	104G11	359040	6393772	indeterminate	1
C2	KTSr	CGR89-128	C167906	104G12	360116	6393971	indeterminate	1
C3	KTS	DBR89-268	C167901	104G11	347336	6385398	indeterminate	1
C5	KTS	DBR90-25	C167921	104G11	358264	6389001	indeterminate	2
C6	KTS	DBR90-26	C167922	104G11	358341	6388844	indeterminate	2
C7	KTS	DBR90-27	C167923	104G11	358351	6388796	indeterminate	2
C8	KTS	DBR90-28	C167924	104G11	353888	6392293	indeterminate	2
C9	KTS	DBR90-29	C167925	104G11	353872	6392340	indeterminate	2
C10	KTS	DBR90-30	C167926	104G11	354065	6392360	indeterminate	2
C11	KTS	DBR90-31	C167927	104G11	353996	6392422	indeterminate	2
HAZELTON								
C12	ImJHv	DBR89-275	C167902	104G11	347282	6385285	indeterminate	1
C13	IJHs	DBR89-424	C167904	104G11	354787	6381410	indeterminate	1

References:

1. Sweet, A.R., 1989, Paleontology Division, ISPG, Calgary, Alberta, Report number AS-1989-6.
2. Sweet, A.R., 1990, Paleontology Division, ISPG, Calgary, Alberta, Report number AS-90-08.

APPENDIX 8
WHOLE-ROCK AND TRACE ELEMENT CHEMISTRY OF STRATIFIED ROCKS

FIELD NO	NTS MAP Zone 9	UTM EAST	UTM NORTH	MAP CODE	ROCK CODE	SiO ₂ %	TiO ₂ %	Al ₂ O ₃ %	Fe ₂ O _{3t} %	MnO %	MgO %	CaO %	Na ₂ O %	K ₂ O %
DETECTION LIMITS:						0.01	0.01	0.01	0.01	0.01	0.01	0.01	0.01	0.01
ANALYTICAL TECHNIQUE:						XRF / ICP	XRF / ICP	XRF / ICP	XRF / ICP	XRF / ICP	XRF / ICP	XRF / ICP	XRF / ICP	XRF / ICP
Unit Mb:														
DBR91-695	104G13	337841	6409497	Mb	BSLT	56.57	0.98	15.09	7.35	0.13	4.28	4.87	3.58	2.29
DBR91-695-2*	104G13	337841	6409497	Mb	BSLT	56.25	0.98	15.00	7.38	0.14	4.52	4.65	3.78	2.23
DBR91-695-3	104G13	337841	6409497	Mb	BSLT	56.14	1.01	15.02	7.50	0.13	4.63	4.52	3.93	2.06
Sloko Group:														
FLOWS and/or SILLS														
DBR89-198-3	104G11	353015	6392471	TS	DCIT	64.13	0.43	16.29	4.44	0.17	0.81	2.51	5.35	2.61
DBR89-458	104G11	351448	6392545	TSd	BSLT	54.10	0.92	17.02	8.67	0.18	3.59	5.44	3.82	2.03
DBR89-459*	104G11	351457	6392485	TSd	RDCT	57.06	0.72	14.50	6.61	0.15	1.77	6.05	2.50	2.09
DBR89-460*	104G11	351269	6391945	TSb	TCAN	55.47	0.77	16.26	7.43	0.16	2.97	6.18	2.50	2.28
DBR89-468	104G11	352432	6392380	TSb	BSLT	59.54	0.70	16.74	6.36	0.17	2.25	5.39	3.89	2.26
DBR89-469	104G11	352432	6392380	TSd	FLOW	61.47	0.65	14.98	6.08	0.18	1.88	4.18	3.90	2.62
DBR89-470	104G11	352432	6392380	TSb	TCAN	55.94	0.94	16.81	8.16	0.17	3.19	6.35	3.50	2.06
DBR89-471	104G11	352738	6392320	TSd	ANDS	60.96	0.42	17.22	4.50	0.15	1.11	3.41	5.15	2.54
VOLCANICLASTIC ROCKS														
DBR89-467	104G11	352272	6392237	TSd	VCCB	60.29	0.62	16.93	5.63	0.17	2.10	4.18	3.90	2.82
Sustut Group:														
FLOWS and/or SILLS														
CGR89-200-2*	104G12	353526	6395831	KTS	ANDS	52.91	0.89	16.47	8.79	0.24	1.83	7.12	3.91	1.79
CGR89-200-3	104G12	353526	6395831	KTS	ANDS	54.82	0.90	17.02	8.22	0.12	3.36	6.04	3.29	1.96
VOLCANICLASTIC ROCKS														
CGR89-200-1	104G12	353526	6395831	KTS	TUFF	74.31	0.15	12.75	1.20	0.02	0.42	0.76	0.92	6.81
Hazelton Group:														
FLOWS and/or SILLS														
CGR89-217	104G12	355389	6378238	ImJHv	ANDS	54.10	0.72	17.74	8.32	0.14	3.41	3.89	5.96	0.64
CGR89-227	104G12	356604	6381458	ImJHv	ANDS	56.74	0.75	16.53	7.90	0.15	3.16	5.99	3.11	2.03
CGR89-237	104G12	356002	6380736	ImJHv	FLOW	56.98	0.79	16.90	7.33	0.17	3.53	7.23	2.70	2.17
CGR89-30	104G11	367720	6388518	ImJHv	ANDS	51.74	1.10	17.03	8.91	0.16	4.13	7.92	3.35	1.85
CGR89-439	104G11	348412	6387905	ImJHv	ANDS	56.35	0.80	16.89	7.39	0.15	2.96	6.93	3.09	1.98
CGR89-467	104G12	355236	6380092	ImJHv	ANDS	52.02	0.69	18.42	8.66	0.18	3.99	9.05	2.71	1.21
CGR89-48	104G11	363364	6390305	ImJHv	FPPP	58.23	0.64	16.93	7.91	0.12	2.10	5.76	2.91	2.18
CGR89-511	104G11	354835	6386287	ImJHv	ANDS	53.11	1.02	16.38	8.91	0.24	5.04	4.11	5.71	0.67
DBR89-155*	104G11	349364	6389572	ImJHv	ANDS	50.56	0.93	16.84	7.98	0.15	2.96	5.92	4.08	1.94
DBR89-303*	104G11	354320	6379905	ImJHd	RYLT	70.73	0.23	14.22	3.06	0.03	1.25	1.27	1.79	3.68
DBR89-377	104G11	348341	6387506	ImJHv	RYLT	71.80	0.24	14.09	3.37	0.01	0.20	0.24	3.40	4.80
DBR89-430	104G11	354407	6381909	ImJHb	BSLT	49.53	0.84	16.00	8.58	0.14	5.55	11.23	2.01	1.17
DBR89-432*	104G11	353476	6381935	ImJHb	BSLT	52.54	1.02	16.24	8.26	0.16	4.62	6.98	2.93	1.82
DBR89-435	104G11	353139	6382257	ImJHv	ANDS	64.75	0.59	15.47	3.87	0.10	0.76	2.55	4.06	4.09
DBR90-151*	104G11	354265	6381506	ImHd	RYLT	47.10	1.05	18.46	6.80	0.14	4.78	5.59	5.05	2.02
DBR90-162*	104G11	355655	6377046	ImHv	ANDS	47.66	1.04	17.70	9.28	0.19	2.96	11.10	2.28	0.60
DBR91-714*	104G12	348865	6385994	ImHv	ANDS	61.25	0.60	15.57	5.88	0.10	1.01	3.48	3.11	2.83
DBR91-715*	104G12	348912	6386070	ImHv	ANDS	50.12	0.92	16.75	10.95	0.17	2.89	5.03	6.96	0.51
DBR91-716	104G12	348917	6386091	ImHv	ANDS	48.58	0.93	17.68	10.27	0.19	3.66	8.49	3.41	2.58
DBR91-719*	104G12	348639	6386112	ImHb	BSLT	47.74	0.89	16.31	8.17	0.31	3.47	7.57	6.17	0.45
DBR91-720	104G12	348626	6386148	ImHb	BSLT	51.64	0.97	16.60	10.88	0.16	3.03	3.82	7.51	0.13

FIELD NO	NTS MAP Zone 9	UTM EAST	UTM NORTH	MAP CODE	ROCK CODE	K ₂ O/Na ₂ O Ratio	P ₂ O ₅ %	LOI %	OX_SUM %	Fe ₂ O ₃ %	FeO %	S %	CO ₂ %	Ni ppm	Mo ppm	Zn ppm
DETECTION LIMITS:							0.01	0.01						5	8	2
ANALYTICAL TECHNIQUE:							XRF / ICP	XRF / ICP	XRF / ICP	calc.	TIT			AAS	AAS	AAS
Unit Mb:																
DBR91-695	104G13	337841	6409497	Mb	BSLT	0.64	0.31	3.79	99.24	5.05	2.07					
DBR91-695-2*	104G13	337841	6409497	Mb	BSLT	0.59	0.31	4.17	99.41	4.59	2.51					
DBR91-695-3	104G13	337841	6409497	Mb	BSLT	0.52	0.32	3.85	99.11	4.19	2.97					
Stoko Group:																
FLOWS and/or SILLS																
DBR89-198-3	104G11	353015	6392471	TS	DCIT	0.49	0.24	2.22	99.20	3.56	0.79	0.01	0.40			91
DBR89-458	104G11	351448	6392545	TSd	BSLT	0.53	0.36	2.95	99.08	3.97	4.23	0.01	0.90			97
DBR89-459*	104G11	351457	6392485	TSd	RDCT	0.84	0.24	8.24	99.93	4.53	1.87	0.01	4.52			89
DBR89-460*	104G11	351269	6391945	TSb	TCAN	0.91	0.27	5.23	99.52	3.24	3.77	0.01	2.66			84
DBR89-468	104G11	352432	6392380	TSb	BSLT	0.58	0.23	2.22	99.75	4.45	1.72	0.01	0.14			81
DBR89-469	104G11	352432	6392380	TSd	FLOW	0.67	0.21	3.30	99.45	5.52	0.50	0.01	0.65			75
DBR89-470	104G11	352432	6392380	TSb	TCAN	0.59	0.26	1.90	99.28	4.17	3.59	0.01	0.14			89
DBR89-471	104G11	352738	6392320	TSd	ANDS	0.49	0.25	3.59	99.30	3.14	1.22	0.01	0.14			95
VOLCANICLASTIC ROCKS																
DBR89-467	104G11	352272	6392237	TSd	VCCB	0.72	0.23	2.58	99.45	3.95	1.51	0.01	0.47			85
Sustut Group:																
FLOWS and/or SILLS																
CGR89-200-2*	104G12	353526	6395831	KTS	ANDS	0.46	0.26	5.49	99.70	4.32	4.02	0.01	3.19			88
CGR89-200-3	104G12	353526	6395831	KTS	ANDS	0.60	0.27	3.70	99.70	5.19	2.73	0.01	0.36			89
VOLCANICLASTIC ROCKS																
CGR89-200-1	104G12	353526	6395831	KTS	TUFF	7.40	0.03	2.81	100.18	0.80	0.36	0.01	0.14			29
Hazelton Group:																
FLOWS and/or SILLS																
CGR89-217	104G12	355389	6378238	ImJHv	ANDS	0.11	0.26	3.92	99.10	6.16	1.94	0.01	1.23			70
CGR89-227	104G12	356604	6381458	ImJHv	ANDS	0.65	0.16	3.26	99.78	4.47	3.09	0.01	1.45			70
CGR89-237	104G12	356002	6380736	ImJHv	FLOW	0.80	0.20	1.67	99.67	3.65	3.31	0.01	0.14			70
CGR89-30	104G11	367720	6388518	ImJHv	ANDS	0.55	0.39	2.77	99.35	5.64	2.94	0.01	0.77			69
CGR89-439	104G11	348412	6387905	ImJHv	ANDS	0.64	0.24	2.84	99.62	4.43	2.66	0.01	1.44			71
CGR89-467	104G12	355236	6380092	ImJHv	ANDS	0.45	0.17	2.31	99.41	4.03	4.17	0.01	0.79			71
CGR89-48	104G11	363364	6390305	ImJHv	FPPP	0.75	0.18	2.38	99.34	3.92	3.59	0.01	0.51			66
CGR89-511	104G11	354835	6386287	ImJHv	ANDS	0.12	0.28	3.62	99.09	5.23	3.31	0.01	1.37			130
DBR89-155*	104G11	349364	6389572	ImJHv	ANDS	0.48	0.45	7.36	99.17	6.62	1.22	0.01	1.08			93
DBR89-303*	104G11	354320	6379905	ImJHd	RYLT	2.06	0.03	3.57	99.86	1.46	1.44	0.01	1.01			52
DBR89-377	104G11	348341	6387506	ImJHv	RYLT	1.41	0.02	1.39	99.56	2.97	0.36	0.01	0.14			44
DBR89-430	104G11	354407	6381909	ImJHb	BSLT	0.58	0.15	4.02	99.22	2.68	5.31	0.01	2.02			59
DBR89-432*	104G11	353476	6381935	ImJHb	BSLT	0.62	0.27	4.60	99.44	3.31	4.45	0.01	2.06			72
DBR89-435	104G11	353139	6382257	ImJHv	ANDS	1.01	0.17	3.55	99.96	3.24	0.57	0.01	1.91			44
DBR90-151*	104G11	354265	6381506	ImHd	RYLT	0.40	0.24	7.49	98.72	1.27	4.97	0.21	3.66			
DBR90-162*	104G11	355655	6377046	ImHv	ANDS	0.26	0.20	5.71	98.72	2.78	5.84	0.01	3.44			
DBR91-714*	104G12	348865	6385994	ImHv	ANDS	0.91	0.15	5.61	99.59	5.15	0.66					
DBR91-715*	104G12	348912	6386070	ImHv	ANDS	0.07	0.21	4.75	99.26	9.28	1.50					
DBR91-716	104G12	348917	6386091	ImHv	ANDS	0.76	0.23	3.02	99.04	6.60	3.30					
DBR91-719*	104G12	348639	6386112	ImHb	BSLT	0.07	0.20	8.19	99.47	4.05	3.70					
DBR91-720	104G12	348626	6386148	ImHb	BSLT	0.02	0.20	4.07	99.01	8.03	2.56					

FIELD NO	NTS MAP Zone 9	UTM EAST	UTM NORTH	MAP CODE	ROCK CODE	Cr ppm 10 XRF	Ba ppm 10 XRF	Sr ppm 5 XRF	Rb ppm 10 XRF	Zr ppm 20 XRF	Y ppm 10 XRF	Nb ppm 5 XRF	Ta ppm NA XRF	V ppm 5 XRF	La ppm 15 XRF	Sn ppm NA XRF	Th ppm NA XRF	U ppm NA XRF
DETECTION LIMITS:																		
ANALYTICAL TECHNIQUE:																		
Unit Mb:																		
DBR91-695	104G13	337841	6409497	Mb	BSLT	113		531	54	171	21	8	<15					
DBR91-695-2*	104G13	337841	6409497	Mb	BSLT	108		469	50	171	23	9	<15					
DBR91-695-3	104G13	337841	6409497	Mb	BSLT	105		431	42	171	20	9	<15					
Sloko Group:																		
FLOWS and/or SILLS																		
DBR89-198-3	104G11	353015	6392471	TS	DCIT	5	1611	405	45	166	25	7		44	25			
DBR89-458	104G11	351448	6392545	TSd	BSLT	15	1418	894	35	115	28	6		154	30			
DBR89-459*	104G11	351457	6392485	TSd	RDCT	14	884	282	48	117	24	7		133	19			
DBR89-460*	104G11	351269	6391945	TSb	TCAN	16	1368	631	33	128	26	5		145	20			
DBR89-468	104G11	352432	6392380	TSb	BSLT	21	1471	594	34	153	27	6		116	27			
DBR89-469	104G11	352432	6392380	TSd	FLOW	23	1868	585	48	135	27	9		106	16			
DBR89-470	104G11	352432	6392380	TSb	TCAN	24	1245	587	39	141	27	8		180	22			
DBR89-471	104G11	352738	6392320	TSd	ANDS	4	1602	500	42	181	26	8		34	29			
VOLCANICLASTIC ROCKS																		
DBR89-467	104G11	352272	6392237	TSd	VCCB	12	1709	660	44	168	29	8		93	20			
Sustut Group:																		
FLOWS and/or SILLS																		
CGR89-200-2*	104G12	353526	6395831	KTS	ANDS	18	1183	396	28	123	28	11		172	20			
CGR89-200-3	104G12	353526	6395831	KTS	ANDS	19	1173	571	36	127	30	9		171	11			
VOLCANICLASTIC ROCKS																		
CGR89-200-1	104G12	353526	6395831	KTS	TUFF	4	1157	72	121	131	22	13		9	33			
Hazleton Group:																		
FLOWS and/or SILLS																		
CGR89-217	104G12	355389	6378238	ImJHv	ANDS	20	447	783	15	82	24	5		183	8	17	<15	<15
CGR89-227	104G12	356604	6381458	ImJHv	ANDS	23	1095	406	37	118	26	7		183	21	<15	<15	<15
CGR89-237	104G12	356002	6380736	ImJHv	FLOW	22	1015	430	49	127	25	11		198	16	<15	<15	<15
CGR89-30	104G11	367720	6388518	ImJHv	ANDS	44	1109	587	30	140	30	11		240	25	<15	<15	<15
CGR89-439	104G11	348412	6387905	ImJHv	ANDS	23	1091	465	41	131	26	7		178	19	17	<15	<15
CGR89-467	104G12	355236	6380092	ImJHv	ANDS	16	689	406	24	83	22	6		196	18	<15	<15	<15
CGR89-48	104G11	363364	6390305	ImJHv	FPPP	15	1127	404	42	109	22	6		183	20	<15	<15	<15
CGR89-511	104G11	354835	6386287	ImJHv	ANDS	100	401	361	19	143	27	9		198	22	<15	<15	<15
DBR89-155*	104G11	349364	6389572	ImJHv	ANDS	19	394	502	40	200	29	13		192	30			
DBR89-303*	104G11	354320	6379905	ImJHd	RYLT	4	1030	178	107	284	30	15		2	31			
DBR89-377	104G11	348341	6387506	ImJHv	RYLT	4	2539	144	101	278	36	12		20	42			
DBR89-430	104G11	354407	6381909	ImJHb	BSLT	158	455	307	22	87	27	8		213	17			
DBR89-432*	104G11	353476	6381935	ImJHb	BSLT	71	811	444	33	145	27	8		185	18			
DBR89-435	104G11	353139	6382257	ImJHv	ANDS	6	1106	153	111	258	31	11		49	18			
DBR90-151*	104G11	354265	6381506	ImHd	RYLT	22	1129	569	10	131	27	7		234	25			
DBR90-162*	104G11	355655	6377046	ImHv	ANDS	36	473	497	10	71	21	5		306	15			
DBR91-714*	104G12	348865	6385994	ImHv	ANDS	<10		222	79	133	20	9	<15					
DBR91-715*	104G12	348912	6386070	ImHv	ANDS	<10		357	<10	71	18	6	<15					
DBR91-716	104G12	348917	6386091	ImHv	ANDS	<10		739	42	76	24	9	<15					
DBR91-719*	104G12	348639	6386112	ImHb	BSLT	17		392	<10	97	25	7	<15					
DBR91-720	104G12	348626	6386148	ImHb	BSLT	20		370	<10	98	23	6	<15					

FIELD NO	NTS MAP Zone 9	UTM EAST	UTM NORTH	MAP CODE	ROCK CODE	SiO ₂ %	TiO ₂ %	Al ₂ O ₃ %	Fe ₂ O _{3t} %	MnO %	MgO %	CaO %	Na ₂ O %	K ₂ O %
DETECTION LIMITS:						0.01	0.01	0.01	0.01	0.01	0.01	0.01	0.01	0.01
ANALYTICAL TECHNIQUE:						XRF / ICP	XRF / ICP	XRF / ICP	XRF / ICP	XRF / ICP	XRF / ICP	XRF / ICP	XRF / ICP	XRF / ICP
VOLCANICLASTIC ROCKS														
CGR89-229	104G12	356793	6381361	lnJHv	CLTF	51.99	0.98	17.89	9.15	0.18	3.83	7.09	4.15	0.49
Stuhini Group:														
FLOWS and/or SILLS														
CGR89-10	104G11	350344	6391596	uTSv	FLOW	49.27	0.91	13.01	11.16	0.21	8.17	9.97	3.27	1.39
CGR89-183	104G11	341342	6391774	uTSv	BSLT	46.74	0.74	12.33	10.83	0.18	8.55	11.86	1.90	2.23
CGR89-183DUF	104G11	341342	6391774	uTSv	BSLT	46.88	0.74	12.33	10.78	0.18	8.56	11.85	1.95	2.26
CGR89-264	104G11	345426	6400750	uTSvb	BSLT	48.71	0.82	14.42	9.38	0.17	6.81	10.40	3.48	0.89
CGR89-268	104G11	345684	6400469	uTSvp	FLOW	48.35	0.86	13.82	10.26	0.19	6.78	9.05	2.74	3.15
CGR89-335	104G12	352292	6376373	uTSvb	BSLT	46.75	0.65	9.76	10.82	0.37	10.76	14.39	1.11	0.57
CGR89-533	104G12	340089	6393659	uTSv	BSLT	46.26	0.70	10.48	11.88	0.22	11.17	13.10	1.83	0.94
CGR89-554	104G12	345251	6396216	uTSv	ANDS	48.11	1.18	16.34	11.37	0.25	4.90	7.43	3.60	2.27
CGR89-563	104G12	346606	6396233	uTSv	BSLT	49.00	1.54	15.09	13.10	0.25	3.68	6.70	4.87	0.69
DBR89-281	104G11	346810	6384970	uTSv	FLOW	47.29	0.72	10.42	11.29	0.21	12.18	11.96	2.00	0.77
DBR89-370	104G12	344967	6392423	uTSvb	BSLT	46.16	0.77	11.92	11.31	0.20	9.00	13.84	1.73	0.95
DBR91-535	104G13	338286	6430030	uTv	BSLT	48.37	0.64	10.97	10.80	0.19	13.21	11.28	1.73	0.77
DBR91-581*	104G13	351503	6418008	uTv	BSLT	43.26	1.17	18.08	12.69	0.20	3.74	8.84	3.30	0.34
DBR91-601	104G13	351704	6421915	uTv	BSLT	50.95	1.07	17.46	10.42	0.18	4.12	8.97	3.04	0.76
DBR91-703	104G13	335493	6398746	uTv	BSLT	50.24	0.81	13.84	9.67	0.15	7.77	8.70	2.51	2.77
JTI91-53	104G13	333875	6430064	uTv	ANDS	46.61	0.97	18.91	10.54	0.23	5.89	10.48	2.74	1.08
MGU88-176	104G06	360496	6369172	uTv	ANDS	50.71	0.98	17.04	9.52	0.20	5.25	10.47	2.16	2.34
MGU89-254	104G12	331650	6392506	uTv	BSLT	54.09	1.04	16.30	9.58	0.16	3.59	7.95	2.24	1.77
MGU89-267	104G12	329571	6392392	uTv	BSLT	47.27	1.00	17.80	10.76	0.21	5.21	6.86	4.00	3.56
MGU89-270-1	104G12	329185	6391797	uTSv	BSLT	49.34	0.83	13.85	10.60	0.20	7.31	9.17	2.23	3.36
MMC88-291*	104G06	356295	6356073	uTv	BSLT	49.83	0.64	15.07	9.86	0.18	6.74	9.25	1.73	4.23
VOLCANICLASTIC ROCKS														
MMC88-283	104G06	357110	6357696	uTv	TUFF	65.53	0.57	14.83	6.09	0.17	1.79	3.36	3.17	1.86
CGR89-387	104G11	335509	6392688	uTSv	LPTF	46.39	0.89	11.96	11.48	0.22	8.39	12.44	2.85	0.76
CGR89-541	104G12	338824	6394075	uTSv	LPTF	46.01	0.83	9.95	11.50	0.21	11.53	11.82	2.62	0.53
CGR89-541DUF	104G12	338824	6394075	uTSv	LPTF	46.06	0.83	9.91	11.49	0.21	11.62	11.83	2.47	0.52
DBR89-362	104G12	338047	6395824	uTSvf	TUFF	77.98	0.21	9.67	3.09	0.04	1.50	1.73	3.14	0.34
CGR89-477-1	104G12	348953	6376500	uTSv	VCCB	48.50	1.13	13.43	11.55	0.20	8.62	9.97	3.10	1.02
CGR89-550	104G12	344435	6396670	uTSv	VCCB	47.96	0.80	13.17	10.75	0.22	6.82	9.58	3.37	2.24
MMC88-18	104G06	361381	6357644	uTs	VCCB	48.26	0.71	12.66	10.67	0.21	9.35	11.72	2.36	2.43

FIELD NO	NTS MAP Zone 9	UTM EAST	UTM NORTH	MAP CODE	ROCK CODE	K ₂ O/Na ₂ O Ratio	P ₂ O ₅ %	LOI %	OX_SUM %	Fe ₂ O ₃ %	FeO %	S %	CO ₂ %	Ni ppm	Mo ppm	Zn ppm	
DETECTION LIMITS:							0.01	0.01						5	8	2	
ANALYTICAL TECHNIQUE:							XRF / ICP	XRF / ICP	XRF / ICP	calc.	TIT				AAS	AAS	AAS
VOLCANICLASTIC ROCKS																	
CGR89-229	104G12	356793	6381361	ImJHv	CLTF	0.12	0.33	3.36	99.44	6.59	2.30	0.01	1.05			83	
Stuhini Group:																	
FLOWS and/or SILLS																	
CGR89-10	104G11	350344	6391596	uTSv	FLOW	0.43	0.31	1.84	99.51	5.66	4.95	0.01	0.14			93	
CGR89-183	104G11	341342	6391774	uTSv	BSLT	1.17	0.43	3.38	99.17	4.47	5.72	0.03	0.14			74	
CGR89-183DUF	104G11	341342	6391774	uTSv	BSLT	1.16	0.43	3.38	99.34	4.40	5.74	0.03	0.14			82	
CGR89-264	104G11	345426	6400750	uTSvb	BSLT	0.26	0.27	3.82	99.17	3.70	5.11	0.01	0.54			79	
CGR89-268	104G11	345684	6400469	uTSvp	FLOW	1.15	0.47	3.58	99.25	5.54	4.25	0.02	1.09			74	
CGR89-335	104G12	352292	6376373	uTSvb	BSLT	0.51	0.23	4.06	99.47	4.66	5.54	0.01	1.89			181	
CGR89-533	104G12	340089	6393659	uTSv	BSLT	0.51	0.26	2.45	99.29	6.45	4.89	0.01	0.14			87	
CGR89-554	104G12	345251	6396216	uTSv	ANDS	0.63	0.64	3.18	99.27	4.57	6.12	0.02	0.72			109	
CGR89-563	104G12	346606	6396233	uTSv	BSLT	0.14	0.70	3.41	99.03	5.42	6.91	0.36	0.14			125	
DBR89-281	104G11	346810	6384970	uTSv	FLOW	0.39	0.14	2.14	99.12	3.61	6.91	0.02	0.29			80	
DBR89-370	104G12	344967	6392423	uTSvb	BSLT	0.55	0.45	3.05	99.38	2.30	8.11	0.01	0.14			74	
DBR91-535	104G13	338286	6430030	uTv	BSLT	0.45	0.19	1.49	99.64	1.71	8.17						
DBR91-581*	104G13	351503	6418008	uTv	BSLT	0.10	0.41	7.47	99.50	4.11	7.71						
DBR91-601	104G13	351704	6421915	uTv	BSLT	0.25	0.16	2.18	99.31	5.03	4.84						
DBR91-703	104G13	335493	6398746	uTv	BSLT	1.10	0.29	2.39	99.14	3.60	5.45						
JT191-53	104G13	333875	6430064	uTv	ANDS	0.39	0.15	1.71	99.31	1.62	8.01						
MGU88-176	104G06	360496	6369172	uTv	ANDS	1.08	0.32	0.96	99.95	1.92	6.84	0.06	0.15	26	8		
MGU89-254	104G12	331650	6392506	uTv	BSLT	0.79	0.22	2.30	99.24	3.83	5.17	0.01	0.33			99	
MGU89-267	104G12	329571	6392392	uTv	BSLT	0.89	0.65	1.91	99.23	4.30	5.81	0.01	0.29			83	
MGU89-270-1	104G12	329185	6391797	uTv	BSLT	1.51	0.53	1.90	99.32	2.31	7.46	0.01	0.14			72	
MMC88-291*	104G06	356295	6356073	uTv	BSLT	2.45	0.31	2.27	100.11	3.84	5.42	0.01	0.15	44	8		
VOLCANICLASTIC ROCKS																	
MMC88-283	104G06	357110	6357696	uTv	TUFF	0.59	0.09	2.34	99.80	4.19	1.71	0.01	0.49	4	8		
CGR89-387	104G11	335509	6392688	uTSv	LPTF	0.27	0.24	3.66	99.28	4.96	5.87	0.01	0.91			80	
CGR89-541	104G12	338824	6394075	uTSv	LPTF	0.20	0.21	4.48	99.69	4.39	6.40	0.01	1.23			81	
CGR89-541DUF	104G12	338824	6394075	uTSv	LPTF	0.21	0.20	4.47	99.61	4.78	6.04	0.01	1.30			79	
DBR89-362	104G12	338047	6395824	uTSvf	TUFF	0.11	0.07	1.98	99.75	1.01	1.87	0.09	0.32			50	
CGR89-477-1	104G12	348953	6376500	uTSv	VCCB	0.33	0.25	1.42	99.19	4.84	6.04	0.01	0.14			49	
CGR89-550	104G12	344435	6396670	uTSv	VCCB	0.66	0.26	4.20	99.37	4.75	5.40	0.02	1.52			87	
MMC88-18	104G06	361381	6357644	uTs	VCCB	1.03	0.30	0.97	99.64	2.36	7.48	0.01	0.15	102	6		

FIELD NO	NTS MAP Zone 9	UTM EAST	UTM NORTH	MAP CODE	ROCK CODE	Cr ppm 10 XRF	Ba ppm 10 XRF	Sr ppm 5 XRF	Rb ppm 10 XRF	Zr ppm 20 XRF	Y ppm 10 XRF	Nb ppm 5 XRF	Ta ppm NA XRF	V ppm 5 XRF	La ppm 15 XRF	Sn ppm NA XRF	Th ppm NA XRF	U ppm NA XRF
VOLCANICLASTIC ROCKS																		
CGR89-229	104G12	356793	6381361	lmJHv	CLTF	31	373	678	11	108	25	7		258	26	15	<15	<15
Stuhini Group:																		
FLOWS and/or SILLS																		
CGR89-10	104G11	350344	6391596	uTSv	FLOW	229	732	507	20	54	15	6		302	19			
CGR89-183	104G11	341342	6391774	uTSv	BSLT	279	499	691	40	51	20	5		282	24			
CGR89-183DUF	104G11	341342	6391774	uTSv	BSLT	279	495	685	45	50	17	6		276	18			
CGR89-264	104G11	345426	6400750	uTSvb	BSLT	192	487	617	20	52	21	3		276	14			
CGR89-268	104G11	345684	6400469	uTSvp	FLOW	166	976	504	72	74	21	5		293	21			
CGR89-335	104G12	352292	6376373	uTSvb	BSLT	463	307	530	10	37	14	5		273	18			
CGR89-533	104G12	340089	6393659	uTSv	BSLT	466	411	943	17	48	18	4		297	18			
CGR89-554	104G12	345251	6396216	uTSv	ANDS	47	1342	762	32	72	25	5		404	14			
CGR89-563	104G12	346606	6396233	uTSv	BSLT	34	407	675	14	115	40	6		398	15			
DBR89-281	104G11	346810	6384970	uTSv	FLOW	439	488	226	13	38	14	5		304	19			
DBR89-370	104G12	344967	6392423	uTSvb	BSLT	347	221	442	19	49	16	4		294	27			
DBR91-535	104G13	338286	6430030	uTv	BSLT	607		299	16	38	14	5	<15					
DBR91-581*	104G13	351503	6418008	uTv	BSLT	<10		200	<10	91	23	9	<15					
DBR91-601	104G13	351704	6421915	uTv	BSLT	12		335	<10	52	20	5	<15					
DBR91-703	104G13	335493	6398746	uTv	BSLT	342		851	54	60	20	7	<15					
JTI91-53	104G13	333875	6430064	uTv	ANDS	25		425	19	56	13	7	<15					
MGU88-176	104G06	360496	6369172	uTv	ANDS	220	1047	527	39	54	15	7	5	305	17			
MGU89-254	104G12	331650	6392506	uTv	BSLT	49	1517	483	33	99	28	8		180	18			
MGU89-267	104G12	329571	6392392	uTv	BSLT	22	850	622	74	68	30	3		352	23			
MGU89-270-1	104G12	329185	6391797	uTv	BSLT	165	935	330	48	73	20	3		314	31			
MMC88-291*	104G06	356295	6356073	uTv	BSLT	196	833	555	91	44	14	5	5	239	15			
VOLCANICLASTIC ROCKS																		
MMC88-283	104G06	357110	6357696	uTv	TUFF	41	1223	524	46	124	24	10	5	176	15			
CGR89-387	104G11	335509	6392688	uTSv	LPTF	250	170	692	18	58	21	3		314	15			
CGR89-541	104G12	338824	6394075	uTSv	LPTF	493	165	226	15	54	19	6		280	15			
CGR89-541DUF	104G12	338824	6394075	uTSv	LPTF	492	164	231	13	50	21	7		277	23			
DBR89-362	104G12	338047	6395824	uTSvf	TUFF	5	536	249	8	139	26	4		15	4			
CGR89-477-1	104G12	348953	6376500	uTSv	VCCB	223	221	341	29	56	21	6		317	11			
CGR89-550	104G12	344435	6396670	uTSv	VCCB	271	697	335	35	55	21	8		273	15			
MMC88-18	104G06	361381	6357644	uTs	VCCB	498	618	416										

FIELD NO	NTS MAP Zone 9	UTM EAST	UTM NORTH	MAP CODE	ROCK CODE	SiO ₂ %	TiO ₂ %	Al ₂ O ₃ %	Fe ₂ O _{3t} %	MnO %	MgO %	CaO %	Na ₂ O %	K ₂ O %
DETECTION LIMITS:						0.01	0.01	0.01	0.01	0.01	0.01	0.01	0.01	0.01
ANALYTICAL TECHNIQUE:						XRF / ICP	XRF / ICP	XRF / ICP	XRF / ICP	XRF / ICP	XRF / ICP	XRF / ICP	XRF / ICP	XRF / ICP
SEDIMENTARY ROCKS														
MGU89-222	104G12	329405	6388264	ST?	SLST	47.85	0.68	10.15	11.47	0.22	11.22	13.10	1.72	1.33
MGU89-227	104G12	329698	6388729	ST?	SLST	47.77	0.90	15.78	10.87	0.25	6.91	9.12	3.23	3.08
Possible Stuhini Group (Missusjay Creek Area)														
MGU89-215	104G12	332770	6387281	PSmt	ANDS	56.72	1.33	15.31	9.39	0.16	5.59	7.19	2.81	0.64
MGU89-237*	104G12	333581	6390282	ST?	BSLT	46.48	0.60	8.75	10.59	0.19	12.87	13.53	1.45	0.63
MGU89-239	104G12	333008	6390054	ST?	BSLT	46.87	0.58	14.02	8.94	0.16	8.68	13.22	1.92	1.35
Stikine Assemblage:														
FLAWS and/or SILLS														
DBR91-360-2	104G12	324451	6402875	ST	BSLT	39.98	3.62	12.67	11.21	0.14	4.54	11.78	3.00	0.78
DBR91-360-3	104G12	324451	6402875	ST	BSLT	39.27	4.05	14.36	12.38	0.12	3.29	10.46	2.84	2.25
MGU89-284	104G12	342586	6373599	ST	ANDS	58.68	0.64	19.80	6.00	0.06	0.89	0.87	6.02	4.16
MGU89-291*	104G12	342430	6374251	ST	BSLT	44.52	3.43	11.72	16.86	0.32	3.79	7.46	2.27	0.04
MGU89-297	104G12	343572	6375215	ST	BSLT	44.93	2.94	15.40	10.28	0.22	7.26	10.96	1.30	2.12
MGU89-303*	104G05	342233	6371247	ST	BSLT	44.92	1.17	13.24	11.58	0.21	10.09	10.69	1.77	1.09
MGU89-307*	104G05	341785	6371397	ST	BSLT	47.76	0.74	13.85	8.78	0.24	6.65	15.04	0.69	1.91
MGU89-314	104G05	341266	6371566	ST	BSLT	49.73	1.06	15.42	9.23	0.16	6.79	7.50	3.48	1.44
MGU89-319*	104G12	340697	6371614	ST	BSLT	46.64	1.09	14.47	9.86	0.18	8.78	9.71	2.06	1.28

FIELD NO	NTS MAP Zone 9	UTM EAST	UTM NORTH	MAP CODE	ROCK CODE	Cr ppm	Ba ppm	Sr ppm	Rb ppm	Zr ppm	Y ppm	Nb ppm	Ta ppm	V ppm	La ppm	Sn ppm	Th ppm	U ppm
DETECTION LIMITS:						10	10	5	10	20	10	5	NA	5	15	NA	NA	NA
ANALYTICAL TECHNIQUE:						XRF	XRF	XRF	XRF	XRF	XRF	XRF	XRF	XRF	XRF	XRF	XRF	XRF
SEDIMENTARY ROCKS																		
MGU89-222	104G12	329405	6388264	ST?	SLST	456	224	345	32	46	17	7		284	24			
MGU89-227	104G12	329698	6388729	ST?	SLST	114	1104	757	64	79	24	6		281	19			
Possible Stuhini Group (Missusjay Creek Area)																		
MGU89-215	104G12	332770	6387281	PSmt	ANDS	31	167	338	15	149	40	7		200	8			
MGU89-237*	104G12	333581	6390282	ST?	BSLT	581	281	265	22	52	17	6		263	31			
MGU89-239	104G12	333008	6390054	ST?	BSLT	274	377	186	21	31	15	8		258	11			
Stikine Assemblage:																		
FLAWS and/or SILLS																		
DBR91-360-2	104G12	324451	6402875	ST	BSLT	133		530	14	263	32	63	<15					
DBR91-360-3	104G12	324451	6402875	ST	BSLT	122		314	34	289	31	62	<15					
MGU89-284	104G12	342586	6373599	ST	ANDS	6	439	330	62	488	36	138		9	79			
MGU89-291*	104G12	342430	6374251	ST	BSLT	19	35	408	4	471	72	22		147	35			
MGU89-297	104G12	343572	6375215	ST	BSLT	189	146	478	36	343	55	65		210	91			
MGU89-303*	104G05	342233	6371247	ST	BSLT	442	562	426	15	71	24	5		375	22			
MGU89-307*	104G05	341785	6371397	ST	BSLT	43	869	571	19	134	35	9		138	35			
MGU89-314	104G05	341266	6371566	ST	BSLT	228	1102	575	24	118	26	4		211	27			
MGU89-319*	104G12	340697	6371614	ST	BSLT	281	735	392	32	94	25	7		249	25			

Notes:

* = altered flow samples that exhibit at least one of the following criteria: LOI > ~4%, CO₂ > 2%, or K₂O / Na₂O > 2

Alteration was not evaluated for the pyroclastic, volcaniclastic or sedimentary samples.

Abbreviations:

BSLT = basalt, DCIT = dacite, RDCT = rhyodacite, RYLT = rhyolite, ANDS = andesite, TCAN = trachyandesite, FPPP = potassium feldspar-plagioclase porphyritic, CLTF = crystal tuff, LPTF = lapilli tuff, VCCB = volcaniclastic breccia.

APPENDIX 9

FILTERING OF GEOCHEMICAL DATA:

Geochemical data were screened for alteration prior to inclusion on discrimination plots. Only analyses from flows of andesite, basalt and dacite were plotted. Most suites/groups contain pyroclastic or volcaniclastic units which were not plotted. Their chemistry is listed in Appendix 8 together with geochemical results for the entire volcanic specimen collection. Metamorphic facies ranges from zeolite to greenschist grade, therefore moderate mobility of large ion elements is expected.

Samples were rejected based on any one of three parameters:

- 1) K_2O/Na_2O greater than 2, eliminates hydrated and potassic-altered samples. High-potassium rocks, such as shoshonites, do not exhibit K_2O/Na_2O ratios of greater than 2, therefore, this is considered to be an appropriate limiting parameter.
- 2) Loss on ignition (LOI) greater than 4 wt.%, eliminates oxidized and carbonate-altered samples.
- 3) CO_2 content greater than 2 wt.%, also eliminates excessively carbonate-altered samples.

APPENDIX 10
PETROGRAPHIC NOTES

SAMPLE NO	UTM EAST	Zn 09 NORTH	LITHOLOGY	METAMORPHIC ASSEMBLAGE	METAMORPHIC GRADE
STIKINE ASSEMBLAGE:					
DBR91- 501	325286	6428982	chloritic phyllite	vnlet: ep, chl, qtz, py; xtls:	greenschist
STUHINI GROUP:					
CGR89- 322	349932	6378251	pyx plag phyric bas	ep, alb, act, qtz	greenschist
CGR89- 325	349786	6378452	amyg ol pyx plag phyric bas	amyg: alb, ep, chl, calc	greenschist
CGR89- 10	350344	6391596	(ol) pyx plag phyric bas	vnlt: ep, chl, qtz, act	greenschist
CGR89- 183	341342	6391774	bsltic xtl lith lap/ash tuff	matrix andt vnlt: ze	zeile
CGR89- 262	345980	6400980	(ol?) pyx plag phyric bas	vnlt: pr, alb, chl, ze(?)	transitional
CGR89- 264	345426	6400750	bsltic (ol-pyx-plag phyric) xtl	matrix: calc, chl, alb(?)	transitional
CGR89- 268	345684	6400469	amyg pyx plag phyric bas	amygs: ze, calc, chl,	zeile
CGR89- 335	352292	6376373	ep amphibolite (metabas,	matrix andt xtls: amph	upper greenschist
CGR89- 380	336800	6393778	bsltic xtl lith lap tuff	matrix: alb, calc, amph(?)	greenschist
CGR89- 387	335509	6392688	pyx-rich bsltic xtl lith lap/ash	matrix: ep, chl, calc, pp,	transitional
CGR89- 407-1	348313	6379142	amyg ol plag pyx bas	amyg: ep, alb, chl, amph,	greenschist
CGR89- 407-3	348313	6379142	amyg plag pyx phyric bas	amygs: ep, alb; vnlt: calc	greenschist
CGR89- 408	348342	6379389	amyg pyx plag phyric bas	amygs andt matrix: alb, act,	greenschist
CGR89- 477-1	348953	6376500	uralitized pyx phyric bas	vnlt: act, alb, qtz; uralitized	greenschist
CGR89- 541	338824	6394075	bsltic xtl lith lap/ash tuff	vnlt: calc, chl, ep; matrix:	transitional
CGR89- 550	344435	6396670	pyx-rich volc brx or xtl lith tuff	matrix andt amygs: calc,	zeolite
CGR89- 551	344783	6396452	bsltic xtl lith lap tuff-brx	matrix: ze (wairakite?)	zeolite
CGR89- 554	345251	6396216	ol(?) pyx plag phyric bas	vnlt: calc, chl, ep, ze(?)	zeolite
CGR89- 563	346606	6396233	pyx plag phyric bsltic andt,	vnlt: calc, qtz, cz(?);	greenschist
DBR89- 127	355489	6402165	amyg ol, pyx, plag phyric bas	amyg and vnlt: ze	zeolite
DBR89- 316	353385	6381112	amyg pyx(?) ol(?) plag phyric	amyg: chl, qtz, calc; vnlt:	transitional
DBR89- 445	350960	6393215	amyg ol pyx plag phyric bas	amyg: ep, qtz, chl, calc, alb	greenschist
DBR89- 126A	355547	6402150	amyg pyx (cpyx and opyx?)	amygs: chl, calc, pp(?)	pr-pp
DBR89- 281	346810	6384970	altered pyx-rich metabas	matrix: act, calc, ep, alb,	greenschist
DBR89- 370	344967	6392423	bsltic lith xtl ash/lap tuff	matrix: act, alb, calc, chl	greenschist
MGU89- 157	359608	6375918	lith xtl (plag pyx) lap/ash tuff	matrix: chl, act	transitional
MGU89- 73-1	359468	6378210	pyx, plag rich metabas	vnlt: chl, calc, ep; amygs:	greenschist
CGR89- 210	355698	6376866	meta-andt	amyg: ep, chl, alb, qtz	greenschist
CGR89- 312	353029	6377225	xtl lith lap tuff-brx	matrix: alb, ep, calc, act	greenschist
CGR89- 209	355757	6376911	amyg pyx plag phyric andt	amygs: ep, alb, chl, qtz;	greenschist
CGR89- 333	351968	6378389	xtl lith andt(?) tuff-brx	vnlt, matrix: ep, act, chl,	greenschist
CGR89- 346	355623	6375885	hornfelsed(?) lith xtl andt(?)	matrix: hb, plag=An30-35	hb-hornfels
DBR89- 357	337577	6395744	lith xtl vitric lap/ash tuff	matrix: chl, calc	transitional
DBR89- 366-3	339521	6396285	xtl lith rhy(?) tuff	vnlt: qtz, calc, chl(?)	transitional
DBR91- 8	344513	6412395	volc sst/sis	matrix: chl, calc; vnlets: calc	transitional
DBR91- 12	345331	6413366	plag pyx xtl lith lap tuff	xtls: calc, chl, opaques;	transitional
DBR91- 15	347855	6417740	plag xtl lith tuff	amygs: chl, pr, calc, qtz;	pr-pp
DBR91- 21	348514	6417145	plag hb pyx xtl lith tuff	matrix: chl, calc, pr	pr-pp
DBR91- 27-2	349852	6417224	pyx plag hb phyric bas	xtls: chl, calc, ser; vnlets:	transitional
DBR91- 31	350816	6417425	pyx hb plag xtl lith lap tuff	matrix: calc, chl, alb; vnlets:	transitional
DBR91- 32	351501	6417435	plag hb pyx phyric bas	matrix: chl, alb, ser, calc;	pr-pp
DBR91- 69	348738	6413859	pyx phyric bas brx	amygs: ze, chl, qtz, calc	zeolite
DBR91- 82	346165	6422754	bladed plag pyx phyric	matrix: chl, calc, ep; vnlt:	greenschist
DBR91- 82-2	345160	6421545	plag hb pyx xtl lith tuff	xtls: chl, calc, opaques;	greenschist
DBR91- 101	342497	6417665	plag pyx xtl tuff	matrix: chl, calc	transitional
DBR91- 124	343747	6423648	bladed plag pyx phyric	matrix: chl, ep	transitional
DBR91- 220	331959	6413569	plag pyx xtl lith lap tuff	matrix: chl, pp; vnlet: pr,	pr-pp
DBR91- 534	338139	6429916	pyx xtl lith tuff	matrix: act, chl, alb	greenschist
DBR91- 535	338286	6430030	pyx xtl lith tuff	matrix: act, chl, alb	greenschist

SAMPLE NO	UTM EAST	Zn 09 NORTH	LITHOLOGY	METAMORPHIC ASSEMBLAGE	METAMORPHIC GRADE	
DBR91-	540	336587	6413755	plag-rich tuff wacke	matrix: calc, pp, pr, chl, ep	pr-pp
DBR91-	552	336246	6414459	plag pyx xtl lith lap tuff	matrix: chl	transitional
DBR91-	556	334893	6415872	amylg hb phyrlic bas	amylgs: calc, chl, ep; vnlts:	transitional
DBR91-	581	351503	6418008	aphyrlic bas	matrix: chl, calc; vnlts:	transitional
DBR91-	584	351213	6418628	plag hb xtl lith lap tuff	matrix: chl, calc	transitional
DBR91-	587	350600	6419317	pyx xtl lith lap tuff	matrix: chl, calc	transitional
DBR91-	593	351482	6420614	hb plag pyx phyrlic bas	matrix: chl, calc, ep	transitional
DBR91-	601	351704	6421915	plag hb xtl lith lap tuff	matrix: chl, calc, opaques;	greenschist
DBR91-	604	322954	6411474	volc sls	vnlts: calc	transitional
DMU91-	13	346104	6414436	amylg pyx plag phyrlic andt	amylgs: chl, calc, ep	transitional
INE91-	7	349079	6416171	plag pyx lith xtl tuff	amylg: chl, qtz, calc, ep, pr;	pr-pp
INE91-	34	344604	6418482	plag pyx xtl lith lap tuff	matrix: chl, calc, qtz	transitional
JTI91-	77	343921	6426027	bsltic ash/xtl tuff - tuffaceous	matrix: act, chl, alb	greenschist
JTI91-	112	330838	6419807	amylg plag phyrlic andt/bas	amylg: chl, calc, pr; matrix:	pr-pp
JTI91-	114	349612	6420129	hb plag phyrlic diabase?	matrix: chl, calc, qtz, ep, pp;	transitional
JTI91-	117	348901	6418473	amylg plag phyrlic bas	amylg: chl, calc, ze?	transitional
JTI91-	118	348941	6418072	tuffac sst/grit	amylgs: chl, calc; vnlts: chl,	transitional
JTI91-	121	348669	6417630	massive andt sill/flow	matrix: act, chl, ep, calc, chl	transitional
JTI91-	126	324983	6415167	amylg hb plag pyx phyrlic bas	matrix: calc; amylgs: qtz,	transitional
JTI91-	128	324594	6414551	amylg hb plag pyx phyrlic bas	amylgs: qtz, chl, calc, pp	pr-pp
JTI91-	136	323697	6413466	plag hb phyrlic andt	matrix: chl, calc	transitional
HAZELTON GROUP:						
CGR89-	51	354443	6390737	amylg ol pyx plag phyrlic bas	amylg: chl, calc, ep; vnlts:	greenschist
CGR89-	162	353593	6388824	ol(?) pyx plag phyrlic bas	vnlts: calc, chl, ep, alb,	greenschist
CGR89-	227	356604	6381458	ol(?) pyx(?) plag phyrlic	vnlts andt matrix: qtz, chl,	transitional
CGR89-	467	355236	6380092	(ol?) pyx plag phyrlic bsltic	Ca-plag (An55); vnlts: calc;	transitional
DBR89-	184	347397	6386705	amylg ol plag pyx phyrlic bas	amylgs andt vnlts: chl, alb,	transitional
DBR89-	430	354407	6381909	ol(?) pyx plag phyrlic bas	Ca-plag; altn: chl, calc after	transitional
CGR89-	160	353953	6388984	meta-andt	matrix: calcic plag, hb	upper greenschist
CGR89-	434	350072	6385284	pyx-plag phyrlic andt	amylg: chl, calc, qtz	transitional
CGR89-	214	355339	6377986	xtl lith andesltic ash tuff	matrix: chl, calc	transitional
CGR89-	217	355389	6378238	xtl (plag) lith andt lap tuff-brx	amylgs andt matrix: chl,	greenschist
CGR89-	229	356793	6381361	sparsely amylg pyx plag andt	amylgs andt vnlts: qtz, chl,	transitional
CGR89-	237	356002	6380736	hb pyx plag phyrlic bsltic andt	plag=An50	transitional
CGR89-	363	352219	6382972	hornfelsed(?) andesltic/felsic	hornfels: biotite, act, alb;	biotite hornfels(?)
CGR89-	437-2	351019	6384718	amylg (pyx) plag	amylg andt matrix: act, alb,	greenschist
CGR89-	439	348412	6387905	pyx plag phyrlic bsltic andt	Ca-plag (An47); altn: chl,	transitional
CGR89-	48	363364	6390305	(hb?) pyx plag phyrlic andt	altn: calc, chl; plag=An48	transitional
CGR89-	511	354835	6386287	amylg hb plag phyrlic andt	amylgs: chl, act, qtz; Ca-	transitional
DBR89-	147	363974	6388675	amylg (ol?) plag phyrlic bsltic	amylg: chl, calc, qtz	indeterminate
DBR89-	136-2	366740	6388629	trachytic amylg andt flow brx	amylgs: calc, chl, ep, qtz	transitional
DBR89-	136-2	366739	6388629	trachytic amylg andt flow brx	amylg: calc, qtz,	transitional
DBR89-	155	349364	6389572	bladed plag phyrlic andt	amylg: calc, qtz, chl, alb(?)	transitional
DBR89-	326	354588	6381203	hb plag phyrlic andt	vnlts: calc, qtz, alb; altn:	transitional
DBR89-	432	353476	6381935	trachytic pyx plag phyrlic	Ca-plag; amylgs: chl, calc,	transitional
DBR89-	69-1	354864	6387519	hb plag phyrlic bsltic(?) andt	matrix andt phenocrysts:	greenschist
MGU89-	92	348900	6387140	amylg andt (vltic) xtl lith lap	amylgs: chl, calc, qtz, alb	transitional
MGU89-	99-1	349497	6386531	amylg pyx plag phyrlic bsltic	amylgs: chl, calc, ep, alb	greenschist
DBR89-	435	353139	6382257	amylg plag phyrlic dac	amylgs: calc, alb, qtz, chl	transitional
SUSTUT GROUP:						
CGR89-	200-3	353526	6395831	amylg pyx plag phyrlic bsltic	amylgs: chl, calc, qtz,	transitional
CGR89-	128-2	360116	6393971	pyx plag phyrlic bsltic andt	amylg: calc, chl; Ca-plag	transitional
CGR89-	200-2	353526	6395831	sparsely amylg plag phyrlic	amylgs: chl, calc, qtz;	transitional
CGR89-	179	351300	6390380	trachytic rhyodac plag	chl, calc, ep?	transitional

SAMPLE NO	UTM EAST	Zn 09 NORTH	LITHOLOGY	METAMORPHIC ASSEMBLAGE	METAMORPHIC GRADE
DBR89- 376	354146	6391935	rhyolitic xtl vitric ash tuff	matrix: ze(?)	zeolite
DBR89- 415-2	370000	6384950	welded lith xtl vitric rhy ash	matrix: ze	zeolite
SLOKO GROUP:					
DBR89- 468	341288	6394369	pyx plag phyric bsitic andt	Ca-plag	transitional
DBR89- 469	341110	6394305	pyx plag phyric bsitic andt	Ca-plag; amys: calc, chl	transitional
DBR89- 470	340904	6394217	pyx plag phyric bas/bsitic	Ca-plag; amys (rare): calc,	transitional
DBR89- 458	341138	6394284	(hb) pyx plag phyric bsitic	amys: chl, calc; plag=An47	transitional
DBR89- 460	341275	6394361	(hb/pyx?) plag phyric andt	amys: chl, calc, qtz; Ca-	transitional
DBR89- 467	341289	6394367	pyx plag phyric andt	Ca-plag; altn: chl, qtz, calc	transitional
DBR89- 471	340902	6394216	hb plag phyric andt flow brx	amys: chl, ze	zeolite
DBR89- 6	353026	6391935	amyl feldspar phyric andt(?)	amys: chl, qtz	transitional
DBR89- 198-3	353015	6392471	amyl hb feldspar phyric	amys: chl, qtz, calc, ze(?)	zeolite
INTRUSIONS WITH METAMORPHIC MINERAL ASSEMBLAGES:					
CGR89- 34	367461	6389197	amyl plag phyric andt	amys: calc, chl, ep	
CGR89- 377	335494	6393085	coarse grained pyx	vnls: pr	pr-pp
DBR89- 64-2	355225	6389852	amyl pyx phyric bas dike	amys: calc, (qtz)	transitional
DBR89- 374	356795	6399091		vnls: calc, pr, chl	pr-pp

Abbreviations: dac - dacite; andt - andesite; bas - basalt; bsitic - basaltic; xtl - crystal; lith - lithic; lap - lapilli; amyl - amygdaloidal; hb - hornblende; pyx - pyroxene; plag - plagioclase; ol - olivine; bio - biotite; chl - chlorite; calc - calcite; qtz - quartz; alb - albiote; ze - zeolite; pr - prehnite; pp - pumpellyite; ep - epidote; act - actinolite; trem - tremolite; py - pyrite; brx - breccia; rhy - rhyolite; cpx - clinopyroxene; opx -

APPENDIX 11
WHOLE-ROCK LITHOGEOCHEMICAL ANALYSES OF PLUTONIC ROCKS

FIELD NO	NTS MAP Zone 9	UTM EAST	UTM NORTH	MAP CODE	ROCK CODE	QAP FIELD	SiO ₂ %	TiO ₂ %	Al ₂ O ₃ %	Fe ₂ O ₃ %	MnO %	MgO %	CaO %	Na ₂ O %	K ₂ O %	P ₂ O ₅ %	
Detection Limits:							0.01	0.01	0.01	0.01	0.01	0.01	0.01	0.01	0.01	0.01	
Analytical Techniques:							XRF/ICP	XRF/ICP	XRF/ICP	XRF/ICP	XRF/ICP	XRF/ICP	XRF/ICP	XRF/ICP	XRF/ICP	XRF/ICP	XRF/ICP
EOCENE - Hyder suite																	
Sawback pluton:																	
DBR88-108	104G05	319895	6367806	Egn	GRNT	MNGRNT	74.88	0.17	13.78	1.46	0.06	0.21	1.09	3.44	4.47	0.03	
DBR88-163	104G05	329826	6365610	Egn	GRNT	GRDR	70.26	0.36	15.20	2.60	0.08	0.67	2.05	4.12	3.54	0.13	
MGU88-76*	104G05	327946	6374268	Egn	MNZN	MNGRNT	75.75	0.14	13.32	1.20	0.05	0.16	1.08	3.28	4.63	0.02	
MGU89-209-3	104G12	333095	6385834	Egn	GRNT	MNGRNT	76.54	0.15	12.83	1.02	0.03	0.06	0.58	3.49	4.71	0.02	
MGU89-213-2	104G12	332545	6386823	Egn	GRNT	MNGRNT	76.48	0.12	13.07	0.80	0.01	0.06	0.37	2.89	5.13	0.01	
MGU89-221	104G12	329227	6387981	Egn	GRNT	MNGRNT	68.28	0.58	15.17	3.55	0.07	1.04	2.35	3.68	4.59	0.18	
MGU89-224	104G12	329990	6388052	Egn	GRNT	MNGRNT	73.73	0.26	13.77	1.53	0.04	0.38	1.14	3.54	4.83	0.06	
MGU89-224DUP	104G12	329990	6388052	Egn	GRNT	MNGRNT	73.81	0.26	13.77	1.53	0.03	0.36	1.14	3.54	4.85	0.06	
MGU89-232	104G12	330680	6388349	Egn	GRNT	MNGRNT	71.35	0.38	14.19	2.29	0.04	0.62	1.11	3.39	5.03	0.11	
Christina pluton:																	
MGU88-48*	104G05	332316	6349874	Egd	GRDR	TNLT	59.28	0.69	18.23	6.56	0.13	2.44	6.51	3.35	1.74	0.25	
DIKES																	
DBR88-290-2*	104G05	347682	6371082	Dikes	RYLT	MNGRNT	63.24	0.59	17.84	4.68	0.12	1.29	4.02	4.87	2.57	0.20	
DBR89-380	104G11	349463	6387294	Dikes	ANDS	GRDR	61.47	0.71	15.02	5.07	0.09	2.28	3.71	3.66	3.17	0.21	
DBR89-380DUP	104G11	349463	6387294	Dikes	ANDS	GRDR	61.69	0.71	14.99	5.10	0.09	2.30	3.70	3.59	3.03	0.20	
MIDDLE JURASSIC - Three Sisters suite																	
Niko pluton:																	
DBR88-328*	104G06	352733	6360764	mJgn	GRNT	MNGRNT	74.11	0.21	13.65	1.96	0.06	0.28	1.37	3.77	3.64	0.04	
Saffron pluton:																	
CGR89-495*	104G11	359129	6384068	mJgn	GRNT	MNGRNT	68.76	0.38	15.26	3.04	0.04	0.69	1.84	4.03	4.58	0.09	
CGR89-517*	104G11	354301	6385459	mJgn	MONZ	QZMZDR	53.73	0.95	16.88	8.05	0.11	3.93	7.43	3.66	2.39	0.32	
CGR89-513	104G11	355410	6386169	Dikes	SYNT	MNGRNT	71.88	0.30	14.14	2.52	0.03	0.35	0.26	3.30	5.47	0.09	
Yehiniko pluton:																	
MGU88-101	104G06	360497	6367640	mJgn	GRNT	MNGRNT	76.60	0.15	12.78	1.39	0.04	0.14	0.88	3.21	4.43	0.02	
MGU88-193	104G06	360944	6365404	mJgn	GRNT	MNGRNT	75.61	0.20	13.31	1.69	0.04	0.25	1.14	3.19	4.30	0.03	
Conover pluton:																	
CGR89-546*	104G12	338140	6393551	mJm	MNZN	GRDR	58.47	0.67	16.72	7.44	0.18	2.74	6.42	3.04	2.34	0.21	
CGR89-34	104G11	367461	6389197	Dikes	FPPP	QZMZDR	51.18	1.31	16.98	9.58	0.22	2.85	4.36	4.94	2.88	0.29	
LATE EARLY JURASSIC - Cone Mountain suite																	
DBR90-40*	104G05	340000	6360530	leJgd	GRDR	MNGRNT	68.42	0.31	15.39	2.96	0.08	0.71	2.52	3.34	4.66	0.08	
Navo pluton :																	
DBR88-329*	104G06	348562	6359899	leJgd	GRDR	GRDR	67.31	0.45	15.98	3.76	0.07	1.34	3.77	4.00	2.23	0.13	
Dokdaon pluton:																	
DBR88-331*	104G06	349807	6371030	leJgd	GRDR	GRDR	65.51	0.49	15.54	5.22	0.09	1.97	4.89	3.08	2.58	0.13	
Strata Glacier pluton																	
MGU88-194	104G06	356351	6366738	leJgd	GRDR	TNLT	64.69	0.57	16.52	4.83	0.09	1.95	4.75	3.90	1.82	0.15	
EARLY JURASSIC - Texas Creek suite																	
Limpoke pluton:																	
DBR91-723*	104G13	331083	6408326	eJmd	QZMZDR	QZMZDR	61.03	0.62	16.88	6.25	0.15	1.96	5.39	3.42	3.10	0.24	
Geology Ridge pluton																	
DBR90-1	104G05	329237	6360819	eJd	DORT	DORT	52.72	0.66	11.41	8.88	0.22	10.30	11.60	1.74	0.33	0.21	
DBR90-1DUP	104G05	329237	6360819	eJd	DORT	DORT	52.77	0.66	11.52	8.88	0.22	10.34	11.56	1.75	0.34	0.21	

FIELD NO	NTS MAP Zone 9	UTM EAST	UTM NORTH	MAP CODE	ROCK CODE	QAP FIELD	LOI %	OX_SUM %	Fe ₂ O ₃ %	FeO %	S %	Co ₂ %	Ni ppm	Mo ppm	Zn ppm	Cr ppm	Ba ppm	Sr ppm	Rb ppm	
							0.01						5	8	2	10	10	5	10	
Detection Limits:							XRF/ICP	XRF/ICP	calc.	TIT										
Analytical Techniques:														AAS	AAS	AAS	XRF		XRF	XRF
EOCENE - Hyder suite																				
Sawback pluton:																				
DBR88-108	104G05	319895	6367806	Egn	GRNT	MNGRNT	0.29	99.88	0.52	0.85	0.01	0.15	2	8		29	722	134	167	
DBR88-163	104G05	329826	6365610	Egn	GRNT	GRDR	0.52	99.53	1.18	1.28	0.01	0.15	3	8		35	2086	527	51	
MGU88-76*	104G05	327946	6374268	Egn	MNZN	MNGRNT	0.21	99.84	0.57	0.57	0.01	0.15	2	8		22	539	112	148	
MGU89-209-3	104G12	333095	6385834	Egn	GRNT	MNGRNT	0.42	99.85	0.62	0.36	0.01	0.14			11	2	308	82	261	
MGU89-213-2	104G12	332545	6386823	Egn	GRNT	MNGRNT	1.05	99.99	0.56	0.22	0.01	0.14			14	2	156	40	238	
MGU89-221	104G12	329227	6387981	Egn	GRNT	MNGRNT	0.39	99.88	1.64	1.72	0.01	0.14			52	14	1964	537	102	
MGU89-224	104G12	329990	6388052	Egn	GRNT	MNGRNT	0.34	99.62	0.65	0.79	0.01	0.14			27	6	930	233	116	
MGU89-224DUP	104G12	329990	6388052	Egn	GRNT	MNGRNT	0.34	99.69	0.50	0.93	0.01	0.14			27	5	905	232	117	
MGU89-232	104G12	330680	6388349	Egn	GRNT	MNGRNT	0.81	99.32	1.01	1.15	0.01	0.14			33	9	1742	447	90	
Christina pluton:																				
MGU88-48*	104G05	332316	6349874	Egd	GRDR	TNLT	0.60	99.78	2.89	3.30	0.01	0.15	2	8		25	1599	921	23	
DIKES																				
DBR88-290-2*	104G05	347682	6371082	Dikes	RYLT	MNGRNT	0.41	99.83	2.32	2.12	0.02	0.15	3	6		13	2017	797		
DBR89-380	104G11	349463	6387294	Dikes	ANDS	GRDR	3.96	99.35	2.84	2.01	0.01	1.88			53	35	1443	597	76	
DBR89-380DUP	104G11	349463	6387294	Dikes	ANDS	GRDR	3.96	99.36	2.87	2.01	0.01	1.88			51	34	1452	595	75	
MIDDLE JURASSIC - Three Sisters suite																				
Niko pluton:																				
DBR88-328*	104G06	352733	6360764	mJgn	GRNT	MNGRNT	0.42	99.51	0.70	1.13	0.01	0.15	2	8		22	1705	163	74	
Saffron pluton:																				
CGR89-495*	104G11	359129	6384068	mJgn	GRNT	MNGRNT	0.85	99.56	1.28	1.58	0.01	0.14			20	7	1254	226	102	
CGR89-517*	104G11	354301	6385459	mJgn	MONZ	QZMZDR	1.92	99.37	2.45	5.04	0.01	0.65			29	41	807	491	62	
CGR89-513	104G11	355410	6386169	Dikes	SYNT	MNGRNT	1.32	99.66	1.80	0.65	0.01	0.14			31	5	1736	101	113	
Yehiniko pluton:																				
MGU88-101	104G06	360497	6367640	mJgn	GRNT	MNGRNT	0.33	99.97	0.45	0.85	0.01	0.15	2	8		46	2386	647	30	
MGU88-193	104G06	360944	6365404	mJgn	GRNT	MNGRNT	0.27	100.03	-1.15	2.56	0.01	0.15	2	8		10	1019	114	117	
Conover pluton:																				
CGR89-546*	104G12	338140	6393551	mJm	MNZN	GRDR	1.04	99.27	3.44	3.60	0.01	0.14			73	29	4299	594	35	
DIKES																				
CGR89-34	104G11	367461	6389197	Dikes	FPPP	QZMZDR	4.48	99.07	4.00	5.02	0.03	1.90			115	21	1436	546	48	
LATE EARLY JURASSIC - Cone Mountain suite																				
DBR90-40*	104G05	340000	6360530	leJgd	GRDR	MNGRNT	0.55	99.02	2.90	1.55	0.05	0.14				10	2102	344	10	
Navo pluton :																				
DBR88-329*	104G06	348562	6359899	leJgd	GRDR	GRDR	0.43	99.47	1.78	1.78	0.01	0.15	4	8		19	1141	514	19	
Dokdaon pluton:																				
DBR88-331*	104G06	349807	6371030	leJgd	GRDR	GRDR	0.54	100.04	2.21	2.71	0.01	0.15	3	8		57	1546	462	38	
Strata Glacier pluton																				
MGU88-194	104G06	356351	6366738	leJgd	GRDR	TNLT	0.48	99.75	1.99	2.56	0.01	0.15	7	8		23	1073	509	18	
EARLY JURASSIC - Texas Creek suite																				
Limpoke pluton:																				
DBR91-723*	104G13	331083	6408326	eJmd	QZMZDR	QZMZDR	0.69	99.73	6.25	2.71						14		912	63	
Geology Ridge pluton																				
DBR90-1	104G05	329237	6360819	eJd	DORT	DORT	1.14	99.21	8.87	5.29	0.01	0.14				650	252	298	10	
DBR90-1DUP	104G05	329237	6360819	eJd	DORT	DORT	1.14	99.39	8.87	6.12	0.01	0.14				649	252	296	10	

FIELD NO	NTS MAP Zone 9	UTM EAST	UTM NORTH	MAP CODE	ROCK CODE	QAP FIELD	Zr ppm 20 XRF	Y ppm 10 XRF	Nb ppm 5 XRF	Ta ppm NA XRF	V ppm 5 XRF	La ppm 15 XRF	Yb ppm XRF	Pt ppm XRF	Pd ppm XRF	Sn ppm NA XRF	Th ppm NA XRF	U ppm NA XRF	
Detection Limits:																			
Analytical Techniques:																			
EOCENE - Hyder suite																			
Sawback pluton:																			
DBR88-108	104G05	319895	6367806	Egn	GRNT	MNGRNT	121	24	24	5	24	19	7						
DBR88-163	104G05	329826	6365610	Egn	GRNT	GRDR	149	13	17	5	53	22	5						
MGU88-76*	104G05	327946	6374268	Egn	MNZN	MNGRNT	100	20	21	5	22	15	6						
MGU89-209-3	104G12	333095	6385834	Egn	GRNT	MNGRNT	102	12	21		7	25							
MGU89-213-2	104G12	332545	6386823	Egn	GRNT	MNGRNT	76	11	22		4	3							
MGU89-221	104G12	329227	6387981	Egn	GRNT	MNGRNT	279	25	18		56	60							
MGU89-224	104G12	329990	6388052	Egn	GRNT	MNGRNT	158	16	13		15	42							
MGU89-224DUP	104G12	329990	6388052	Egn	GRNT	MNGRNT	155	17	13		15	38							
MGU89-232	104G12	330680	6388349	Egn	GRNT	MNGRNT	189	29	12		37	36							
Christina pluton:																			
MGU88-48*	104G05	332316	6349874	Egd	GRDR	TNLT	179	18	12	5	137	35	5						
DIKES																			
DBR88-290-2*	104G05	347682	6371082	Dikes	RYLT	MNGRNT													
DBR89-380	104G11	349463	6387294	Dikes	ANDS	GRDR	134	17	6		108	24							
DBR89-380DUP	104G11	349463	6387294	Dikes	ANDS	GRDR	144	17	7		103	17							
MIDDLE JURASSIC - Three Sisters suite																			
Niko pluton:																			
DBR88-328*	104G06	352733	6360764	mJgn	GRNT	MNGRNT	158	24	16	5	31	33	8						
Saffron pluton:																			
CGR89-495*	104G11	359129	6384068	mJgn	GRNT	MNGRNT	276	26	11		34	24							
CGR89-517*	104G11	354301	6385459	mJgn	MONZ	QZMZDR	116	30	6		226	25							
CGR89-513	104G11	355410	6386169	Dikes	SYNT	MNGRNT	170	24	10		22	13							
Yehiniko pluton:																			
MGU88-101	104G06	360497	6367640	mJgn	GRNT	MNGRNT	118	16	10	5	116	22	7						
MGU88-193	104G06	360944	6365404	mJgn	GRNT	MNGRNT	126	16	15	5	30	17	6						
Conover pluton:																			
CGR89-546*	104G12	338140	6393551	mJm	MNZN	GRDR	111	22	3		174	22							
DIKES																			
CGR89-34	104G11	367461	6389197	Dikes	FPPP	QZMZDR	145	32	9		287	22							
LATE EARLY JURASSIC - Cone Mountain suite																			
DBR90-40*	104G05	340000	6360530	leJgd	GRDR	MNGRNT	197	22	19		43	43							
Navo pluton :																			
DBR88-329*	104G06	348562	6359899	leJgd	GRDR	GRDR	128	15	14	5	72	15	5						
Dokdaon pluton:																			
DBR88-331*	104G06	349807	6371030	leJgd	GRDR	GRDR	125	16	11	5	128	23	9						
Strata Glacier pluton																			
MGU88-194	104G06	356351	6366738	leJgd	GRDR	TNLT	149	16	11	5	99	22	6						
EARLY JURASSIC - Texas Creek suite																			
Limpoke pluton:																			
DBR91-723*	104G13	331083	6408326	eJmd	QZMZDR	QZMZDR	151	26	7	<15						<15	<15	<15	
Geology Ridge pluton																			
DBR90-1	104G05	329237	6360819	eJd	DORT	DORT	97	25	5		202	15							
DBR90-1DUP	104G05	329237	6360819	eJd	DORT	DORT	94	26	12		207	21							

FIELD NO	NTS MAP Zone 9	UTM EAST	UTM NORTH	MAP CODE	ROCK CODE	QAP FIELD	SiO ₂ % 0.01 XRF/ICP	TiO ₂ % 0.01 XRF/ICP	Al ₂ O ₃ % 0.01 XRF/ICP	Fe ₂ O ₃ % 0.01 XRF/ICP	MnO % 0.01 XRF/ICP	MgO % 0.01 XRF/ICP	CaO % 0.01 XRF/ICP	Na ₂ O % 0.01 XRF/ICP	K ₂ O % 0.01 XRF/ICP	P ₂ O ₅ % 0.01 XRF/ICP	
Detection Limits:							0.01	0.01	0.01	0.01	0.01	0.01	0.01	0.01	0.01	0.01	
Analytical Techniques:							XRF/ICP	XRF/ICP	XRF/ICP	XRF/ICP	XRF/ICP	XRF/ICP	XRF/ICP	XRF/ICP	XRF/ICP	XRF/ICP	XRF/ICP
LATE TRIASSIC TO EARLY JURASSIC - Copper Mountain suite																	
Rugged Mountain pluton - syenites																	
INE91-121	104G13	343900	6410055	eJs	SYNT	FSYNT	51.86	0.64	19.29	5.65	0.15	1.41	6.33	2.45	8.68	0.29	
INE91-122	104G13	343815	6409693	eJs	SYNT	FSYNT	52.51	0.76	19.26	5.56	0.17	1.51	5.51	3.24	8.27	0.28	
INE91-316	104G13	345938	6408895	eJs	SYNT	FSYNT	53.72	0.52	20.78	4.51	0.13	0.99	4.91	2.96	9.03	0.24	
INE91-317	104G13	346111	6408964	eJs	SYNT	FSYNT	50.42	0.63	18.93	5.75	0.15	1.41	6.71	2.23	8.49	0.34	
INE91-320	104G13	346465	6409053	eJs	SYNT	FSYNT	51.17	0.85	18.71	7.30	0.18	1.78	7.74	1.75	8.51	0.46	
INE91-322	104G13	346472	6408613	eJs	SYNT	FSYNT	54.12	0.68	20.35	4.79	0.13	0.70	4.59	2.25	10.70	0.16	
INE91-324	104G13	346493	6408088	eJs	SYNT	FSYNT	51.52	0.99	20.09	6.00	0.12	1.32	4.98	2.34	10.24	0.32	
INE91-82	104G13	345489	6410465	Dikes	SYNT	FSYNT	58.74	0.28	19.88	2.23	0.08	0.40	2.62	1.87	11.78	0.01	
INE91-64	104G13	347313	6409513	Dikes	SYNT	FSYNT	60.28	0.14	21.06	1.74	0.03	0.14	2.88	5.29	7.49	0.01	
INE91-73-2	104G13	346298	6410221	Dikes	SYNT	FSYNT	57.09	0.54	19.21	4.62	0.10	1.06	4.86	3.79	8.00	0.22	
INE91-76	104G13	346069	6409865	eJs/TJcpx	SYNT/PRXN	NA	46.43	0.97	15.24	9.71	0.20	3.43	10.79	1.16	7.73	0.83	
INE91-115	104G13	345096	6410460	eJs/TJcpx	SYNT/PRXN	NA	47.73	0.99	15.23	9.89	0.17	3.33	10.33	0.79	7.03	0.82	
INE91-336	104G13	343829	6410644	eJs/TJcpx	SYNT/PRXN	NA	48.56	0.92	15.52	9.32	0.18	3.88	9.91	1.38	7.54	0.91	
Rugged Mountain ultramafic phase																	
INE91-78-2	104G13	345738	6409800	TJcpx	PRXN	NA	38.90	1.54	3.20	21.02	0.34	9.96	21.33	0.81	0.06	2.58	
INE91-80-2	104G13	345626	6410045	TJcpx	PRXN	NA	37.59	1.47	4.47	18.55	0.32	7.91	20.24	0.87	1.23	2.31	
INE91-80-2DU	104G13	345626	6410045	TJcpx	PRXN	NA	37.16	1.44	4.42	18.30	0.32	7.78	20.04	0.85	1.30	2.28	
Ultramafite bodies																	
Latimer Lake pluton																	
DBR91-382-2	104G13	338833	6417196	TJcpx	CPXN	NA	39.21	1.50	5.34	19.51	0.20	10.95	20.46	0.23	0.18	1.34	
DBR91-387	104G13	338096	6416989	TJcpx	CPXN	NA	39.55	1.59	5.74	21.01	0.20	11.00	18.59	0.23	0.28	0.04	
Damnation pluton																	
INE91-282	104G13	348525	6416034	TJcpx	CPXN	NA	40.20	1.50	4.04	22.25	0.20	11.44	18.21	0.26	0.31	0.18	
Quartz monzonite variation																	
Perelshin pluton:																	
MGU88-102*	104G05	341169	6352116	eJqm	MNZN	QZMZDR	60.16	0.59	17.85	6.10	0.17	1.77	6.69	3.34	2.30	0.24	
MGU88-190	104G05	335928	6355747	eJqm	MNZN	GRDR	64.80	0.50	16.15	4.82	0.13	1.42	4.94	3.05	3.31	0.16	
MIDDLE(?) TO LATE TRIASSIC - Polaris suite																	
Mount Hickman Complex																	
MGU88-184	104G06	374058	6347932	ITcx	CPXN	NA	49.58	0.35	1.16	9.22	0.19	17.31	19.52	0.19	0.01	0.01	
DBR88-314	104G06	375952	6350727	ITcx	PRXN	NA	43.99	0.18	1.16	12.00	0.21	24.52	11.95	0.01	0.00	0.01	
Middle Scud Creek body																	
MMC88-224	104G06	360224	6350671	ITcx	CPXN	NA	43.70	0.47	7.66	10.26	0.18	20.89	9.58	0.78	0.27	0.11	
DBR88-243	104G06	361339	6349375	ITcx	GBBR	NA	43.22	0.36	5.31	11.03	0.18	29.10	6.69	0.30	0.05	0.07	
Yehinko Lake body																	
MGU89-111	104G11	360372	6380596	ITcx	CPXN	NA	42.41	0.32	4.92	10.89	0.18	27.78	7.05	0.47	0.08	0.08	
MGU89-114	104G11	360008	6380195	ITcx	CPXN	NA	40.27	0.32	4.71	10.87	0.18	30.86	4.71	0.30	0.03	0.07	
MGU89-121	104G11	359714	6377724	ITcx	CPXN	NA	41.26	0.29	4.16	10.60	0.16	29.96	5.31	0.15	0.04	0.07	
MGU89-156	104G11	359684	6376552	ITcx	CPXN	NA	40.43	0.34	4.39	10.77	0.19	29.86	6.02	0.32	0.10	0.09	
MIDDLE TO LATE TRIASSIC - Stikine suite																	
Hickman batholith																	
DBR88-322	104G06	365956	6350407	ITm	MNZN	GRDR	63.56	0.51	16.57	4.95	0.10	2.01	4.43	4.14	2.52	0.18	
MGU88-192	104G06	369187	6356802	ITm	GRDR	GRDR	65.28	0.47	16.28	4.16	0.09	1.74	4.04	4.10	2.56	0.14	
DBR88-325	104G06	363815	6352467	ITm	MNZN	QZMZDR	53.73	1.00	17.61	8.88	0.18	3.59	8.00	3.42	2.07	0.34	
MGU88-197	104G06	362995	6351733	ITm	MNZN	QZMZDR	57.76	0.82	19.10	5.81	0.12	1.49	5.42	4.05	4.37	0.53	
Nightout pluton																	
MGU88-204	104G06	375004	6373914	ITgd	GRDR	GRDR	66.13	0.38	16.85	3.30	0.07	1.28	3.94	4.76	2.19	0.11	
MGU89-52	104G11	361593	6402281	ITgd	GRDR	TNLT	59.44	0.60	17.71	6.19	0.14	2.46	6.21	4.19	0.88	0.21	
CGR89-525	104G11	363661	6375334	ITgd	GRDR	GRDR	64.34	0.51	16.12	4.44	0.09	1.89	4.18	4.18	2.73	0.15	

FIELD NO	NTS MAP Zone 9	UTM EAST	UTM NORTH	MAP CODE	ROCK CODE	QAP FIELD	LOI %	OX_SUM %	Fe ₂ O ₃ %	FeO %	S %	Co ₂ %	Ni ppm 5	Mo ppm 8	Zn ppm 2	Cr ppm 10	Ba ppm 10	Sr ppm 5	Rb ppm 10	
Detection Limits:							0.01													
Analytical Techniques:							XRF/ICP	XRF/ICP	calc.	TIT			AAS	AAS	AAS	XRF	XRF	XRF	XRF	
LATE TRIASSIC TO EARLY JURASSIC - Copper Mountain suite																				
Rugged Mountain pluton - syenites																				
INE91-121	104G13	343900	6410055	eJs	SYNT	FSYNT	2.32	99.07	2.74	2.81			52	INT	92	<10		1603	175	
INE91-122	104G13	343815	6409693	eJs	SYNT	FSYNT	3.67	100.74	3.19	2.19						<10		1762	135	
INE91-316	104G13	345938	6408895	eJs	SYNT	FSYNT	2.58	100.37	2.33	2.03			<50	<1	73	13		1505	145	
INE91-317	104G13	346111	6408964	eJs	SYNT	FSYNT	4.06	99.12	2.97	2.77						<10		2095	169	
INE91-320	104G13	346465	6409053	eJs	SYNT	FSYNT	2.01	100.46	3.46	3.60						<10		2157	200	
INE91-322	104G13	346472	6408613	eJs	SYNT	FSYNT	2.39	100.86	2.51	3.25						<10		1105	204	
INE91-324	104G13	346493	6408088	eJs	SYNT	FSYNT	2.93	100.85	1.57	3.21						16		1498	274	
INE91-82	104G13	345489	6410465	Dikes	SYNT	FSYNT	1.76	99.65	1.08	1.07						<10		2155	210	
INE91-64	104G13	347313	6409513	Dikes	SYNT	FSYNT	1.44	100.50	0.82	0.85						<10		1624	132	
INE91-73-2	104G13	346298	6410221	Dikes	SYNT	FSYNT	1.39	100.88	2.10	2.33						<10		2377	134	
INE91-76	104G13	346069	6409865	eJs/TJcpx	SYNT/PRXN	NA	3.71	100.20	4.67	4.93			<50	<1	110	13		1909	152	
INE91-115	104G13	345096	6410460	eJs/TJcpx	SYNT/PRXN	NA	2.61	98.92	4.59	5.21						<10		2932	150	
INE91-336	104G13	343829	6410644	eJs/TJcpx	SYNT/PRXN	NA	1.73	99.85	4.00	5.09			<50	<1	130	26		2554	179	
Rugged Mountain ultramafic phase																				
INE91-78-2	104G13	345738	6409800	TJcpx	PRXN	NA	0.18	99.92	10.08	10.10			<50	<1	200	24		1038	<10	
INE91-80-2	104G13	345626	6410045	TJcpx	PRXN	NA	4.83	99.79	9.25	9.45			<50	<1	210	<10		1247	24	
INE91-80-2DU	104G13	345626	6410045	TJcpx	PRXN	NA	4.89	98.78	9.25	9.45						<10		1249	20	
Ultramafite bodies																				
Latimer Lake pluton																				
DBR91-382-2	104G13	338833	6417196	TJcpx	CPXN	NA	0.16	99.08	19.51	6.12						<10		177	<10	
DBR91-387	104G13	338096	6416989	TJcpx	CPXN	NA	0.43	98.66	21.01	7.94						<10		130	11	
Damnation pluton																				
INE91-282	104G13	348525	6416034	TJcpx	CPXN	NA	0.31	98.90	22.25	9.20						32		113	<10	
Quartz monzonite variation																				
Perelshin pluton:																				
MGU88-102*	104G05	341169	6352116	eJqm	MNZN	QZMZDR	0.91	100.12	3.26	2.56	0.01	0.15	2	8		22	1062	102	126	
MGU88-190	104G05	335928	6355747	eJqm	MNZN	GRDR	0.33	99.61	2.13	2.42	0.01	0.15	3	8		58	2446	517	57	
MIDDLE(?) TO LATE TRIASSIC - Polaris suite																				
Mount Hickman Complex																				
MGU88-184	104G06	374058	6347932	ITcx	CPXN	NA	0.81	98.35	9.21	5.69	0.01	0.14	104	6		790	100	90		
DBR88-314	104G06	375952	6350727	ITcx	PRXN	NA	5.61	99.64	11.98	4.28	0.02	0.14	430	6		1900	100	66		
Middle Scud Creek body																				
MMC88-224	104G06	360224	6350671	ITcx	CPXN	NA	5.12	99.02	10.24	7.18	0.02	0.99			51					
DBR88-243	104G06	361339	6349375	ITcx	GBBR	NA	3.76	100.07	4.23	6.12	0.23	0.15	1300	6	32	2100	100	120		
Yehinko Lake body																				
MGU89-111	104G11	360372	6380596	ITcx	CPXN	NA	5.58	99.76	5.72	4.65	0.01	0.14			49	1728	55	93	7	
MGU89-114	104G11	360008	6380195	ITcx	CPXN	NA	7.13	99.45	5.25	5.06	0.01	0.14			36	2305	18	140	8	
MGU89-121	104G11	359714	6377724	ITcx	CPXN	NA	7.62	99.62	5.93	4.20	0.04	0.14			50	2020	14	114	5	
MGU89-156	104G11	359684	6376552	ITcx	CPXN	NA	6.77	99.28	5.78	4.49	0.04	0.14			48	1853	53	173	11	
MIDDLE TO LATE TRIASSIC - Stikine suite																				
Hickman batholith																				
DBR88-322	104G06	365956	6350407	ITm	MNZN	GRDR	0.92	99.89	2.11	2.56	0.01	0.15	10	8		56	1053	759	39	
MGU88-192	104G06	369187	6356802	ITm	GRDR	GRDR	0.85	99.71	1.95	1.99	0.01	0.15	8	8		48	1430	693	44	
DBR88-325	104G06	363815	6352467	ITm	MNZN	QZMZDR	1.06	99.88	5.40	3.13	0.01	0.15	16	8		44	815	688	16	
MGU88-197	104G06	362995	6351733	ITm	MNZN	QZMZDR	0.51	99.98	2.01	3.42	0.01	0.15	2	8		23	908	582	125	
Nightout pluton																				
MGU88-204	104G06	375004	6373914	ITgd	GRDR	GRDR	0.61	99.62	1.74	1.40	0.01	0.15	6	8		38	1036	835	35	
MGU89-52	104G11	361593	6402281	ITgd	GRDR	TNLT	1.51	99.54	2.84	3.01	0.01	0.14			66	21	852	827	16	
CGR89-525	104G11	363661	6375334	ITgd	GRDR	GRDR	0.72	99.35	1.81	2.37	0.01	0.14			59	26	1451	660	68	

FIELD NO	NTS MAP Zone 9	UTM EAST	UTM NORTH	MAP CODE	ROCK CODE	QAP FIELD	Zr ppm 20 XRF	Y ppm 10 XRF	Nb ppm 5 XRF	Ta ppm NA XRF	V ppm 5 XRF	La ppm 15 XRF	Yb ppm XRF	Pt ppm XRF	Pd ppm XRF	Sn ppm NA XRF	Th ppm NA XRF	U ppm NA XRF	
Detection Limits:																			
Analytical Techniques:																			
LATE TRIASSIC TO EARLY JURASSIC - Copper Mountain suite																			
Rugged Mountain pluton - syenites																			
INE91-121	104G13	343900	6410055	eJs	SYNT	FSYNT	85	20	10	<15	<5	25	1.7			<15	<15	<15	
INE91-122	104G13	343815	6409693	eJs	SYNT	FSYNT	93	22	8	<15						<15	<15	<15	
INE91-316	104G13	345938	6408895	eJs	SYNT	FSYNT	77	26	6	<15	<5	18	3.2			<15	<15	<15	
INE91-317	104G13	346111	6408964	eJs	SYNT	FSYNT	80	20	<5	<15						<15	<15	<15	
INE91-320	104G13	346465	6409053	eJs	SYNT	FSYNT	80	22	<5	<15						18	<15	<15	
INE91-322	104G13	346472	6408613	eJs	SYNT	FSYNT	67	17	<5	<15						16	<15	<15	
INE91-324	104G13	346493	6408088	eJs	SYNT	FSYNT	48	18	6	<15						<15	<15	<15	
INE91-82	104G13	345489	6410465	Dikes	SYNT	FSYNT	76	11	7	<15						<15	<15	<15	
INE91-64	104G13	347313	6409513	Dikes	SYNT	FSYNT	105	<10	5	<15						<15	<15	<15	
INE91-73-2	104G13	346298	6410221	Dikes	SYNT	FSYNT	134	18	13	<15						15	<15	<15	
INE91-76	104G13	346069	6409865	eJs/TJcpx	SYNT/PRXN	NA	81	22	<5	<15	<5	26	2.2			19	<15	<15	
INE91-115	104G13	345096	6410460	eJs/TJcpx	SYNT/PRXN	NA	61	21	<5	<15						28	<15	<15	
INE91-336	104G13	343829	6410644	eJs/TJcpx	SYNT/PRXN	NA	58	19	<5	<15	<5	25	1.8			15	<15	<15	
Rugged Mountain ultramafic phase																			
INE91-78-2	104G13	345738	6409800	TJcpx	PRXN	NA	52	26	7	<15	<5	36	2.0			29	<15	<15	
INE91-80-2	104G13	345626	6410045	TJcpx	PRXN	NA	68	23	10	<15	<5	51	2.1			23	<15	<15	
INE91-80-2DU	104G13	345626	6410045	TJcpx	PRXN	NA	64	20	<5	<15						24	<15	<15	
Ultramafite bodies																			
Latimer Lake pluton																			
DBR91-382-2	104G13	338833	6417196	TJcpx	CPXN	NA	41	19	8	<15						15	<15	<15	
DBR91-387	104G13	338096	6416989	TJcpx	CPXN	NA	32	13	8	<15						16	<15	<15	
Damnation pluton																			
INE91-282	104G13	348525	6416034	TJcpx	CPXN	NA	25	10	<5	<15						<15	<15	<15	
Quartz monzonite variation																			
Perelshin pluton:																			
MGU88-102*	104G05	341169	6352116	eJqm	MNZN	QZMZDR	129	19	15	5	22	19	6						
MGU88-190	104G05	335928	6355747	eJqm	MNZN	GRDR	124	16	10	5	111	15	5						
MIDDLE(?) TO LATE TRIASSIC - Polaris suite																			
Mount Hickman Complex																			
MGU88-184	104G06	374058	6347932	ITcx	CPXN	NA								15	2				
DBR88-314	104G06	375952	6350727	ITcx	PRXN	NA								37	3				
Middle Scud Creek body																			
MMC88-224	104G06	360224	6350671	ITcx	CPXN	NA								7	12				
DBR88-243	104G06	361339	6349375	ITcx	GBBR	NA								10	9				
Yehinko Lake body																			
MGU89-111	104G11	360372	6380596	ITcx	CPXN	NA	20	8	9		142	6		6	11				
MGU89-114	104G11	360008	6380195	ITcx	CPXN	NA	20	9	5		110	4		2	8				
MGU89-121	104G11	359714	6377724	ITcx	CPXN	NA	17	8	4		108	1		2	9				
MGU89-156	104G11	359684	6376552	ITcx	CPXN	NA	20	9	8		125	3		3	8				
MIDDLE TO LATE TRIASSIC - Stikine suite																			
Hickman batholith																			
DBR88-322	104G06	365956	6350407	ITm	MNZN	GRDR	148	12	8	5	113	15	6						
MGU88-192	104G06	369187	6356802	ITm	GRDR	GRDR	138	10	8	5	103	15	5						
DBR88-325	104G06	363815	6352467	ITm	MNZN	QZMZDR	63	17	7	5	259	22	5						
MGU88-197	104G06	362995	6351733	ITm	MNZN	QZMZDR	272	32	20	5	127	19	6						
Nightout pluton																			
MGU88-204	104G06	375004	6373914	ITgd	GRDR	GRDR	144	12	7	5	72	15	6						
MGU89-52	104G11	361593	6402281	ITgd	GRDR	TNLT	115	20	1		125	21							
CGR89-525	104G11	363681	6375334	ITgd	GRDR	GRDR	146	23	5		87	8							

FIELD NO	NTS MAP Zone 9	UTM EAST	UTM NORTH	MAP CODE	ROCK CODE	QAP FIELD	SiO ₂ %	TiO ₂ %	Al ₂ O ₃ %	Fe ₂ O ₃ %	MnO %	MgO %	CaO %	Na ₂ O %	K ₂ O %	P ₂ O ₅ %	
Detection Limits:							0.01	0.01	0.01	0.01	0.01	0.01	0.01	0.01	0.01	0.01	
Analytical Techniques:							XRF/ICP	XRF/ICP	XRF/ICP	XRF/ICP	XRF/ICP	XRF/ICP	XRF/ICP	XRF/ICP	XRF/ICP	XRF/ICP	XRF/ICP
Tahltan Lake pluton																	
DBR91-724	104G13	342364	6425433	TJgd	QZMNZN	QZMZDR	59.45	0.51	17.88	5.81	0.14	1.97	6.46	3.69	1.78	0.25	
INE91-244	104G13	344238	6425218	TJgd	QZDORT	QZMZDR	53.94	0.68	18.16	8.39	0.20	2.82	8.67	3.19	1.16	0.25	
JTI91-72	104G13	345075	6425634	TJgd	QZDORT	DORT	49.59	0.75	19.42	9.06	0.21	3.38	10.09	3.12	1.49	0.28	
Little Tahltan Lake pluton																	
INE91-225	104G13	326042	6425687	TJhqd	GRDR	GRDR	60.85	0.50	18.16	5.24	0.16	1.37	5.10	3.87	1.91	0.20	
Tahltan River pluton																	
WMC91-52	104G13	342555	6430607	TJhqm	QZMZDR	GRDR	64.33	0.47	16.97	4.21	0.10	1.32	4.92	4.43	1.72	0.14	
WMC91-52DUP	104G13	342555	6430607	TJhqm	QZMZDR	GRDR	64.29	0.47	17.04	4.20	0.11	1.31	4.92	4.41	1.81	0.13	

FIELD NO	NTS MAP Zone 9	UTM EAST	UTM NORTH	MAP CODE	ROCK CODE	QAP FIELD	LOI %	OX_SUM %	Fe ₂ O ₃ %	FeO %	S %	Co ₂ %	Ni ppm	Mo ppm	Zn ppm	Cr ppm	Ba ppm	Sr ppm	Rb ppm		
Detection Limits:							0.01						5	8	2	10	10	5	10		
Analytical Techniques:							XRF/ICP	XRF/ICP	calc.	TIT				AAS	AAS	AAS	XRF		XRF	XRF	
MGU88-197	104G06	362995	6351733	ITm	MNZN	QZMZDR	0.51	99.98	2.01	3.42	0.01	0.15	2	8		23	908	582	125		
Nightout pluton																					
MGU88-204	104G06	375004	6373914	ITgd	GRDR	GRDR	0.61	99.62	1.74	1.40	0.01	0.15	6	8		38	1036	835	35		
MGU89-52	104G11	361593	6402281	ITgd	GRDR	TNLT	1.51	99.54	2.84	3.01	0.01	0.14			66	21	852	827	16		
CGR89-525	104G11	363661	6375334	ITgd	GRDR	GRDR	0.72	99.35	1.81	2.37	0.01	0.14			59	26	1451	660	68		
Tahltan Lake pluton																					
DBR91-724	104G13	342364	6425433	TJ	QZMNZN	QZMZDR	1.56	99.50	5.81	2.51						<10		564	38		
INE91-244	104G13	344238	6425218	TJ	QZDORT	QZMZDR	1.58	99.04	8.39	4.39						<10		484	22		
JTI91-72	104G13	345075	6425634	TJ	QZDORT	DORT	2.12	99.51	9.06	6.40						<10		466	31		
Little Tahltan Lake pluton																					
INE91-225	104G13	326042	6425687	TJ	GRDR	GRDR	1.97	99.33	5.24	2.16						<10		596	48		
Tahltan River pluton																					
WMC91-52	104G13	342555	6430607	TJ	QZMZDR	GRDR	0.88	99.49	4.21	1.78						11		666	37		
WMC91-52DUP	104G13	342555	6430607	TJ	QZMZDR	GRDR	0.87	99.56	4.20	1.75						<10		665	41		

FIELD NO	NTS MAP Zone 9	UTM EAST	UTM NORTH	MAP CODE	ROCK CODE	QAP FIELD	Zr ppm	Y ppm	Nb ppm	Ta ppm	V ppm	La ppm	Yb ppm	Pt ppm	Pd ppm	Sn ppm	Th ppm	U ppm		
Detection Limits:							20	10	5	NA	5	15				NA	NA	NA		
Analytical Techniques:							XRF	XRF	XRF	XRF	XRF	XRF	XRF	XRF	XRF	XRF	XRF	XRF	XRF	
MGU88-197	104G06	362995	6351733	ITm	MNZN	QZMZDR	272	32	20	5	127	19	6							
Nightout pluton																				
MGU88-204	104G06	375004	6373914	ITgd	GRDR	GRDR	144	12	7	5	72	15	6							
MGU89-52	104G11	361593	6402281	ITgd	GRDR	TNLT	115	20	1		125	21								
CGR89-525	104G11	363661	6375334	ITgd	GRDR	GRDR	146	23	5		87	8								
Tahltan Lake pluton																				
DBR91-724	104G13	342364	6425433	TJ	QZMNZN	QZMZDR	80	16	<5	<15						<15	<15	<15		
INE91-244	104G13	344238	6425218	TJ	QZDORT	QZMZDR	67	19	<5	<15						<15	<15	<15		
JTI91-72	104G13	345075	6425634	TJ	QZDORT	DORT	34	16	<5	<15						<15	<15	<15		
Little Tahltan Lake pluton																				
INE91-225	104G13	326042	6425687	TJ	GRDR	GRDR	86	16	7	<15						<15	<15	<15		
Tahltan River pluton																				
WMC91-52	104G13	342555	6430607	TJ	QZMZDR	GRDR	91	13	<5	<15						<15	<15	<15		
WMC91-52DUP	104G13	342555	6430607	TJ	QZMZDR	GRDR	91	11	<5	<15						<15	<15	<15		

Rock code abbreviations: GRNT = granite, MNGRNT = monzogranite, GRDR = granodiorite, TNLT = tonalite, SYNT = syenite, QZMNZN = quartz monzonite, QZMZDR = quartz monzodiorite, QZDORT = quartz diorite, DORT = diorite, MNZN = monzonite, PRXN = pyroxenite, CPXN = clinopyroxenite, RYLT = rhyolite, ANDS = andesite, FPPP = feldspar plagioclase porphyric, na = not applicable. Rock Code = classification based on modal mineralogy (Streckeisen, 1976); QAP Field = normalized geochemical classification. * = radiometric date sample.

APPENDIX 12
 POTASSIUM-ARGON ANALYTICAL DATA AND DATES FOR
 STRATIFIED AND PLUTONIC ROCKS

FIELD NO.	MAP CODE	NTS MAP	UTM EAST	(ZN 09) NORTH	ROCK TYPE	PLUTON/ GROUP	DATING METHOD	MINERAL	K (%)	⁴⁰ Ar (x10 ⁻⁶ cc/gm)	⁴⁰ Ar (%)	AGE (Ma)
MGU88-76	Egn	104G05	327946	6374268	Biotite granite	Sawback	K-Ar	Bi	6.65 ± 0.07	12.574	59.7	48.0 ± 1.7
DBR89-471	TSd	104G11	352738	6392320	Andesite tuff	Sloko	K-Ar	Hb	0.577 ± 0.001	1.110	79.6	48.8 ± 1.7
DBR88-290-2	Ef	104G05	347688	6371094	Felsite dike	Dike	K-Ar	Bi	6.090 ± 0.030	11.922	90.9	49.7 ± 1.7
DBR89-376	KTS	104G11	354146	6391935	Tuff	Sustut	K-Ar	WR	4.170 ± 0.010	8.490	85.2	51.6 ± 1.8
MGU88-48	Egd	104G05	332316	6349874	Granodiorite	Christina	K-Ar	Bi	5.78 ± 0.04	12.368	53.6	54.2 ± 1.9
MGU88-48	Egd	104G05	332316	6349874	Granodiorite	Christina	K-Ar	Hb	0.695 ± 0.001	1.539	83.4	56.1 ± 2.0
DBR89-25	KTS	104G11	358247	6388689	Wacke	Sustut	K-Ar	Bi	5.82 ± 0.02	19.815	62.2	85.6 ± 3.0
CGR89-217	ImJHv	104G12	355389	6378238	Andesite tuff	Hazelton	K-Ar	WR	0.475 ± 0.002	2.843	86.9	148 ± 5
MGU89-314	uCSv	104G05	341176	6371611	Hb schist	Stikine	K-Ar	Hb	0.647 ± 0.004	4.073	3.29	155 ± 5
DBR88-331	leJgd	104G05	349807	6371030	Granodiorite	Dokdaon	K-Ar	Hb	0.712 ± 0.005	4.58	88.8	158 ± 6
CGR89-495	mJgn	104G12	359129	6384068	Granite	Saffron	K-Ar	Bi	4.42 ± 0.14	29.200	94.7	162 ± 7
CGR89-517	mJmd	104G11	354301	6385459	Monzonite	Saffron	K-Ar	Hb	0.345 ± 0.016	2.272	82.3	162 ± 7
DBR88-329	leJgd	104G06	348562	6359899	Granodiorite	Navo	K-Ar	Bi	6.980 ± 0.020	46.357	88.4	163 ± 6
CGR89-439	ImJHv	104G11	348412	6387905	Andesite	Hazelton	K-Ar	WR	1.660 ± 0.010	11.245	94.6	166 ± 6
DBR88-328	leJgd	104G06	352733	6360764	Pink granite	Niko	K-Ar	Bi	5.930 ± 0.200	42.932	81.4	177 ± 7
CGR89-546	mJm	104G12	338140	6393551	Monzonite	Conover	K-Ar	Hb	0.802 ± 0.001	5.804	92.7	177 ± 6
DBR88-329	leJgd	104G05	348562	6359899	Granodiorite	Navo	K-Ar	Hb	1.21 ± 0.04	8.995	91.7	182 ± 7
DBR91-723	eJmd	104G13	331062	6408246	Monzonite	Limpoke	K-Ar	Hb	0.601 ± 0.007	4.481	89.8	182 ± 5
CGR89-78	ITgd	104G11	366699	6391077	Monzonite	Nightout	K-Ar	Hb	0.567 ± 0.003	4.668	90.7	200 ± 7
MGU88-102	eJqm	104G05	341169	6352216	Qtz monzonite	Pereshin	K-Ar	Hb	0.773 ± 0.004	6.495	95.5	204 ± 7

* = Radiogenic argon; na = not available; WR = whole rock.

Decay constants: 40K epsilon=0.581 x 10⁻¹⁰ year⁻¹; 40K beta=4.96 x 10⁻¹⁰ year⁻¹; 40K/K = 1.167 x 10⁻⁴.

Potassium determined at the University of British Columbia geochronology laboratory; Ages given with 1 sigma error.

Argon determination and age calculation by J.E. Harakal, University of British Columbia.

APPENDIX 13
URANIUM-LEAD ANALYTICAL DATA

Zircon fraction	Wt. (mg.)	U (ppm)	Pb ^a (ppm)	$\frac{^{206}\text{Pb}^b}{^{204}\text{Pb}}$	Pb ^c (pg)	$^{208}\text{Pb}^a$ (%)	$\frac{^{206}\text{Pb}^d}{^{238}\text{U}}$	$\frac{^{207}\text{Pb}^d}{^{235}\text{U}}$	Corr. Coeff. ^e	$\frac{^{207}\text{Pb}^d}{^{206}\text{Pb}}$	$^{207}\text{Pb}/^{206}\text{Pb}$ age (Ma)
Hazelton Group andesitic tuff (Sample DBR-90-162) ¹											
A. N1 +74-105 A	0.023	425	13	1298	14	8.8	0.03032 ± 0.10%	0.2101 ± 0.28%	0.56	0.05027 ± 0.23%	207.3 ± 10.8
B. N1 +62-74 A	0.013	527	15	784	16	10.7	0.02887 ± 0.14%	0.1982 ± 0.51%	0.60	0.04980 ± 0.44%	185.8 ± 20.5
C. N1 +149 A	0.010	1189	35	2198	10	11.1	0.02908 ± 0.11%	0.1995 ± 0.21%	0.65	0.04978 ± 0.16%	184.5 ± 7.5
Hazelton Group flow-banded rhyolite (Sample DBR-90-717) ¹											
A. M2 +45-63	0.2	532	13	675	247	13.2	0.02389 ± 0.15%	0.1632 ± 0.21%	0.70	0.04954 ± 0.15%	173 ± 7
B. N2 +63-100	0.5	107	3	651	141	12.1	0.02617 ± 0.15%	0.1806 ± 0.21%	0.70	0.05005 ± 0.15%	197 ± 7
C. M2 +80-100	0.4	325	9	996	226	12.0	0.02663 ± 0.15%	0.1828 ± 0.18%	0.83	0.04978 ± 0.10%	185 ± 5
D. N2 +100-350	1.3	491	13	334	1120	12.0	0.02611 ± 0.15%	0.1787 ± 1.35%	0.43	0.04964 ± 1.32%	178 ± 15
E. N2 +100-350 A	0.2	386	11	1266	108	11.7	0.02747 ± 0.15%	0.1878 ± 0.17%	0.89	0.04957 ± 0.08%	175 ± 4
Cone Mountain granodiorite (Sample DBR-90-40) ¹											
A. N1 +105 A	0.044	537	16	1576	28	12.6	0.02905 ± 0.10%	0.1993 ± 0.17%	0.70	0.04976 ± 0.13%	183.9 ± 5.9
B. N2 +105 A	0.089	429	13	1657	42	11.4	0.02906 ± 0.09%	0.1993 ± 0.15%	0.77	0.04973 ± 0.10%	182.6 ± 4.5
C. M2 +149 A	0.062	402	12	2460	18	13.5	0.02908 ± 0.10%	0.1995 ± 0.16%	0.70	0.04976 ± 0.11%	183.9 ± 5.3
D. N2 +105-149 A	0.102	606	17	2597	42	11.8	0.02813 ± 0.09%	0.1937 ± 0.13%	0.82	0.04994 ± 0.07%	192.1 ± 3.5
Limpoke quartz monzodiorite (Sample DBR-91-723) ²											
A. N2 +30-45	1.1	759	20	5108	269	13.8	0.02568 ± 0.15%	0.1767 ± 0.15%	0.99	0.04991 ± 0.02%	191 ± 1
B. N2 +45-80	1.7	466	12	4297	100	12.7	0.02525 ± 0.15%	0.1736 ± 0.16%	0.96	0.04986 ± 0.04%	188 ± 2
C. N2 +80-100	1.8	422	11	3793	112	12.3	0.02615 ± 0.15%	0.1799 ± 0.22%	0.67	0.04991 ± 0.17%	191 ± 8
D. N2 +100-125	1.9	410	11	3910	111	12.2	0.02606 ± 0.15%	0.1791 ± 0.22%	0.68	0.04985 ± 0.16%	188 ± 8
E. N2 +125-350	0.8	304	8	3377	119	11.9	0.02569 ± 0.15%	0.1767 ± 0.15%	0.98	0.04989 ± 0.03%	190 ± 2
F. N2 +145-350	0.4	398	11	6104	47	12.8	0.02794 ± 0.15%	0.1924 ± 0.15%	1.00	0.04993 ± 0.01%	192 ± 1
Rugged Mountain dyke (Sample DBR-91-725) ³											
A. N2 +74-105	0.031	2206	66.8	107	1250	21.2	0.02643 ± 0.36%	0.1819 ± 2.22%		0.04991 ± 2.04%	191.0 ± 95.0
B. N2 +105-134, a	0.010	1319	46.3	524	46	23.2	0.02982 ± 0.15%	0.2044 ± 0.74%		0.04972 ± 0.66%	181.7 ± 30.9
C. N2 +74-105, a	0.011	993	34.4	474	40	25.0	0.02872 ± 0.12%	0.1984 ± 0.65%		0.05011 ± 0.58%	199.9 ± 27.1
D. N2 +74-134, a	0.010	2071	69.0	398	100	21.3	0.02901 ± 0.12%	0.2002 ± 0.72%		0.05004 ± 0.65%	197.0 ± 30.1

N1 = non-magnetic at <1°, 1.7 amps on Frantz magnetic separator; N2 = non-magnetic at <2°, 1.7 amps; M2 = magnetic at >2°, 1.7 amps; A = abraded. Numbers such as +105 refer to size in microns; a = abraded. $^{207}\text{Pb}/^{206}\text{Pb}$ age errors are 2 standard errors in Ma. Blank compositions for GSC analyses are $^{206}\text{Pb}/^{204}\text{Pb}=17.92$; $^{207}\text{Pb}/^{204}\text{Pb}=15.37$; $^{208}\text{Pb}/^{204}\text{Pb}=37.4$. Blank compositions for UCSB analyses are $^{206}\text{Pb}/^{204}\text{Pb}=18.6$; $^{207}\text{Pb}/^{204}\text{Pb}=15.5$; $^{208}\text{Pb}/^{204}\text{Pb}=38.0$.

^a Radiogenic Pb, corrected for blank and spike.

^b Corrected for fractionation and spike Pb.

^c Total common Pb in analysis in picograms.

^d Corrected for blank Pb and U in common Pb; errors are 1 standard error of mean in %.

^e Correlation coefficient of errors in $^{206}\text{Pb}/^{238}\text{U}$ and $^{207}\text{Pb}/^{235}\text{U}$.

¹ Analysis and age determination by Mary Lou Bevier, GSC, Ottawa, Ontario.

² Analysis and age determination by William C. McClelland, University of California, Santa Barbara, California.

³ Analysis and age determination by James Mortensen, University of British Columbia, Vancouver, B.C..

APPENDIX 14
LITHOGEOCHEMICAL DATA

FIELD NO.	NTS MAP	UTM EAST	(Zn 09)	SAMPLE DESCRIPTION NORTH	Au ppb	Ag ppm	Cu ppm*	Pb ppm*	Zn ppm*	As ppm*	Sb ppm
DBR88-5-2	104G05	346050	6356750	Rusty argillite with 5-10% diss py, po	<20	1	36	16	380	3	1
DBR88-20	104G06	350630	6348450	Limonitic, buff limestone	<20	<0.5	5	7	27	5	<0.5
DBR88-101	104G06	360000	6357550	Quartz vein in siltstone	<20	<0.5	21	7	29	36	<0.5
DBR88-107	104G05	319000	6367100	Pyritic quartz vein in altered intrusion (F)	112	20	9	42	22	1	<0.5
DBR88-113-1	104G05	322200	6365800	Quartz vein with 25% gal, cpy, py (F)	<20	37	0.27%	2.30%	1.44%	<1	3
DBR88-113-2	104G05	322200	6365800	Quartz vein with 25% py (F)	730	66	181	760	950	54	2
DBR88-115	104G05	322900	6365500	Pyritic quartz vein in Eocene granite	<20	<0.5	4	39	10	3	0.7
DBR88-130-1	104G05	348600	6351640	Fine-grained mafic rock with malachite (F)	97	2	620	5	440	7	0.6
DBR88-130-2	104G05	348600	6351640	Altered limestone with mt, py, cpy	58	0.5	0.31%	3	173	8	<0.5
DBR88-187	104G06	361330	6359720	Mafic sandstone with pyritic Fe-carb vein	5	<0.5	154	3	66	9	5
DBR88-213	104G06	361040	6354820	Altered limestone with pyrite	2	<0.5	208	3	38	112	11
DBR88-215	104G06	361090	6354440	Fe-carb altered limestone with py, arpr	1	1.5	232	3	35	232	260
DBR88-222-2	104G06	360040	6350930	Fe-carb altered limestone along fault	1	<0.5	92	3	55	7	2
DBR88-286-1	104G05	348140	6371700	Quartz vein	154	6	128	19	15	39	0.9
DBR88-286-3	104G05	348140	6371700	Massive sulphide pod with mt, py	102	25	91	20	24	54	<0.5
DBR88-288	104G05	347830	6371430	Pyrite-quartz zone in volcanics	226	0.8	14	14	7	8	3
DBR88-302-2	104G06	357650	6375300	Fe-Carb vein with py, splr, gal	450	20	450	0.58%	3.50%	258	321
DBR88-336	104G05	320650	6366225	Stck clcp-mlbd in altered felsic int (T)	1	<0.5	15	20	30	<1	0.5
DBR88-337	104G05	320650	6366225	Stck clcp-mlbd in altered felsic int (T)	1	2	18	75	103	<1	0.5
DBR88-338	104G05	320650	6366225	Srct-altered felsic int (D)	1	7	28	24	30	<1	0.5
DBR88-339	104G05	320650	6366225	Srct-altered felsic int with qt-mlbd stck (D)	4	<0.5	17	20	22	<1	0.5
DBR88-340	104G05	320650	6366225	Srct-altered felsic int with qt-py stck (D)	1	<0.5	10	10	15	<1	0.5
DBR88-341	104G05	320650	6366225	Srct-altered felsic int with mlbd stck (D)	1	0.5	9	20	16	<1	0.5
DBR88-342	104G05	320650	6366225	Srct-altered felsic int with qt-py stck (D)	1	0.6	6	23	25	<1	0.5
DBR88-343	104G05	320650	6366225	Srct-altered felsic int with mlbd stck (D)	2	0.5	7	44	12	<1	0.5
DBR88-344	104G05	320650	6366225	Srct-altered felsic int with diss py (D)	1	13	495	0.14%	0.23%	2	0.5
DBR88-345	104G05	320650	6366225	Srct-altered felsic int with diss py (D)	15	1	8	12	50	<1	0.5
DBR88-346	104G05	320650	6366225	Srct-altered felsic int with qt-mlbd stck (D)	1	7	12	63	82	<1	0.5
MGU88-16	104G05	340350	6349150	Sheared margin of volcanic pendant with	10	<0.5	115	18	50	2	<0.5
MGU88-44-2	104G05	333730	6350420	Gabbroic dike with 5% diss py	1	<0.5	52	18	152	<1	<0.5
MGU88-106	104G05	342370	6350470	Sheared granodiorite with py	7	<0.5	123	6	87	3	1
MGU88-130-2	104G05	341300	6356640	Altered sill in limestone with py, cpy	5	0.8	133	14	158	2	0.9
MGU88-181	104G06	360950	6371250	Qt - Fe-Carb vein in volcanics with py, cpy	11	<0.5	264	5	13	14	5
MMC88-48	104G06	362390	6354000	Rusty, mylonitic fault zone	<20	<0.5	72	13	59	8	0.9
MMC88-54	104G06	362450	6352730	Sheared quartz monzonite with malachite	<20	<0.5	330	13	55	4	<0.5
MMC88-55-3	104G06	362400	6352440	Sheared quartz monzonite with malachite	<20	<0.5	40	18	63	2	0.9
MMC88-68-1	104G05	342200	6358090	Sheared siliceous rock with py	35	1	45	19	17	288	2
MMC88-157-2	104G06	361000	6360230	Rusty, silicified dike with py	<20	<0.5	34	3	59	N.A.	2
MMC88-202	104G05	340190	6372790	Silicified quartz monzonite with py	1	<0.5	10	8	21	<1	0.5
MMC88-207	104G05	339780	6373900	Fine-grained basalt with py, pyr (F)	1	<0.5	256	9	69	1	0.7
MMC88-218-2	104G06	361300	6353560	Rusty fine-grained basalt with py	1	<0.5	156	6	49	2	0.6
MMC88-249	104G05	347370	6371670	Rusty quartz monzonite with diss py	10	<0.5	20	9	48	10	2
MMC88-250	104G05	347400	6371430	Malachite-stained volcanic breccia with py	4	<0.5	103	14	102	5	<0.5
MMC88-279-2	104G05	341560	6354350	Fine-grained siliceous rock with diss py	1	<0.5	59	5	115	3	0.5
CGR89-7-2	104G12	350651	6390820	cm-scale quartz and carbonate vein	<2	2.0	260	5	8	13	20.0
CGR89-46	104G11	363807	6389993	pyritic felsite dike	4	0.8	5	5	19	17	2.0
CGR89-47-2	104G11	363624	6390051	pyritic felsite dike	<2	0.8	8	11	31	73	4.0
CGR89-69	104G11	367856	6389075	cm-scale quartz vein with malachite and	40	<0.5	0.24%	9	118	10	0.6
CGR89-93	104G12	346559	6397567	pyritic, siliceous dust tuff	<2	<0.5	225	2	83	6	1.0
CGR89-116	104G11	362252	6391394	py, pyr, chl, qz open space filling in rhyolite	<2	<0.5	186	7	145	6	1.0
CGR89-120	104G11	360342	6391750	disseminated py in carbonaceous(?)	<2	<0.5	48	7	55	52	3.0
CGR89-153-1	104G11	353947	6388416	py and cb breccia filling	<2	<0.5	14	2	27	2	<0.5
CGR89-153-2	104G11	353947	6388416	pyritic altered pluton or felsite dike	<2	<0.5	44	2	15	2	<0.5
CGR89-153-3	104G11	353947	6388416	pyritic felsite dike	<2	<0.5	40	2	6	1	<0.5
CGR89-166	104G11	351657	6389893	quartz vein with cpy, mal, up to 5 cm	<2	51.0	4.7%	7	57	29	50.0
CGR89-166DUF	104G11	351657	6389893	quartz vein with cpy, mal, up to 5 cm	12	66.0	5.3%	10	55	62	3.0
CGR89-188	104G12	340725	6391456	Fe carbonate and quartz veining, minor py.	<2	<0.5	108	4	42	8	23.0
CGR89-191	104G12	340178	6391377	Fe carbonate vein-breccia along dike	8	<0.5	24	65	140	64	79.0
CGR89-194	104G12	340469	6391222	pyritic, siliceous dust tuff	<2	<0.5	141	5	86	11	3.0
CGR89-195	104G12	340675	6391222	pyritic, siliceous dust tuff	3	<0.5	87	12	103	2	0.7
CGR89-196	104G12	340845	6391268	pyritic, siliceous dust tuff	<2	<0.5	159	7	83	6	0.9
CGR89-196DUF	104G12	340845	6391268	pyritic, siliceous dust tuff	<2	<0.5	163	7	83	6	0.7
CGR89-197	104G11	353967	6395595	pyritic, siliceous dust tuff	<2	<0.5	158	5	85	7	0.6
CGR89-213	104G11	355423	6377783	black carbonate veining and breccia fillings	5	<0.5	63	9	35	13	0.6
CGR89-218	104G11	355351	6378311	pyritic feldspar porphyry dike	<2	<0.5	25	7	59	21	0.9
CGR89-220	104G11	355397	6378716	tourmalinized(?) feldspar porphyry dike	<2	<0.5	8	7	37	3	0.7
CGR89-224	104G11	356579	6381817	cm-scale hematitic cb-qz veins	3	<0.5	31	2	49	2	<0.5
CGR89-247	104G12	350289	6386230	5-15 cm Fe carbonate vein-breccia	22	3.0	210	0.58%	0.37%	17	10.0

FIELD NO.	NTS MAP	UTM EAST	(Zn 09)	SAMPLE DESCRIPTION NORTH	Au ppb	Ag ppm	Cu ppm*	Pb ppm*	Zn ppm*	As ppm*	Sb ppm
CGR89-291-2	104G12	337511	6400131	siliceous tuff with disseminated py,	<2	<0.5	200	9	105	4	2.0
CGR89-293	104G12	338259	6399941	siliceous tuff with disseminated py,	<2	<0.5	144	4	82	5	0.7
CGR89-307	104G11	353660	6377330	cm-scale qz-cb veinlets @ py, gal, sph, py,	43	45.0	0.86%	0.51%	162	3	2.0
CGR89-307-2	104G11	353660	6377330	cm-scale qz-cb veinlets @ py, gal, sph, py,	136390	19.0	0.29%		27	10	2 0.7
CGR89-324	104G12	349748	6378342	float: qz vein @ ep, hem, cpy, py, mal	7	3.0	0.73%		7	28	8 2.0
CGR89-337	104G11	353071	6376673	silicified, chloritized and ep-rich plutonic	5	<0.5	118	7	71	11	3.0
CGR89-341	104G11	354520	6376545	cb vng & hematitic/potassic altn in plut host	<2	<0.5	4	7	55	6	0.7
CGR89-359	104G11	351903	6381529	pyritic and chloritic wallrock to dike swarm	10	<0.5	68	10	17	3	<0.5
CGR89-382	104G12	337371	6393580	cb veining and vein-breccia	<2	<0.5	17	2	20	7	<0.5
CGR89-411	104G12	347667	6379730	silicified and potassically(?) altered plut rock	5158	2.0	28	267	171	7	3.0
CGR89-412	104G12	347476	6379970		18	<0.3	121	15	25		
CGR89-460	104G12	346971	6389455	cm-scale qz veinlet with py	312	12.0	0.50%	15	83	5	2.0
CGR89-481	104G12	347824	6376597	soil sample from limonitic zone	21	<0.5	315	24	102	113	3.0
CGR89-492-2	104G11	358011	6383849	sub-cm qz veinlet @ mal, py, ep	18	<0.5	0.52%	2	55	8	2.0
CGR89-524	104G11	363564	6375622	float: qz veinlet @ vfg chalcocite(?), mal	560	22.0	1.8%	79	44	11	6.0
CGR89-532	104G12	340283	6393699	Fe carb and chalcocite qz vein-breccia	<2	<0.5	72	5	36	6	7.0
CGR89-532-2	104G12	340283	6393699	qz and Fe carb veining	<2	<0.5	68	2	40	9	3.0
CGR89-536-2	104G12	339639	6393835	chalcocite qz vng & limonite open space	<2	<0.5	40	7	158	10	24.0
CGR89-539	104G12	339105	6394010	Fe carb altn & drusy qz open space filling	<2	<0.5	8	2	63	1	0.9
CGR89-540	104G12	338936	6394031	qz veining and Fe cb altn	<2	<0.5	40	2	35	2	5.0
DBR89-17	104G11	365042	6382784	Fe carb altered granodiorite	<2	0.8	6	5	56	14	2.0
DBR89-65	104G11	355316	6389710	disseminated py in altered andesite	<2	0.8	136	5	23	6	0.7
DBR89-101	104G12	339180	6389323	Cu-Fe skarn	338	19.0	2	11	162	130	3.0
DBR89-119-2	104G11	355942	6401780	py stringers in wacke	23	0.8	168	5	50	36	4.0
DBR89-139	104G11	366035	6388511	epidote-flooded tuff	<2	0.8	28	5	35	12	1.0
DBR89-247-2	104G12	342741	6401677	quartz vein in shale	<2	1.0	50	4	162	17	7.0
DBR89-256	104G11	354366	6377045	massive py with epidote and quartz	24	1.0	20	16	30	25	3.0
DBR89-258	104G11	354058	6377815	float: qz py vein in volcanic breccia	822	8.0	502	147	13	0.17%	21.0
DBR89-261	104G11	353956	6378067	disseminated py in siltstone	30	1.1	25	120	17	0.15%	28.0
DBR89-266	104G11	353336	6379465	qz-calcite vein @ cpy, gal, py	3977	29.0	3.5%	120	8	10	0.9
DBR89-266DUF	104G11	353336	6379465	qz-calcite vein @ cpy, gal, py	2898	33.0	1.5%	51	6	12	1.0
DBR89-273	104G12	347412	6385901	qz vein @ py, cpy	142	75.0	6.1%	84	67	11	11.0
DBR89-277-1	104G12	347013	6385242	1-2% py in fine grained chloritized(?) host	13	0.8	441	5	28	9	1.0
DBR89-277-2	104G12	347013	6385242	float: qz vein @ py	342	2.0	0.12%	31	0.22%	322	14.0
DBR89-298	104G11	354563	6379169	qz-calcite vein @ cpy, gal, py	856	37.0	2.5%	0.36%	57	4	0.7
DBR89-298DUF	104G11	354563	6379169	qz-calcite vein @ cpy, gal, py	2561	29.0	1.9%	1.7%	47	3	1.0
DBR89-302	104G11	354555	6379720	qz vein @ mal	300	261.0	11.8%	4	15	60	20.0
DBR89-367	104G12	339187	6395997	silicified host @ 2% disseminated py	167	<0.5	10	19	63	158	4.0
DBR89-367-2	104G12	339187	6395997	qz-calcite veins in clay-altered volcanic host	86	<0.5	49	56	71	160	4.0
DBR89-367-3	104G12	339187	6395997	qz-calcite veins in clay-altered volcanic host	140	<0.5	10	9	42	83	2.0
DBR89-382	104G12	349193	6383577	qz-Fe cb vein @ py	786	12.0	7	0.31%	0.43%	819	8.0
DBR89-383	104G12	349343	6383521	disseminated py in altered volcanic breccia	38	4.0	203	0.11%	0.33%	397	21.0
DBR89-384	104G12	349343	6383521	qz-calcite vein @ gal, py	548	40.0	485	2.2%	3.8%	638	55.0
DBR89-388	104G12	349486	6383569	qz-calcite vein @ py, gal	3	5.0	20	585	0.45%	33	39.0
DBR89-397	104G12	347156	6384568	float: limonitic, pyritic altered breccia	17	1.7	6	56	50	14	2.0
DBR89-398	104G12	347157	6384569	float: clay-altered conglomerate	6	0.8	11	41	28	35	7.0
DBR89-408-2	104G12	347488	6382841	vein	6	2.0	68	58	53	119	47.0
MGU89-73	104G11	359468	6378210	chloritized mafic tuff	<2	2.0	46	5	46	5	0.8
MGU89-73DUF	104G11	359468	6378210	chloritized mafic tuff	<2	2.0	47	5	52	6	0.6
MGU89-112-2	104G11	360073	6380466	up to 10% py in hb qz diorite dike	<2	0.8	120	5	51	1	<0.5
MGU89-115	104G11	360008	6380002	up to 10% py in hb qz diorite dike	56	0.8	246	5	51	1	<0.5
MGU89-115DUF	104G11	360008	6380002	up to 10% py in hb qz diorite dike	77	0.8	282	5	55	1	<0.5
MGU89-124	104G12	340509	6382959	pyritic metavolcanic	15	0.8	43	5	85	9	3.0
MGU89-125	104G12	340515	6383126	pyritic metavolcanic	3	0.8	53	5	58	5	2.0
MGU89-126	104G12	340468	6383222	pyritic metavolcanic	<2	0.8	85	17	48	6	2.0
MGU89-126DUF	104G12	340468	6383222	pyritic metavolcanic	<2	0.8	84	17	46	6	2.0
MGU89-141	104G12	340370	6381134	pyritic siliceous tuff	3	0.8	6	17	34	22	1.0
MGU89-143	104G12	340508	6380666	pyritic siliceous tuff	<2	0.8	15	23	62	11	1.0
MGU89-144	104G12	340500	6380258	pyritic siliceous tuff	8	0.8	40	5	688	5	0.7
MGU89-144DUF	104G12	340500	6380258	pyritic siliceous tuff	11	0.8	45	5	0	3	<0.5
MGU89-180-2	104G12	334859	6387323	pyritic andesite dike	<2	<0.5	134	12	41	7	0.6
MGU89-184	104G12	334242	6386648	pyritic andesite dike	4	<0.5	52	5	31	43	1.0
MGU89-189-2	104G12	333426	6386410	pyritic recrystallized limestone	14	1.3	199	38	54	2	<0.5
MGU89-209-2	104G12	333095	6385834	pyritic recrystallized limestone	<2	<0.5	104	17	19	116	1.0
MGU89-238	104G12	333400	6390208	pyritic metapelite	6	<0.5	0.10%	9	45	45	3.0
MGU89-252	104G12	332081	6392931	pyritic hb, plagioclase porphyritic dike	<2	<0.5	35	10	97	4	0.6
MGU89-279-2	104G12	327858	6391153	dacite tuff @ 5-10% layer-parallel pyrite	<2	<0.5	28	14	82	17	2.0
DBR88-243	104G06	361339	6349375	Wrx/PGE of a gabbro/peridotite	3	<0.5	48	5	32	3	0.9
MGU88-157-2	104G05	341290	6356620		1	<0.5	34	3	59	2	2
MGU88-224					1	<0.5	74	5	51	6	<0.5
MGU90-518	104G12	340043	6383679		4198	3.7	578	7	19	10	5
MGU90-580-3	104G05	339764	6371561		5	0.1	14	6	6	5	2
INE91-45	104G13	322521	6403596	Pyritic siltstone	7	<5	47	12	100	4	0.9
INE91-45-2	104G13	322521	6403596	Pyritic siltstone	<5	<5	25	12	23	11	1.1

FIELD NO.	NTS MAP	UTM EAST	(Zn 09)	SAMPLE DESCRIPTION NORTH	Au ppb	Ag ppm	Cu ppm*	Pb ppm*	Zn ppm*	As ppm*	Sb ppm
JTI91-50A	104G13	322775	6426500	10 m thick rusty altered zone	<5	<5	114	10	180	5	2.2
JTI91-50Adup	104G13	322775	6426500	10 m thick rusty altered zone	6	<5	125	12	181	6	2.3
INE91-50	104G13	322846	6403450	Pyritic siltstone	13	<5	19	34	29	68	5
DBR91-471	104G13	325259	6424810	Fe-carb.-qtz-py vein-5 cm wide	<5	<5	56	12	85	140	56
DBR91-470	104G13	325387	6424854	Fe-carb.-qtz-py veinlets(float)	<5	<5	59	6	53	1300	99
DBR91-469	104G13	325458	6424876	Rusty pyrite in vuggy-quartz(float)	22	<5	40	4	37	1100	110
JTI91-19A	104G13	327750	6408352	Pyritic, chl/ep. altered andesite	24	<5	416	22	105	9	3.2
JTI91-17	104G13	329270	6406695	Fe-carb., malachite in quartz vein	417	6	545	120	300	72	1.2
JTI91-96C	104G13	329906	6413005	Limonitic dike	<5	<5	28	6	14	3100	410
JTI91-14	104G13	330309	6406770	Epidote, mal. alteration along fault	106	5	1400	12	38	<2	0.3
JTI91-11	104G13	330392	6409065	Rusty zone with qtz veins & pyrite	<5	<5	128	6	9	<2	<0.2
DBR91-697-2	104G13	335641	6409581	Malachite infilling of fractures	12	<5	1.51%	44	413	5	1.6
DBR91-530	104G13	336983	6429701	Pyritic tuff mudstone	<5	<5	35	12	200	7	2.9
DBR91-252-2	104G13	339417	6407830	Pyritic, altered volcanic rock	12	<5	112	8	55	7	1
DBR91-699	104G13	340114	6408405	Rusty, pyritic syenite	28	<5	292	28	36	8	1.2
JTI91-79	104G13	342037	6425680	Altered granodiorite, mal. staining	647	22	0.29%	10	54	89	1.8
DBR91-171	104G13	342215	6412266	Pyritic, altered syenite dike	7	<5	224	12	68	5	0.4
DBR91-309	104G13	342234	6428432	Limonitic zone	<14	<5	69	6	41	26000	870
JTI91-82	104G13	343662	6424797	Limonitic diorite	8	<5	367	8	31	8	2.5
JTI91-65	104G13	343738	6425127	Rusty, altered quartz veins	2380	27	180	10	325	1700	<0.2
DBR91-84	104G13	345474	6422070	Pyritic, iron carbonate altered rx	86	<5	43	8	50	11	1.2
INE91-81-3	104G13	345521	6410352	Biotite, magnetite, pyrite, malachite	1810	<5	1.17%	18	117	3	0.3
INE91-78-3	104G13	345738	6409800	Altered syenite	1190	31	0.90%	36	153	<2	2.6
DMU91-3	104G13	349836	6415602	Limonite and epidote altered rx	21	<5	48	22	54	250	5.5
DBR91-594	104G13	351488	6420711	Fe-carb. altered volcanic rock	<5	<5	60	6	91	4	4

ABBREVIATIONS:

"=given in percent where indicated, alt=alteration, arpr=arsenopyrite, cb=carbonate, chl=chlorite, cm=centimetres, cpy=chalcopyrite, (D)=drill core sample, diss=disseminated, DUP=duplicate analysis, ep=epidote, (F)=float, Fe-Carb=iron carbonate, gal=galena, hb=hornblende, hem=hematite, int=intrusion, mal=malachite, mibd=molybdenum, mt=magnetite, plut=plutonic, py=pyrite, pyr=pyrrhotite, qz=quartz, sph=sphalerite, (T)=trench, vfg=very fine grained, vng=veining

ANALYTICAL TECHNIQUES:

SAMPLE PREPARATION:

Samples were pulverized to minus 200 mesh using tungsten carbide equipment.

TRACE ELEMENT ANALYSIS—Ag, Cu, Pb, Zn, As, Sb:

Samples, typically 0.5 gram, were digested in mixed acids (including HF) within Teflon beakers. The residue was then diluted to a specific volume and the elements measured using atomic adsorption spectroscopy. As and Sb determination used a method whereby an evolved hydride was passed through a heated quartz tube in the light path of the spectrometer. Background corrections were made for Pb, As and Sb.

TRACE ELEMENT ANALYSIS—Au:

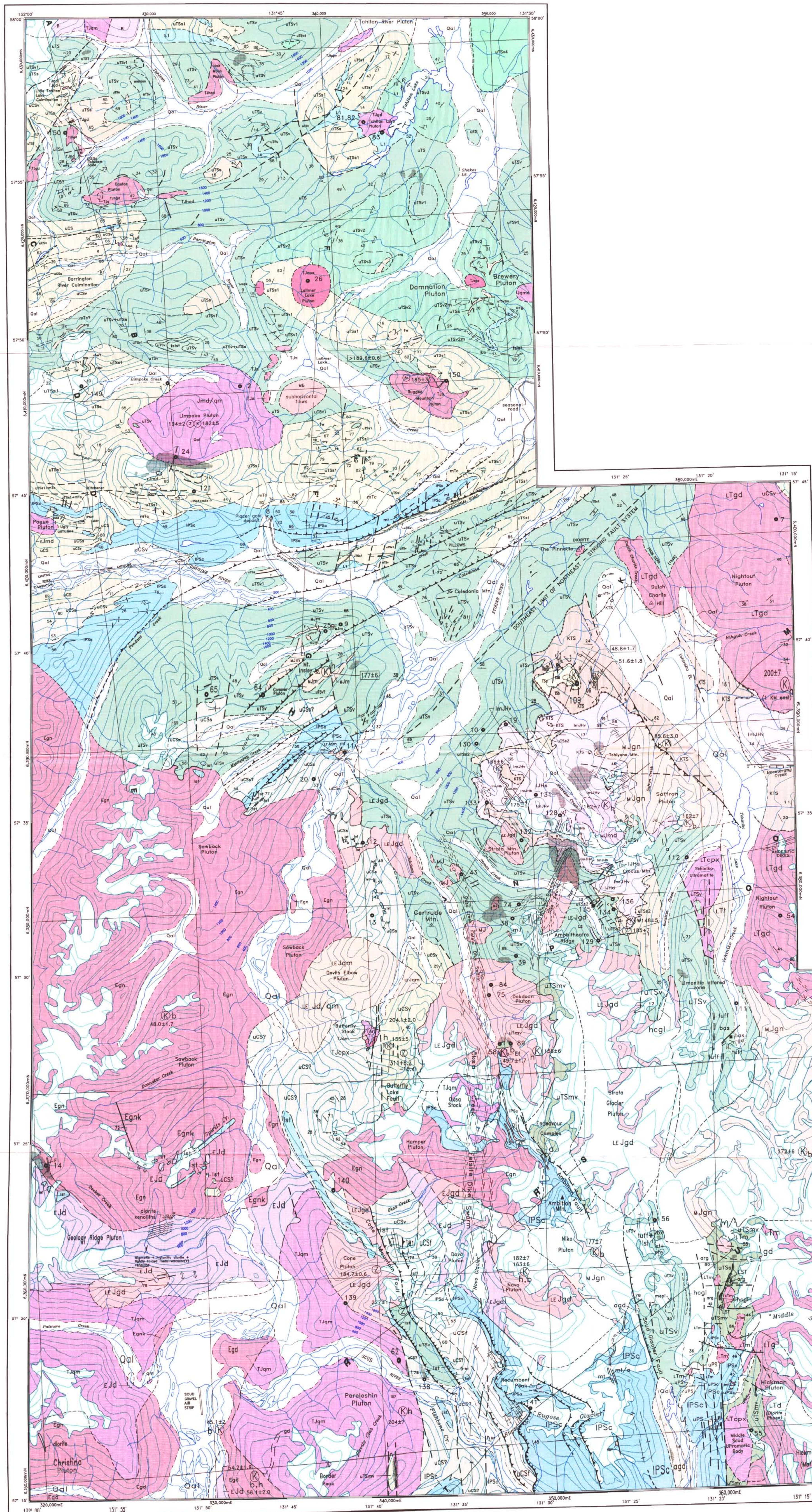
Gold analyses were performed by Acme Analytical Laboratories of Vancouver, British Columbia. A 20-gram sample was concentrated by fire assay into a silver bead, dissolved in aqua regia, and then gold was determined by graphite furnace atomic adsorption spectroscopy.

GEOLOGY OF WESTERN TELEGRAPH CREEK MAP AREA

NTS 104G/5,6,11W,12,13

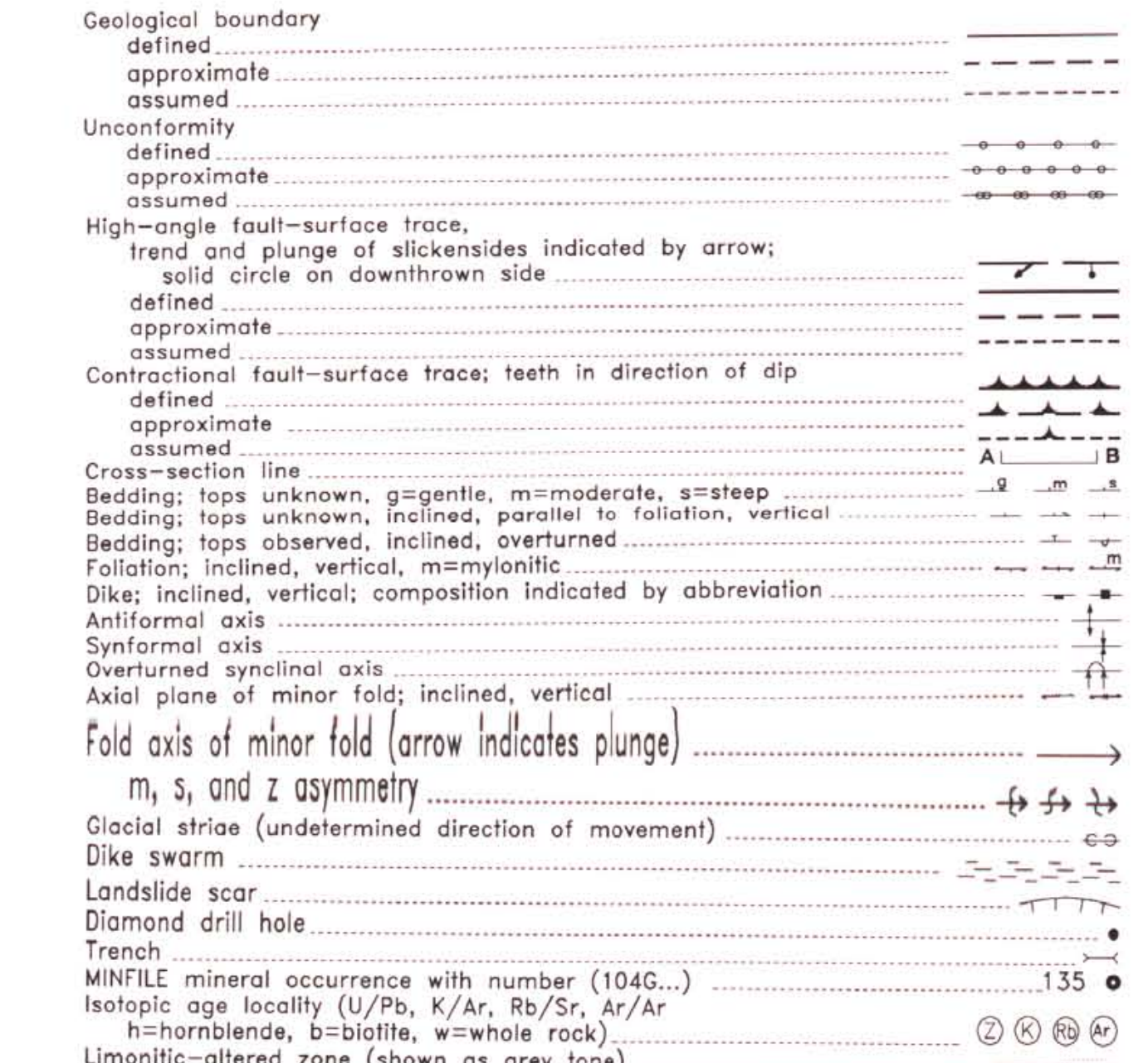
By D.A. Brown, M.H. Gunning, and C.J. Greig

Scale 1 : 100 000



- STRATIFIED ROCKS**
- QUATERNARY**
- Qal Alluvium, glacial fill, unconsolidated glacial/fluvioglacial deposits
- MIOCENE OR YOUNGER (?)**
- Mb Dark brown weathering, columnar jointed potassic andesite flows, minor tuff
- TERTIARY-EOCENE SLOKO GROUP**
- Tsd Pale green to white, locally welded, dacite and rhyolite; minor olive green andesite flows and breccia; hornblende crystals; thin lignitic tuff-breccia and tuff
 - Tsb Dark brown weathering, columnar jointed, plagioclase-phyric trachyandesite and basalt flows
- UPPER CRETACEOUS (?) TO PALEOGENE SUSTUT GROUP**
- KTS Bushes Peak Formation Poorly indurated, brick-red, brown and grey polymictic conglomerate, lesser sandstone, wacke, siltstone, rare shale; granitoid cobble conglomerate (gcn); white rhyolite to rhyodacite ash to lapilli tuff horizons (<10m thick); rhyolite to rhyodacite flows, minor basalt and andesite flows & breccia (?)
- LOWER TO MIDDLE JURASSIC HAZELTON GROUP**
- ImJhv Undifferentiated volcanic and minor sedimentary rocks
 - ImJhr Amygdaloidal olivine basalt flows, carbonate-cemented pillow breccia; rare bioclastic limestone lenses (<2m thick)
 - ImJht Flow-banded, pink to red, hematitic rhyodacite/dacite ignimbrite flows, locally subvolcanic and flow-fused
 - ImJhw Maroon, purple, magenta, brick-red and green dacite to basaltic andesite pyroxene-plagioclase porphyritic, flow-banded and amygdaloidal flows, crystal lithic tuff-breccia and lapilli tuff; local tuffaceous gneiss
 - Ljhs Lumpy sandstone, feldspathic wacke, oreille, discontinuous limestone lenses, fossiliferous-biotenites, ammonites, terebratulid brachiopods, rare Weyo, small bioherms
 - Ljhd Buff to rusty, flow-banded aphanitic rhyolite flow (or silt?)
 - Ljgl Polymictic conglomerate
- UPPER TRIASSIC STIKINE GROUP**
- UTS Undifferentiated volcanic and sedimentary rocks; argillite (arg); micritic limestone (L); limestone breccia (lx); tuffaceous wacke (tw)
 - UTSs Sedimentary rocks; undifferentiated
 - UTS2 Upper Noron Thin to thick-bedded, buff, grey, green & magenta sandstone, siltstone & argillite; andesite (and); silty-siltstone; minor subvolcanic andesite flows; minor grey chert
 - UTS1 Carnian-Lower Noron Well-bedded to massive, tuffaceous siltstone, wacke, minor argillite, interformational limestone-bearing conglomerate; grey arkosic wacke with limestone clasts, siltstone, argillite shale, rare black chert; rare granitoid-bearing polymictic conglomerate; breccia; discontinuous limestone lenses with Carnian to early Noron conodonts (L1); intertuffaceous with Ludlowian to Carnian conodonts (L2); limestone sedimentary breccia (bx); limestone (L)
 - UTSV Volcanic rocks, undifferentiated; volcanic breccia (vbx); maroon volcanic breccia (mvbx); andesite (and); silty-siltstone; pyroxene-phyric basalt (pb); maroon epilitite (mp); felsic volcanic rocks; subaqueous felsic ash tuff, laminated, pale to dark green, columnar, pyritic; "shrapnel" silty wacke/breccia, pale to dark green, silty-siltstone; locally welded ignimbrite (subvent?)
 - UTSV4 Banded plagioclase-phyric basalt or basaltic andesite flows (p), locally pillowed
 - UTSV3 Massive, medium-grained, plagioclase-rich, tuffaceous wacke
 - UTSV2 Intermediate volcanic rocks (a); massive, green hornblende-plagioclase-rich andesite block-tuff, tuff, minor flows, green & maroon andesite lithic fragments; maroon & green (UTSV2m); limestone boulder conglomerate (lc); light grey, well-bedded, hornblende-rich tuff (m), red-brown to purple plagioclase-rich volcanic breccia and tuff; fine-grained, massive, green to olive-ophitic andesite
 - UTSV1 Mafic volcanic rocks (b); augite-phyric basalt to basaltic andesite flows and breccia; pyroxene-rich crystal lithic lapilli tuff; volcanic wacke, dark green to olive-green, medium-grained, massive, minor plagioclase
- UPPER TRIASSIC (OR OLDER ?)**
- UTSm Possibly metamorphosed Stikine Group equivalents; foliated to massive metavolcanic rocks; biotite schist (bs sch); chert (chrt); chlorite schist (ch sch); siliceous rock (sil. rx.)
- EARLY PERMIAN TO (AND?) MIDDLE TRIASSIC**
- mtc Buff, pale green, grey and black chert, ribbon chert, siliceous siltstone; maroon and green ash tuff, and tuffaceous mudstone
- PALEOZOIC STIKINE ASSEMBLAGE**
- UPS Undifferentiated sedimentary rocks; granitic argillite (uPsc), black, red and green chert (uPsc), green tuffaceous siltstone, sandstone and greywacke (uPsc)

- LOWER TO UPPER PERMIAN AMBITION FORMATION**
- uPSi Maroon tuffaceous limestone
 - IPSc Dark to light grey and black calcarenites with minor chert layers and nodules, locally bioclastic, minor argillite (a), maroon and green plagioclase crystal lithic tuff, mudstone, (m) and green tuffaceous siltstone
 - IPSa Pyrite & pyrrhotite-bearing argillite and siltstone
- UPPER CARBONIFEROUS TO LOWER PERMIAN**
- uCSi Bedded to laminated sericitic ash tuff and tuffaceous siltstone; varicoloured chert; buff calcareous siltstone, dolomite layers
- UPPER CARBONIFEROUS**
- uCSa Foliated argillite, siltstone, calcareous siltstone, conglomerate, recrystallized limestone (rs)
 - uCSv Foliated, chloritic, pyroxene-plagioclase phytic, andesite flows and/or sills, crystal tuff and thin lapilli tuff, massive andesite (a), recrystallized limestone (rs)
- UPPER CARBONIFEROUS (?)**
- uCS? Foliated to massive siltstone, conglomerate, andesite, crystal lithic lapilli tuff (possibly Sulphurets Creek)
- PERMIAN OR OLDER**
- uCS Undifferentiated foliated volcanic & sedimentary rocks; recrystallized limestone (rs); pillow basalt (p)
- INTRUSIVE ROCKS**
- TERTIARY AND OLDER DIKES**
- Andesite (A); basalt (B); felsite (F); dark green, pyroxene-phyric olivine basalt (W); trachyte, quartz, syenite (S)
- TERTIARY (OR EARLY JURASSIC)**
- agg Chlorite-altered, plagioclase-phyric granodiorite
- EOCENE - HYDER SUITE**
- Egn Well-jointed, medium to coarse-grained (hornblende) biotite granite (gn); locally K-feldspar megacrystic (<5%; gn); equigranular, medium-grained hornblende-biotite granodiorite (gpd); gneiss K-feldspar megacrystic granodiorite felsite (f)
- MIDDLE JURASSIC - THREE SISTERS SUITE**
- wjn Hornblende granite to quartz monzonite stocks; spatially associated pink plagioclase-ultra-trachyte, quartz, syenite, quartz monzonite dikes, typically biotite-hornblende-plagioclase porphyritic
 - wjm Texturally heterogeneous, sorted to crowded plagioclase-porphyrific, locally trachytic, hornblende monzonite to monzonitic groundmass of fine to medium grained, subequal to subhedral hornblende and potassium feldspar
- LATE EARLY JURASSIC - COCKE MOUNTAIN SUITE**
- ltdg Equigranular, medium-grained (biotite) hornblende granodiorite; quartz monzonite
- EARLY JURASSIC - TEXAS CREEK SUITE**
- ltdm Medium-grained hornblende monzonite; quartz monzonite
- EARLY JURASSIC (?) - DIORITE SUITE**
- ltd Heterogeneous, medium to coarse-grained quartz diorite, hornblende diorite, hornblende and pyroxene
- LATE TRIASSIC TO EARLY JURASSIC - COPPER MOUNTAIN SUITE**
- ltdpx Medium-grained magnetite biotite clinopyroxene
 - ltds Medium-grained, biotite clinopyroxene potassium-feldspar syenite, equigranular to potassium-feldspar megacrystic, locally melonite garnel bearing
 - ltdm Medium-grained, potassium feldspar-megacrystic hornblende quartz monzonite
- MIDDLE TO LATE TRIASSIC - STIKINE SUITE**
- ltd Coarse-grained, plagioclase-megacrystic, magnetite-bearing hornblende quartz diorite
 - ltdg Heterogeneous, fine to medium-grained hornblende gabbro and hornblende
 - ltdm Heterogeneous quartz monzonite (qm); foliated to massive hornblende biotite granodiorite (gd); monzonitic, quartz diorite, quartz monzonite
- ALASKAN TYPE ULTRAMAFIC ROCKS**
- ltd Medium to coarse-grained olivine clinopyroxene (cp); dunite (du)
- TRIASSIC TO JURASSIC**
- tj Medium-grained, diorite to granodiorite
- UNKNOWN AGE**
- b Amphibolite (from Sauter, 1972)



ACKNOWLEDGMENTS

Field assistance and additional geology by: D. Carmichael, M. McDonough (1988), E. Moeckelburg (1988), D. Munro, I. Neill and J. Timmerman (1991). Macrofossil and microfossil identifications by E.W. Bombar, M.J. Orchard, T.P. Poulton, Lin Rui, A.R. Sweet, H.W. Tipper and E.L. Tozer of the Geological Survey of Canada. Radiometric age determinations by M.L. Bevier, W.C. McClelland, and J. Hasek; includes K-Ar dates from Holbak (1988), and White et al. (1968).

Base map compiled from 1 : 250 000 digital map produced by B.C. Ministry of Environment, Lands and Parks, Surveys and Resource Mapping Branch; Universal Transverse Mercator coordinate system. The datum used is the North American Datum defined in 1927 (NAD27). UTM Zone 11. Ice coverage is less than depicted on this map. Contour interval is 200 metres.

